AUG 6 1987 173 1051-H-11 Y 3.N 88:25/4919

NUREG/CR-4919

Field Testing of Bentonite and Cement Borehole Plugs in Granite

Prepared by A. F. Kimbrell, T. S. Avery, J. J. K. Daemen

University of Arizona
Department of Mining and Geological Engineering

Prepared for
U.S. Nuclear Regulatory
Commission

COMPLETED ORIGINAL

BEST COPY AVAILABLE

NOTICE

This report was prepared as an account of work sponsored by an agency of the United States Government. Neither the United States Government nor any agency thereof, or any of their employees, makes any warranty, expressed or implied, or assumes any legal liability of responsibility for any third party's use, or the results of such use, of any information, apparatus, product or process disclosed in this report, or represents that its use by such third party would not infringe privately owned rights.

NOTICE

Availability of Reference Materials Cited in NRC Publications

Most documents cited in NRC publications will be available from one of the following sources:

1. The NRC Public Document Room, 1717 H Street, N.W.
   Washington, DC 20555
2. The Superintendent of Documents, U.S. Government Printing Office, Post Office Box 37082, Washington, DC 20013-7082
3. The National Technical Information Service, Springfield, VA 22161

Although the listing that follows represents the majority of documents cited in NRC publications it is not intended to be exhaustive.

Referenced documents available for inspection and copying for a fee from the NRC Public Document Room include NRC correspondence and internal NRC memoranda, NRC Office of Inspection and Enforcement bulletins, circulars, information notices, inspection and investigation notices, Licensee Event Reports, vendor reports and correspondence, Commission papers, and applicant and licensee documents and correspondence.

The following documents in the NUREG series are available for purchase from the GPO Sales Program: formal NRC staff and contractor reports, NRC-sponsored conference proceedings, and NRC booklets and brochures. Also available are Regulatory Guides, NRC regulations in the *Code of Federal Regulations*, and *Nuclear Regulatory Commission Issuances*.

Documents available from the National Technical Information Service include NUREG series reports and technical reports prepared by other federal agencies and reports prepared by the Atomic Energy Commission, forerunner agency to the Nuclear Regulatory Commission.

Documents available from public and special technical libraries include all open literature items, such as books, journal and periodical articles, and transactions. *Federal Register* notices, federal and state legislation, and congressional reports can usually be obtained from these libraries.

Documents such as theses, dissertations, foreign reports and translations, and non NRC conference proceedings are available for purchase from the organization sponsoring the publication cited.

Single copies of NRC draft reports are available free, to the extent of supply, upon written request to the Division of Information Support Services, Distribution Section, U.S. Nuclear Regulatory Commission, Washington, DC 20555.

Copies of industry codes and standards used in a substantive manner in the NRC regulatory process are maintained at the NRC Library, 7920 Norfolk Avenue, Bethesda, Maryland, and are available there for reference use by the public. Codes and standards are usually copyrighted and may be purchased from the originating organization or, if they are American National Standards, from the American National Standards Institute, 1430 Broadway, New York, NY 10018.

BEST COPY AVAILABLE

NUREG/CR-4919

Field Testing of Bentonite and Cement Borehole Plugs in Granite

Manuscript Completed: March 1987
Date Published: July 1987

Prepared by
A. F. Kimbrell, T. S. Avery, J. J. K. Daemen

University of Arizona
Department of Mining and Geological Engineering
Tucson, AZ 85721

Prepared for
Division of Engineering Safety
Office of Nuclear Regulatory Research
U.S. Nuclear Regulatory Commission
Washington, DC 20555
NRC FIN B6627
Under Contract No. NRC-04-78-271

ABSTRACT

This technical report describes in-situ flow tests on bentonite and cement borehole plugs installed in granite, as well as laboratory back-up experiments on similar plugs. Prior to sealing, the hydraulic conductivity of the boreholes is tested. These measurements, together with core logs and borehole videologs, permit the selection of suitable seal test intervals. Commercial expansive cement and standard waterwell sealing bentonite products and emplacement procedures are used for borehole sealing. Transient (short-term) and steady-state (long-term) testing determines the sealing performance of the plugs under various stress conditions.

Both laboratory and field experiments confirm the great difficulty of obtaining even moderately accurate performance values for bentonite plugs as installed here, due to the simultaneous saturation, swelling, and consolidation effects. Nevertheless, conventional installation of readily available seals can provide adequate borehole seals (i.e., seals with a hydraulic conductivity of about the same order of magnitude as that of intact granite). Bentonite plugs of this type are heterogeneous and weak. Improved testing procedures and analyses are needed if actual conductivity values are to be obtained in a reasonable testing time (e.g., months). Laboratory investigations on failure mechanisms in cementitious and bentonitic plugs, not covered in this research study, are needed to identify and prevent plug failure.

TABLE OF CONTENTS

Page

ABSTRACT iii

LIST OF FIGURES x

LIST OF TABLES xvi

ACKNOWLEDGEMENTS xix

LIST OF SYMBOLS xxi

EXECUTIVE SUMMARY 1

1. In-situ Testing 1
2. Laboratory Testing 1
3. Conclusions 2

1. INTRODUCTION 3

1.1 Objective 3
1.2 Scope and Limitations 4
1.3 Organization 5
1.4 Rock Mass Sealing Contact No. NRC-40-78-271 - Reports Issued 5

2. SITE CHARACTERIZATION AND PREPARATION 9

2.1 Introduction 9
2.2 Access 9
2.3 Regional Geologic Setting 11
2.4 Local Geologic Setting 11
2.5 Whole Rock Analysis 18
2.6 Drilling History 18
2.7 Site and Hole Geology 20
2.8 Site Preparation 24
2.9 Electrical Hook-up 28

3. BOREHOLE CHARACTERIZATION TESTING 29

3.1 Introduction 29
3.2 Borehole Preparation 29
3.3 Photologging 30
    3.3.1 Photologging Equipment 30
    3.3.2 Photologging Procedures 34
    3.3.3 Photologging Results 34
    3.3.4 Videologging 40
3.4 Borehole Hydraulic Conductivity Testing: A Literature Review 42

TABLE OF CONTENTS--Continued

Page

3.4.1 Introduction 42
3.4.2 Approaches to the Problem 42
3.4.3 Field Test Objectives 43
3.4.4 Single-Hole Packer Tests 44
3.4.5 Injection Tests 45
3.4.6 Slug Tests 48
3.4.7 Cross-Hole Packer Tests 51
3.5 Borehole Hydraulic Conductivity Field Tests 53
3.5.1 Introduction 53
3.5.2 Pressure Slug Test Theory 53
3.5.3 Pressure Slug Testing Equipment 57
3.5.4 Pressure Slug Test Procedures 63
3.5.5 Pressure Slug Test Results 65
3.5.5.1 Borehole CCR/C-3 65
3.5.5.2 Borehole CCR/C-1 67
3.5.5.3 Borehole CCR/D-4 67
3.5.5.4 Borehole CCR/C-2 71
3.5.6 Pressure Slug Test Analysis 71
3.6 Constant Pressure Injection Test 80
3.6.1 Introduction 80
3.6.2 Constant Pressure Injection Test Procedures and Equipment 83
3.6.3 Results and Analysis of Constant Pressure Injection Test 83
3.7 Neutron Probe Measurements 87
3.7.1 Introduction 87
3.7.2 Theory of Neutron Moisture Probe Operations . . . 87
3.7.3 Neutron Moisture Probe Equipment and Procedures . 88

4. IN-SITU TESTING OF BOREHOLE PLUGS 92

4.1 Introduction 92
4.2 Site Preparation 92
4.3 Plug Design 95
4.4 Injection Test Equipment 95
4.5 Plug Installation 99
4.5.1 Bentonite Plug Installation in Borehole CCR/C-1 . 99
4.5.2 Cement Plug Installation in Borehole CCR/C-3 . . 103
4.5.2.1 Plug Emplacement Procedure 106
4.5.2.2 Post-Installation Work 106
4.5.3 Cement Plug Installation in Borehole CCR/C-2 . . 108
4.6 Transient Testing of Bentonite Seals 109
4.6.1 Introduction 109
4.6.2 Equipment and Procedures 109
4.6.3 Analysis of the Hydraulic Conductivity of Bentonite Plugs 110
4.6.4 Analysis of Bentonite Plug Storativity 113
4.6.5 Results of Transient Pulse Testing of Bentonite Seals 114

TABLE OF CONTENTS--Continued

Page

4.7 Long-term In-situ Performance Testing of Bentonite Plugs 126
4.8 Constant Head Injection Tests on Cement Plugs 129
4.9 Transient Flow Testing of Cement Plugs 129
4.10 Influence of Temperature Variations on In-Situ Testing . 132

5. LABORATORY INVESTIGATION OF BENTONITE BOREHOLE PLUGS 135

5.1 Introduction 135
5.2 Significant Characteristics of Bentonite Used in Seal Testing 136
5.3 Constant Injection Hydraulic Conductivity Test 139
    5.3.1 Test Objectives 139
    5.3.2 Constant Injection Pressure Test Theory 141
    5.3.3 Constant Injection Pressure Testing Equipment and Procedures 144
5.4 Consolidation Testing 147
    5.4.1 Introduction 147
    5.4.2 Consolidation Test Theory 147
    5.4.3 Consolidation Test Equipment and Procedures . . . 149
5.5 Swelling Rate/Moisture Content Testing 152
    5.5.1 Introduction 152
    5.5.2 Swelling Rate/Moisture Content Test Theory . . . 153
    5.5.3 Swelling Rate/Moisture Content Testing Equipment and Procedures 154
5.6 Reference Testing 154
    5.6.1 Introduction 154
    5.6.2 Liquid Limit Tests 154
    5.6.3 Plastic Limit Test 157
    5.6.4 Harvard Miniature Compaction Test 157
5.7 Transient Hydraulic Conductivity Testing 158
    5.7.1 Introduction 158
    5.7.2 Transient Hydraulic Conductivity Analysis 158
    5.7.3 Transient Hydraulic Conductivity Testing Equipment and Procedures 163
5.8 Saturation Test 163
    5.8.1 Introduction 163
    5.8.2 Theory 164
    5.8.3 Saturation Test Equipment and Procedures 165
5.9 Large-Scale Transient Testing 165
    5.9.1 Introduction 165
    5.9.2 Large-Scale Transient Test Theory 166
    5.9.3 Large-Scale Transient Testing Equipment and Procedures 166
5.10 Plug Prototype Study 166

6. RESULTS AND ANALYSIS OF LABORATORY TESTING OF BENTONITE BOREHOLE PLUGS 170

6.1 Introduction 170
6.2 Hydraulic Conductivity: Constant Pressure Injection . . 171

TABLE OF CONTENTS--Continued

Page

6.3 Consolidation Test Results and Analysis 178
6.4 Swelling/Moisture Content Testing 197
6.5 Reference Testing 206
    6.5.1 Liquid Limits 206
    6.5.2 Plastic Limit Test 211
    6.5.3 Harvard Miniature Compaction Test 211
6.6 Transient Hydraulic Conductivity Testing 216
6.7 Saturation Test 221
6.8 Large Scale Transient Tests 225
6.9 Plug Prototype 226

7. LABORATORY TESTING OF CEMENT PLUGS 231

7.1 Introduction 231
7.2 Plug Prototype 231
    7.2.1 Prototype Construction 231
    7.2.2 Equipment Calibration 232
7.3 Effects of Pipe Penetrating Through Plugs 232
    7.3.1 Test Equipment and Procedure 232
    7.3.2 Analysis 234
    7.3.3 Results of Constant Head Tests 234
    7.3.4 Conclusion 243
7.4 Thermal Contraction Test 243
    7.4.1 Procedure 243
    7.4.2 Results 243
    7.4.3 Conclusions 245
7.5 Piping Test 245
    7.5.1 Procedure 246
    7.5.2 Results 246
    7.5.3 Recommendations 248

8. SUMMARY, CONCLUSIONS, AND RECOMMENDATIONS FOR FURTHER RESEARCH 249

8.1 Summary 249
8.2 Conclusions 250
8.3 Recommendations for Further Research 254

REFERENCES 259

APPENDIX A: PRESSURE TRANSDUCER CALIBRATION CURVES 271

APPENDIX B: TYPE CURVES FOR SLUG TEST ANALYSIS 274

APPENDIX C: LABORATORY MEASUREMENTS OF BENTONITE PLUG HYDRAULIC CONDUCTIVITY AND DEGREE OF SATURATION . . 278

APPENDIX D: BENTONITE PLUG CONSOLIDATION TEST DATA 293

TABLE OF CONTENTS--Continued

Page

APPENDIX E: LATE TIME SOLUTIONS FOR TRANSIENT TEST LABORATORY PLUG HYDRAULIC CONDUCTIVITY TESTING 304

APPENDIX F: TYPE CURVES FOR LABORATORY PLUG TRANSIENT HYDRAULIC CONDUCTIVITY TESTING 314

LIST OF FIGURES

Figure		Page
2.1	Location of the Cargodera Canyon field test site	10
2.2	Geologic map of the Rincon-Santa Catalina-Tortolita complex	12
2.3	Schematic illustration of the Western Santa Catalina Mountains looking southeast	14
2.4	Cross-section of Santa Catalina Mts. looking southwest .	17
2.5	Cargodera Canyon lower drill site	21
2.6	Cargodera Canyon upper drill site	22
2.7	Cargodera Canyon lower drill site fracture system	23
2.8	Schematic of bunker positioned over boreholes CCR/C-1 and C-3	27
3.1	"Cactus grabber" borehole cleaner	31
3.2	Downhole camera assembly designed and constructed for photologging	32
3.3	Focus target being inserted into borehole	33
3.4	Example of downhole photograph	35
3.5	Downhole photograph with horizontal features	35
3.6	Borehole photograph in relatively damaged rock	36
3.7	Borehole CCR/C-1 core log	37
3.8	Borehole CCR/C-2 core log	38
3.9	Borehole CCR/C-3 core log	39
3.10	Schematic of borehole videologging equipment	41
3.11	Illustration of the effect of test section length on borehole hydraulic conductivity measurements	44
3.12	Assumed flow patterns in analysis of single-hole packer tests	46

LIST OF FIGURES--Continued

Figure Page

3.13 Schematic diagram showing two methods of conducting slug tests 49

3.14 Conceptual picture of a fracture network and cross-hole injection and monitoring intervals 52

3.15a Schematic of straddle-packer for pressure slug testing . 59

3.15b Schematic of straddle-packer for pressure slug testing . 60

3.16 Schematic diagram showing packer construction 61

3.17 Single packer assembly used to test conductivity of borehole section between packer and hole bottom 62

3.18 Nitrogen over water injection pump 64

3.19 Borehole CCR/D-4 core fracture map 70

3.20 Pressure decay curve measured in borehole CCR/C-1 76

3.21 Borehole CCR/C-1 test data over type curve 77

3.22 Pressure decay test 1. Borehole CCR/D-4 78

3.23 Pressure decay test 2. Borehole CCR/D-4 79

3.24 Pressure decay curve measured in borehole CCR/C-2 82

3.25 Field arrangement for constant pressure injection test . 84

3.26 Hydraulic conductivity determined from constant pressure injection test in borehole CCR/D-4 86

3.27 Neutron moisture probe inserted in a standard calibration barrel 90

3.28 Neutron moisture probe container and shield on leveling platform above a hole 90

4.1 Lower drill site, showing location of bunkers 93

4.2 Inside view of instrument protection bunker 94

4.3 Protective bunkers 94

4.4 Double plug with injection, collection, and tracer monitoring system 96

LIST OF FIGURES--Continued

Figure		Page
4.5	Twin-plug bentonite test arrangement with concentric penetrating tubing	97
4.6	Bottom collection zone with tracer collection system and bottom seal	98
4.7	Injection test apparatus for borehole CCR/C-1	100
4.8	Bentonite plugs and sand-filled collection intervals in borehole CCR/C-1 test interval	102
4.9	Cement plug in borehole CCR/C-3	105
4.10	Schematic for borehole CCR/C-3 with new top plug	107
4.11	Axial and radial flow from an injection section between two plugs	111
4.12	Pressure decay test, bentonite plugs in borehole CCR/C-1 - injection interval, Test 1	121
4.13	Pressure decay test, bentonite plugs in borehole CCR/C-1 - injection interval, Test 2	121
4.14	Pressure decay in upper collection interval, borehole CCR/C-1	123
4.15	Pressure decay in lower collection interval, borehole CCR/C-1	124
4.16	Water injected during long-term constant pressure bentonite plug testing in borehole CCR/C-1	127
4.17	Water flow into the collection intervals during long-term constant pressure bentonite plug testing in borehole CCR/C-1	128
4.18	Change in pressure over a two-day period, presumably as a result of thermal effects	134
5.1	Hydraulic conductivity of bentonite as a function of void ratio and of water chemistry	140
5.2	Schematic of constant head permeability test arrangement	142
5.3	Experimental arrangement for laboratory constant pressure testing of bentonite plugs	145
5.4	Constant pressure flow testing of bentonite plugs in PVC pipe	146

LIST OF FIGURES--Continued

Figure **Page**

5.5 Schematic of apparatus for consolidation testing of bentonite plugs 150

5.6 Apparatus for consolidation testing of bentonite plugs: tubes 5 through 8 151

5.7 Experimental arrangement for swelling rate and moisture content experiments on bentonite plugs 155

5.8 Apparatus for bentonite swelling rate and moisture content testing 156

5.9 Apparatus and sample dimensions for laboratory transient pulse testing of bentonite plug 159

5.10 Large scale transient pulse test apparatus 167

5.11 Laboratory prototype for field bentonite plug simulation tests 168

6.1 Apparent hydraulic conductivity of bentonite in tubes 1 and 4 174

6.2 Apparent hydraulic conductivity of bentonite in tubes 2 and 3 175

6.3 Consolidation outflow. Bentonite plug 5 at 69 kPa . . . 180

6.4 Consolidation outflow. Bentonite plug 6 at 69 kPa . . . 181

6.5 Consolidation outflow. Bentonite plug 7 at 69 kPa . . . 182

6.6 Consolidation outflow. Bentonite plug 8 at 69 kPa . . . 183

6.7 Consolidation outflow. Bentonite plug 5 at 69 kPa . . . 185

6.8 Consolidation outflow. Bentonite plug 6 at 69 kPa . . . 186

6.9 Consolidation outflow. Bentonite plug 7 at 69 kPa . . . 187

6.10 Consolidation outflow. Bentonite plug 8 at 69 kPa . . . 188

6.11 Consolidation outflow. Bentonite plug 5 at 138 kPa . . . 189

6.12 Consolidation outflow. Bentonite plug 6 at 138 kPa . . . 190

6.13 Consolidation outflow. Bentonite plug 7 at 138 kPa . . . 191

6.14 Consolidation outflow. Bentonite plug 5 at 207 kPa . . . 192

LIST OF FIGURES--Continued

Figure Page

6.15 Consolidation outflow. Bentonite plug 6 at 207 kPa . . . 193

6.16 Consolidation outflow. Bentonite plug 7 at 207 kPa . . . 194

6.17 Consolidation of bentonite plug 6 at 69, 138 and 207 kPa 196

6.18 Change in water content for plugs 9 through 12 at 34 kPa injection pressure 202

6.19 Change in water content for bentonite plugs 1 through 4 at 34 kPa injection pressure 205

6.20 Results of bentonite liquid limit determination, Test 1 . 209

6.21 Results of bentonite liquid limit determination, Test 2 . 210

6.22 Harvard Miniature Compaction Mold Test curve for bentonite used in sealing experiments 215

6.23 Transient pulse test 217

6.24 Transient pulse testing on bentonite plug 218

6.25 Transient pulse testing on bentonite plug 219

6.26 Lower reservoir pressure build-up as a result of upper reservoir pressure during bentonite saturation test . . . 222

6.27 Lower reservoir pressure build-up as a result of upper reservoir pressure during bentonite saturation test . . . 223

6.28 Relation between lower reservoir pressure and moisture content for bentonite saturation tests 224

6.29 Sand drying adjacent to bentonite plugs, presumably due to water adsorption by bentonite from sand 228

6.30 Separation between bentonite plugs and sand-filled adjacent reservoirs 230

7.1 Schematic of pipe through plug test 233

7.2 Cumulative inflow for tests on cement plugs with embedded steel pipes 235

7.3 Outflow from tube 1 236

7.4 Outflow from tube 2 237

7.5 Outflow from tube 3 238

LIST OF FIGURES--Continued

Figure **Page**

7.6 Outflow from tube 4 239

7.7 Outflow from tube 5 240

7.8 Outflow from tube 6 240

7.9 Outflow from tube 8 241

7.10 Cement plug outflow for pipe thermal contraction test . . 244

7.11 Cement plug piping test apparatus 247

LIST OF TABLES

Table		Page
2.1	Whole Rock Analysis of Tortolita Quartz Monzonite from Lower Drilling Site, CCR/C-1	19
2.2	Preliminary Estimate of Unfractured or Slightly Fractured Intervals Longer than One Foot for the Cargodera Canyon Study Area Lower Drill Site	25
3.1	Pressure Slug Test, Borehole CCR/C-1, Interval from 98 to 158 cm (39 to 63 inches)	68
3.2	Pressure Slug Test, Borehole CCR/C-2, Interval from 105 to 193 cm (42 to 77 inches)	68
3.3	Long-Term Pressure Slug Test, Borehole CCR/C-1	69
3.4	Long-Term Pressure Decay Test #1, Borehole CCR/D-4 . . .	72
3.5	Pressure Decay Test #2, Borehole CCR/D-4	72
3.6	Summary of Pressure Slug Test Analyses	81
3.7	Constant Pressure Injection Test Results, Borehole CCR/D-4	85
4.1	Weight of Bentonite Tablets Required for Borehole Seal with a Depth of 30 cm (1 ft)	104
4.2	Borehole CCR/C-1 Injection Interval Pressure Decay Test #1	115
4.3	Borehole CCR/C-1 Injection Interval Pressure Decay Test #2	116
4.4	Borehole CCR/C-1 Upper Collection Interval Pressure Decay	119
4.5	Borehole CCR/C-1 Lower Collection Interval Pressure Decay	120
4.6	Results of Pressure Slug Testing of Bentonite Seals . . .	125
4.7	Constant Head Injection Test #1, Borehole CCR/C-3	130
4.8	Constant Head Injection Test #2, Borehole CCR/C-3	130
4.9	Temperature Effect Test - Injection Interval CCR/C-1 . .	133
5.1	Whole Rock Analysis of Samples from Two Batches of Bentonite Ordered for This Sealing Study	137

LIST OF TABLES--Continued

Table		Page
6.1	Apparent Hydraulic Conductivity of Tubes 1-4, May-July 1985	172
6.2	Apparent Hydraulic Conductivity in Tubes 1 through 4. Constant Pressure at 10 psi	179
6.3	Summary of Slopes, Outflow vs. Square Root of Time for Consolidation Tests	179
6.4	Volumetric and Linear Deformation Measurements during Bentonite Plug Consolidation Testing	198
6.5	Saturation Tests on Bentonite Plugs in Tubes 9 through 12	199
6.6	Moisture Content of Bentonite Plugs in Tubes 1 through 4	204
6.7	Summary of Bentonite Plug Longitudinal Expansion Measurements for Tubes 9 through 12	204
6.8	Results of Bentonite Liquid Limit Test 1	207
6.9	Results of Bentonite Liquid Limit Test 2	208
6.10	Bentonite Plastic Limit Test Results	212
6.11	Harvard Miniature Compaction Test Results	213
6.12	Harvard Miniature Compaction Test - Water Content	214
6.13	Results of Small-Scale Transient Pulse Testing on Bentonite Plugs	220
6.14	Results of Large Scale Bentonite Plug Transient Pulse Tests	227

ACKNOWLEDGEMENTS

The research reported on has been performed by the University of Arizona, Department of Mining and Geological Engineering, for the U.S. Nuclear Regulatory Commission (NRC). Project monitor for the NRC is Mr. Jacob Philip. The project is under Dr. F.A. Costanzi, Chief, Waste Management Branch, Division of Engineering Safety, Office of Nuclear Regulatory Research.

Dr. Jaak J.K. Daemen, Associate Professor, Department of Mining and Geological Engineering, University of Arizona, is the Principal Investigator. Dr. James G. McCray, Acting Director, Nuclear Fuel Cycle Research Program, Department of Nuclear and Energy Engineering, University of Arizona, has provided project management assistance and nuclear waste technical assistance. Allen F. Kimbrell and Timothy S. Avery have performed the experimental and theoretical work as part of their M.Sc. degree requirements, with considerable help by Mike Gaudette, whose contribution is especially acknowledged. Experimental assistance has been provided by laboratory technicians and undergraduate assistants Charles Williams, George Shosted, Terrance Miley, Behrooz Kousari, and Robert Armstrong. Valuable discussions have been held with Bill Greer, particularly with regard to field testing and transient pulse test analysis. Mike Porter has assembled, typed and produced the report.

We gratefully acknowledge the assistance of the Dowell Division of Dow Chemical, U.S.A., in providing cement and additives, and especially the technical help provided by Erik B. Nelson.

American Colloid Company supplied precompressed Volclay® bentonite tablets. Valuable technical discussions with Chris Jepsen, Mark Bertane and Todd Harriet of American Colloid are gratefully acknowledged.

LIST OF SYMBOLS

Roman Symbols:

a: parallel plate hydraulic aperture (equation 7.2)

a_a, a_w: air and water fractional areas (equation 5.30)

a_v: coefficient of compressibility

A: sample cross-sectional area

c: constant in cubic law fracture flow equation (equation 7.3)

C_c: compression index (equation 6.6)

C_h: wellbore storage term (equation 3.9)

C_{ps}: pseudo-compressibility term; combined water and test equipment compliance

c_v: coefficient of consolidation (equation 6.3)

C_s: swell index

C_w: water compressibility

D: characteristic conduit length

e: void ratio

g: acceleration of gravity

h: hydraulic head, piezometric head

H: length of (consolidation) drainage path (equation 6.3)

h_d: head in downstream reservoir (equation 5.10)

h_o: ambient (undisturbed by test) hydraulic head

h_u: head in upstream reservoir (equation 5.11)

h_w: hydraulic head at a wellbore

i: hydraulic gradient

J_o, J_1, Y_o, Y_1: Bessel functions, zero and first-order, first and second kind

K: hydraulic conductivity

K_h: horizontal permeability

K_o: shape factor in Kozeny-Carman equation (equation 5.3)

L: test interval, plug, or sample length

L_f: length of rectangular parallel plate flowpath (eqution 7.4)

n: porosity

N_R: Reynolds Number (equation 5.2)

P: pressure

P_w: density of water

Q: volumetric flowrate

Q_i: inflow for plug i (equation 7.1)

Q_o: total outflow (equation 7.1)

Q_T: total inflow (equation 7.1)

r: radial distance from wellbore axis

r_c: casing or standpipe radius

r_e: radius of influence

r_w: borehole radius

s: residual drawdown

S: storage coefficient (or storativity)

S_d: compressive storage of downstream reservoir (equation 5.12)

S_s: specific storage

S_p: specific surface area (equation 5.12)

S_u: compressive storage of upstream reservoir (equation 5.13)

S_w: packer compliance, plug compliance

t: time

T: transmissivity

t_b: basic lag time (equation 3.9)

t_D: dimensionless time

u: integration variable

u^*: equivalent pore pressure in partially saturated clay (equation 5.30)

u_a: gas (air) pore pressure (equation 5.30)

u_w: water (fluid) pore pressure (equation 5.30)

v: flow velocity

V: water volume

V_c: outflow volume due to consolidation

V_w: compressed water volume; water volume in test interval

W_f: width of rectangular parallel plate flowpath (equation 7.4)

$W(t_D)$: well function

z: axial (vertical) coordinate

Greek Symbols:

α: transient pulse type curve parameter

β: dimensionless time transient pulse type curve parameter

γ: unit weight of a permeant

γ: ratio of downstream to upstream reservoir volumes (Sections 5.7.2, 6.6, Appendix F)

γ_w: specific weight of water

γ_s: unit weight of solid

μ: fluid viscosity

ρ: density

σ: total stress

$\bar{\sigma}$: effective stress

σ_{va}: average vertical stress in confined compression (equation 6.6)

ϕ_1: solution of equation (5.25)

ϕ_m: solutions of equations (5.20),(5.27)

EXECUTIVE SUMMARY

1. In-situ Testing

In-situ testing at the Cargodera Canyon study area is divided chronologically and is the focus of research into three basic areas. The first stage involves site characterization of the study area and the surrounding geologic environment. It has as objective determining the suitability of the site for the proposed seal testing. Detailed mapping of the site area determines the geologic and natural features of the site that must be taken into account in the testing program. The location of the study area presents a security problem if the site is to be instrumented as testing requires. Site preparation must take into account power requirements and the meteorological conditions that could interfere with access or actual testing.

The second stage of in-situ testing at Cargodera Canyon has as objective the geologic and hydrogeologic characterization of the geologic medium to be sealed. The first step in this process is a detailed review of the drilling histories and drilling logs of the boreholes at the site. Holes selected for testing are photologged. Once suitable testing intervals have been chosen, packer tests determine the hydraulic conductivity of the rock before it is sealed. Finally, on-going testing provides long-term permeability information as a control for both short-term testing and actual plug testing. In addition, these tests and neutron probes record the impact of injection for plug testing on the degree of saturation in the surrounding rock mass.

The third stage of in-situ testing involves the emplacement of bentonite and cement plugs as well as their performance testing. This is initiated with the construction of structures to secure the required equipment and to protect it from the elements. Plug design and emplacement methods tested on laboratory prototypes are then used to seal the borehole intervals selected for testing. Transient testing is used to determine if the plug injection and collection structures are competent and ready for testing. Finally, long-term performance testing of the in-place plugs is initiated.

2. Laboratory Testing

The laboratory study has as objective providing an experimental control for the equipment, methods and materials used for in-situ testing. Whenever possible, an effort is made to reproduce field conditions. Several scale sizes are used to help control the impact of size effects on field analysis.

The laboratory work has three principal areas of focus. The first is equipment testing and calibration. A number of the tests used in the field require precise equipment testing and calibration so that compliance factors can be computed. The low permeabilities of both the host rock and the sealing materials tested necessitate long-term study of equipment performance under a variety of pressure and temperature regimes.

Bentonite is a complex material and many of its characteristics significant to sealing are not well understood. The second area of laboratory research involves prototype study of the behavior of bentonite plugs in the laboratory. Once plugs have been emplaced in the field, they are no longer accessible for inspection. Laboratory prototypes allow the rheological aspects of plug behavior to be studied. The behavior of plugs in the field can then be predicted and explained. In addition, the permeability of the plug material can be estimated without the influence of the host rock.

A third area of laboratory research involves reference testing of the bentonite used in this study. A number of these reference values have never been determined. Others are problematic and often a function of testing methods not suited to pure bentonites. An effort is made in these reference tests to use bentonite in the same form it has as plugs in the field. Finally, a number of the tests are repeated over time to determine if the established reference values are time dependent.

Laboratory tests assess a critical aspect of the field plug design, a pipe penetrating through the plug. The results show that as the penetrating pipe diameter increases, so does the permeability. A test aimed at assessing the effects of water channeling through fresh cement paste was inconclusive.

3. Conclusions

The results confirm that conventional borehole sealing, e.g. bailer-emplaced cement plugs and bentonite pellets dropped through water, can provide satisfactory short-term sealing of holes in granite. Such simple installation of widely used products provides a hydraulic conductivity of the sealed hole less than or about equal to that of intact granite. Detailed predictions of such bentonite installations (e.g. actual hydraulic conductivity) are highly uncertain due to complications associated with installation (e.g. pronounced heterogeneity) and with behavior (in particular swelling, consolidation, and saturation). As is to be expected, the strength of such bentonite installations is exceedingly low, suggesting the need for bentonite plug support, e.g. by means of cementitious plugs.

Precise determination of bentonite seal parameters will require extremely lengthy testing, if conventional steady state testing is used, or will require the development of reliable short term (transient) testing procedures and analysis methods for soft, porous low permeability materials such as clay, that, moreover, are subject to volume changes (swelling and consolidation).

CHAPTER ONE

INTRODUCTION

1.1 Objective

The fundamental objective of this "Rock Mass Sealing" research project is to assess experimentally the performance of existing products and methods for sealing rock masses, in the current phase of the project to conduct an experimental evaluation of borehole plug performance. This work is aimed at determining the feasibility of sealing boreholes intersecting a repository rock mass to a level where it can reasonably be assured that the plugged boreholes will not become preferential radionuclide migration paths. This project studies experimentally the likelihood of preventing such migrations by sufficiently reducing the hydraulic conductivity of the plugged borehole (including the plug-rock interface). The work performed provides direct input to an assessment as to whether or not 10 CFR 60.134 (U.S. Nuclear Regulatory Commission, 1983, and, as amended, 1985) is likely to be satisfied by any particular proposed sealing methods. Some aspects of this study have broader implications, e.g. directly for 10 CRF.133 (d), and indirectly for 10 CFR.133 (a)(1),(2),(f) (U.S. Nuclear Regulatory Commission 1983, and as amended, 1985), (h).

The study is conducted to establish a factual data basis on borehole sealing performance. Although some types of borehole sealing have been performed for many years, relatively little testing and sealing performance verification has been reported on.

Concern about boreholes and their potential influence on the isolation performance of the rock mass surrounding repositories has been expressed in a number of basic reviews on underground HLW (High level radioactive waste) disposal (e.g. Atomic Energy of Canada Limited, 1978, p. 72; Bredehoeft et al., 1978, p. 8; Committee on Radioactive Waste Management, 1978, pp. 5,10; Heineman et al., 1978, p. 4; U.S. Department of Energy, 1979, p. 3.1.328; Arnett et al., 1980, p. 139; Barbreau et al., 1980, p. 528; Burkholder, 1980, p. 15; Irish, 1980, p. 42; OECD, 1980, Foreword; Pedersen and Lindstrom-Jensen, 1980, p. 195; U.S. Department of Energy, 1982, p. 29; Deju, 1983, p. 4; Kocher et al., 1983, p. 54; National Research Council, 1983, p. 8-9, 21, 63; U.S. Department of Energy, 1983, p. 25).

It deserves pointing out that the need for borehole plugging, and particularly for very high performance (e.g. very low hydraulic conductivity), is not universally accepted, nor obvious, and certainly might be a somewhat site dependent requirement, as shown by consequence assessments (e.g. Pedersen and Lindstrom-Jensen, 1980, p. 195; Klingsberg and Duguid, 1980, p. 43; Intera Environmental Consultants, Inc., 1981). These authors do recognize that borehole seals will provide "... an important redundant barrier ..." or "... will satisfy the concept of multiple barriers ...". A panel of experts convened by the Commission of the European Communities and the OECD Nuclear Energy Agency simultaneously considers backfilling and sealing (OECD, 1984, Section III.4) and, after stressing the host rock specificity of backfill and sealing functions, states that "they (i.e. seals) would be designed so as not to present any preferential flow paths ... there is confidence that they (i.e. the functional requirements) can be met by a number of different materials." That the controversy about sealing requirements is far from resolved is particularly well illustrated by the recently published disagreements among the ONWI Exploratory Shaft Peer Review Group (Kalia, 1986, p. 14). Site-specific analyses are most likely to provide information needed to finalize specific performance requirements (e.g. Stormont, 1984; Fernandez and Freshley, 1984; Seitz et al., 1987).

General guidelines for the separation of radioactive waste from the physical environment, and in particular for the acceptable radionuclide releases following repository closure, have been finalized by EPA (U.S. Environmental Protection Agency, 1986; 40 CRF 191). Detailed implementation of the requirements is governed by 10 CFR 60 (U.S. Nuclear Regulatory Commission, 1983, 1985). The research performed as part of this ongoing contract addresses specifically some of the remaining uncertainties associated with the sealing requirements in 10 CFR 60, including §60.51,(a); §60.102,b(2),e(1),(2); §60.113; §60.133,(h), §60.142,(c), but particularly §60.134, Design of seals for shafts and boreholes.

1.2 Scope and Limitations

Experimental investigations have been conducted on the sealing performance of bentonite and of cementitious borehole plugs in granite. Steady state constant pressure and transient (pulse) injection tests have been used to determine the hydraulic characteristics of in-situ plugs. Related back-up laboratory testing included construction (installation) of prototype plugs simulating field installation and test procedures, detailed characterization of plug materials, and a variety of experimental plug flow investigations.

Readying the Cargodera Canyon field site for in-situ testing has been a major part of the effort described here. This includes design, acquisition, installation and operation of the field instrumentation, as well as necessary preliminary site and borehole characterization. The latter included, in particular, hydrological testing of the holes.

Cement plugs have been installed in two short vertical boreholes, two bentonite plugs in one hole. The hydraulic conductivity of the plugs has been tested by steady state (constant pressure) and by transient (pulse) injection tests.

Hydraulic conductivity of bentonite plugs has been studied in the laboratory with particular emphasis on the influence of consolidation, swelling, and saturation, on the flow results. A transient approach to bentonite flow testing has been initiated. Standard soil mechanics characterization tests have been performed on bentonite in a state as installed in the field.

Field test installation procedures required the installation of piping penetrating the plugs. The influence of such penetrations through cement and through bentonite plugs has been tested in the laboratory.

The main limitation on the experimental field work is the short duration for which the experiments have been run, resulting in a rather limited data basis, compromised by uncertainties regarding transient effects.

1.3 Organization

This introductory chapter briefly summarizes the regulatory context of rock mass sealing requirements, quotes commentaries and viewpoints on rock mass sealing from the literature on HLW disposal, outlines the organization of this report, and lists related reports issued under this contract.

Site characterization and geological environment of the Cargodera Canyon field site are described in Chapter 2, as well as preparation of the site for testing. Characterization of the boreholes used for field plug testing is described in Chapter 3. This includes borehole photologging and hydraulic testing.

Plug installation and plug testing in the boreholes at the site are described in Chapter 4.

Chapter 5 includes a description of the laboratory investigations on bentonite borehole plugs. Results are presented in Chapter 6.

Laboratory work on cement plugs is reported in Chapter 7.

Chapter 8 summarizes the work, as well as conclusions drawn, and identifies promising future research topics.

1.4 Rock Mass Sealing Contract No. NRC-04-78-271 - Reports Issued

This Technical Report is the latest in a series of reports issued for the subject contract. A complete list of reports issued (to be issued for Schaffer and Daemen, 1987) is given below, to facilitate a general overview of work performed to date and of the overall context of ongoing work.

The first four reports, as well as the seventh, are literature surveys.

The fifth report is primarily a description of planning, experimental design and some preliminary tests.

The topical report by Jeffrey (1980) gives a comprehensive theoretical (analytical) discussion of transverse plug-rock interaction, based on elastic and viscoelastic calculations. This is complemented by the axial interaction discussed in Stormont and Daemen (1983), a report which is primarily experimentally oriented, but includes extensive analytical discussions.

The topical reports by Mathis and Daemen (1982) and by Fuenkajorn and Daemen (1986) present a detailed experimental assessment of drilling damage in granites and in basalts.

Experimental flow studies under polyaxial stress conditions are described in Cobb and Daemen (1982), under radially symmetric external loading in South and Daemen (1986), and on unloaded samples in Akgun and Daemen (1986). Additional data on plug performance under stressed and unstressed conditions are included in virtually all other reports.

Schaffer and Daemen (1987) describe experiments on rock fracture grouting, emphasizing the considerable lack of detailed knowledge and need for further research in this area.

All annual reports subsequent to (5) include a combination of experiments, results, conclusions, and plans for future work, similar to the present annual report.

Quarterly progress reports are not listed as all information contained therein also is included in the annual reports.

1. South, D.L., R.G. Jeffrey, L.W. Kiejbuk, and J.J.K. Daemen, 1979, "Rock Mass Sealing - Annual Report, October 1, 1978 - September 30, 1979," prepared for the U.S. Nuclear Regulatory Commission, SAFER Division, for Contract NRC-04-78-271, by the Department of Mining and Geological Engineering, University of Arizona, Tucson.

2. Daemen, J.J.K., 1979, "Rock Mass Sealing (Research in Europe)," 48 pp., Foreign Travel Trip Report to the U.S. Nuclear Regulatory Commission, SAFER Division, for Contract NRC-04-78-271, by the Department of Mining and Geological Engineering, University of Arizona, Tucson.

3. South, D.L., 1979, "Well Cementing," 75 + vii pp., Topical Report to the U.S. Nuclear Regulatory Commission, SAFER Division, for Contract NRC-04-78-271, by the Department of Mining and Geological Engineering, University of Arizona, Tucson.

4. Sultan, H.A., "Chemical Grouting for Rock Mass Sealing - a Literature Review," 45 + iv pp., Topical Report to the U.S. Nuclear Regulatory Commission, SAFER Division, for Contract NRC-04-78-271, by the Department of Mining and Geological Engineering, University of Arizona, Tucson.

5. South, D.L., R.G. Jeffrey, S.L. Cobb, S.P. Mathis, and J.J.K. Daemen, 1979, "Rock Mass Sealing - Annual Report, October 1, 1979 - September 30, 1980," prepared for the U.S. Nuclear Regulatory Commission, SAFER Division, for Contract NRC-04-78-271, by the Department of Mining and Geological Engineering, University of Arizona, Tucson.

6. Jeffrey, R.G., 1980, "Shaft or Borehole Plug-Rock Mechanical Interaction," 145 + xi pp., Topical Report to the U.S. Nuclear Regulatory Commission, SAFER Division, for Contract NRC-04-78-271, by the Department of Mining and Geological Engineering, University of Arizona, Tucson.

7. South, D.L., 1980, "Borehole Sealing with Clay (Part A). Considerations in Clay Mineral Stability (Part B)," 50 + iv pp.; 25 + ii pp., Topical Report to the U.S. Nuclear Regulatory Commission, SAFER Division, for Contract NRC-04-78-271, by the Department of Mining and Geological Engineering, University of Arizona, Tucson.

8. Cobb, S.L., W.B. Greer, R.G. Jeffrey, S.P. Mathis, D.L. South, and J.J.K. Daemen, 1981, "Rock Mass Sealing - Annual Report, September 1, 1980 - May 31, 1981," prepared for the U.S. Nuclear Regulatory Commission, SAFER Division, for Contract NRC-04-78-271, by the Department of Mining and Geological Engineering, University of Arizona, Tucson.

9. South, D.L., W.B. Greer, N.I. Colburn, S.L. Cobb, B. Kousari, S.P. Mathis, R.G. Jeffrey, C.A. Wakely, and J.J.K. Daemen, 1982, "Rock Mass Sealing - Annual Report, June 1, 1981 - May 31, 1982," prepared for the U.S. Nuclear Regulatory Commission, SAFER Division, for Contract NRC-04-78-271, by the Department of Mining and Geological Engineering, University of Arizona, Tucson.

10. Mathis, S.P. and J.J.K. Daemen, 1982, "Borehole Wall Damage Induced by Drilling: An Assessment of Diamond and Percussion Drilling Effects," 171 + xii pp., Topical Report to the U.S. Nuclear Regulatory Commission, SAFER Division, for Contract NRC-04-78-271, by the Department of Mining and Geological Engineering, University of Arizona, Tucson.

11. Cobb, S.L. and J.J.K. Daemen, 1982, "Polyaxial Testing of Borehole Plug Performance," 180 + xi pp., Topical Report to the U.S. Nuclear Regulatory Commission, SAFER Division, for Contract NRC-04-78-271, by the Department of Mining and Geological Engineering, University of Arizona, Tucson.

12. Daemen, J.J.K., D.L. South, W.B. Greer, J.C. Stormont, S.A. Dischler, G.S. Adisoma, N.I. Colburn, K. Fuenkajorn, D.E. Miles, B. Kousari, and J. Bertuca, 1983, "Rock Mass Sealing - Annual Report, June 1, 1982 - May 31, 1983," NUREG/CR-3473, prepared for the U.S. Nuclear Regulatory Commission, Division of Health, Siting and Waste Management, for Contract NRC-04-78-271, by the Department of Mining and Geological Engineering, University of Arizona, Tucson.

13. Stormont, J.C. and J.J.K. Daemen, 1983, "Axial Strength of Cement Borehole Plugs in Granite and Basalt, NUREG/CR-3594, Topical Report to the U.S. Nuclear Regulatory Commission, Division of Health, Siting and Waste Management, for Contract

NRC-04-78-271, by the Department of Mining and Geological Engineering, University of Arizona, Tucson.

14. Daemen, J.J.K., W.B. Greer, G.S. Adisoma, K. Fuenkajorn, W.D. Sawyer, Jr., A. Yazdandoost, H. Akgun, and B. Kousari, 1985, "Rock Mass Sealing - Annual Report, June 1983 - May 1984," NUREG/CR-4174, prepared for the U.S. Nuclear Regulatory Commission, Division of Radiation Programs and Earth Sciences, Office of Nuclear Regulatory Research, Contract No. NRC-04-78-271, by the Department of Mining and Geological Engineering, University of Arizona, Tucson.

15. Fuenkajorn, K. and J.J.K. Daemen, 1986, "Experimental Assessment of Borehole Wall Drilling Damage in Basaltic Rocks," NUREG/CR-4641, Technical Report to the U.S. Nuclear Regulatory Commission, Division of Radiation Programs and Earth Sciences, Office of Nuclear Regulatory Research, Contract No. NRC-04-78-271, by the Department of Mining and Geological Engineering, University of Arizona, Tucson.

16. Daemen, J.J.K., W.B. Greer, K. Fuenkajorn, A. Yazdandoost, H. Akgun, A. Schaffer, A.F. Kimbrell, T.S. Avery, J.R. Williams, B. Kousari, and R.O. Roko, 1986, "Rock Mass Sealing - Annual Report, June 1984 - May 1985," NUREG/CR-4642, prepared for the U.S. Nuclear Regulatory Commission, Division of Radiation Programs and Earth Sciences, Office of Nuclear Regulatory Research, Contract No. NRC-04-78-271, by the Department of Mining and Geological Engineering, University of Arizona, Tucson.

17. Akgun, H., and J.J.K. Daemen, 1986, "Size Influence on the Sealing Performance of Cementitious Borehole Plugs," NUREG/CR-4738, Technical Report to the U.S. Nuclear Regulatory Commission, Division of Engineering Safety, Office of Nuclear Regulatory Research, Contract No. NRC-04-78-271, by the Department of Mining and Geological Engineering, University of Arizona, Tucson.

18. South, D.L. and J.J.K. Daemen, 1986, "Permeameter Studies of Water Flow through Cement and Clay Borehole Seals in Granite, Basalt and Tuff," NUREG/CR-4748, Technical Report to the U.S. Nuclear Regulatory Commission, Division of Engineering Safety, Office of Nuclear Regulatory Research, Contract No. NRC-04-78-271, by the Department of Mining and Geological Engineering, University of Arizona, Tucson.

19. Schaffer, A., and J.J.K. Daemen, 1987, "Experimental Assessment of the Sealing Effectiveness of Rock Fracture Grouting", Technical Report to the U.S. Nuclear Regulatory Commission, Division of Engineering Safety, Office of Nuclear Regulatory Research, Contract No. NRC-04-78-271, by the Department of Mining and Geological Engineering, University of Arizona, Tucson. (Submitted to NRC)

CHAPTER TWO

SITE CHARACTERIZATION AND PREPARATION

2.1 Introduction

Site characterization at Cargodera Canyon has as objective to determine the suitability of this site for in-situ performance testing of borehole seals. The criteria for this assessment are a function of the overall objective of the field testing program: to determine the in-hole performance of borehole plugs in granite. The site must provide rock with appropriate lithology. Boreholes must be deep enough for testing and must include intervals of relatively competent rock. The regional setting must provide year-round access and must permit research installations.

2.2 Access

The Cargodera Canyon study site is approximately 40 km (25 mi) north of the University of Arizona, Tucson, Arizona (Figure 2.1). It is at an elevation of approximately 1122 m (3680 ft) in the SE 1/4 Section 25 (unsurveyed), T 11 S, R 14 E (Gila and Salt River Meridian), within the Santa Catalina Ranger District of the Coronado National Forest, Pima County, Arizona. The Cargodera Canyon area access road runs east from U.S. Highway 89 immediately south of the town of Catalina, at the Golder Ranch road turnoff. The road is paved to the Canada del Oro Wash. For 8 to 10 km (5 to 6 mi) the road is graded dirt. After Sutherland Wash, the Forest Service rock-surfaced route 643 is accessible only by four wheel drive vehicles. The site is approximately 1.25 km (3/4 mi) beyond the gate marking the boundary of the National Forest.

The access road is adjacent to the site, which is advantageous for transporting equipment, but is detrimental in that the site is exposed to all who travel the road. A small ephemeral stream parallels the road to the southeast and proved useful as a water supply for construction. Over the duration of this study the stream contained water from the middle of August until the end of May or early June.

A line supplying power to Summerhaven, a small community at the top of the Catalinas, is approximately 100 m (300 ft) from the site. The line is maintained by Trico Electric Company and was used to supply electric power to the site.

The temperature range at the site is similar to that in Tucson. Highs in the summer reach 43°C (110°F). In the winter the lows fall below freezing for short periods of time. This is an important factor to consider due to the use of precision electronic measuring devices and computer equipment.

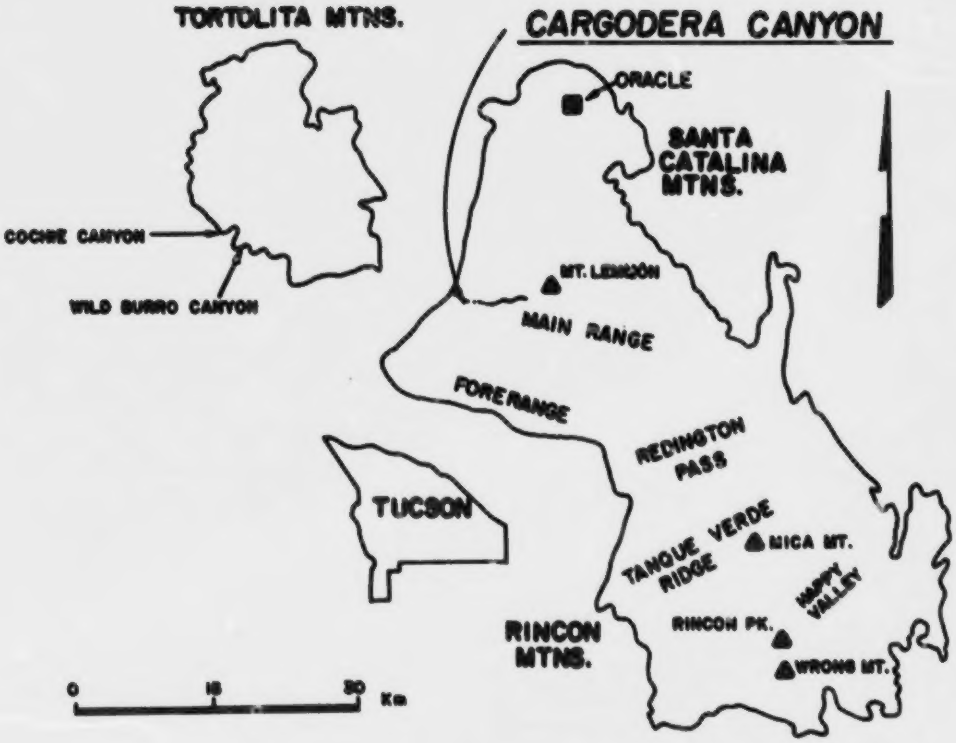
TORTOLITA MTNS.
CARGODERA CANYON
ORACLE
SANTA CATALINA MTNS.
COCHISE CANYON
WILD BURRO CANYON
MT. LEMMON
MAIN RANGE
FORERANGE
REDINGTON PASS
TUCSON
TANQUE VERDE RIDGE
MICA MT.
HAPPY VALLEY
RINCON PK.
WRONG MT.
RINCON MTNS.
0
15
30
Km

Figure 2.1 Location of the Cargodera Canyon field test site.

(Reproduced with permission from Keith, S.B., et al., 1980, "Evidence for Multiple Intrusion and Deformation within the Santa-Catalina-Rincon-Tortolita Crystalline Complex, Southeastern, Arizona," pp. 217-269, Geological Society of America, Memoir 153, Cordilleran Metamorphic Core Complexes.)

BEST COPY AVAILABLE

2.3 Regional Geologic Setting

The Santa Catalina Mountains reach elevations of 3,000 m and are among the highest in the Basin and Range province of the state of Arizona. The physiography of the region is distinctively broad, bulbous and domical. It is characterized by long, flat-topped topographic profiles and elongate northeast-, north-, or northwest-trending plan outlines. The region features visible high angle faulting that seriously disrupts the arch morphology.

The study site is within the Basin and Range physiographic province. Exposures in the province consist of Precambrian granitic and metamorphic basement, upper Precambrian to Paleozoic stratified rocks, and a variety of Mesozoic-Cenezoic sedimentary, volcanic, plutonic and metamorphic rocks (Rehrig and Reynolds, 1980).

The region was tectonically active intermittently between 1.8 and 1.4 billion years before present (b.y.B.P.). It became more stable during later Precambrian time. It was entirely within the continental cratonic environment of thin Paleozoic sedimentation during the Paleozoic. During the Mesozoic, southern Arizona was the site of magmatism, metamorphism, tectonic unrest and accumulation of locally thick sections of stratified rock. A Triassic-Jurassic volcanic arc trended northwest through the region. During the early Cretaceous, the region was the site of clastic and carbonate deposition. In addition, thick sections of impure arkose are widespread and indicate unstable tectonic conditions. Laramide time (80 to 50 m.y.B.P.) was characterized by compressional deformation, plutonism and volcanism. During the Eocene, widespread erosion and sparse continental sedimentation may have occurred over most of the region. During Oligocene and Miocene time, the region was dominated by tectonism, plutonism, metamorphism, silicic volcanism and continental sedimentation (Banks, 1980; Rehrig and Reynolds, 1980).

The test site is in an area of intense geologic interest, the Rincon-Santa Catalina-Tortolita complex (Figure 2.2). This complex has been affected by a number of superposed deformations, including high temperature extensional deformation, which was regional in extent, and ductile to brittle tectonic denudation. The result of these processes is presently considered a metamorphic core complex (Davis, 1980).

The metamorphic core complex including the Catalina-Rincon complex is of early to middle Tertiary age. The core complex fabrics and related decollements are superimposed on plutons as young as 50 m.y. The complex features a complicated history of plutonism, deformation and metamorphism which continues to be a focus of study (Keith et al., 1980).

2.4 Local Geologic Setting

Cargodera Canyon is on the northwest flank of the Santa Catalina Mountains. Figure 2.3 locates the three major plutonic intrusions that outcrop in the vicinity of the study area.

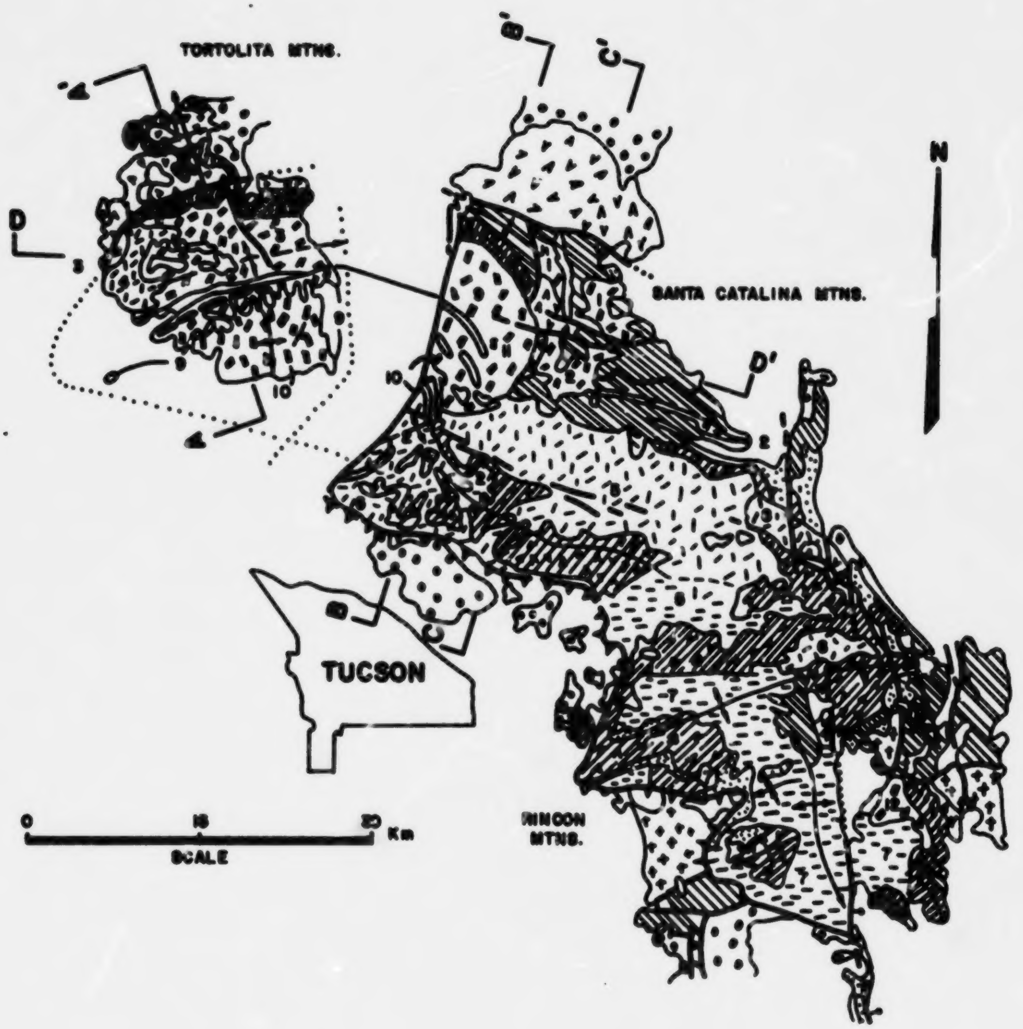
TORTOLITA MTNS.
A
A'
B'
C'
D
D'
N
SANTA CATALINA MTNS.
TUCSON
B
C
0
10
20 Km
SCALE
RINCON MTNS.

Figure 2.2 Geologic map of the Rincon-Santa Catalina-Tortolita complex.

(Reproduced with permission from Keith, S.B., et al., 1980, "Evidence for Multiple Intrusion and Deformation within the Santa-Catalina-Rincon-Tortolita Crystalline Complex, Southeastern, Arizona," pp. 217-269, Geological Society of America, Memoir 153, Cordilleran Metamorphic Core Complexes.)

BEST COPY AVAILABLE

Figure 2.2 Geologic map of the Rincon-Santa Catalina-Tortolita complex.

EXPLANATION

	□	LATE TERTIARY AND QUATERNARY BASIN FILL SEDIMENTS (13 m.y. to Recent)
	⁘	MID-TERTIARY CLASTIC SEDIMENTARY AND LOCALLY INTERCALATED VOLCANIC ROCKS (36 to 15 m.y.)
	░	MYLONITIC SCHIST AND SCHISTOSE ROCKS OF UNCERTAIN PARENT MATERIALS AND AGE
LATE CRETACEOUS TO OLIGOCENE BATHOLITH INTRUSIONS	▪	OLIGOCENE QUARTZ MONZONITE PLUTONS (28 to 25 m.y.)
	⁄	EOCENE MUSCOVITE GRANITES AND ASSOCIATED APLO-PEGMATITES (51 to 44 m.y.)
	″	LATE CRETACEOUS - EARLY TERTIARY DIORITE TO GRANODIORITE PLUTONS (75 to 60 m.y.)
	∴	MESOZOIC (MOSTLY CRETACEOUS) SEDIMENTARY AND METASEDIMENTARY ROCKS
	▨	YOUNGER PRECAMBRIAN SEDIMENTARY DIABASE AND METASEDIMENTARY AND METADIABASE ROCKS AND PALEOZOIC SEDIMENTARY AND METASEDIMENTARY ROCKS
OLDER PRE-CAMBRIAN ROCK	▧	PORPHYRITIC GRANITIC ROCKS (1.45 to 1.4 b.y.)
	+	GRANODIORITE AND DIORITE (1.65 to 1.6 b.y.)
	▩	PINAL SCHIST (1.7 b.y.)

PLUTONS ARE NUMBERED AS FOLLOWS:

1. RICE PEAK GRANODIORITE
2. LEATHERWOOD QUARTZ/DIORITE
3. CHIRREON WASH GRANODIORITE
4. DERRIO CANYON GRANITE
5. WILDERNESS GRANITE & ASSOCIATED LEMMON ROCK LEUCOGRANITE
6. ESPIRITU CANYON GRANITE
7. WRONG MOUNTAIN GRANITE
8. YOUTEY GRANITE
9. CATALINA QUARTZ MONZONITE
10. TORTOLITA QUARTZ MONZONITE
11. REEF OF ROCK GRANITE
12. HAPPY VALLEY QUARTZ MONZONITE

(Reproduced with permission from Keith, S.B., et al., 1980, "Evidence for Multiple Intrusion and Deformation within the Santa-Catalina-Rincon-Tortolita Crystalline Complex, Southeastern, Arizona," pp. 217-269, Geological Society of America, Memoir 153, Cordilleran Metamorphic Core Complexes.)

BEST COPY AVAILABLE

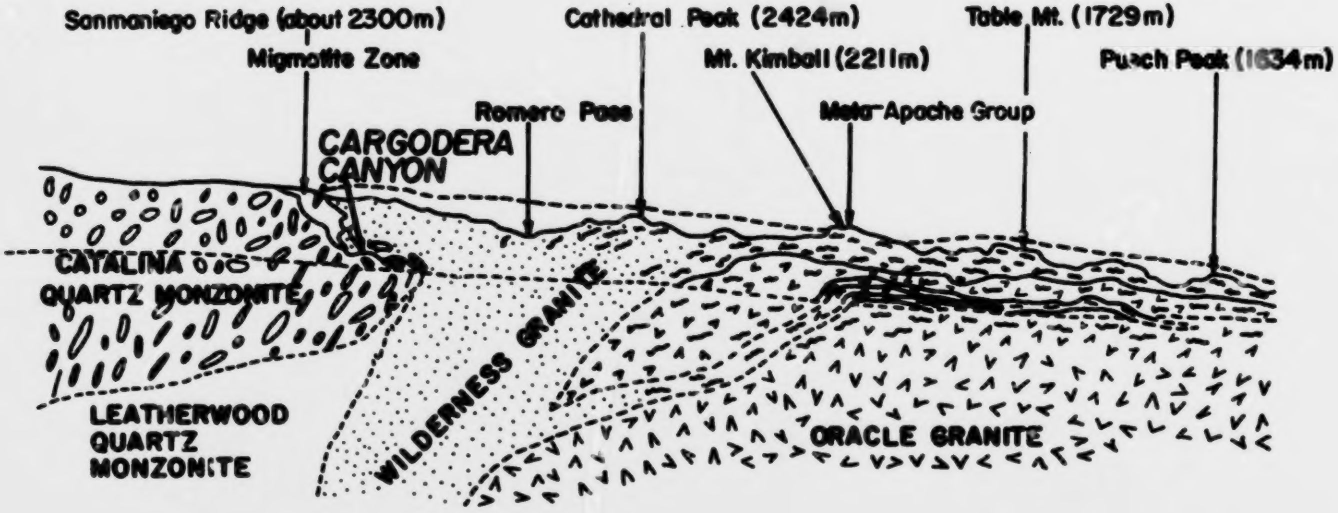
Sanmaniego Ridge (about 2300m)
Migmatite Zone
Cathedral Peak (2424m)
Mt. Kimball (2211m)
Table Mt. (1729m)
Pusch Peak (1634m)
Romero Pass
Meta-Apache Group
CARGODERA CANYON
CATALINA QUARTZ MONZONITE
LEATHERWOOD QUARTZ MONZONITE
WILDERNESS GRANITE
ORACLE GRANITE

Figure 2.3 Schematic illustration of the Western Santa Catalina Mountains looking southeast.

(Reproduced with permission from Keith, S.B., et al., 1980, "Evidence for Multiple Intrusion and Deformation within the Santa-Catalina-Rincon-Tortolita Crystalline Complex, Southeastern, Arizona," pp. 217-269, Geological Society of America, Memoir 153, Cordilleran Metamorphic Core Complexes.)

The Wilderness granite is one of five members of the Wilderness suite, all asymmetric, laccolithic granitic intrusions. The Wilderness granite is a batholith-sized laccolith trending west-northwest in the main range of the Santa Catalina Mountains. Average modes for the Wilderness granite are (Keith et al., 1980):

Quartz - 28
Plagioclase - 29
K-feldspar - 27
Biotite - 4
Muscovite - 7
Magnetite - 1
Garnet - 1-2.

(Reproduced with permission from Keith, S.B., et al., 1980, "Evidence for Multiple Intrusion and Deformation within the Santa-Catalina-Rincon-Tortolita Crystalline Complex, Southeastern, Arizona," pp. 217-269, Geological Society of America, Memoir 153, Cordilleran Metamorphic Core Complexes.)

The Wilderness granite that outcrops in Cargodera Canyon is described as the Lemmon Rock leucogranite phase of the Wilderness granite. Rb-Sr isotope data indicate the rock is approximately 47 m.y. in age. K-Ar data seems to confirm this dating with analyses of coarse muscovite suggesting an age of 47.9 m.y. Field relationships require that the Wilderness suite granites postdate Late Cretaceous and early Tertiary plutons but predate the middle Tertiary plutons that also outcrop in the Cargodera Canyon region (Keith et al., 1980).

Catalina quartz monzonite is one of four Middle Tertiary plutons that make up the Catalina Suite. The Catalina Quartz monzonite forms a large, half-circle-shaped pluton in the northwestern Santa Catalina Mountains. The Catalina quartz monzonite is mineralogically distinct from the Wilderness granite. Field identification is facilitated by visible hornblende and sphene in all samples. Established modes for the Catalina quartz monzonite are as follows:

Quartz - 26.8
K-feldspar - 34.3
Plagioclase - 26.7
Biotite - 7.5
Hornblende - 0.8
Opaque grains - 1.3
Sphene - 0.6
Apatite - 0.4.

(Reproduced with permission from Keith, S.B., et al., 1980, "Evidence for Multiple Intrusion and Deformation within the Santa-Catalina-Rincon-Tortolita Crystalline Complex, Southeastern, Arizona," pp. 217-269, Geological Society of America, Memoir 153, Cordilleran Metamorphic Core Complexes.)

Isotopic analyses suggest a reference age of approximately 26 m.y. for the Catalina quartz monzonite. Field relationships confirm that the pluton is younger than the Eocene Wilderness suite (Keith et al., 1980).

Cargodera Canyon is the site of intrusive contact of the Catalina quartz monzonite into the Lemmon Rock leucogranite phase of the Wilderness granite (Figure 2.4). Much of the contact is occupied by a steeply inclined migmatite zone that contains an interleaved assemblage of metasedimentary rocks. These include quartzites, calc-silicate skarns and siliceous gneiss. Also present are foliated Lemmon Rock leucogranite and Catalina quartz monzonite. The migmatite has been interpreted as a screen of metamorphosed and highly injected, pre-Catalina intrusive and metasedimentary rocks. Both plutons contain metasedimentary inclusions (Keith et al., 1980).

The youngest pluton in the Cargodera Canyon area is the Tortolita quartz monzonite. The Tortolita quartz monzonite is included in the Catalina suite. In Cargodera Canyon, two large north-northwest-striking dikes of Tortolita quartz monzonite crosscut both the Catalina quartz monzonite and the Wilderness granite. These dikes have been correlated with the main Tortolita pluton in the southern Tortolita Mountains which occupies the entire southern third of the mountain range. Tortolita quartz monzonite can be distinguished from Catalina quartz monzonite in the field by its finer grain size and nonporphyritic, hypidiomorphic-granular texture. Modal analysis is as follows (Keith et al., 1980):

Quartz - 39.2
K-feldspar - 31.2
Plagioclase - 26.4
Biotite - 3.2
Opaque grains - trace

(Reproduced with permission from Keith, S.B., et al., 1980, "Evidence for Multiple Intrusion and Deformation within the Santa-Catalina-Rincon-Tortolita Crystalline Complex, Southeastern, Arizona," pp. 217-269, Geological Society of America, Memoir 153, Cordilleran Metamorphic Core Complexes.)

Wherever Tortolita quartz monzonite and Catalina quartz monzonite are in contact, the Tortolita quartz monzonite clearly cuts the Catalina quartz monzonite. So, even though both plutons are best dated with reference to the 26 m.y. isochron previously discussed, field relationships indicate the Tortolita quartz monzonite is younger (Banks, 1980; Keith et al., 1980).

Some confusion in earlier discussions of the Cargodera Canyon site demonstrates the complex and interrelated nature of the various granitic suites present at the site and the significance of their contacts. Recent research has confirmed that the Tortolita quartz monzonite dike discussed above is, in fact, the rock unit where the

BLANK PAGE

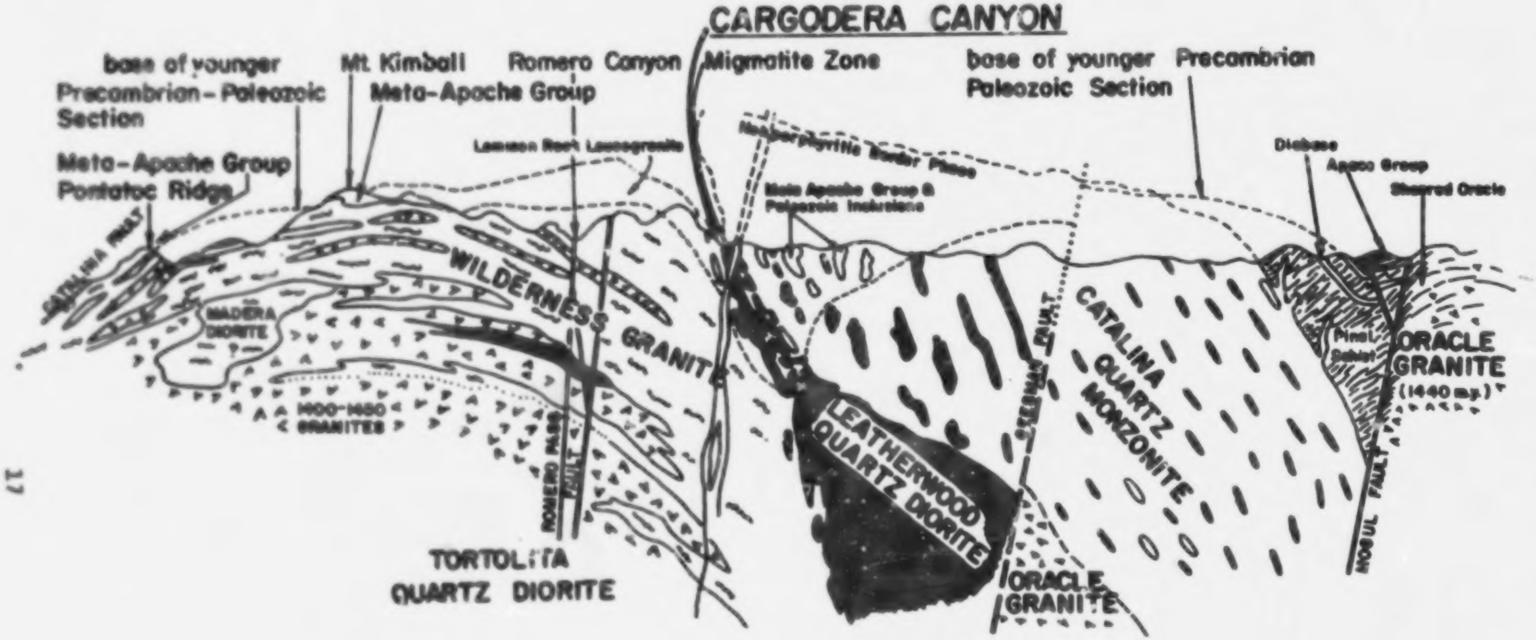
CARGODERA CANYON
base of younger Precambrian-Paleozoic Section
Mt Kimball
Romero Canyon
Migmatite Zone
Meta-Apache Group
base of younger Precambrian Paleozoic Section
Meta-Apache Group Pontatoc Ridge
Lemmon Rock Leucogranite
Meta-Apache Group & Paleozoic Inclusions
Diabase
Apache Group
Sheared Oracle
CATALINA FAULT
MADERA DIORITE
WILDERNESS GRANITE
1400-1450 GRANITES
ROMERO PASS FAULT
TORTOLITA QUARTZ DIORITE
LEATHERWOOD QUARTZ DIORITE
GEESAMAN FAULT
CATALINA QUARTZ MONZONITE
ORACLE GRANITE
Pinal Schist
ORACLE GRANITE (1440 m.y.)
MOGUL FAULT

Figure 2.4 Cross-section of Santa Catalina Mountains looking southwest.

(Reproduced with permission from Keith, S.B., et al., 1980, "Evidence for Multiple Intrusion and Deformation within the Santa-Catalina-Rincon-Tortolita Crystalline Complex, Southeastern, Arizona," pp. 217-269, Geological Society of America, Memoir 153, Cordilleran Metamorphic Core Complexes.)

BEST COPY AVAILABLE

boreholes to be studied were drilled.* Lack of agreement on dating the other units present allows for the possibility that those units experienced some form of metamorphic alteration. The Tortolita quartz monzonite, however, postdates those possible metamorphic events. Its unfoliated, undeformed non-metamorphic character recommends it as the object of study designed to identify engineering aspects of crystalline rocks as a whole.

2.5 Whole Rock Analysis

A whole rock analysis of a sample of Tortolita quartz monzonite from the Cargodera Canyon study area was peformed by Copper State Analytical Lab, Inc., of Tucson, Arizona. The test was performed on a piece of core from borehole CCR/C-1 of the lower drill site (Section 2.6). Table 2.1 presents the results.

Quartz monzonite is a granitic rock containing major plagioclase, orthoclase and quartz, with minor biotite, hornblende, apatite and zircon. Quartz comprises 10 to 50 percent of the felsic constituents. The alkali feldspar to total feldspar ratio should range from 35 to 65 percent. It differs from granite primarily in its low feldspar to total feldspar ratio of 65 to 90 percent (American Geological Institute, 1974, p. 582). The results in Table 2.1 indicate a higher percentage of Na than K, which suggests that the alkali feldspar to total feldspar ratio of the study area rock is chemically more a quartz monzonite than a granite. The composition of quartz monzonite falls between alkali granites and quartz diorites. A comparison of Table 2.1 with average compositions of calc alkalic granite, alkali granite and quartz diorite (e.g. Ehlers and Blatt, 1980, Table 4.1, p. 103) with respect to FeO, MgO, CaO, Na_2O and K_2O suggests that the Tortolita quartz monzonite resembles the quartz diorite in composition for Na and Fe values and the alkali granites with respect to high Si and K values.

2.6 Drilling History

Drilling at the Cargodera Canyon site was done by American Mining and Drilling Co.,a company based in Tucson, Arizona. A Joy 12B/Gardner Denver 83 rig was used for drilling. Fifteen holes with an aggregate drilled footage of 97 m (317 ft) were completed between September and November 1981. Available drill-hole footage includes 51 m (168 ft) of 6.275 cm (2 1/2 inch) diameter holes and 20 m (67 ft) of 16.3 cm (6 1/2 inch) diameter holes. Open footage in the large diameter holes is less than drilled because core barrels and contained core were lost and not retrieved from two holes.

Five percussion holes with diameters of 6.275 cm (2 1/2 inches) were drilled, each to a depth of 4.6 m (15 ft). These holes are designated CCR/P-1 through 5 and are located on the lower (eastern) portion of the

---

*Stephen J. Reynolds, Arizona Bureau of Geology and Mineral Technology, Geological Survey Branch, Tucson, AZ. Personal communication, 1985.

Table 2.1 Whole Rock Analysis of Tortollita Quartz Monzonite from Lower Drilling Site, CCR/C-1

	Percent of Total
SiO_2	71.4
Al_2O_3	8.9
CaO	0.68
MgO	1.22
K_2O	4.3
Na_2O	5.6
Fe_2O_3	4.29
TiO_2	0.48
P_2O_5	0.29
MnO	0.28
LiO	1.96

site (Figure 2.5). Five 6.275 cm (2 1/2 inch) diameter diamond core holes, designated CCR/D-1 through 5, were drilled to depths varying from 4.6 to 6.7 m (15 to 22 ft) on the lower site. One 6.275 cm (2 1/2 inch) diamond core hole, CCR/D-6, was drilled to a depth of 13 m (42.5 ft) on the upper (western) site (Figure 2.6). Four 16.3 cm (6 1/2 inch) diameter holes, designated CCR/C-1 through 4, were drilled by overcoring 3.765 cm (1 1/2 inch) diameter diamond holes with a 16.3 cm (6 1/2 inch) diamond bit. CCR/C-1 through 3 are located on the lower site, CCR/C-4 on the upper site. CCR/C-4 was drilled to 8 m (26 ft), but core barrel loss reduced the available depth to 6.4 m (21 ft). CCR/C-3 also had its effective depth reduced to 3 m (9.5 ft) by the loss of core barrel. CCR/C-1 was drilled to a depth of 4.3 m (14 ft), CCR/C-2 to approximately 6 m (19.5 ft). All core holes were drilled with water only. Mud was not used because it might affect hole wall permeability. Dry drilling was attempted for about a meter in several holes, but was not successful. The driller cleaned and capped all holes.

2.7 Site and Hole Geology

A preliminary evaluation of the geology of the Cargodera Canyon study area was made by members of the research group, principally Nora Colburn, consulting geologist, from November 1981 through May of 1982 (Daemen et al., 1982). This evaluation had as objectives determining the lithological and structural features that characterized the site as well as finding intervals in the diamond holes competent enough to recommend plug testing.

Some confusion existed at the time with respect to the actual rock unit represented by the lower site. Rock descriptions were made using representative core. Both sites are composed of a distinctly biotitic granitic rock. At the lower site, the rock is fine to medium grained. The upper site rock is coarser grained, almost porphyritic, with K-feldspar and sphene phenocrysts. Both sites show one or two cross foliation sets, with visible alignment of biotite flakes, feldspar lath and quartz-plagioclase zones. The upper site rock features numerous oriented inclusions, including rock fragments and septa, clots and pods and schlieren zones. A few biotite-enriched schlieren zones were found in the lower site rock.

Several aplite dikes crosscut the study area, some apparently extending for miles. The widths of these dikes vary from a few to about thirty centimeters. The dikes, in turn, are crosscut by conjugal joint sets.

The lower site features what may be a through-going, erosionally widened gap which varies in width from 10 to 30 cm. This gap was logged in all the diamond holes in the lower site except CCR/C-2 and CCR/D-5. It occurs at approximately the same elevation in the holes where it was noted. Figure 2.7 suggests how some of the larger fracture systems, including the predominating gap, may be interconnected and linking the logged holes of the lower site. Several surface indications may express the same large gap in the lower site outcrop. A large opening at the northern tip of the outcrop has allowed partial collapse of part of the unsupported overhang which, in

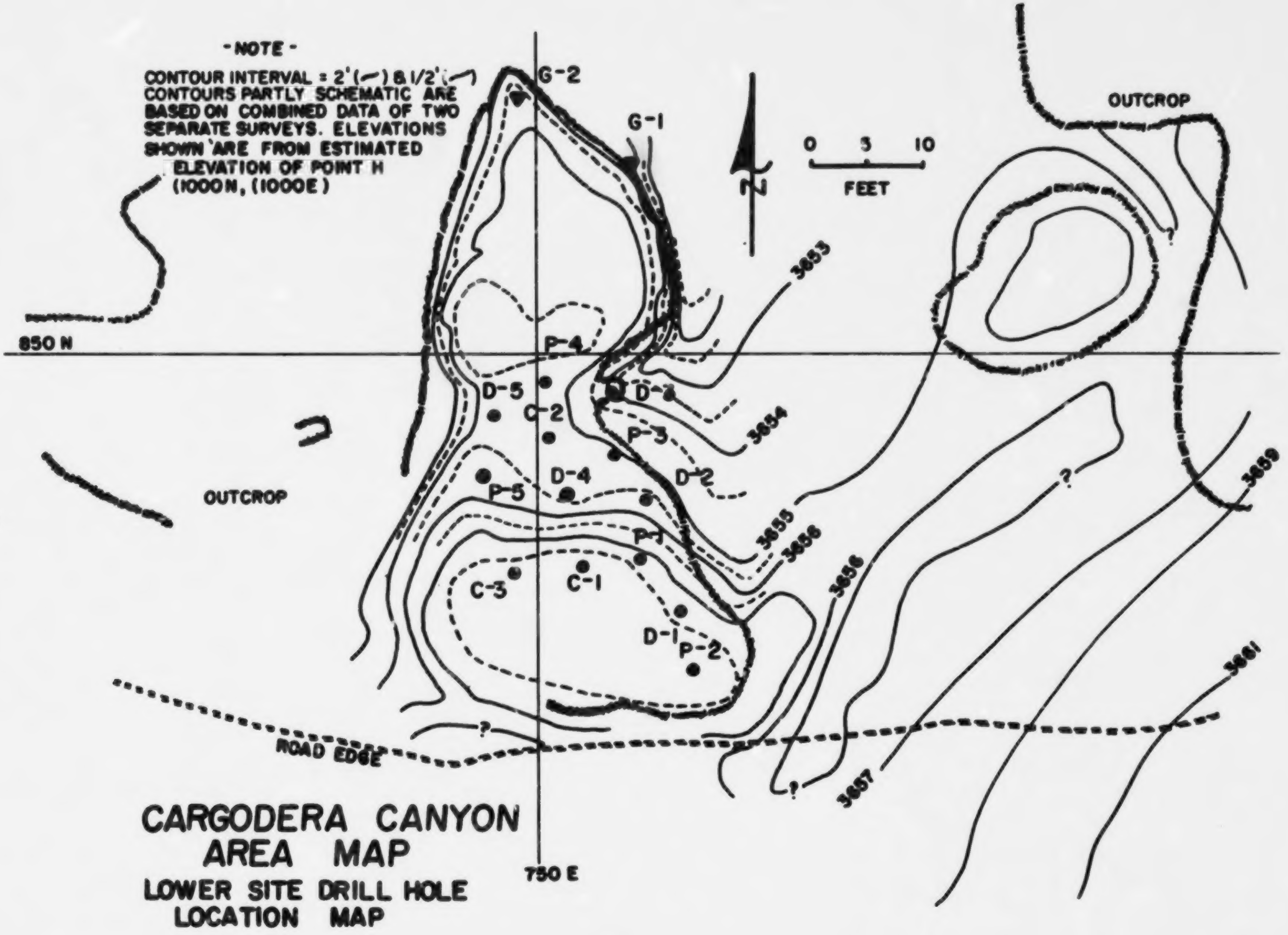
- NOTE -
CONTOUR INTERVAL = 2'(—) & 1/2'(---)
CONTOURS PARTLY SCHEMATIC ARE BASED ON COMBINED DATA OF TWO SEPARATE SURVEYS. ELEVATIONS SHOWN ARE FROM ESTIMATED ELEVATION OF POINT H (1000N, (1000E)
G-2
G-1
N
0 5 10
FEET
OUTCROP
3653
850 N
P-4
D-5
D-3
C-2
3654
P-3
D-2
P-5
D-4
?
3659
OUTCROP
3655
3656
P-1
3656
C-3
C-1
D-1
P-2
3661
?
ROAD EDGE
?
3657
CARGODERA CANYON AREA MAP
LOWER SITE DRILL HOLE LOCATION MAP
750 E

Figure 2.5 Cargodera Canyon Lower Drill site.

BEST COPY AVAILABLE

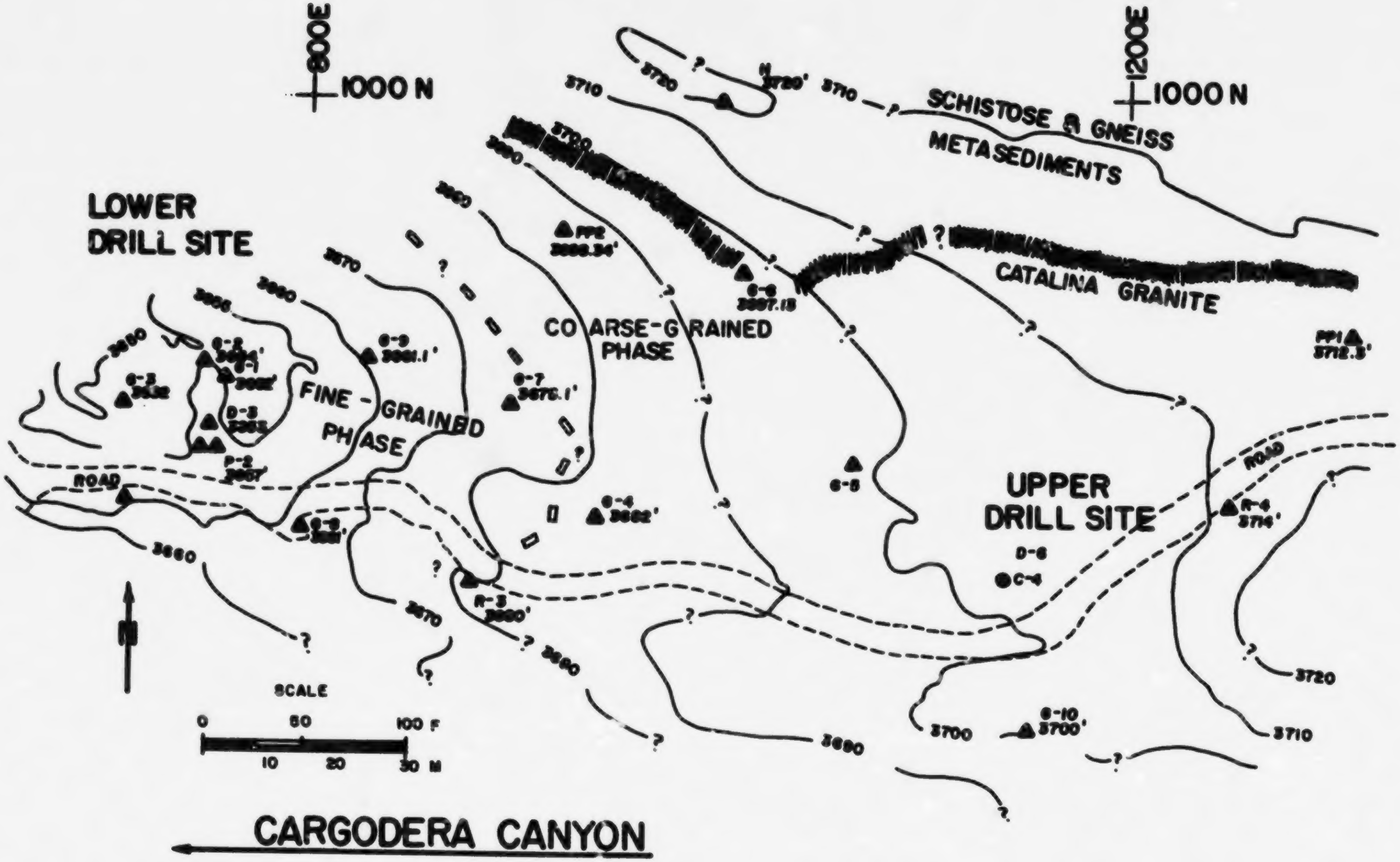
800E
1000 N
1200E
1000 N
SCHISTOSE & GNEISS
METASEDIMENTS
CATALINA GRANITE
LOWER
DRILL SITE
FINE - GRAINED
PHASE
COARSE-GRAINED
PHASE
UPPER
DRILL SITE
ROAD
ROAD
3720
3720'
3710
3710
3700
3690
3680
3670
3660
3650
3660
3670
3680
3690
3700
3710
3720
PP2
3688.34'
G-6
3697.15
G-9
3661.1'
G-7
3675.1'
G-4
3662'
G-5
PP1
3712.3'
R-4
3714'
D-6
C-4
G-10
3700'
R-3
3660'
G-3
G-2
G-1
D-3
P-2
3657'
?
N
SCALE
0
50
100 F
10
20
30 M
CARGODERA CANYON

Figure 2.6 Cargodera Canyon Upper Drill Site.

BEST COPY AVAILABLE

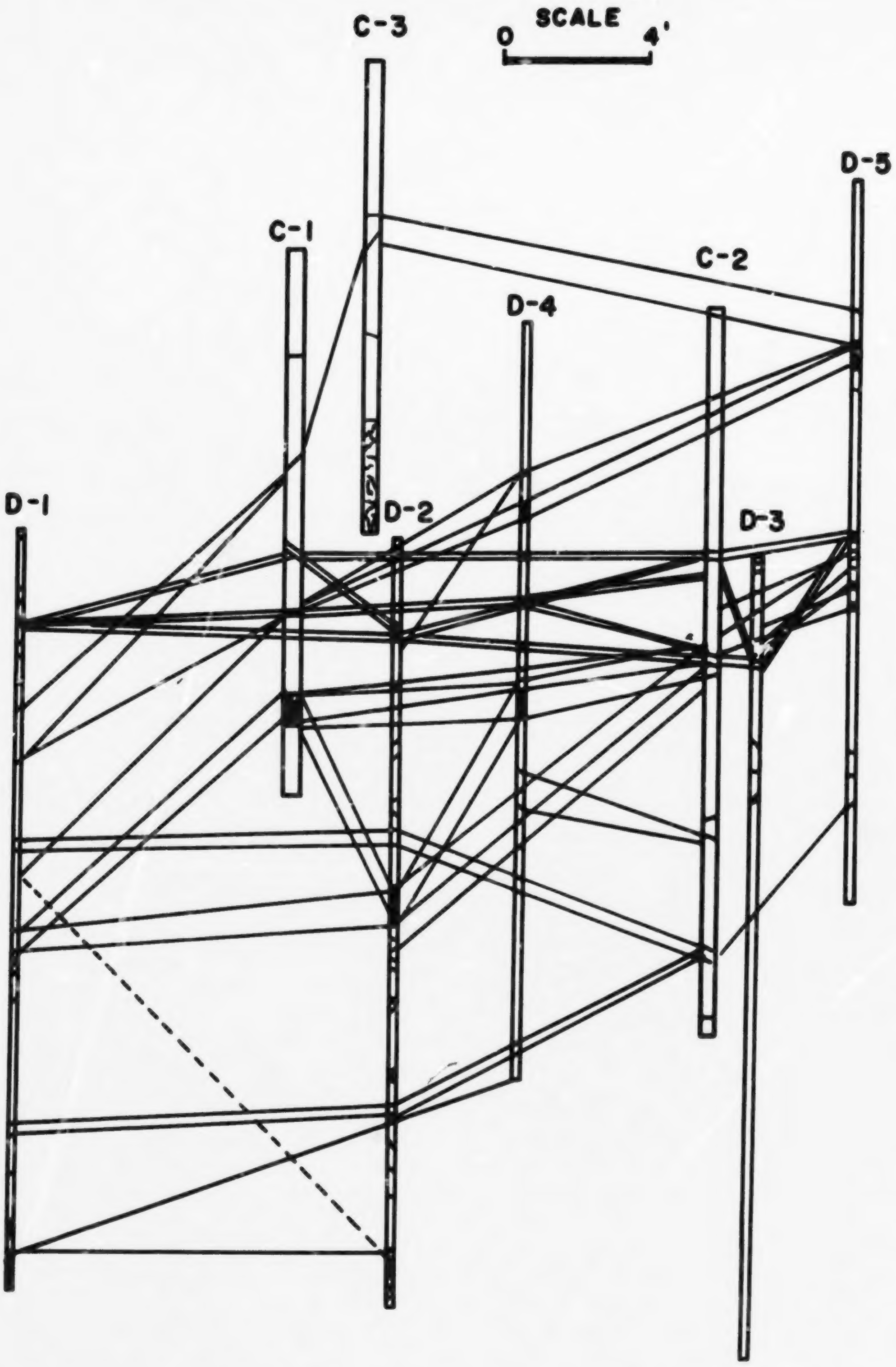
C-3
SCALE
0
4'
D-5
C-1
C-2
D-4
D-1
D-2
D-3

Figure 2.7 Cargodera Canyon Lower Drill site fracture system.

BEST COPY AVAILABLE

turn, has opened fractures on the surface of the outcrop. This large "fracture" feature led original investigators to suggest that the portion of the drilled outcrop above the fracture may have moved some small distance. A minimal offset of several centimeters was noted in the extended trends of two aplite dikes that crosscut the drill site.

A preliminary estimate of intervals suitable for testing was based on core logging and site investigation. The results of this evaluation are included in Table 2.2.

2.8 Site Preparation

The Rock Mass Sealing program demands sophistication in equipment design to be able to monitor the small flow rates associated with low permeability materials. With sophistication comes delicacy. Proper conditions can be guaranteed in the laboratory; no such guarantees exist in the field. The conditions in the field add difficulty, and cost, to any test, especially when accurate data monitoring is essential. The ability to overcome problems in the field that do not exist in the lab may determine whether a field test will fail or succeed.

Cargodera Canyon provided many challenges that had to be overcome before a single test could be conducted. The testing apparatus had to be compatible with the restrictions imposed by the environment. Potentially dangerous nitrogen bottles were a major concern when the site plan was developed. Other items involved in the design included precision gages and burettes, LVDT's, pressure transducers, and a data logging device with peripherals.

Security was the highest priority when Cargodera Canyon was considered as a field site. The drill holes are located adjacent to a dirt road that is accessible to four-wheel drive vehicles. The presence of a test facility in such a remote area provides a tempting target for vandals.

The area supports populations of deer, javalina and quail, which are prime game in Southern Arizona. While the majority of hunters are law-abiding, a high-powered rifle can be most destructive. Several years ago in this area, two teenagers shot at an explosives shack with armor-piercing bullets. One of them was killed instantly and the other died later in the hospital. Minor damage has been done to the equipment bunker described later in this section during the last deer season. Permission to store high explosives at the site was denied early on in the planning stage.

Permission to test had to be acquired from the Coronado National Forest District Ranger. A detailed description of test plans had to be submitted and approved. A permit was granted to build up to three equipment bunkers and conduct tests for one year. At the end of that time the permit had to be renewed. If, for some reason, the permit was not renewed, or if the project were terminated for any reason at any time, the bunkers and equipment had to be removed and the site returned to its original state.

Table 2.2 Preliminary Estimate of Unfractured or Slightly Fractured Intervals Longer than One Foot for the Cargodera Canyon Study Area Lower Drilled Site (After Daemen et al., 1982, p. 116)

Hole No.	Diameter (in)	Total Depth (ft)	Interval (ft)	Interval Length (ft)	Remarks
C1	6.5	15.0	0 - 2.9	2.9	(2)
			3.0 - 6.0	3.0	(2)
			6.3 - 8.1	1.8	(1)
			10.3 - 12.1	1.8	(1)
			13.5 - 15.0	1.8	(1)
C2	6.5	19.6	0 - 6.7	6.7	(1)
			10.8 - 14.0	3.2	(1)
			14.3 - 17.5	3.2	(1)
C3	6.5	13.0	0 - 4.3	4.3	(2)
			5.7 - 10.9	5.2	(1)
D1	2.5	21.0	0.2 - 4.6	4.4	(2)
			5.0 - 6.2	1.2	(2)
			6.4 - 9.2	2.8	(1)
			11.6 - 18.9	7.3	(2)
D2	2.5	21.0	6.0 - 7.5	1.5	(1)
			7.6 - 9.6	2.0	(1)
			10.6 - 12.6	2.0	(1)
			13.0 - 14.6	1.6	(1)
			15.7 - 19.5	3.8	(1)
D3	2.5	35.0	0 - 4.7	4.7	(2)
			6.6 - 9.7	3.1	(1)
D4	2.5	21.0	0 - 3.8	3.8	(1)
			5.7 - 9.7	4.0	(1)
			10.9 - 12.2	1.3	(1)
			13.3 - 20.6	7.3	(1)
D5	2.5	20.0	0 - 4.6	4.6	(2)
			5.9 - 10.0	4.1	(1)
			12.0 - 15.8	3.8	(1)
			16.6 - 20.0	3.4	(1)

(1) Apparently unfractured throughout interval.

(2) Slightly fractured, i.e. apparently containing only a few hairline fractures (apertures of about 0.1 mm or less) over the interval.

The shelter requirements were determined to be:

1. Protect apparatus and test environment from vandalism and the surrounding environment.

2. Adequately house all apparatus.

3. Be transportable by four-wheel drive vehicle over a rough road.

4. Blend with the surroundings as best as possible.

5. Be removable.

A masonry structure was the selected solution. A structure built of slump block could be customized to fit any size requirements. Slump block filled with mortar would also be an effective barrier against most high-powered rifles, ensuring the safety of the equipment in the shelter, or "bunker". The ease in transporting the slump block to the site would be a function of how many blocks could be safely carried over the road at one time. Light grey slump block would match the light tones of the granite outcrop surroundings. A bunker could be removed with minimal difficulty by chiseling apart the mortar joints and transporting the blocks back down the road.

The bunker size was standardized at 2.5 m x 1.5 m. Two boreholes can be enclosed per bunker. The first bunker contains two 16.5 cm diameter boreholes, each one plugged (Figure 2.8). The second bunker contains a 16.5 cm borehole and a 6.4 cm borehole. The 16.5 cm hole was plugged with cement, the smaller hole was used to conduct hydrologic tests.

The building materials used for the bunker were 40 cm x 20 cm x 10 cm (16" x 8" x 4") grey slump block, mortar, 40 cm x 20 cm x 5 cm (16" x 8" x 2") cap block and a custom-made steel lid. The construction of the bunker required masonry skills and ingenuity. Normally blocks are laid on a cement pad or footer. A footer was not used in this case due to the complexity it would add when the bunker had to be removed. A cement footer would have made the work easier. The area for the first bunker varies about 15 cm (6 inches) in elevation, and includes a rather steep slope at the back wall location. The slope was compensated for by cutting brick to the slope angle. To adjust for the varying elevation, blocks were sliced lengthwise to 2.5, 5 and 7.5 cm (1", 2" and 3") thicknesses. These blocks were used wherever a block shorter than 10 cm (4") was needed. The angles and short blocks provided a level base upon which the rest of the bunker could be built. Once all blocks were laid, the access doors were brought to the site and fastened in place.

The frame and door assembly are one unit, weighing approximately 180 kg (400 lbs). The outer dimensions of the frame are 120 x 260 cm (48 x 104.5 inches). The access doors are two 0.475 cm (3/16 inch) thick steel plates mounted by hinges to a cross-member of the door frame. The door frame is constructed of 7.5 cm (3 inch) angle iron with 5 x 1.25 cm (2 x 1/2 inch) box tubing reinforcement. Another set of doors 0.31 cm (1/8 inch) thick can be slid into slots below the first set of

BLANK PAGE

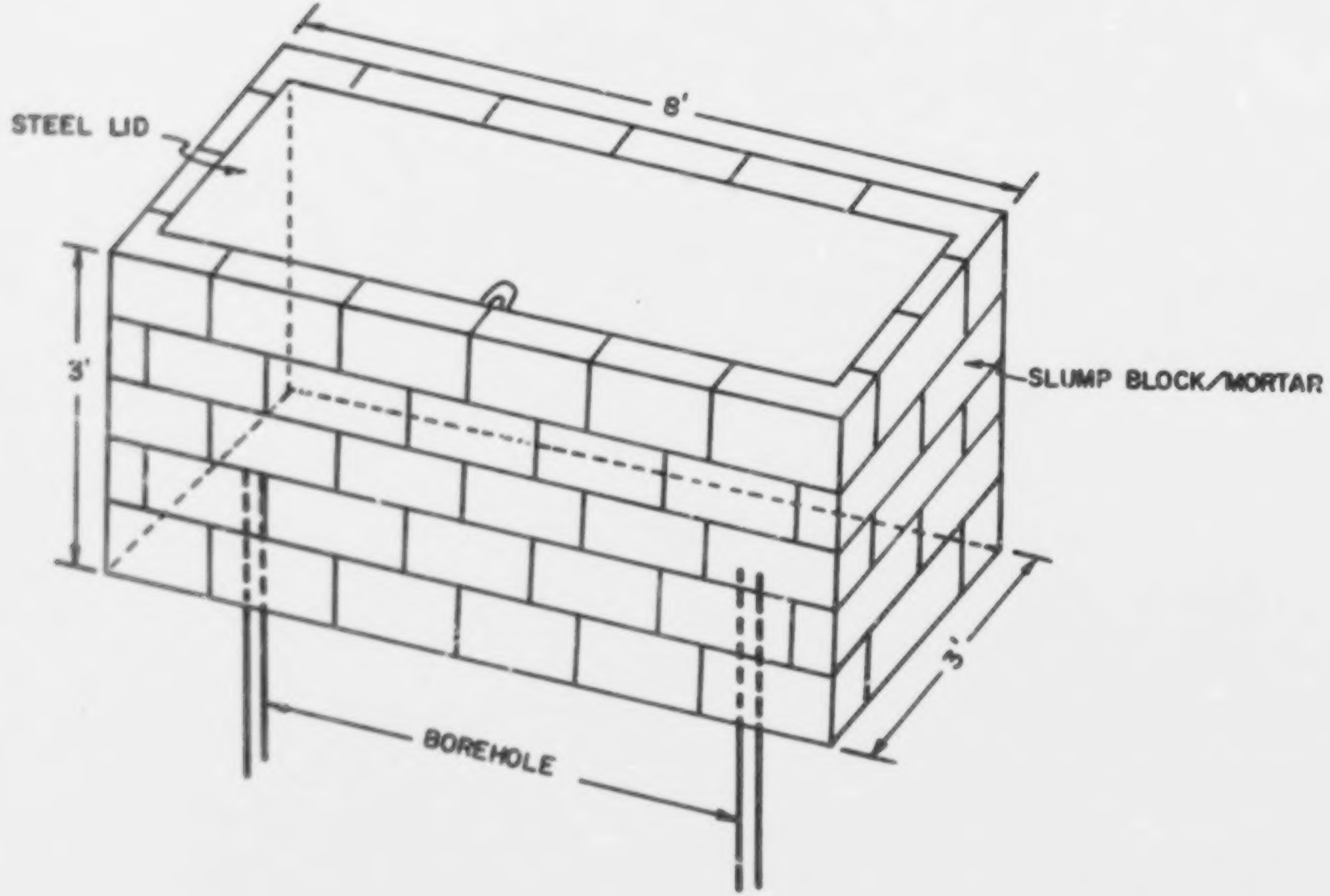
STEEL LID
8'
3'
SLUMP BLOCK/MORTAR
3'
BOREHOLE

Figure 2.8 Schematic of bunker positioned over boreholes CCR/C-1 and C-3.

doors, providing added security. These additional doors have not been used - the outer doors have proven to be more than adequate.

The doors were fastened to the bunker by laying 5 cm (2 inch) thick cap block over the 7.5 cm (3 inch) lip of the frame. The lip of the frame covers the inner 7.5 cm (3 inch) of the bunker wall, which allows the cap block to be laid flush with the outside wall. While the lid assembly is not secured by anything other than a mortar joint and a 5 cm (2 inch) thick cap block, its weight alone would prevent it from being moved easily off the top of the bunker.

2.9 Electrical Hook-up

Data gathering components require a power supply, either 12V DC or 115V AC. The selection was a function of cost, reliability and ease in use. It was decided that 115V AC from a nearby utility line would best satisfy the requirements. Heavily in its favor was that it would be useful for purposes such as powering electric mixers and drills.

Battery power was considered but ruled out for several reasons. The cost to equip all the data logging gear with battery power would be substantial. The equipment on hand was designed for a 115V AC power supply. Batteries would have to be checked and rotated with fresh ones. The reliability of the system would depend on the batteries, for which we would be responsible. By using the power at the site, the electric company would be responsible for power losses, which could be restored faster than we could replace a faulty battery.

Obtaining power from the nearby pole was not readily accepted due to the potential for power loss from a break in the line due to vandalism or from natural causes. Compared to the difficulties anticipated with battery power, it was felt that the advantages outweighed the disadvantages. The power is obtained from the utility line that serves Summerhaven. This line was run up Cargodera Canyon at the same time the boreholes were drilled. At our request, a breaker box and meter were installed on the pole nearest the drill site.

Power was supplied to the first bunker through 300 ft of Romex cable. A trench was dug 2-3 inch deep where possible and the line buried in it. The line was tucked under granite slabs as best as possible where it went over exposed rock. Where the line runs to the bunkers over the exposed granite, it is enclosed in 2.5 cm (1 inch) galvanized conduit. The second bunker, which houses the computer equipment, was powered by tapping into the line to the first bunker.

CHAPTER THREE

BOREHOLE CHARACTERIZATION TESTING

3.1 Introduction

Borehole characterization testing has as objectives determining the geologic and hydrogeologic characteristics of the boreholes selected for sealing experiments. The geologic characteristic most critical for the selection of suitable test intervals is the presence, extent and density of fracturing. Once suitable intervals in selected boreholes have been chosen, the in-situ hydraulic conductivities of the intervals are determined. The hydraulic conductivity of an unsealed interval and its conductivity when sealed provides a criterion for estimating the effectiveness of the seal. In addition, hydraulic testing can reveal fractures in the interval that otherwise go undetected.

The three 16.3 cm (6 1/2 inch) diameter diamond holes, CCR/C-1 through 3, drilled at the lower site at Cargodera Canyon, were field tested to determine suitable intervals for sealing. These three holes offer diameters large enough to require larger scale emplacement and testing methods than previously used in laboratory sealing studies at the University of Arizona. The three holes are close enough together to make containing them and the instrumentation necessary for testing easy. In addition, one 6.3 cm (2 1/2 inch) diameter diamond hole, CCR/D-4, was selected for long-term field testing.

Intervals of low hydraulic conductivity in the borehole need to be identified prior to placing borehole plugs. The optimum performance characteristics of a borehole plug can be assessed by placing and testing it in such a region. The objective of the borehole characterization testing was to determine zones in the borehole which would be suitable for plugging. The methods used in the selection of the appropriate interval(s) were core log studies, photo and video logging of the borehole and packer testing.

Core logs provided initial target intervals subsequently investigated by photo and video logging. The objective was to identify fracture-free intervals approximately 75 cm (30 inches) long. The intervals selected became the initial target zones for packer testing.

3.2 Borehole Preparation

A preliminary reconnaissance of the site, prior to testing, revealed that a number of the holes, including three of the four 16.315 cm (6.5 inch) holes, had been uncapped since drilling was completed. Some had been filled to within a foot or two (30 to 60 cm) from the surface. CCR/C-1 was filled to 60 cm (two feet) from the surface with what appeared to be large and small rocks. CCR/C-2 was clogged with rocks, twigs and debris 90 cm (three feet) from the surface. The filled holes evidence human intrusion at the site and underscore the necessity for containing and securing instrumentation and equipment.

Figure 3.1 is a schematic of the "cactus grabber" used to clean boreholes CCR/C-1 and 2. The device consists of a long pole with two hand cultivators attached to one end. Springs attached to the cultivators hold the jaws closed. The jaws are opened by pulling a cable that is attached to them and extends to the surface. The cleaner is operated by lowering the pole in the hole until the jaws are just above a rock or other obstruction. The jaws are opened, and the pole is rammed down on top of the obstruction. The jaws are then closed by releasing the cable and the pole is lifted out of the hole. Perhaps one out of every three tries is successful in removing rocks and other bits of debris. The mechanical grabber was successfully used to clear hole CCR/C-1. CCR/C-2 contained a large quantity of dirt and sand. An industrial vacuum cleaner with a long 7.5 cm (3 inch) diameter extension hose was used to complete cleaning of CCR/C-2. Both holes were washed down with water prior to photologging.

3.3 Photologging

3.3.1 Photologging Equipment

Boreholes CCR/C-1 and CCR/C-3 were investigated using a downhole camera assembly designed and constructed to meet the requirements of the site. Figure 3.2 is a schematic of the device. A 35 mm camera is mounted on a pole. The camera shield stabilizer, a 15 cm (6 inch) diameter section of PVC tubing, protects the camera and keeps it centered in the borehole. The trigger assembly allows the camera to be operated by a cable reaching to the surface. Light is provided by three small flashlights with adjustable beam focus mounted approximately 120 degrees apart inside the stabilizer. The focus target is circular, painted red and white for visibility, and marked with a prominent North symbol for compass orientation. The focus target is mounted on an extendable target mount consisting of two rods fixed to the camera stabilizer (Figure 3.3). The level centering platform with four adjustable legs provides a stable, secure and level guide for the camera mount as the camera is raised and lowered.

Two cameras were used for borehole photologging. A Canon AF 35 ML was selected for features including small size, rugged construction, auto/film advance, power rewind and built-in auto flash. These features facilitated downhole operations by simplifying the remote use of the camera and allowing an entire roll of film to be shot before the camera assembly had to be returned to the surface. Unfortunately, the focus on the Canon does not allow the precise adjustments required for borehole photography. Also, the 40 mm f/1.9 lens can not easily be exchanged and does not provide a field of view wide enough for boreholes of 16.3 cm (6 1/2 inch) diameter.

An Olympus OM-1 is used instead. Its advantages include a wide-angle lens and refined manual focusing features. However, this Olympus does

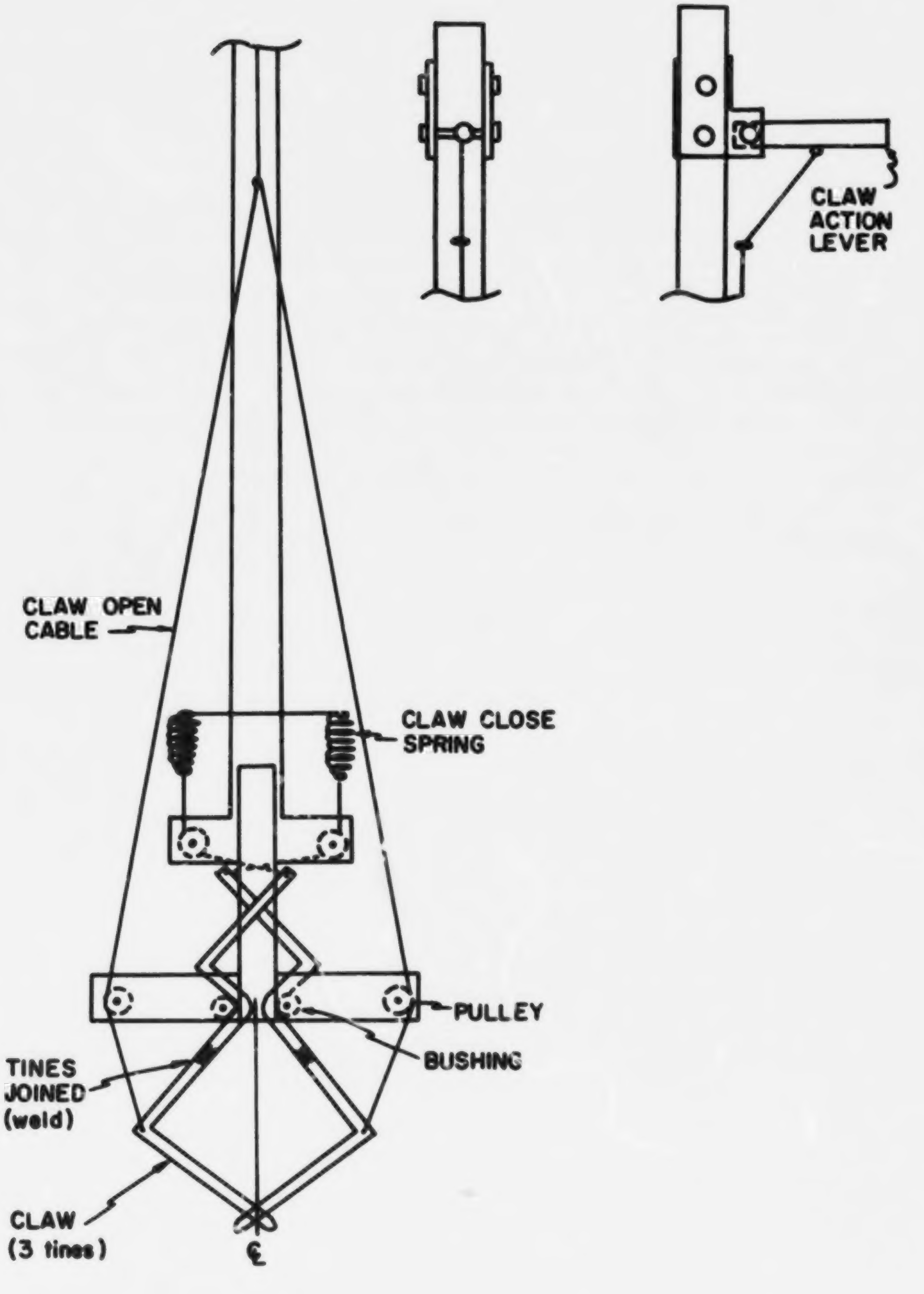
CLAW ACTION LEVER
CLAW OPEN CABLE
CLAW CLOSE SPRING
PULLEY
BUSHING
TINES JOINED (weld)
CLAW (3 tines)
℄

Figure 3.1 "Cactus grabber" borehole cleaner.

BEST COPY AVAILABLE

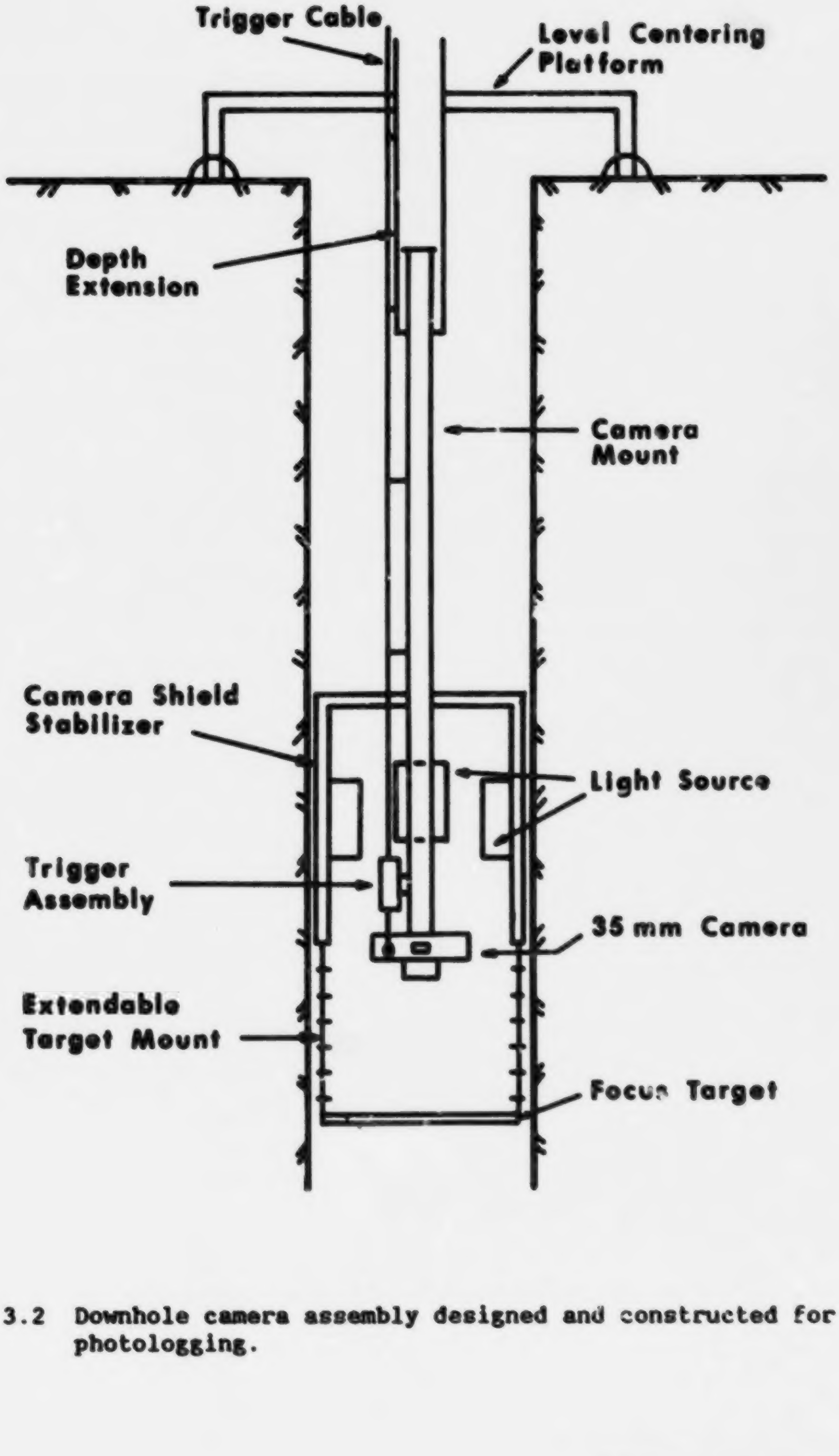
Trigger Cable
Level Centering Platform
Depth Extension
Camera Mount
Camera Shield Stabilizer
Light Source
Trigger Assembly
35 mm Camera
Extendable Target Mount
Focus Target

Figure 3.2 Downhole camera assembly designed and constructed for photologging.

BEST COPY AVAILABLE

Figure 3.3 Focus target being inserted into borehole.

BEST COPY AVAILABLE

not have an automatic film advance. The entire camera assembly has to be raised each time a picture is taken.

3.3.2 Photologging Procedures

Several rolls of film were shot downhole to determine the correct target distance, lens focus and shutter speed. The best results are achieved with a 400 film speed, a 54 cm (1.75 ft) focal distance, and the shutter speed set at .25 seconds. Aperture setting was not recorded. Several different films were used. 36 exposure, black and white Ilford XP1 400 was found to be the most suitable. The focus target is set at 21 inches from the camera lens.

The camera is lowered to the desired position within the borehole, determined by marks on the camera pole. A cable is pulled to trigger the shutter. The camera is brought to the surface and advanced to the next frame. Each borehole is photologged at intervals of 7.5 cm (3 inches). Results indicate that this interval provides the detail necessary for estimating fracture location, orientation, density and apertures (Figure 3.4).

3.3.3 Photologging Results

CCR/C-3 and CCR/C-1 were photologged at least twice. Several intervals considered for sealing were photologged separately. Study of the photolog for CCR/C-3 indicates that a major fracture which had been mapped as dipping from approximately 1.72 m (4 ft 9 in) to 1.87 m (5 ft 2 in) from the surface actually begins at 1.89 m (5 ft 3 in) and dips to 2.01 m (5 ft 7 in). The fracture is actually composed of 2 fractures dipping in the same direction. The photolog also shows what seem to be several smaller fractures nearer to the surface, though their horizontal orientation makes them difficult to distinguish from drilling break marks (Figure 3.5).

The photologging procedures for CCR/C-1 were changed to provide a better record of the full 360 degree borehole wall. After the first picture at any depth, the camera is rotated 90 degrees so that the North symbol points due west. A second picture is then taken at the same depth. Study of the CCR/C-1 photolog shows that at approximately 2.1 m (7 ft) from the surface the borehole wall is damaged or altered by microfracturing or weathering (Figure 3.6). The photolog shows that the borehole interval from near the surface to a depth of 2 m (6 ft 7 in) is relatively fracture-free and suitable for seal testing.

Photologs and preliminary core log fracture maps were studied to determine intervals suitable for sealing in CCR/C-1, CCR/C-2 and CCR/C-3. In CCR/C-1, the interval from 105 cm (3 ft 6 in) to 196 cm (6 ft 6 in) from the surface was selected for testing and sealing (Figure 3.7). In CCR/C-2, the interval from 3 to 3.7 m was selected (Figure 3.8), and in CCR/C-3, the interval from 79 cm (31.5 in) to 147 cm (58.5 in) (Figure 3.9).

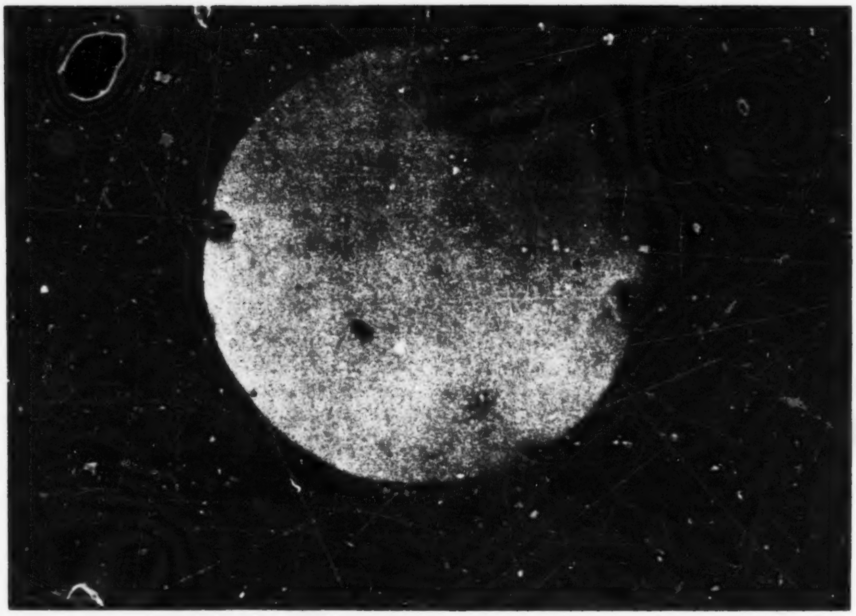

Figure 3.4 Example of downhole photograph.

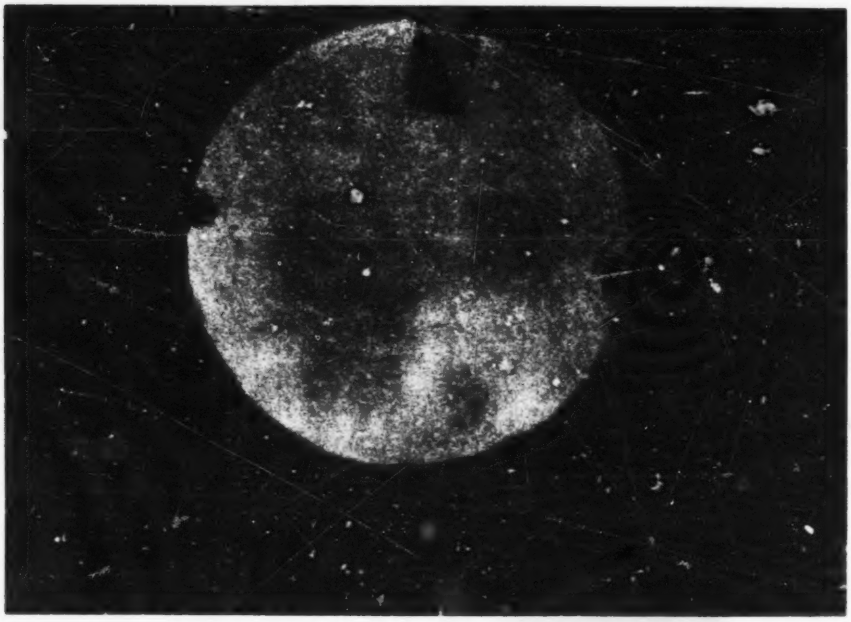

Figure 3.5 Downhole photograph with horizontal features, possibly drilling marks or break, or fracture(s).

BEST COPY AVAILABLE

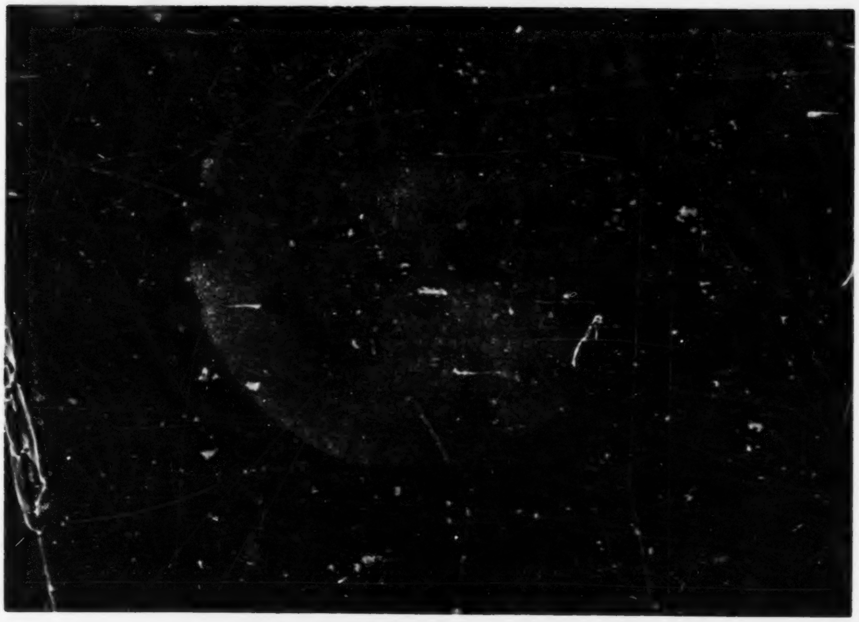

Figure 3.6 Borehole photograph in relatively damaged rock.

BEST COPY AVAILABLE

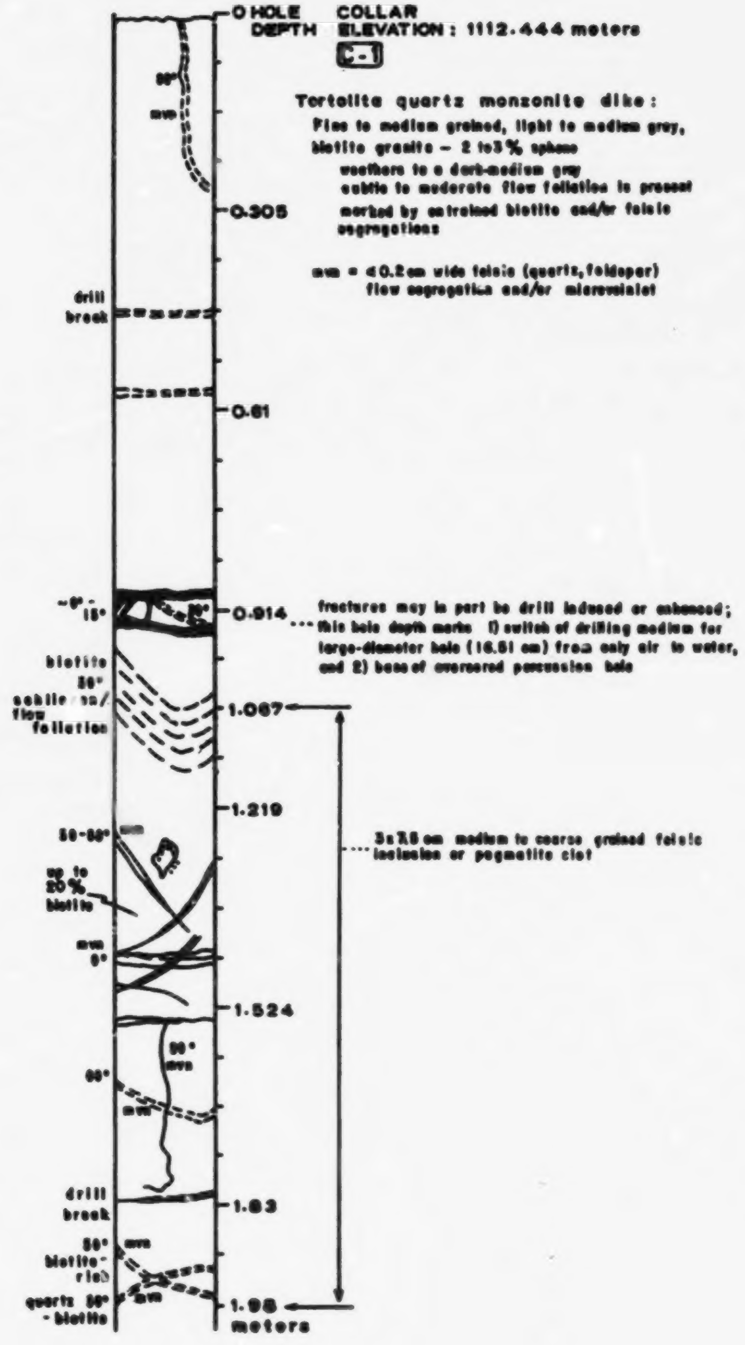

0 HOLE DEPTH
COLLAR ELEVATION : 1112.444 meters
C-1
Tortolite quartz monzonite dike:
Fine to medium grained, light to medium grey, biotite granite – 2 to 3 % sphene
weathers to a dark-medium grey
subtle to moderate flow foliation is present
marked by entrained biotite and/or felsic segregations
mvn = ≤0.2cm wide felsic (quartz, feldspar) flow segregation and/or microveinlet
80°
mvn
0.305
drill break
0.61
~0° - 15°
30°
0.914
fractures may in part be drill induced or enhanced; this hole depth marks 1) switch of drilling medium for large-diameter hole (16.51 cm) from only air to water, and 2) base of overcored percussion hole
biotite 30° schlieren/ flow foliation
1.067
1.219
50-60°
3x7.5 cm medium to coarse grained felsic inclusion or pegmatite clot
up to 20% biotite
mvn 0°
1.524
80° mvn
60°
mvn
drill break
1.83
30° mvn
biotite-rich
quartz 30° - biotite
mvn
1.98 meters

Figure 3.7 Borehole CCR/C-1 core log. Hole depth is given in m.

BEST COPY AVAILABLE

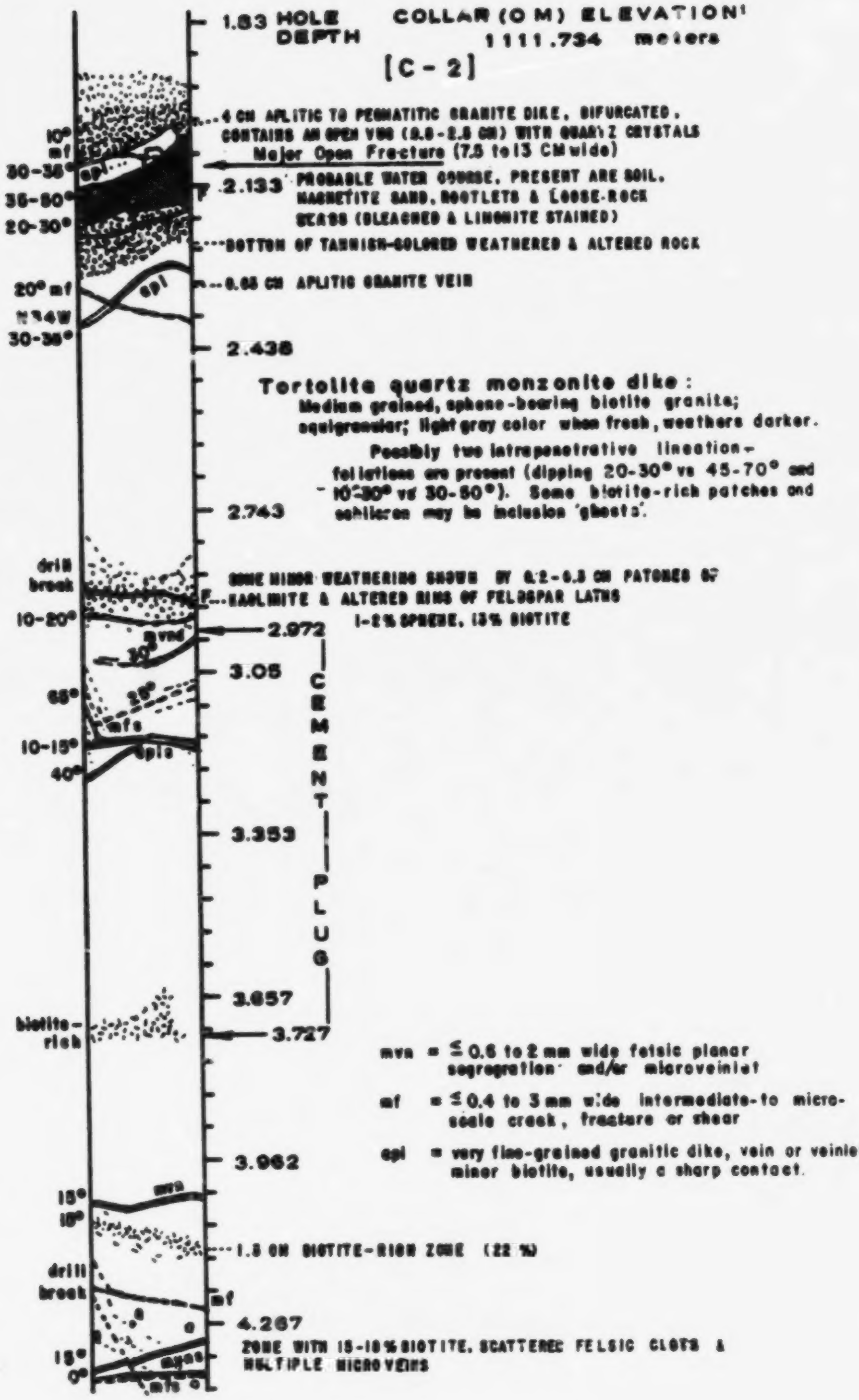
1.83 HOLE DEPTH
COLLAR (O M) ELEVATION
1111.734 meters
[C - 2]
4 CM APLITIC TO PEGMATITIC GRANITE DIKE, BIFURCATED, CONTAINS AN OPEN VUG (0.8-2.5 CM) WITH QUARTZ CRYSTALS
Major Open Fracture (7.5 to 13 CM wide)
2.133
PROBABLE WATER COURSE. PRESENT ARE SOIL, MAGNETITE SAND, ROOTLETS & LOOSE-ROCK SCABS (BLEACHED & LIMONITE STAINED)
BOTTOM OF TANNISH-COLORED WEATHERED & ALTERED ROCK
0.05 CM APLITIC GRANITE VEIN
10°
mf
30-35°
apl
35-50°
20-30°
20° mf
N34W
30-35°
apl
2.438
Tortolite quartz monzonite dike:
Medium grained, sphene-bearing biotite granite; equigranular; light gray color when fresh, weathers darker.
Possibly two interpenetrative lineation-foliations are present (dipping 20-30° vs 45-70° and 10-30° vs 30-50°). Some biotite-rich patches and schlieren may be inclusion 'ghosts'.
2.743
drill break
SOME MINOR WEATHERING SHOWN BY 0.2-0.3 CM PATCHES OF KAOLINITE & ALTERED RIMS OF FELDSPAR LATHS
F
1-2% SPHENE, 13% BIOTITE
10-20°
mvd
30°
2.972
3.05
65°
25°
mfs
10-15°
apls
40°
CEMENT PLUG
3.353
3.657
biotite-rich
3.727
mva = ≤ 0.6 to 2 mm wide felsic planar segregation and/or microveinlet
mf = ≤ 0.4 to 3 mm wide intermediate-to micro-scale crack, fracture or shear
apl = very fine-grained granitic dike, vein or veinlet, minor biotite, usually a sharp contact.
3.962
15°
mva
10°
1.3 CM BIOTITE-RICH ZONE (22 %)
drill break
mf
4.267
ZONE WITH 15-18% BIOTITE, SCATTERED FELSIC CLOTS & MULTIPLE MICROVEINS
15°
mvas
0°
mfs

Figure 3.8 Borehole CCR/C-2 core log. Hole depth is given in m.

BEST COPY AVAILABLE

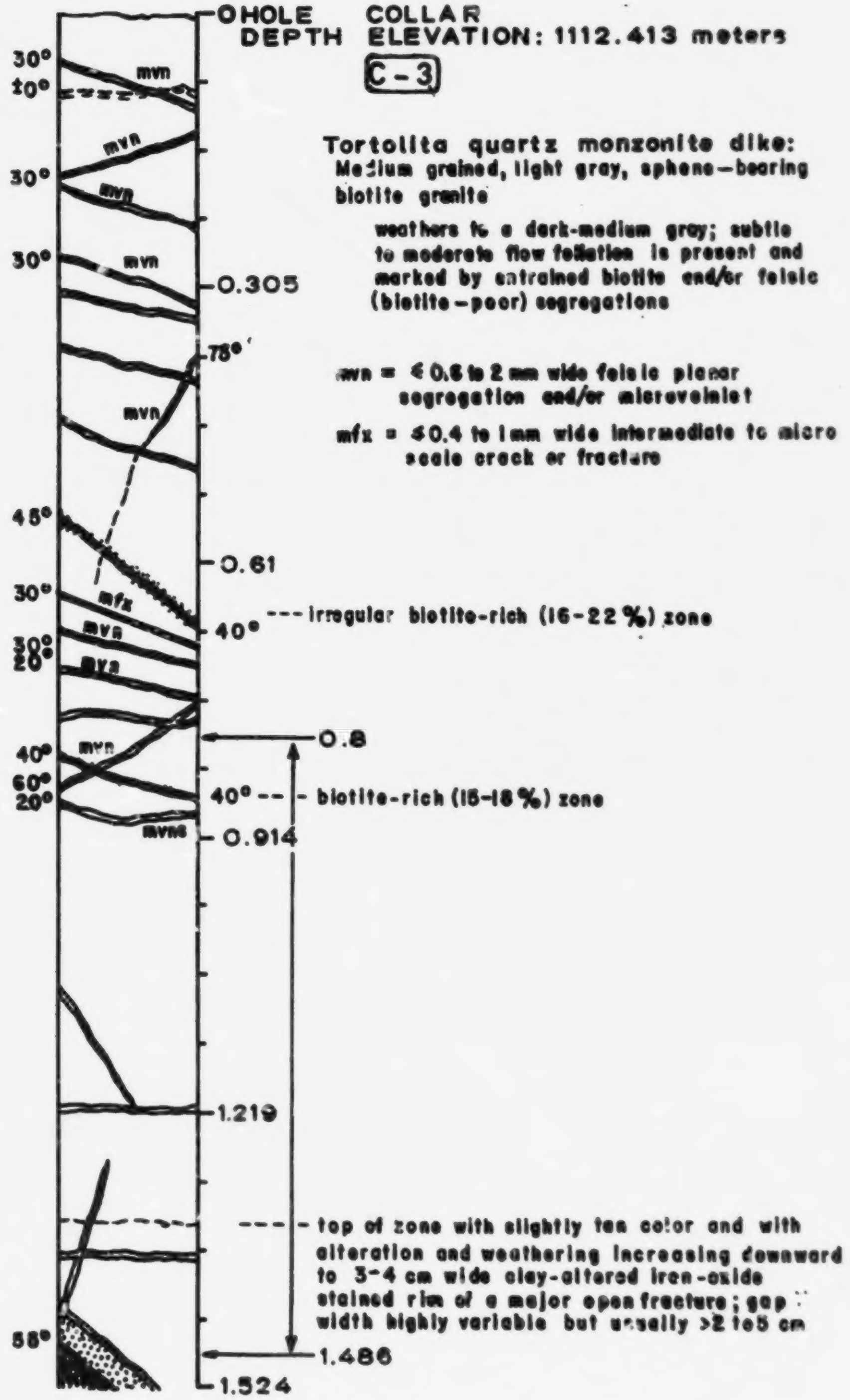

0 HOLE DEPTH
COLLAR ELEVATION: 1112.413 meters
C-3
Tortolita quartz monzonite dike:
Medium grained, light gray, sphene-bearing biotite granite
weathers to a dark-medium gray; subtle to moderate flow foliation is present and marked by entrained biotite and/or felsic (biotite-poor) segregations
mvn = ≤ 0.5 to 2 mm wide felsic planar segregation and/or microveinlet
mfx = ≤ 0.4 to 1 mm wide intermediate to micro scale crack or fracture
30°
10°
mvn
mvn
30°
mvn
30°
mvn
0.305
75°
mvn
45°
0.61
30°
mfx
40°
irregular biotite-rich (16-22 %) zone
30°
20°
mvn
mvn
0.8
40°
60°
20°
mvn
40°
biotite-rich (15-18 %) zone
mvns
0.914
1.219
top of zone with slightly tan color and with alteration and weathering increasing downward to 3-4 cm wide clay-altered iron-oxide stained rim of a major open fracture; gap width highly variable but usually >2 to 5 cm
58°
1.486
1.524

Figure 3.9 Borehole CCR/C-3 core log. Depth below collar is indicated in m.

BEST COPY AVAILABLE

3.3.4 Videologging

The photologging in borehole CCR/C-3 indicated that the objective of identifying fractures missed during core logging would be difficult to meet with the camera logging device. The photos obtained showed only the large fractures, already identified on the core logs. Resolution of the system was not detailed enough to detect smaller fractures.

An interval suitable for testing and sealing in CCR/C-2 was determined in July, 1985, using a videolog of the borehole. Well Scan Video Surveys, Inc., of Phoenix, Arizona, performed the video logging of CCR/C-2 and CCR/C-4 with the assistance of members of the University of Arizona research team.

Well Scan has a van that offers a completely contained borehole logging service with both downhole and sidescan video cameras. Inspection of the van indicated that it would not have the clearance to drive to the site. A portable unit was improvised and the necessary equipment transported to the site with University of Arizona four-wheel drive vehicles.

Figure 3.10 is a schematic of the downhole video assembly. The camera is a Panasonic 800-line resolution, low light level, black-and-white video camera with a 4.8 mm "fish eye" lens. The light source is a 40 watt bulb. Tape is recorded by an industrial grade Panasonic VHS recorder. The film is viewed on a Panasonic 700-line resolution monochrome monitor with an improvised hood to shade the screen from reflected sunlight.

The view from the camera was immediately displayed on the monitor. Portions of the borehole that looked interesting could be studied in more detail by raising the camera above the zone and then lowering it slowly until the desired view was obtained. Distance down the borehole was determined by hanging a tape measure from the top, the tape being read on the display monitor.

The videologs of CCR/C-2 and CCR/C-4 provide an excellent record of the condition of both boreholes. Fracture resolution seems to include all fractures with apertures greater than 1 or 2 mm. The tape speed is slow enough to allow logging significant features. Each hole was videologged from the surface to the depth allowed by the assembly and then back up to the surface.

The videolog for CCR/C-2 shows that a fracture previously logged at approximately 2.1 m (7 ft) from the surface actually dips from 200 cm (6 ft 8 in) to 223 cm (7 ft 5 in). Above and below it a damaged and weathered zone extends for more than 18 cm (7 inches). The video also reveals that the fracture is a source of moisture in the borehole, with visible seeping from all parts of the fracture and damaged zones.

A comparison of procedures and results for the two forms of photologging used at Cargodera Canyon suggests that the videologging is superior in a number of ways. Videologging is much faster. CCR/C-2 and CCR/C-4 were videologged in one 6-to-8 hour day. Photographic

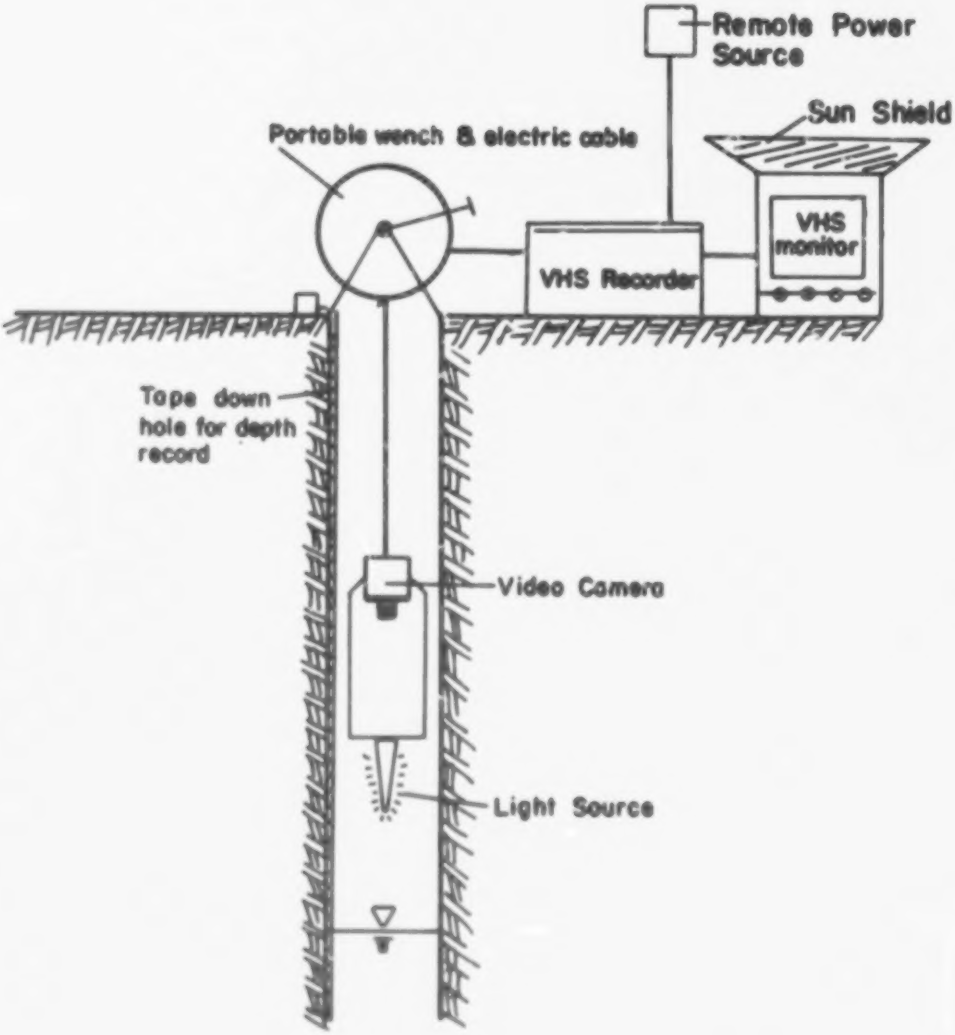

Remote Power Source
Sun Shield
Portable wench & electric cable
VHS monitor
VHS Recorder
Tape down hole for depth record
Video Camera
Light Source

Figure 3.10 Schematic of borehole videologging equipment.

BEST COPY AVAILABLE

logging of CCR/C-3 and CCR/C-2 required at least three full days each. The video record provides a better fracture resolution than the photolog and it is very easy to relog highly fractured or damaged zones since the borehole is being viewed on the monitor as the camera is lowered. On the other hand, the photolog equipment is easily assembled, less vulnerable to damage from off-road travel and extreme temperatures, and the final record of individual photographs is easier to correlate with the equivalent core logs.

3.4 Borehole Hydraulic Conductivity Testing: A Literature Review

3.4.1 Introduction

The field study of rock permeability has been the focus of a number of investigations over the past decade (Bouwer and Rice, 1976; Bredehoeft and Papadopulos, 1980; Earlougher, 1977; Zeigler, 1976; Hsieh, 1983). This section reviews and compares the most commonly used methods. Criteria used for comparison include the theoretical foundations of the method, how appropriate the method is for different types of rock mass study, and the cost and time involved in the implementation of the method. The theory and practice of this type of site evaluation is still in the research and development stage. No hard and fast rules are available. Every field experience is unique in the problems encountered and in the validity of analysis and results.

3.4.2 Approaches to the Problem

From a hydrologic point of view, fractured rock masses can be regarded as consisting of two components: the intact rock and the system of interconnected fractures, the primary conduit of fluid flow in saturated rock.

Two approaches are used to describe fluid flow through rock masses. The discrete approach treats fluid flow in individual fractures. The fracture is represented as a conduit formed by two parallel plates. Flow is assumed to be steady, viscous and laminar. With these assumptions, the flow can be described by the "cubic law", which states that, for a given hydraulic gradient, the discharge through a fracture is proportional to the cube of the fracture hydraulic aperture. The discrete approach requires that the geometry of the fracture be known. Flow through a fracture network is modeled as flow through sets of individual fractures.

The continuum approach uses a fictitious continuum to represent a network of fractures. At each point in the flow region two values can be assigned for pressure, porosity, specific discharge, hydraulic conductivity and specific storage. One value represents the fracture continuum. The other value represents the continuum that models the blocks between fractures. If the blocks are impermeable, the system can be represented solely by the fracture continuum. The mathematical treatment of such a system is identical to that of porous media flow.

Which of the two approaches is most appropriate for a given investigation is a function of the size of the flow region, the scale of observation and the fracture density (Figure 3.11). Local flow regions containing few fractures may require a discrete approach. When fracture density is high enough, the continuum approach may prove more useful. Unfortunately, real investigations often involve regions where fracture density is too high for the discrete approach, but where observation is not adequate or detailed enough to make the continuum approach meaningful.

3.4.3 Field Test Objectives

Two methods used for determining hydraulic conductivity of fractured rock in the field are single-hole tests and cross-hole tests. Packers isolate intervals in boreholes for testing. Single-hole tests are performed on packed-off intervals in a single borehole. Cross-hole tests require packed-off intervals in several holes. Fluid is injected through one borehole interval. Hydraulic head, temperature and tracer are monitored in the packed-off intervals of the other holes.

3.4.4 Single-Hole Packer Tests

Single-hole packer tests can be conducted in several ways. For steady state injection tests water is injected under constant hydraulic head into a packed-off interval. Hydraulic head and flow rate in the interval are monitored. Slug tests involve the instantaneous increase or decrease of hydraulic head in a packed-off interval. Subsequent head decay or recovery is monitored.

These single-hole packer tests are interpreted assuming the rock is homogenoous, isotropic, and a porous medium. Flow is assumed to be governed by (e.g. Freeze and Cherry, 1979, p. 65; Todd, 1980, p. 100):

$$\nabla^2 h = \frac{S_s}{K} \frac{\partial h}{\partial t} \tag{3.1}$$

where K is the scalar hydraulic conductivity, S_s is specific storage, h is hydraulic head, and t is time. Various solutions to the given equation are available. Which one is used depends on the assumed flow pattern in the rock. If steady state analysis is used, hydraulic conductivity only is obtained. Transient analysis allows determination of hydraulic conductivity and of specific storage.

Single-hole packer tests are simple to perform. Once the equipment has been set up, the tests can be conducted rapidly. This is an important advantage when a large number of measurements are required. There are disadvantages to the method. The volume of rock tested is small and limited to the immediate vicinity of the tested interval. Results cannot be interpreted as characteristic of the rock mass as a whole. Single-hole tests cannot be used to investigate anisotropic hydraulic conductivity.

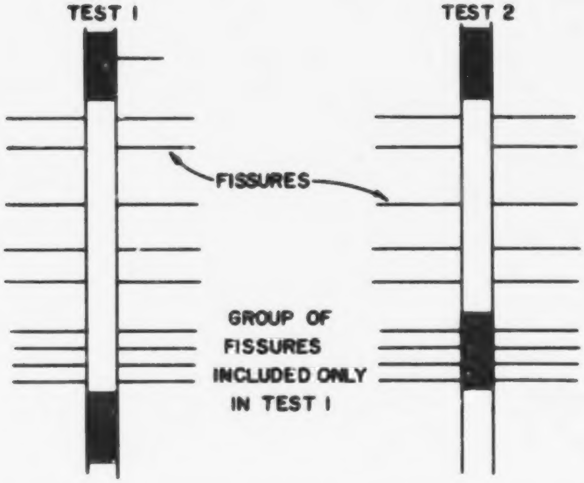
TEST 1
TEST 2
FISSURES
GROUP OF FISSURES INCLUDED ONLY IN TEST 1

a. FISSURES INCLUDED OR EXCLUDED FROM THE TEST SECTION

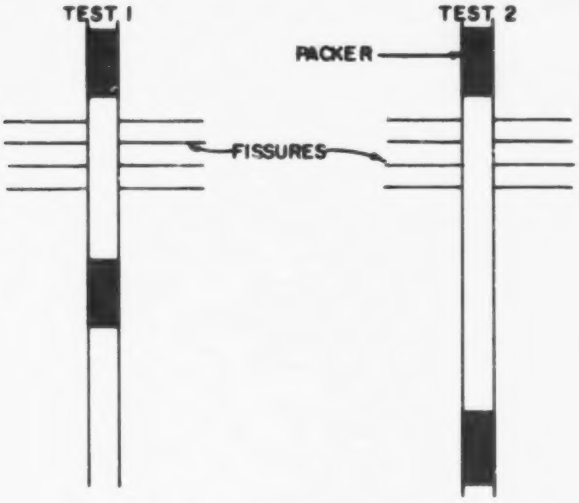
TEST 1
TEST 2
PACKER
FISSURES

b. CHANGE IN TEST SECTION LENGTH WHILE FISSURES INTERSECTED REMAIN UNCHANGED

Figure 3.11 Illustration of the effect of test section length on borehole hydraulic conductivity measurements. (From Zeigler, 1976, p. 56)

BEST COPY AVAILABLE

3.4.5 Injection Tests

Injection tests can be used in both saturated and unsaturated rock. The traditional analysis assumes steady state flow. Steady-state analysis requires that injection into the packed-off interval continue until the flow rate has stabilized. The formulae used to calculate conductivity differ in the flow patterns assumed for their derivations. The most commonly used flow patterns are radial and prolate spheroidal or ellipsoidal (Figure 3.12).

Radial flow assumes all flow is perpendicular to, and radially symmetric about, the borehole axis. It also assumes all flow is confined to a region bounded by impermeable boundaries extending from the upper and lower ends of the test interval. Steady radial flow is described by (e.g. Todd, 1980, p. 100):

$$\frac{\partial}{\partial r}\left(r\frac{\partial h}{\partial r}\right) = 0 \qquad (3.2)$$

where r is the radial distance from the wellbore axis. Boundary conditions include:

$$h = h_w \quad \text{at} \quad r = r_w$$

$$r\frac{\partial h}{\partial r} = \frac{Q}{2\pi KL} \quad \text{at} \quad r = r_w$$

where h_w is the hydraulic head at the wellbore, r_w is the radius of the borehole, Q is the volumetric injection rate, and L is the length of the injection interval. The solution for hydraulic conductivity is (e.g. Hsieh, 1983, p. 13; Zeigler, 1976, p. 41):

$$K = \frac{Q}{2\pi L\Delta h_w}\ln\frac{r_e}{r_w} \qquad (3.3)$$

where r_e is an assumed radius of influence, beyond which no head increase is measured ($h = h_o$, ambient head), and $\Delta h_w = h_w - h_o$.

Prolate ellipsoidal flow assumes all flow to emerge uniformly from a line source at the vertical axis of the borehole. The equipotential surfaces that result are confocal prolate ellipsoids whose foci are the endpoints of the line source. Following Hsieh (1983, p. 13), the solution developed by Hvorslev (1951) is:

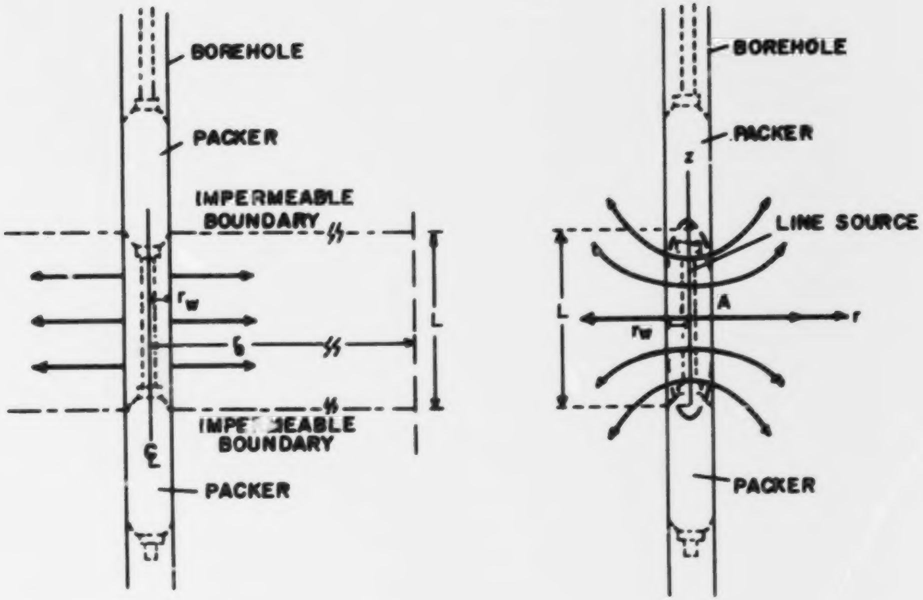
BOREHOLE
PACKER
IMPERMEABLE BOUNDARY
r_w
r_b
L
IMPERMEABLE BOUNDARY
℄
PACKER
BOREHOLE
PACKER
z
LINE SOURCE
A
r
r_w
L
PACKER

(a) radial flow

(b) prolate - ellipsoidal flow

Figure 3.12 Assumed flow patterns in analysis of single-hole packer tests. (From Hsieh, 1983, p. 12)

BEST COPY AVAILABLE

$$\Delta h_w = \frac{Q}{4\pi KL}\left[\sinh^{-1}\left(\frac{L/2 + z}{r}\right) + \sinh^{-1}\left(\frac{L/2 - z}{r}\right)\right] \tag{3.4}$$

where

$$\Delta h = h_w - h_0$$

and r and z are cylindrical coordinates. If r is taken as r_w and z is set equal to zero, i.e. the injection head is referenced at the origin or center of the injection interval (Fig. 3.12.b), then

$$K = \frac{Q}{2\pi L\Delta h_w} \ln\left[\frac{L}{2r_w} + \sqrt{1 + \left(\frac{L}{2r_w}\right)^2}\right] \tag{3.5}$$

This solution does not require assuming a radius of influence.

Transient flow analysis is not used frequently because accurate volumetric measurements are difficult to make during the transient portion of the test. The analysis also is more difficult than steady-state analysis and the results are often ambiguous. Transient analysis assumes radial flow. Its theory is identical to that of constant drawdown aquifer tests given by Jacob and Lohman (1952). Flow is described by (e.g. Todd, 1980, p. 100):

$$\frac{1}{r}\frac{\partial}{\partial r}\left(r\frac{\partial h}{\partial r}\right) = \frac{S_s}{K}\frac{\partial h}{\partial t} \tag{3.6}$$

With the initial condition

$$h = h_0 \quad \text{at} \quad t = 0$$

and boundary conditions

$$h = h_w \quad \text{at} \quad r = r_w$$
$$h = h_0 \quad \text{as} \quad r \to \infty$$

the solution is (Jacob and Lohman, 1952; Hsieh, 1983, p. 18):

$$Q(t) = 2\pi KL\Delta h_w W(t_D) \tag{3.7}$$

where t_D is dimensionless time and $W(t_D)$ is a well function whose values have been tabulated and developed into type curves. When these type curves are used, K can be estimated. The similar shapes of the curves make curve matching difficult over a wide range of values. The value of specific storage that results from this analysis is unreliable (Freeze and Cherry, 1979, p. 342; Hsieh, 1983, p. 16). Steady-state testing appears preferable because of its simplicity and because of the reliability of its conductivity results.

3.4.6 Slug Tests

The slug test can be performed quickly and requires less equipment than injection tests. Two types of slug tests are commonly used (Hsieh, 1983, pp. 18-23). In the conventional, or gravity, method, the test interval is in contact with a standing column of fluid open to the atmosphere. Hydraulic head in the interval is subjected to a step change by instantaneously raising or lowering the fluid level in the column. The pressure slug method uses an isolated test interval. The hydraulic head in the interval is instantaneously increased by injecting fluid into the interval or by plunging a displacement piston into the interval (Figure 3.13).

The fundamental difference between the two test methods is the rate of head recovery after the step change is induced in the test interval. The conventional method has a slow recovery rate because the test fluid must flow into or out of the test interval before a head change will be registered. The pressure slug method has a quick head recovery because the response in the interval is governed by the compressibility effects.

Both test methods assume radial flow out of the test interval. Methods for analyzing the test results differ significantly in their assumptions and in the testing factors they include.

The method developed by Hvorslev (1951) assumes the empirical relationship (e.g. Freeze and Cherry, 1979, p. 340):

$$Q_{sf} = -KF\Delta S \tag{3.8}$$

describing Darcian flow. It allows for different vertical and horizontal conductivities if vertical and horizontal are the principal flow directions. F is a shape factor. ΔS is the difference between pressure changes in the wellbore and pressure in the surrounding medium. For the gravity slug test, Hvorslev's solution can be written as:

$$K_h = \frac{C_h \ln \left[m \frac{L}{D} + \sqrt{1 + \left(m \frac{L}{D}\right)^2}\right]}{2\pi t_b L} \tag{3.9}$$

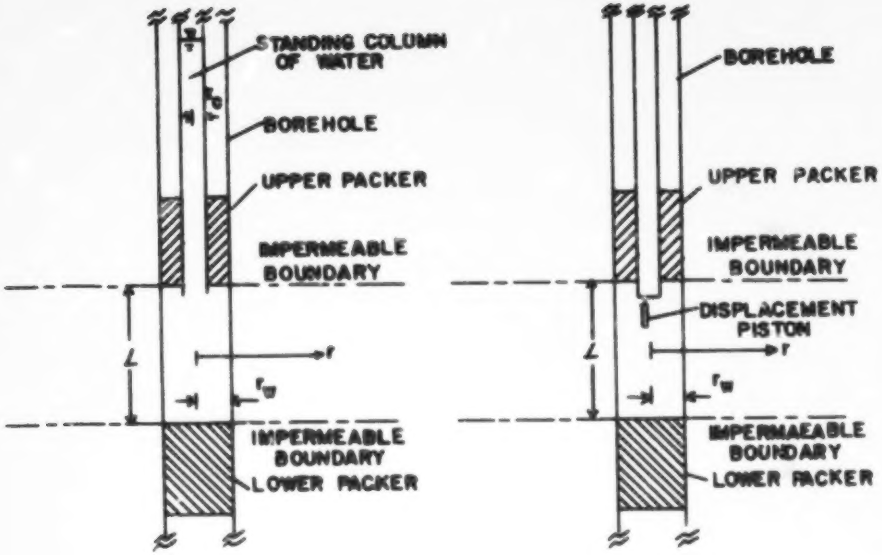
STANDING COLUMN OF WATER
r_c
BOREHOLE
UPPER PACKER
IMPERMEABLE BOUNDARY
L
r
r_w
IMPERMEABLE BOUNDARY
LOWER PACKER
BOREHOLE
UPPER PACKER
IMPERMEABLE BOUNDARY
DISPLACEMENT PISTON
L
r
r_w
IMPERMAEABLE BOUNDARY
LOWER PACKER

Figure 3.13 Schematic diagram showing two methods of conducting slug tests. (From Hsieh, 1983, p. 19)

BEST COPY AVAILABLE

where K_h is the horizontal permeability, m is the square root of the ratio of horizontal to vertical permeability, L/D is the ratio of test interval length to diameter, C_h is a wellbore storage term and t_B is the basic time lag or time it takes for induced pressure changes to be recovered in observation. Hvorslev's solution for the pressure slug test is the same except that the C_w term now expresses the compressibility of water as well as the volume of the test zone.

Skibitzke (1963) and Ferris and Knowles (1963) developed solutions for both types of tests based on the expression (e.g. Ferris and Knowles, 1962; Ferris et al., 1962):

$$s = \frac{V}{4\pi Tt(e^{-r^2 S/4Tt})} \qquad (3.10)$$

where s is residual head (or drawdown in a "bailer" test), V is water volume in the slug, T is transmissivity, S is storativity, t is time since slug was introduced into borehole interval, and r is the radius from the borehole center. For large values of time and small values of r, the exponential goes to unity, and:

$$s = \frac{V}{4\pi Tt} \qquad (3.11)$$

The slope of an arithmetical plot of s against 1/t can be used to calculate T. For the pressure slug test, a compressibility factor is included in the solution.

The most recent analytical approach is that of Bredehoeft and Papadopulos (1980). Their solution is developed into the relationship (e.g. Hsieh, 1983, p. 21):

$$\frac{\Delta H_w}{\Delta H_o} = F(\alpha,\beta) \qquad (3.12)$$

where ΔH_o is the instantaneous head increase, ΔH_w is the time-dependent head change in the test interval, and parameters α and β are defined by:

$$\alpha = \frac{\pi r_w^2 L S_s}{S_w} \qquad (3.13) \qquad\qquad \beta = \frac{\pi KLt}{S_w} \qquad (3.14)$$

The factor S_w takes into account that neither the isolation equipment nor water are perfectly rigid. Type curves are provided for $F(\alpha,\beta)$ against β. A semi-log plot of change in head over time can be matched to calculate hydraulic conductivity as well as specific storage. The parameters computed for these type curves cover a wide range of conditions and results compare favorably with other methods.

Cooper et al. (1967) developed a similar solution for the gravity, or open hole, test method. This solution also includes the compressibility of water.

The Hvorslev method is simple and provides results close to those developed by other methods. The mathematical assumptions it is based on do not have a strong theoretical foundation and no terms account for compressibility effects of water, equipment, or rock. The method only provides hydraulic conductivity. The Skibitzke/Ferris and Knowles method is also simple. Its theoretical basis is sound. It accounts for the compressibility of water. It is only useful for long-term tests and it can only provide hydraulic conductivity. The Bredehoeft and Papadopulos solution is the most rigorous. It accounts for the radius of the borehole, the compressibility of water, and the compliance of the testing equipment. It also allows the calculation of specific storage.

3.4.7 Cross-Hole Packer Tests

The cross-hole packer test is still in the research stage. The object of the test is to measure, on field scale, the hydraulic conductivity tensor and the specific storage of fractured rock. Fluid is injected into a packed-off interval in one borehole. The resultant hydraulic head variations are monitored in the packed-off intervals of adjacent boreholes In this way, it should be possible to investigate the degree to which a given fractured rock mass behaves as a homogeneous, anisotropic, porous medium (Figure 3.14).

Cross-hole test procedures are an extension of single hole testing. The success of the test depends, to a large extent, on how carefully the test intervals are selected. Current test procedures assume the existence of only two fracture types; high conductivity fractures and low conductivity fractures. Overall hydraulic conductivity is assumed to be dominated by the high conductivity fracture network. The low conductivity fracture network is assumed to contribute little to overall flow. For this reason, the test intervals should be selected to intersect high conductivity fractures. This is especially true of the monitoring intervals. The injection intervals can be chosen with less rigor as it is assumed that fluid injected into low conductivity fractures will find its way into the high conductivity network. However, the high injection pressures this procedure might require could interfere with head monitoring in adjacent holes.

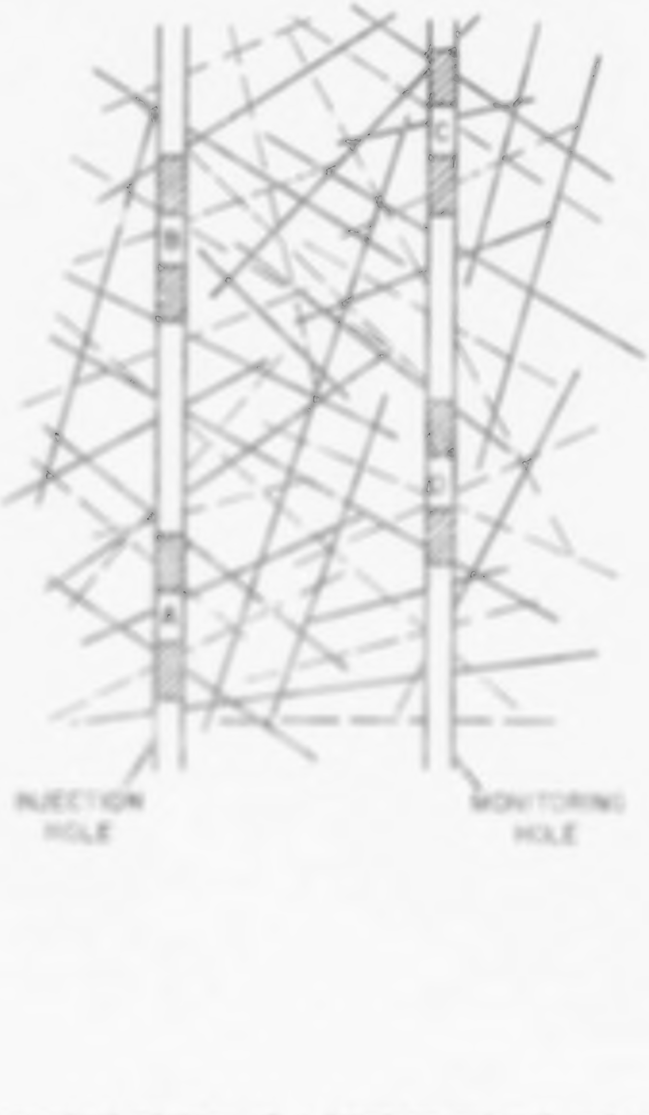
B
A
C
D
INJECTION HOLE
MONITORING HOLE

Figure 3.14 Conceptual picture of a fracture network and cross-hole injection and monitoring intervals. (From Hsieh, 1983, p. 76)

BEST COPY AVAILABLE

3.5 Borehole Hydraulic Conductivity Field Tests

3.5.1 Introduction

Field testing with the goal of determining the in-situ hydraulic conductivity of borehole intervals selected for sealing is described. Two types of tests are used. The pressure slug test, using the procedures and analysis developed by Bredehoeft and Papadopulos (1980), provides an estimate of the hydraulic conductivity in the selected intervals under the flow conditions that exist prior to sealing. Long-term changes in conditions brought about by the injection flows and pressures used to test seals are monitored by a long-term constant injection test in a borehole left unsealed. These changes may be significant over long-term periods as the degree of saturation in the host rock increases. It can be expected that, as the saturation in the host rock increases, the apparent hydraulic conductivity of the rock will increase (Evans, 1983).

Long-term moisture content changes in the host rock as sealing tests continue are also monitored by neutron probe measurements made at regular intervals in boreholes around the seal test holes.

3.5.2 Pressure Slug Test Theory

Pressure slug testing was initiated in early 1985. The pressure slug method is used because of the relative simplicity of its procedures, the short period of time available for testing, and the rigor of solutions available for the test. A review of available analysis methods suggests the solutions developed by Cooper et al. (1967), Papadopulos et al. (1973), and Bredehoeft and Papadopulos (1980) are the most appropriate ones for the conditions and low hydraulic conductivities expected at the Cargodera Canyon study area (see Section 3.4).

The pressure slug test used at Cargodera Canyon is a modification of the conventional slug test. In the conventional slug test, an instantaneous change is induced in the water level of an open standpipe in the well to be tested. The water level decay in the standpipe is monitored (e.g. Freeze and Cherry, 1979, p. 339; Zeigler, 1976). The pressure slug test involves introducing an instantaneous increase in pressure into a filled and shut-in test interval and monitoring the decay of the induced additional head. The analysis assumes that all flow out of the tested interval is radial (Bredehoeft and Papadopulos, 1980).

The differential equation that describes non-steady, radial groundwater flow in a confined formation is

$$\frac{\partial^2 h}{\partial r^2} + \frac{1}{r}\frac{\partial h}{\partial r} = \frac{S}{T}\frac{\partial h}{\partial t} \qquad (3.15)$$

where r is the radial distance from the center of the borehole; S is the storage coefficient of the tested interval; T is the transmissivity of the tested interval; h is the head change in the tested interval due to the induced pressure change; and t is time (Cooper et al., 1967).

When the test starts, the head change due to pressurization of the test interval is zero everywhere in the formation being tested. This is described by the equation

$$h(r,0) = 0. \tag{3.16}$$

At large distances from the test interval the head change induced in the test interval is never experienced and

$$h(\infty,t) = 0. \tag{3.17}$$

At the wall of the borehole, the formation or rock experiences the same head change as does the tested interval

$$h(r_w,t) = H(t) \tag{3.18}$$

where r_w is the radius of the borehole and H is the head change.

The initial head change in the system induced by the pressurization that begins the test is H_0 and

$$H(0) = H_0 \tag{3.19}$$

The solution assumes that the water flowing from the test interval into the rock obeys Darcy's law and that the water flow rate equals the rate at which the water stored in the pressurized interval expands as the pressure in the system declines. These assumptions are expressed by

$$2\pi r_w T \frac{\partial h}{\partial r}(r_w,t) = V_w C_w \rho_w g \frac{\partial H}{\partial t}(t) \tag{3.20}$$

where V_w is the volume of water within the pressurized interval; C_w is the compressibility of water; ρ_w is the density of water; and g is gravitational acceleration.

Expression (3.20) distinguishes the solution from the conventional slug test analysis by Cooper et al. (1967). In that solution, the expression that describes the rate of flow from the test interval into the formation is

$$2\pi r_w T[\partial h(r_w,t)]/\partial r = \pi r_c^2[\partial H(t)/\partial t] \tag{3.21}$$

where r_c is the radius of the standpipe. In the Bredehoeft and Papadopulos (1980) solution, r_c^2 is replaced by $V_w C_w \rho_w g/\pi$, which expresses the influence of the compressibility of the fluid used on the rate at which the fluid will flow into the rock around the test interval.

The Cooper et al. (1967) solution uses the Laplace transform with respect to time to reduce the problem to

$$\frac{\partial^2 \bar{h}}{\partial r^2} + \frac{1}{r}\left(\frac{\partial \bar{h}}{\partial r}\right) = \left(\frac{S}{T}\right)(p\bar{h}) \qquad (3.22)$$

where

$$\bar{h}(\infty,p) = 0 \qquad (3.23)$$

and

$$\frac{[\partial \bar{h}(r_w + 0,p)]}{\partial r} = \left(\frac{r_c^2}{2r_w T}\right)[p\bar{h}(r_w + 0,p) - H_0] \qquad (3.24)$$

The solution is

$$\bar{h}(r,p) = \frac{r_w S H_0 K_0(rq)}{Tq(r_w q K_0(r_w q) + 2\alpha K_0(r_w q)} \qquad (3.25)$$

where

$$q = \left(\frac{pS}{T}\right)^{1/2} \qquad (3.26)$$

and

$$\alpha = r_w^2 S/r_c^2 \qquad (3.27)$$

An analogous problem in heat flow was solved by Carslaw and Jaeger (1959) and the inverse transform solution for $h(r,t)$ is

$$h = \frac{2H_0}{\pi} \int_0^\infty e^{-\beta u^2/\alpha} \{J_0(ur/r_w)[uY_0(u) - 2\alpha Y_1(u)]$$

$$- Y_0(ur/r_w)[uJ_0(u) - 2\alpha J_1(u)]\} \frac{du}{\Delta(u)} \quad (3.28)$$

where $\beta = Tt/r_c^2$
and

$$\Delta(u) = [uJ_0(u) - 2\alpha J_1(u)]^2 + [uY_0(u) - 2\alpha Y_1(u)]^2 \quad (3.29)$$

$J_0(u)$, $J_1(u)$, $Y_0(u)$ and $Y_1(u)$ are the zero and first-order Bessel functions of the first and second kind. To find the head (H) inside the borehole interval, the radius of the borehole (r_w) is substituted for (r) in the inverse transform solution. H as a function of time in the borehole interval is

$$H = (8H_0\alpha/\pi^2) \int_0^\infty e^{-\beta u^2/\alpha} \frac{du}{u\Delta(u)} \quad (3.30)$$

The dimensionless decline in head in the test interval is then

$$\frac{\Delta H}{\Delta H_0} = \left(\frac{8\alpha}{\pi^2}\right) \int_0^\infty e^{-\beta u^2/\alpha} \frac{du}{u\Delta(u)} \quad (3.31)$$

If this solution for pressure decay in the borehole interval is considered a function such that

$$\frac{\Delta H}{\Delta H_0} = F(\alpha,\beta) \quad (3.32)$$

then for Cooper et al. (1967)

$$\frac{\Delta H}{\Delta H_0} = F\left(\frac{r_w^2 S}{r_c^2} , \frac{Tt}{r_c^2} \right) \tag{3.33}$$

while for Bredehoeft and Papadopulos (1980)

$$\frac{\Delta H}{\Delta H_0} = F\left(\frac{\pi r_w^2 S}{V_w C_w \rho_w g} , \frac{\pi Tt}{V_w C_w \rho_w g} \right) \tag{3.34}$$

with the difference again being the substitution of compressibility terms for the radius of the standpipe in the Cooper et al. (1967) solution.

The analysis assumes that only the compressibility of water influences the rate at which water flows from the test interval into the surrounding rock. This implies that the test equipment is perfectly rigid, as well as the rock within which the test is performed. A number of authors argue that this assumption is not valid for actual testing conditions (Hsieh, 1983, p. 20; Forster and Gale, 1980). Hsieh (1983) suggests a modified compliance term for the Bredehoeft and Papadopulos (1980) solution that includes the effect of packer compliance. The r_c^2 term introduced by Cooper et al. (1967) in his solution for the falling head test, which was replaced by $V_w C_w \rho_w g/\pi$ in the Bredehoeft and Papadopulos (1980) solution, is replaced by an S_w term in the solution presented by Hsieh (1983, pp. 20, 87), where

$$S_w = V_w \gamma_w C_{ps} \tag{3.35}$$

$$\gamma_w = \rho_w g \tag{3.36}$$

and $C_{ps} = (1/V_w)(\Delta V/\Delta P)$. (3.37)

ΔV = volume of water injected for pressure pulse

ΔP = resultant pressure increase.

The influence of the packer compliance factors on computed hydraulic conductivities is discussed in Section 3.5.6.

3.5.3 Pressure Slug Testing Equipment

Four packers are used for pressure slug testing at the Cargodero Canyon study area. Two can be inflated to seal the 16.3 cm (6 1/2 inch) diameter holes at the study site and two will inflate to seal the 6.3 cm (2 1/2 inch) diameter holes. The packers are used in two straddle-packer assemblies, one for each size of hole to be tested.

Figures 3.15a,b show the straddle-packer assembly as used in the field for pressure slug testing. The packers are connected by wire cable or rigid aluminum brace. The wire cable creates a flexible, adjustable straddle joint and makes handling the larger packers easier. High pressure plastic tubing is used for injection. Separate injection lines allow each packer to be inflated separately. Normally, there is some axial shortening and creep during packer inflation and it may be difficult to estimate precisely the length of borehole exposed to injection pressure. Inflating the lower packer first provides one definite boundary and allows visual inspection of the success of inflation and sealing.

Figure 3.16 is a schematic of the type of packer used for field testing at Cargodera Canyon. The packers are manufactured by Roctest, Inc. The upper packer of the large diameter assembly has an overall length of 148 cm (59 inches) and an uninflated gland length of 88 cm (35 inches). The lower packer of the large diameter assembly has an overall length of 171 cm (68 inches) and an uninflated gland length of 141 cm (56 inches). The packer is sheathed in a thick rubber cover. Both packers inflate to a diameter of 20 cm (8 inches). The upper packer of the small-diameter assembly has an overall length of 138 cm (55 inches) and an uninflated gland length of 68 cm (27 inches). The lower packer of the small diameter assembly has an overall length of 143 cm (57 inches) and an uninflated gland length of 68 cm (27 inches). Both packers inflate to a diameter of 7.5 cm (3 inches). The interval between the two packers in the small diameter assembly is fixed at 85 cm (34 inches). The interval between the two packers in the large-diameter assembly is adjustable and the packers can be used individually for single packer tests.

Single packer tests can be performed near the bottom of a hole (Figure 3.17). The test interval then is located between the packer and the hole bottom.

All four packers were tested in the laboratory over periods of one week to a month. Steel pipes with 15 cm (6 inches) and 6.3 cm (2 1/2 inches) diameters were used for testing the packers and test instrumentation. Compliance of the packers was measured over a range of inflation and interval injection pressures, and compliance factors were calculated for each straddle-packer assembly.

The pressure decay in the test interval is monitored using an externally mounted 345 kPa (50 psi) Dynisco transducer, an AD converter designed and built by the University of Arizona instrument shop, and a 3-pen, quartz controlled Servogor 430 strip chart recorder capable of measuring from 0 to 110 volts. For some testing, the 345 kPa (50 psi) transducer is replaced by a 172 kPa (25 psi) Dynisco transducer to provide greater decay resolution at the lower testing pressures. The entire monitoring system was tested over a range of pressures to determine the linearity of signal output in the laboratory. A transducer calibration curve is provided in Appendix A. Calibration of the monitoring system is repeated after each field test to

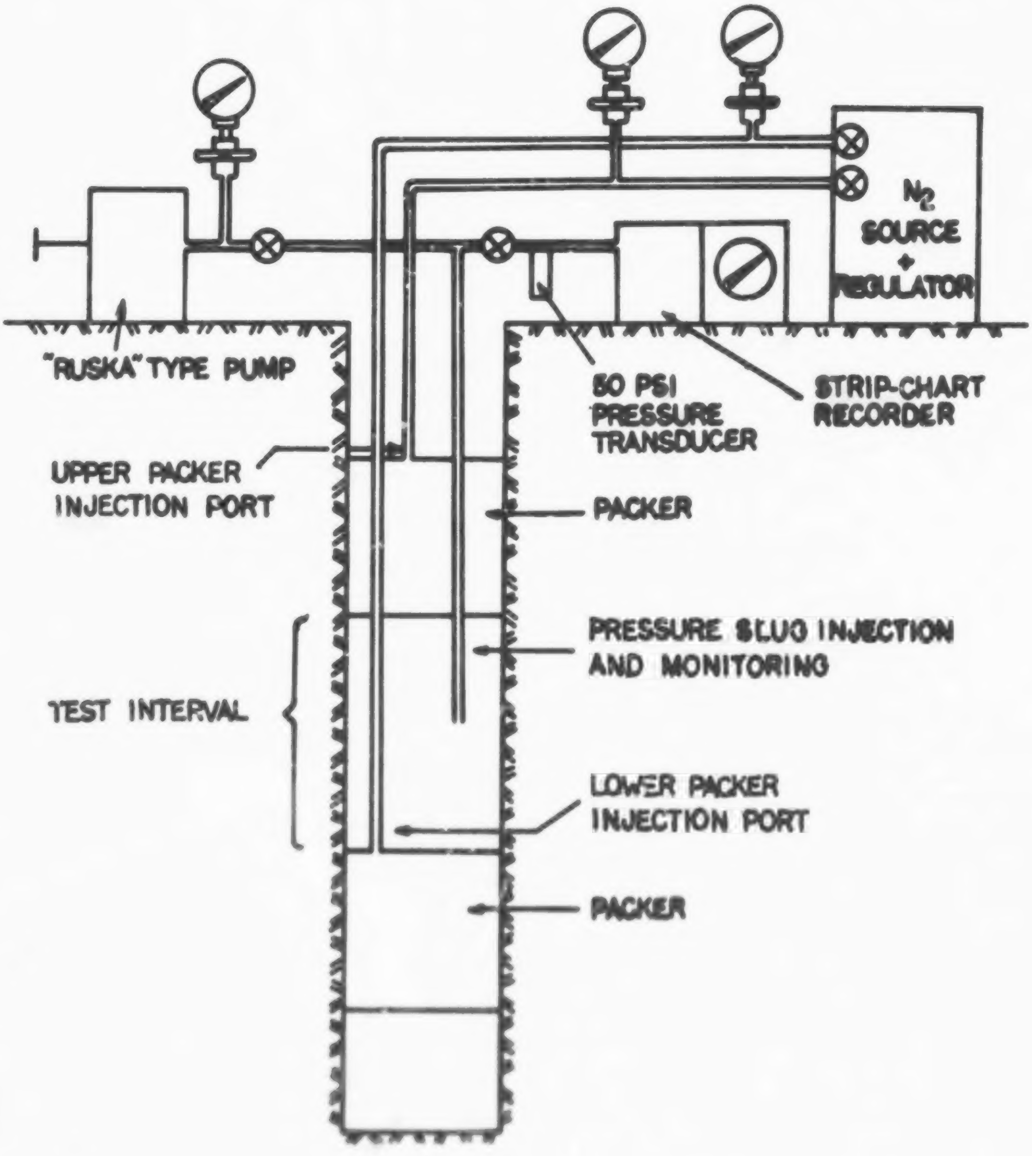
N2
SOURCE
+
REGULATOR
"RUSKA" TYPE PUMP
50 PSI
PRESSURE
TRANSDUCER
STRIP-CHART
RECORDER
UPPER PACKER
INJECTION PORT
PACKER
PRESSURE SLUG INJECTION
AND MONITORING
TEST INTERVAL
LOWER PACKER
INJECTION PORT
PACKER

Figure 3.15a Schematic of straddle-packer assembly for pressure slug testing. Not to scale.

The Ruska pump is a high-precision manually operated screw displacement pump.

BEST COPY AVAILABLE

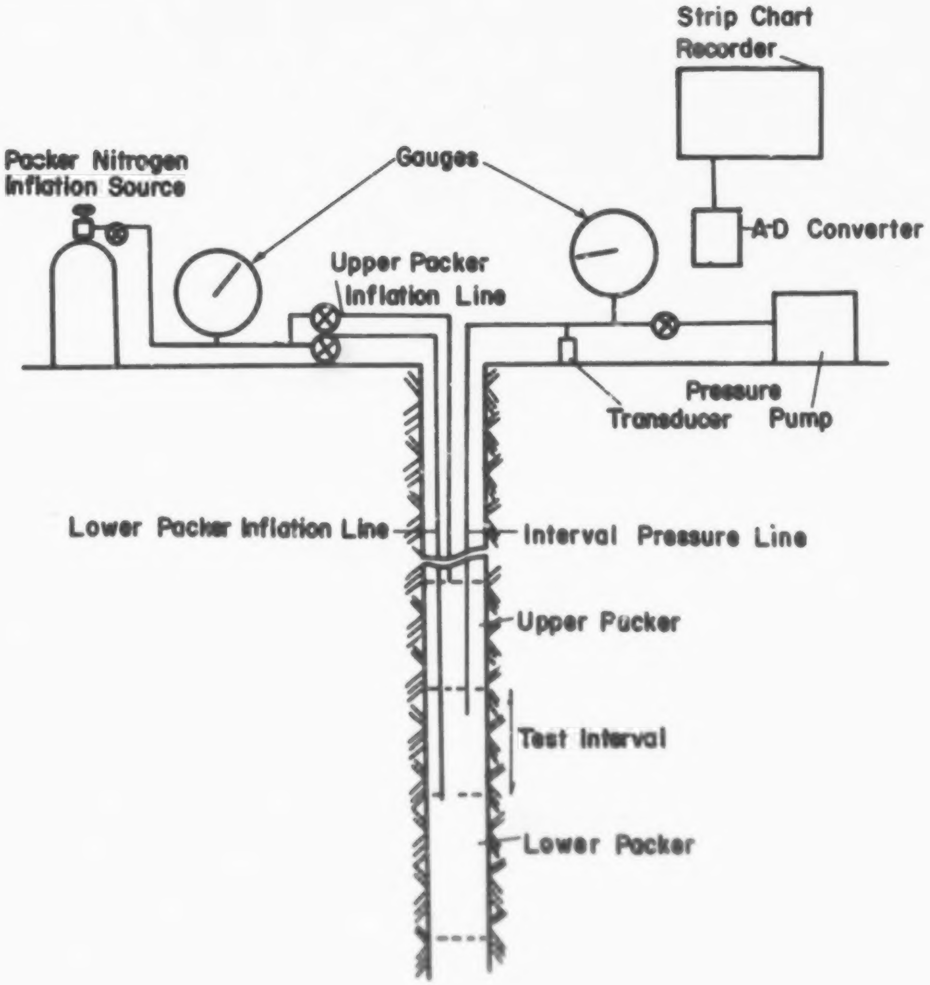
Strip Chart Recorder
Packer Nitrogen Inflation Source
Gauges
A-D Converter
Upper Packer Inflation Line
Pressure Transducer
Pump
Lower Packer Inflation Line
Interval Pressure Line
Upper Packer
Test Interval
Lower Packer

Figure 3.15b Schematic of straddle-packer assembly for pressure slug testing. Not to scale.

Pressure monitoring system is illustrated schematically.

BEST COPY AVAILABLE

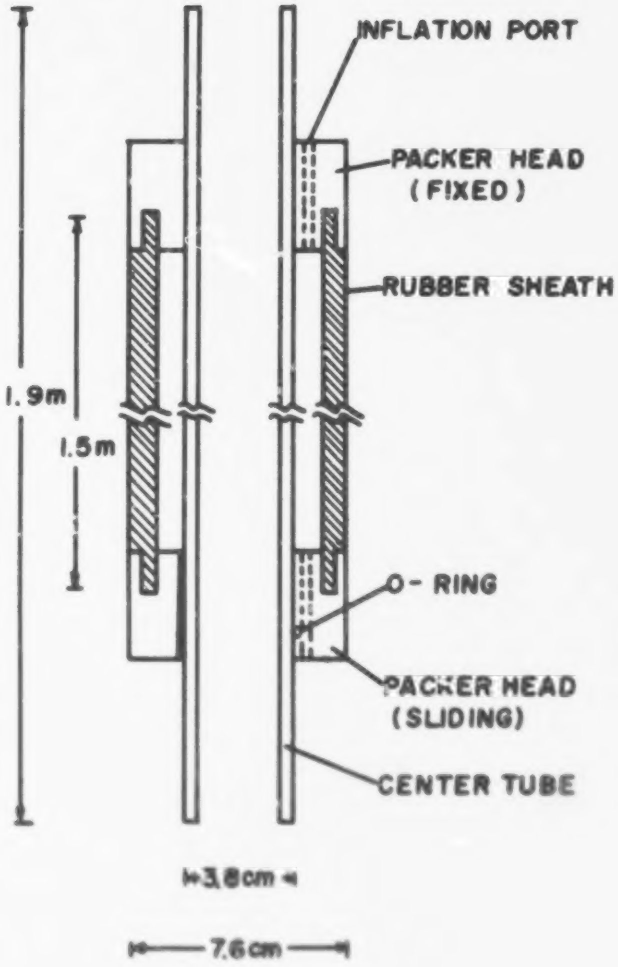
INFLATION PORT
PACKER HEAD (FIXED)
RUBBER SHEATH
O- RING
PACKER HEAD (SLIDING)
CENTER TUBE
1.9m
1.5m
3.8cm
7.6cm

Figure 3.16 Schematic diagram showing packer construction. (From Hsieh, 1983, p. 78)

BEST COPY AVAILABLE

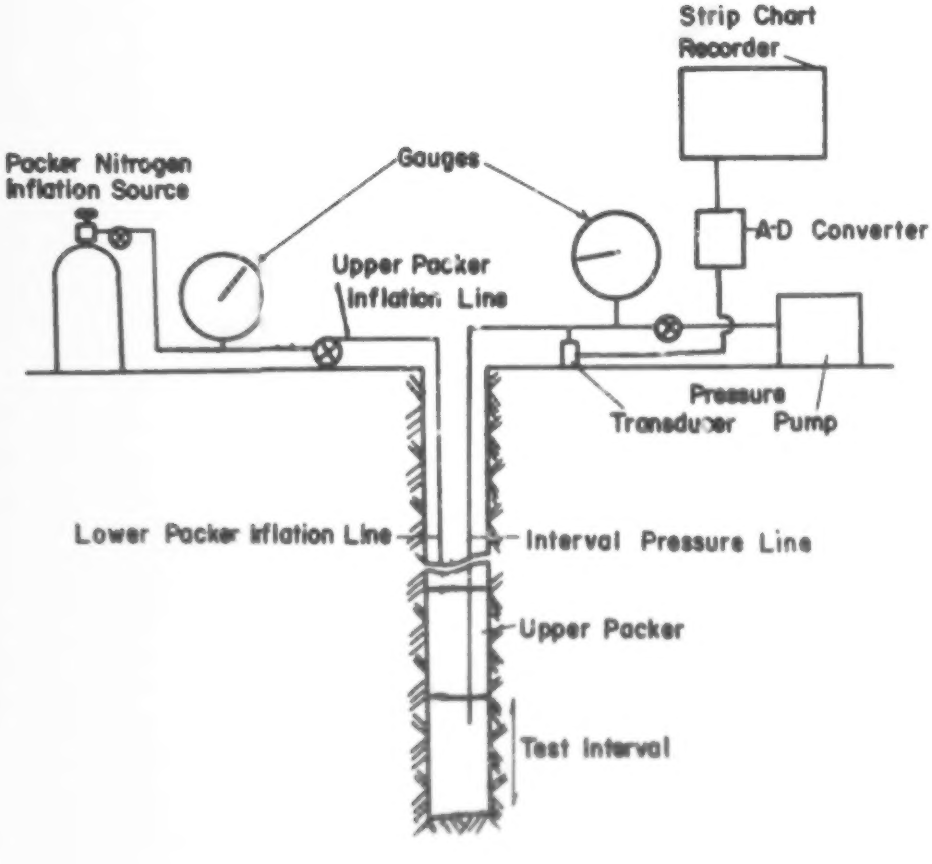
Strip Chart Recorder
Packer Nitrogen Inflation Source
Gauges
A-D Converter
Upper Packer Inflation Line
Pressure Transducer
Pump
Lower Packer Inflation Line
Interval Pressure Line
Upper Packer
Test Interval

Figure 3.17 Single pcker assembly used to test conductivity of boreholesection between packer and hole bottom.

BEST COPY AVAILABLE

compensate for effects of temperature, pressure surges, volt surges, and off-road travel.

Pressure is induced in the test interval with either of two types of pumps. Initial testing was done using a manual screw positive displacement pump in which a piston is displaced when the screw handle is turned. Several problematic test runs indicated that the pump leaked at back pressures greater than 140 kPa (20 psi). To avoid this possibility, the testing system was designed to isolate the pressure slug ahead of the source of the slug. A bleed valve allows the creation of the exact pressure required in the upstream system before any pressure is delivered to the test interval. A second pump, developed for a variety of test applications, uses nitrogen over water. Figure 3.18 shows a schematic of this pump. A piece of 6.3 cm (2 1/2 inch) O.D. clear PVC tubing was capped at both ends. The cap fittings allow connecting lines to the interval and from a nitrogen source. The tube is pressurized from the regulator on the nitrogen bottle. The pressure in the lines is read by a precision pressure gage. The nitrogen over water system proved to be a better device for applying the pressure slug into the intervals. Valves at both ends of the system and a bleed valve allow a pressure pulse to be isolated in the reservoir before any pressure is delivered to the test interval. This pump has the advantage of providing an accurate estimate of fluid injected into the test interval to create the pressure pulse.

3.5.4 Pressure Slug Test Procedures

Procedures for pressure slug testing at Cargodera Canyon are designed to insure that the tested borehole interval is effectively isolated from any pressure other than the pulse introduced for monitoring. Possible sources of pressure influence include improper packer seals, packers leaking inflation pressure into the test interval, fractures in the interval acting as conduits for fluid flow, and the effects of temperature and atmospheric pressure.

The procedure for straddle packer testing is simple, yet care must be taken to ensure that it is conducted properly. If not, leakage can occur through either or both packers, injection lines, fittings and valves. The leakage may be slow enough to avoid recognition and yet influence the test results.

The packers, when used together to straddle an interval, are separated by a cable, which can be adjusted to accommodate different interval lengths. The packers were lowered into the hole by hand with 6.3 mm (1/4 inch) nylon rope.

Nylon tubing with a 3.1 mm (1/8 inch) O.D. was used to connect the packers and injection interval to their respective fixtures on the surface. The tubing is rated to approximately 4.14 MPa (600 psi), which is much higher than the test requirements, and its flexibility makes it desirable for packer testing. After conducting several packer tests, it would now be recommended to consider the use of larger diameter tubing, such as 4.7 mm (3/16 in) or even perhaps 6.3

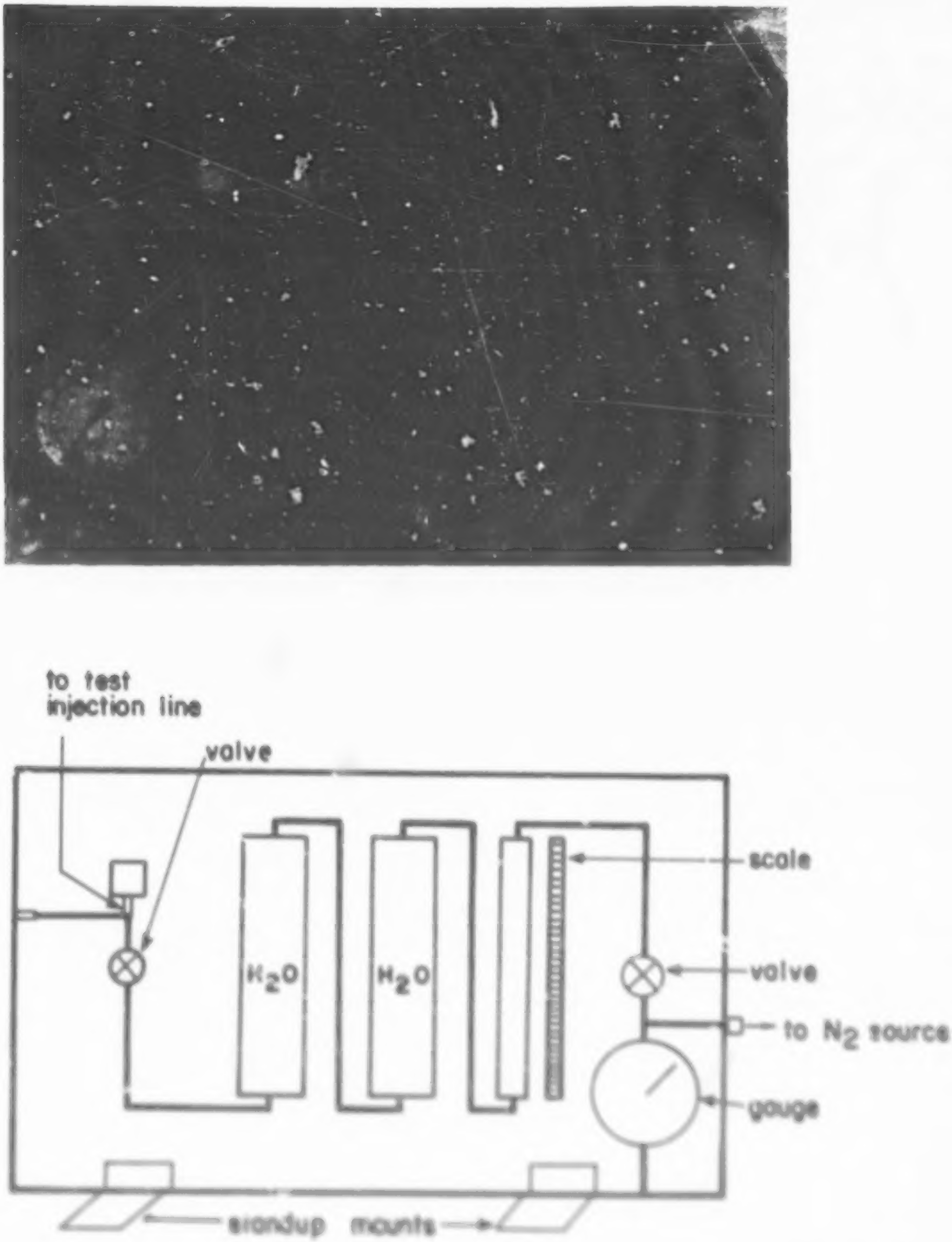
to test
injection line
valve
H_2O
H_2O
scale
valve
to N_2 source
gauge
standup mounts

Figure 3.10 Nitrogen over water injection pump.

BEST COPY AVAILABLE

mm (1/4 inch) O.D., to reduce the friction losses (e.g. Zeigler, 1976, p. 51). It is not obvious, however, that this would really be necessary in very low permeability rock, i.e. with very low flowrates throughout the system. A more detailed analysis might be worthwhile.

Pressure slug testing is initiated by lowering the straddle packer assembly to the depth at which the interval to be tested will be isolated when the packers are inflated. Injection lines are connected to the nitrogen source. The lower packer is inflated to the desired pressure and allowed sufficient time, about 10 minutes, to equilibrate. Water is then piped down the borehole to fill the interval to be tested. The top of the inflated gland of the lower packer is tagged and its depth from the surface recorded. The upper packer is then inflated to the desired pressure and allowed to equilibrate. Some excess water is introduced into the interval before upper packer inflation, and, as the packer inflates, this water is forced up the open injection line to the surface. Before the upper packer has completely expanded to the borehole wall, the pump is activated to de-air the lines to the injection interval. The packers are allowed to equilibrate in the borehole for another 30 minutes prior to test initiation. Water in the injection line prevents air from being introduced into the interval during testing. The top of the inflated gland of the upper packer is located and its depth from the surface recorded. Nitrogen inflation pressure to the packers is maintained for the duration of the test.

The straddle-packer assembly is allowed to equilibrate until there is no movement of water in the open injection line. The injection line is connected to the pressure delivery system but kept isolated from the pump. The pressure monitoring system is zeroed to the actual pressure in the test interval and a preliminary zero calibration is recorded on the strip record. The required pressure pulse is generated and isolated in the pressure reservoir. The pressure pulse is introduced into the pressure monitoring system and the pressure is recorded as calibration on the strip record. Pressure is then introduced into the test interval, the pressure monitoring system is engaged, and the pressure system is isolated by means of a shut-off valve on the surface. The time and actual initial pressure are recorded, as well as the speed of the strip chart recorder. Actual initial pressure is usually slightly less than the original pressure pulse as some pressure is lost to the compliance of the surface equipment.

The packers are inflated to pressures from 0.7 to 1.4 MPa (100 to 200 psi). Injection pressures never exceed 0.14 MPa (20 psi). Pressures are kept low to avoid the lifting some researchers associate with high injection and packer pressures in shallow boreholes (Zeigler, 1976, pp. 39-40).

3.5.5 Pressure Slug Test Results

3.5.5.1 Borehole CCR/C-3. Pressure slug testing was initiated in January of 1985. Borehole CCR/C-3 was selected for the first test as it had remained capped and clean. The available depth was only 2.5 m

(8 ft 4 in). A core barrel blocked access to the rest of the hole. The straddle-packer assembly to be used for testing requires a minimum depth of 2.7 m (9 ft) for proper operation. However, a single packer test could be performed if the bottom of the hole were plugged.

The center of the stuck core barrel was plugged with a rock dropped into the hole. A volume of saturated sand sufficient for a 15 cm (6 in) plug was then poured into the hole. This sand plug was capped by dropping approximately 1000 1.25 cm (1/2 inch) diameter bentonite tablets (American Colloid) through approximately 3 liters (0.8 gallon) of water. These were intended to form a 15 cm (6 in) clay plug above the sand. Four days later the top of this clay plug was measured at 216 cm (7 ft 2 in) from the surface.

Repeated trials proved the system incapable of holding a pressure pulse long enough for meaningful decay measurements. Raising and lowering the packer did not improve the test results. The packer was lowered to within 5 cm (2 in) of the clay plug with no success. It was concluded that the plug itself was failing as an effective seal.

The hole section immediately above the plug was filled with sand and gravel. The sand and gravel layer was capped with a 15 cm (6 inch) cement cap. The top of the cement cap was measured at 1.58 m (5 feet 3 inches) from the surface. Another series of packer tests were run in this interval. The system never maintained pressure.

The intervals may have lost the pressure build-up through fissures in the rock, in which case it was a legitimate assessment of the hydraulic conductivity. Other factors, however, may have caused the rapid pressure decay. The lower clay plug tested in the first series of packer tests may have been incapable of supporting the applied pressure during the pressure decay tests. The pressure may have dissipated through consolidation of the clay plug or through fissures and cracks that may have formed or enlarged after the plug was constructed. A pressure loss through the clay plug may not be an indictment against plugging with clay, but an observation about the sealing performance characteristics of a 15 cm (6 inch) long, i.e. a very short, clay plug. Perhaps if the water pressure in the borehole were maintained for a longer period of time, the clay plug may have equilibrated under that pressure. Perhaps then, any pressure decay thereafter would be due to flow into small fractures or pores in the rock itself.

The second series of packer tests performed on the cement plug as lower base showed the rapid decay typical for the first ones. If the pressure decay was not due to fracture flow into the rock, neglecting any equipment malfunction, it might have been due to a faulty bottom cement base. The cement base may not have expanded sufficiently to seal the borehole interface. Injected water would then pass through the interface into the permeable base of sand and gravel beneath the plug.

The plug may have caused the rapid decay of the injected pressure slug. However, subsequent plug tests performed on cement and bentonite plugs of a similar size showed the plugs to perform quite well. The most probable cause of pressure loss in the borehole is flow into borehole wall joints and fractures. Table 2.3 lists only one apparently unfractured interval in this borehole and a marginal interval above it. The approximately 40 cm (1 foot 4 inches) zone between these two intervals is not listed, which indicates it has a higher number of fractures than desired for seal testing. This zone may account for the pressure losses during both tests.

Borehole C-3 was not the most desirable hole at the site for borehole plugging tests, due to its shallow depth and apparent abundance of fractures. To better determine the actual cause of such pressure losses in the future, it is recommended that when performing single packer tests above a man-made base, video or photographic logs of the plugs be taken prior to packer testing. Perhaps a visual inspection of the plug would reveal a flaw in the plug that would account for pressure losses during slug testing. Similarly, it would be highly desirable to recover installed plugs, e.g. by means of overcoring, to allow detailed plug inspection.

3.5.5.2 Borehole CCR/C-1. Testing on borehole CCR/C-1 began in March 1985. Initial tests determined upper and lower boundaries for an interval competent for sealing. The first interval selected for testing extended from 158 cm (63 inches) to 98 cm (39 inches) from the surface. Table 3.1 summarizes the results of testing over a range of interval pressures. These results suggested that the interval was free of major fractures or damaged zones. The interval, however, was only 60 cm (24 inches) long. In addition, a review of the core log suggested that the bottom of the the upper packer gland may have been inflated against a double set of healed fractures which might interfere with proper seating and sealing.

The bottom of the top packer was lowered to 105 cm (42 inches) from the surface and the top of the bottom packer was lowered to a depth of 193 cm (77 inches). This provided a test interval of 88 cm (35 inches). Packer pressure was set to 1 MPa (145 psi). Table 3.2 summarizes the results of the initial testing. To determine the influence of injection pressures and packer pressures, the inflation pressure was increased to 1.4 MPa (200 psi) and the injection pressure reduced to 69 kPa (10 psi). The results of this test are included in Table 3.2. No meaningful differences in decay results were measured.

A long-term pressure slug test was conducted on March 13 through 14, 1985. Packer pressure was set to 1.03 MPa (150 psi). The interval tested extended from 105 to 193 cm (42 to 77 inches) from the surface. Table 3.3 is a record of the test decay values taken from the strip chart. The test ran for approximately 18 hours. Pressure introduced into the test interval was 62 kPa (9 psi).

3.5.5.3 Borehole CCR/D-4. Pressure slug testing on CCR/D-4 was begun in June of 1985. For these tests, the positive displacement pump used previously was replaced by the nitrogen over water pump and reservoir system discussed in Section 3.4. A review of the core log (Figure 3.19) suggested a suitable interval for testing between 173 cm (5 ft 9

Table 3.1 Pressure Slug Test, Borehole CCR/C-1, Interval from 98 to 158 cm (39 to 63 inches)

Duration* (min)	High Pressure (psi)	Low Pressure (psi)
14.36	11.0	10.3
3.67	15.0	14.8
6.70	14.8	14.6
6.23	14.6	14.4
6.42	14.4	14.2
6.88	14.2	14.0
2.58	17.0	16.8
3.27	16.8	16.6
3.27	19.8	19.6
2.77	19.6	19.4
2.38	19.4	19.2
2.85	19.2	19.0

*Duration is the time elapsed between the high and low pressures.

Table 3.2 Pressure Slug Test, Borehole CCR/C-1, Interval from 105 to 193 cm (42 to 77 inches)

Duration* (min)	High Pressure (psi)	Low Pressure (psi)
13.82	20.0	19.8
7.96	19.8	19.6
9.72	19.6	19.4
8.15	19.4	19.2
11.27	19.2	19.0
16.58	10.0	9.8
13.59	9.8	9.6
10.00	9.6	9.4
12.91	9.4	9.2

*Duration is the time elapsed between the high and low pressures.

Table 3.3 Long-Term Pressure Slug Test, Borehole CCR/C-1

Time (min)	Pressure (psi)	H/H_o* (%)
0	9.00	100
15	8.50	94.4
30	8.25	91.7
60	7.50	83.3
90	6.75	75.0
120	6.00	66.7
150	5.75	63.9
180	5.40	60.0
210	5.00	55.6
240	4.50	50.0
300	3.75	41.7
360	3.50	38.9
420	3.00	33.3
480	2.75	30.6
540	2.50	27.8
600	2.00	22.2
660	1.75	19.4
720	1.50	16.7
780	1.25	13.9
840	1.00	11.1
900	0.75	8.3
960	0.50	5.6
1020	0.30	3.3
1080	0.10	1.1
1110	0	0

*Pressure H as a percent of initial pressure H_o.

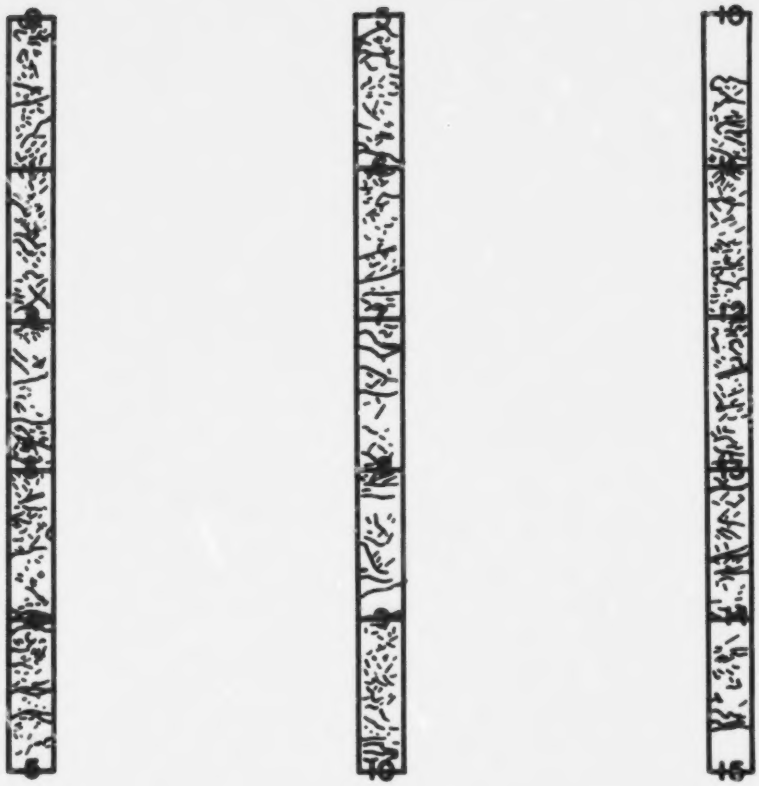

Figure 3.19 Borehole CCR/D-4 core fracture map.

BEST COPY AVAILABLE

in) and 294 cm (9 ft 9 in) from the surface. The straddle packer assembly used for this testing has a fixed test interval length of 85 ± 5 cm (34 ± 2 inches) to account for gland slide during inflation. The bottom of the top packer was set at 200 cm (80 inches) from the surface. Packer pressure was set at 1.24 MPa (180 psi). Table 3.4 lists the results of the first long-term pressure slug test on CCR/D-4. The test ran for approximately 40 hours. The test began at 12:45 p.m. Initial interval pressure was set at 159 kPa (23 psi).

A second long-term pressure slug test was conducted on CCR/D-4 eleven days after the first test. The test began at 11:30 a.m. and ran for approximately 46 hours. Table 3.5 lists the results. Packer pressure was set at 1.24 MPa (180 psi) and initial interval pressure was set at 97 kPa (14 psi).

3.5.5.4 Borehole CCR/C-2. Hole C-2 was cleaned out and made ready for testing in July of 1985. The first interval selected for testing was between 3 and 4.3 m (10 and 14 feet). This interval was long enough, or so it was thought, to hold both packers. The lower packer, however, would not go past 3.6 m (12 feet) in the borehole. An obstruction in the bottom of the hole would not allow the packer to be lowered to its desired position. Several unsuccessful attempts were made to remove the obstruction.

Single packer tests were utilized to select a suitable interval. The effective hole bottom was raised 20 cm (8 inches) by pouring sand down the hole and capping it with 13 cm (5 inches) of cement. The hole bottom was measured at 4 m (13 feet 4 inches) from the surface. Packer tests were conducted in the interval between 4 m (13 feet 4 inches) and 3.26 m (10 feet 10 inches). The decay, while not as rapid as that observed in hole CCR/C-3, was high enough to cause concern. The hydraulic conductivity calculated from the decay curve was in the order of 10^{-6} cm/s, which made the interval of marginal quality and desirability as a host for plug tests. Upon careful review of the video logs, two very small fractures were observed at approximately 3.92 m (13 feet). This observation was confirmed by that of the project geologist, Nora Colburn. This is testimony to the merit and usefulness of borehole videologging.

A new interval was prepared for testing by pouring more sand and then a cement cap on the bottom. The depth was brought to 3.7 m (12 feet 3 inches). The new interval tested was between 3.69 m (12 feet 3 inches) and 2.94 m (9 feet 9 inches) - a 75 cm (30 inch) interval. The packer test conducted in this interval indicated that it would be suitable for plug tests.

The packer test was conducted starting July 31 and ended August 2 for a duration of 52 hours. The packer pressure throughout the test was maintained at 1.03 MPa (150 psi).

3.5.6 Pressure Slug Test Analysis

Analysis of the pressure slug tests conducted in boreholes CCR/C-1, CCR/C-2 and CCR/D-4 utilizes the type curve method discussed in

Table 3.4 Long-Term Pressure Decay Test #1, Borehole CCR/D-4

Time (min)	Pressure (psi)	H/H_o * (%)
0	23.00	100
30	20.10	87.4
60	16.77	72.9
120	13.63	59.3
180	12.60	54.8
240	11.41	49.6
300	10.05	43.7
360	9.88	43.0
420	9.03	39.3
480	8.52	37.0
540	8.18	35.6
600	7.16	31.1
660	6.82	29.7
720	6.65	28.9
780	5.79	25.2
840	5.45	23.7
900	5.11	22.2
960	4.77	20.7
1020	4.26	18.5
1080	3.75	16.3
1140	3.58	15.6
1200	4.26	18.5
1260	4.94	21.5
1320	5.62	24.4
1380	6.47	28.1
1440	6.99	30.4
1500	8.52	37.0
1560	8.45	36.7
1620	7.67	33.3
1680	6.99	30.4
1740	6.65	28.9
1800	5.96	25.9
1860	5.28	23.0
1920	4.60	20.0
1980	3.92	17.0
2040	3.24	14.1
2100	2.56	11.1
2160	2.21	9.6
2220	1.53	6.7
2280	1.02	4.4
2340	0.51	2.2
2400	0.07	0.3

---

*Pressure H as a percent of initial pressure H_o.

Table 3.5 Pressure Decay Test #2, Borehole CCR/D-4

Time (min)	Pressure (psi)	H/H_o * (%)
0	13.24	100
20	12.82	96.83
40	12.57	94.94
60	12.37	93.43
120	11.99	90.56
180	11.69	88.29
240	11.54	87.16
300	11.34	85.65
360	11.01	83.16
420	10.36	78.25
480	9.78	73.87
540	9.28	70.09
600	8.88	62.07
720	8.34	65.26
780	8.10	61.18
840	7.90	59.67
900	7.70	58.16
960	7.60	57.40
1020	7.57	57.18
1080	7.43	56.12
1140	7.24	54.68
1200	7.07	53.40
1260	7.21	54.46
1320	7.44	56.19
1380	7.67	57.93
1440	8.04	60.73
1500	8.33	62.92
1560	8.66	65.41
1620	8.88	67.07
1680	8.74	66.01
1740	8.52	64.35
1800	8.34	62.99
1860	8.04	60.73
1920	7.65	57.78
1980	7.28	54.98
2040	7.03	53.10
2100	6.83	51.59
2160	6.60	49.85
2220	6.43	48.56
2280	6.30	47.58
2340	6.21	46.90
2400	6.12	46.22
2460	6.06	45.77
2520	5.88	44.41

Table 3.5 Pressure Decay Test #2, Borehole CCR/D-4--Continued

Time (min)	Pressure (psi)	H/H_o * (%)
2580	5.81	43.88
2640	5.78	43.66
2700	5.81	43.88
2760	5.89	44.49

[*] Pressure H as a percent of initial pressure H_o.

Section 3.5.2. Type curves for α values of .1, .2, .5, 1, 1, 5 and 10 were drawn using the values presented by Bredehoeft and Papadopulos (1980). For α values of 10^{-1} to 10^{-5}, type curves were developed from values calculated by Cooper et al. (1967). Type curves for α values from 10^{-6} to 10^{-10} were taken from values developed by Papadopulos et al. (1973). These type curves are included in Appendix B.

The results of the long-term pressure decay test for borehole CCR/C-1 are plotted in Figure 3.20. This decay curve is matched to the appropriate type curve by superimposing the curves and moving the decay curve horizontally while keeping the abscissa coincident. A good match is found for the type curve of α equal to 10^{-6}. Figure 3.21 shows the points of the decay curve as they fall along the type curve. The small deviation at early time suggests the test was started before the pressure in the interval was allowed to equilibrate. A match point of β equal 1 gives a time value of 90 minutes. Using the equations discussed in Section 3.5.2 and the packer compliance term developed from laboratory testing, a hydraulic conductivity of 1.19×10^{-8} cm/s is calculated for this interval.

The results of the pressure decay tests in CCR/D-4 are plotted in Figures 3.22 and 3.23. These are matched to type curves as described above. For the first decay test, a match point at $\beta = 1$ is selected for α values between 10^{-4} and 10^{-5}. The time used for calculation is 320 minutes. The match is good for the test time after the first 100 minutes. The early time decay is shallow and does not fit either curve. This may be a result of waiting too long for pressure to equilibrate before starting the test. It may also be a function of temperature. The test was conducted in July with afternoon temperatures approaching 38°C (100°F). The early part of the test corresponds with the warmest time of the day. Though temperatures in the borehole should remain relatively constant, the transducers at the surface are susceptible to drift induced by high temperature. A temperature test discussed in Section 4.10 suggests this drift can approach 20 percent of actual pressure values.

Using the later time match, a hydraulic conductivity of 8.78×10^{-10} cm/s is calculated for this interval. To determine the sensitivity of this value to proximate α values, the hydraulic conductivity at an α of 10^{-4} and of 10^{-5} was calculated. For $\alpha = 10^{-4}$, a time of 290 minutes is used. Hydraulic conductivity is calculated to be 9.69×10^{-10} cm/s. At $\alpha = 10^{-5}$, time is 370 minutes and hydraulic conductivity is 7.60×10^{-10} cm/s. These results suggest that the analysis is similar over the range of α values used to match an individual curve.

The decay plot for the second test in CCR/D-4 shows a distinct pressure increase pulse in the late time portion. During the time the test was conducted, thunderstorms occurred. Several volt surges were noted in the actual strip chart record. These may have resulted

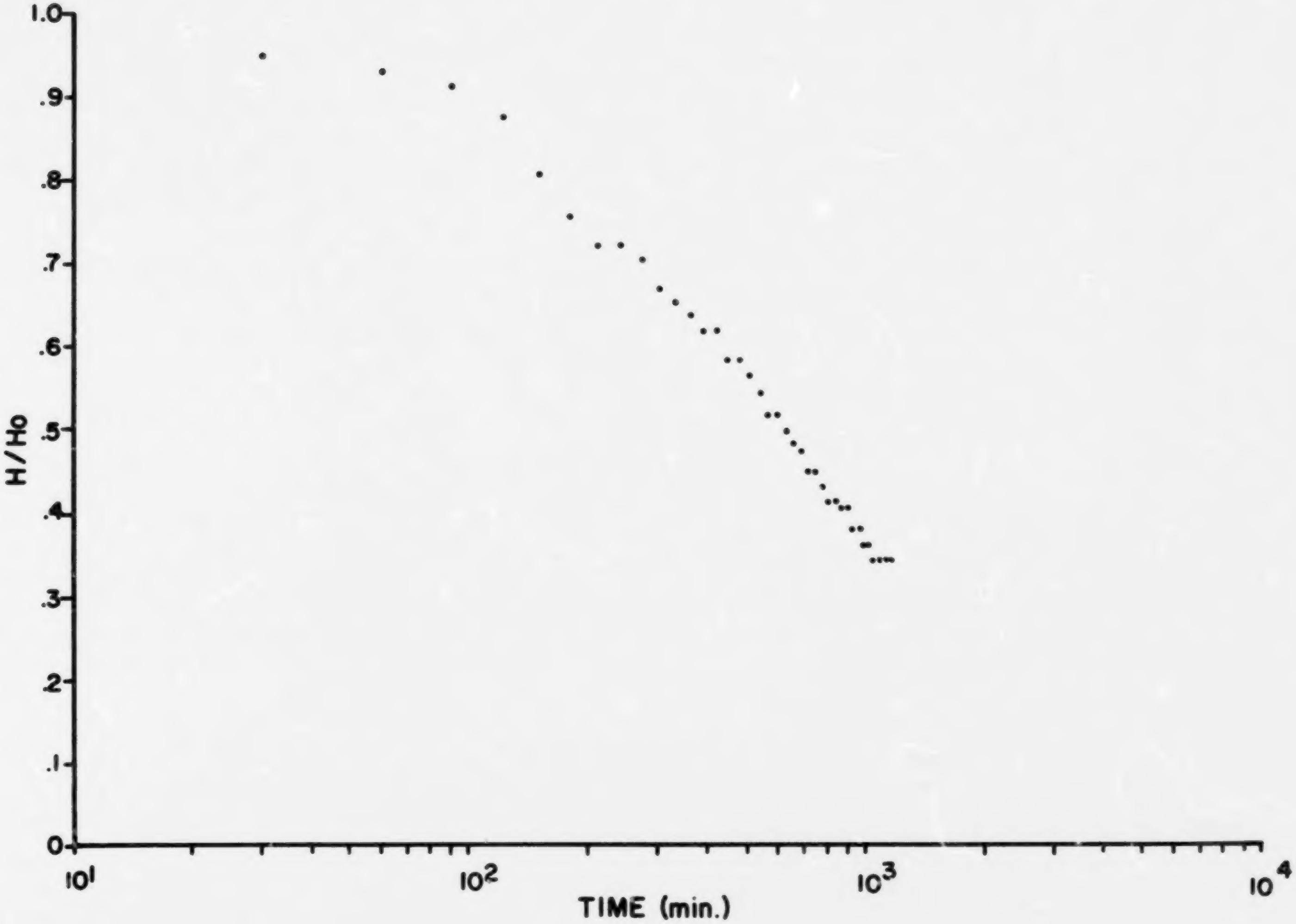

Figure 3.20 Pressure decay curve measured in borehole CCR/C-1. H/H_o is the relative (dimensionless) head monitored in the test section, expressed as a fraction of the suddenly applied H_o head.

BEST COPY AVAILABLE

BLANK PAGE

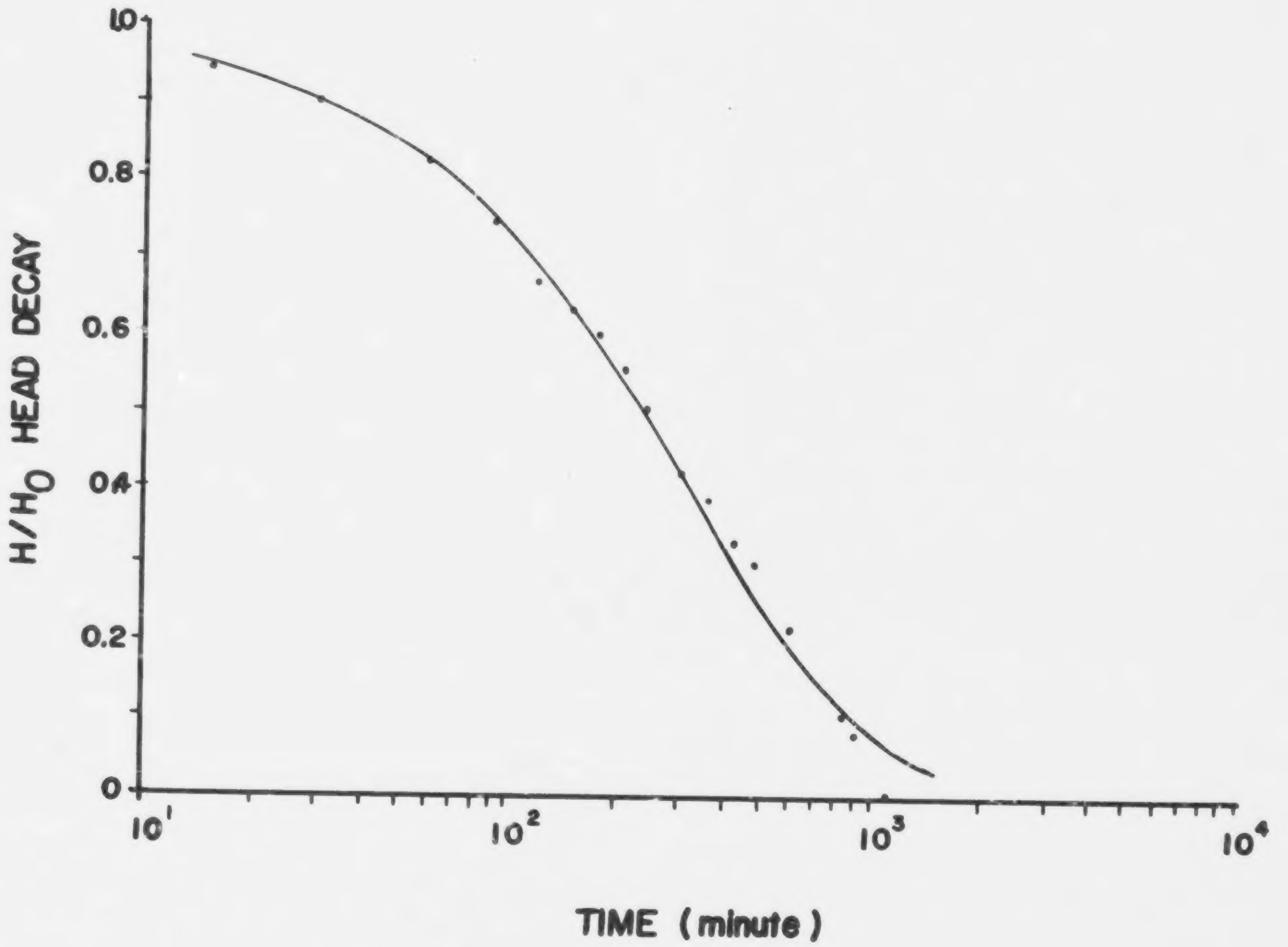

Figure 3.21 Borehole CCR/C-1 test data over type curve. Transient pulse testing.

BEST COPY AVAILABLE

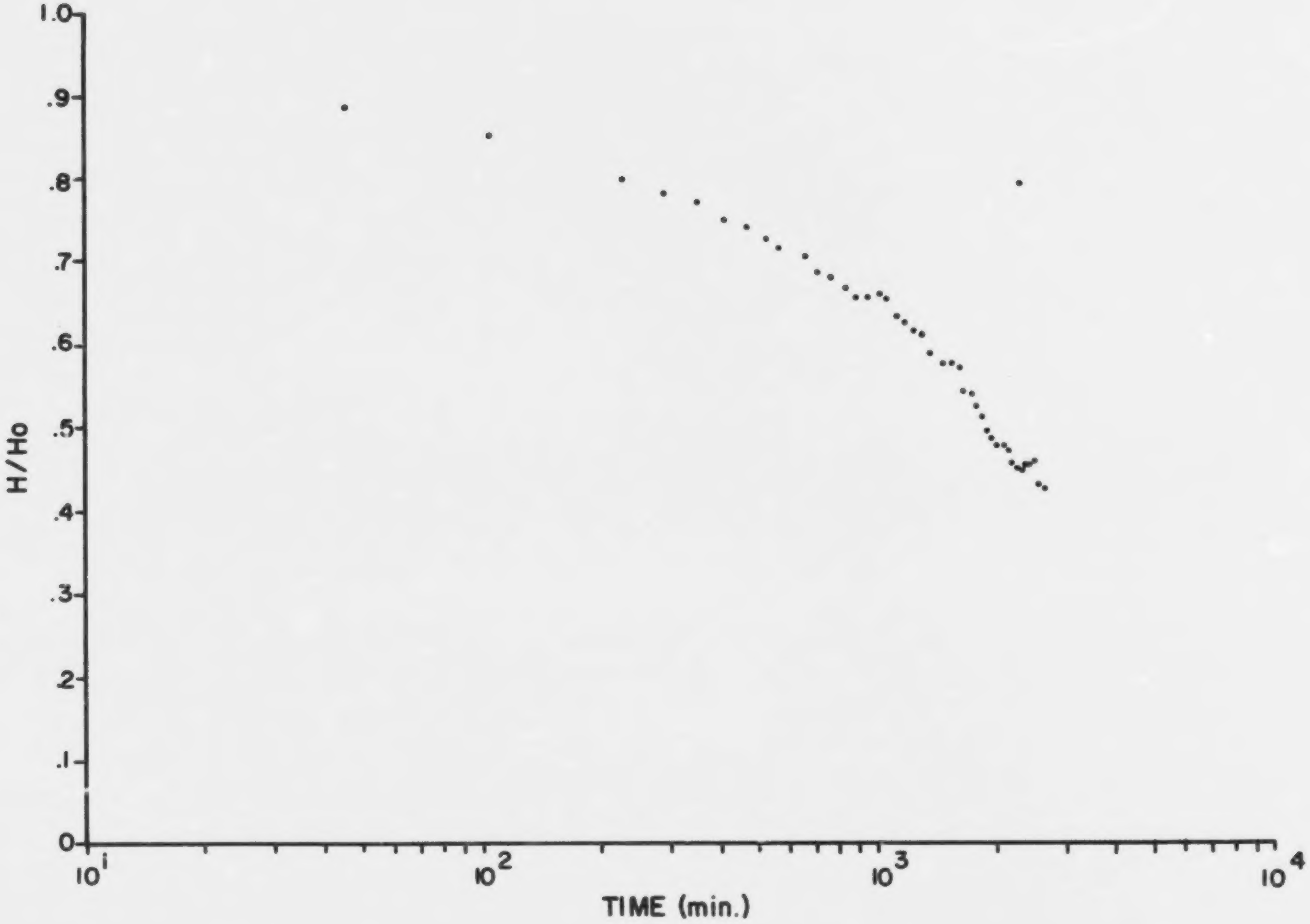

Figure 3.22 Pressure decay test 1. Borehole CCR/D-4.

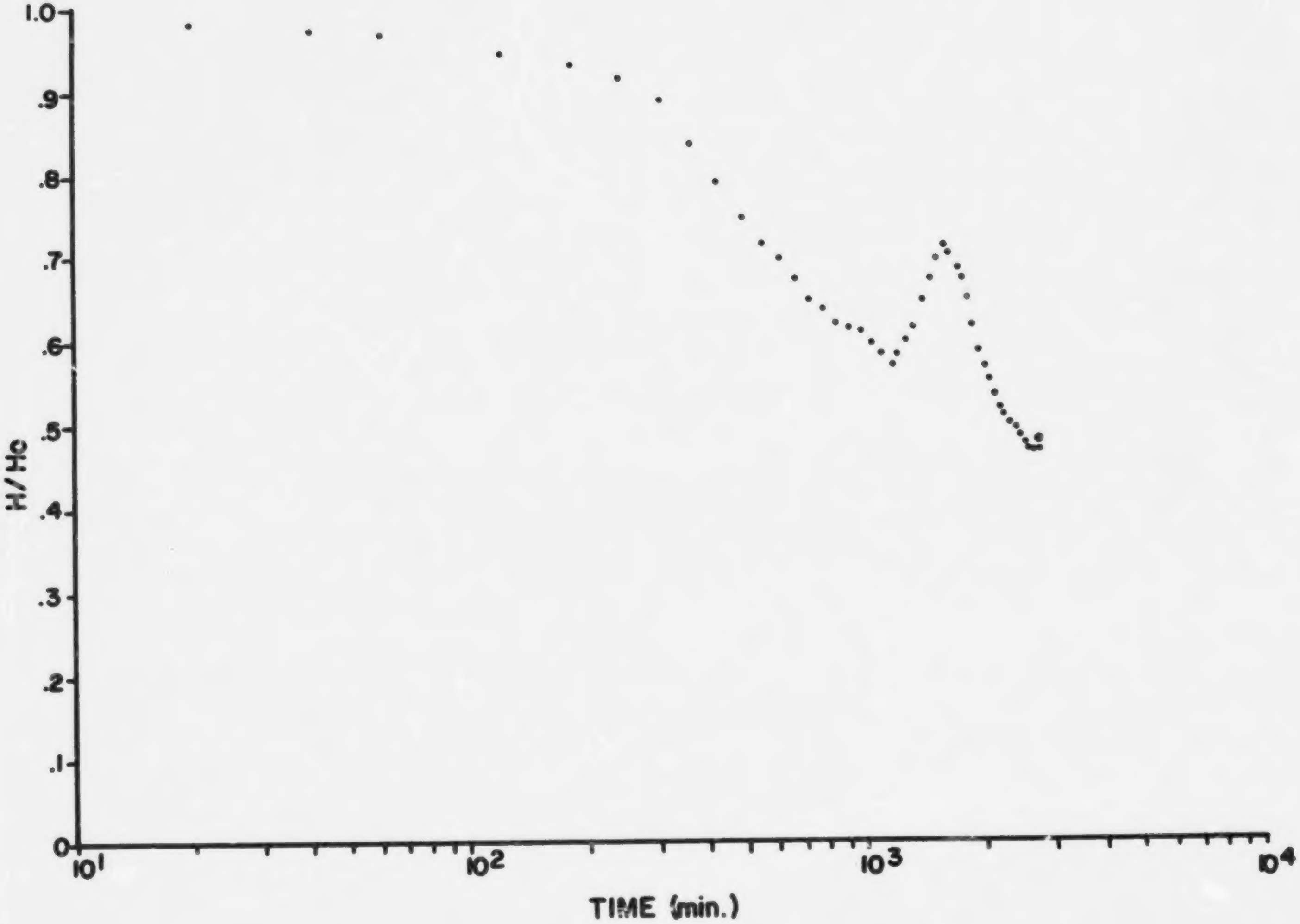

Figure 3.23 Pressure decay test 2. Borehole CCR/D-4.

in a malfunction of the recording equipment over a brief period of time. If the curve is analyzed using the early time portion, the α value curve with the best fit is .1. The match point is $\beta = .01$ and time = 180 minutes. The resulting hydraulic conductivity for the test is 1.56×10^{-11} cm/s. If the later time portion is used, and the pressure pulse ignored, $\alpha = 10^{-6}$, $\beta = 1$, and time is 470 minutes. A hydraulic conductivity of 5.98×10^{-10} cm/s is computed for this portion of the curve. Table 3.6 summarizes the analyses of these tests.

Figure 3.24 is the pressure decay curve for borehole CCR/C-2. A hydraulic conductivity of 7.88×10^{-10} cm/s was computed for the interval between 3.69 and 2.94 m (12 ft 3 in to 9 ft 9 in).

The results of the test in CCR/C-1 are significantly higher than the hydraulic conductivities in CCR/D-4 and CCR/C-2. A review of the core logs suggests that the permeability of the interval in CCR/C-1 may be influenced by microfracturing near the top of the interval as well as some of the seams and infillings found throughout its length. If this is true, the values from the tests in CCR/D-4 are a better representation of the hydraulic conductivity of the competent portions of the host rock. The various compliance terms used in the solutions are approximations depending, in part, on the precision of laboratory packer testing. The large volumes of the packers used in testing CCR/C-1 may have contributed to the difference in hydraulic conductivity values as any error in determining their compliance is magnified by their size with respect to the volume of the interval tested. Both intervals are approximately 90 cm (3 feet) long, but the diameter of CCR/C-1 is more than twice that of CCR/D-4. However, so is the diameter of CCR/C-2.

Freeze and Cherry (1979, p. 29) report hydraulic conductivity values of 10^{-9} cm/s for relatively unfractured granite measured in boreholes. They indicate an expected range of 10^{-8} to 10^{-11} cm/s for igneous rocks in general. The values determined in this study are in this range. They do vary significantly from borehole to borehole.

3.6 Constant Pressure Injection Test

3.6.1 Introduction

A prime goal of borehole characterization testing at the Cargodera Canyon site is to determine the hydraulic conductivity of borehole intervals selected for sealing. Two factors qualify conductivity values established by pressure slug testing. The tests are conducted prior to sealing and all seals are placed in unsaturated rock. Once performance testing of seals is underway, the degree of saturation of the surrounding rock changes as fluid is injected into the test intervals. A corresponding change in the hydraulic conductivity of the surrounding rock should occur. Maintaining a long-term constant injection test in a suitable proximate borehole provides a continuous

Table 3.6 Summary of Pressure Slug Test Analyses

Borehole	Test	α	β	Time (min)	Hydraulic Conductivity K (cm/s)
CCR/C-1	1	10^{-6}	1	90	1.19×10^{-8}
CCR/D-4	1	$10^{-4}-10^{-5}$	1	320	8.78×10^{-10}
CCR/D-4	1	10^{-4}	1	290	9.69×10^{-10}
CCR/D-4	1	10^{-5}	1	370	7.67×10^{-10}
CCR/D-4	2	.1	.01	180	1.56×10^{-11}
CCR/D-4	2	1	1	470	5.98×10^{-10}
CCR/C-2					7.88×10^{-10}

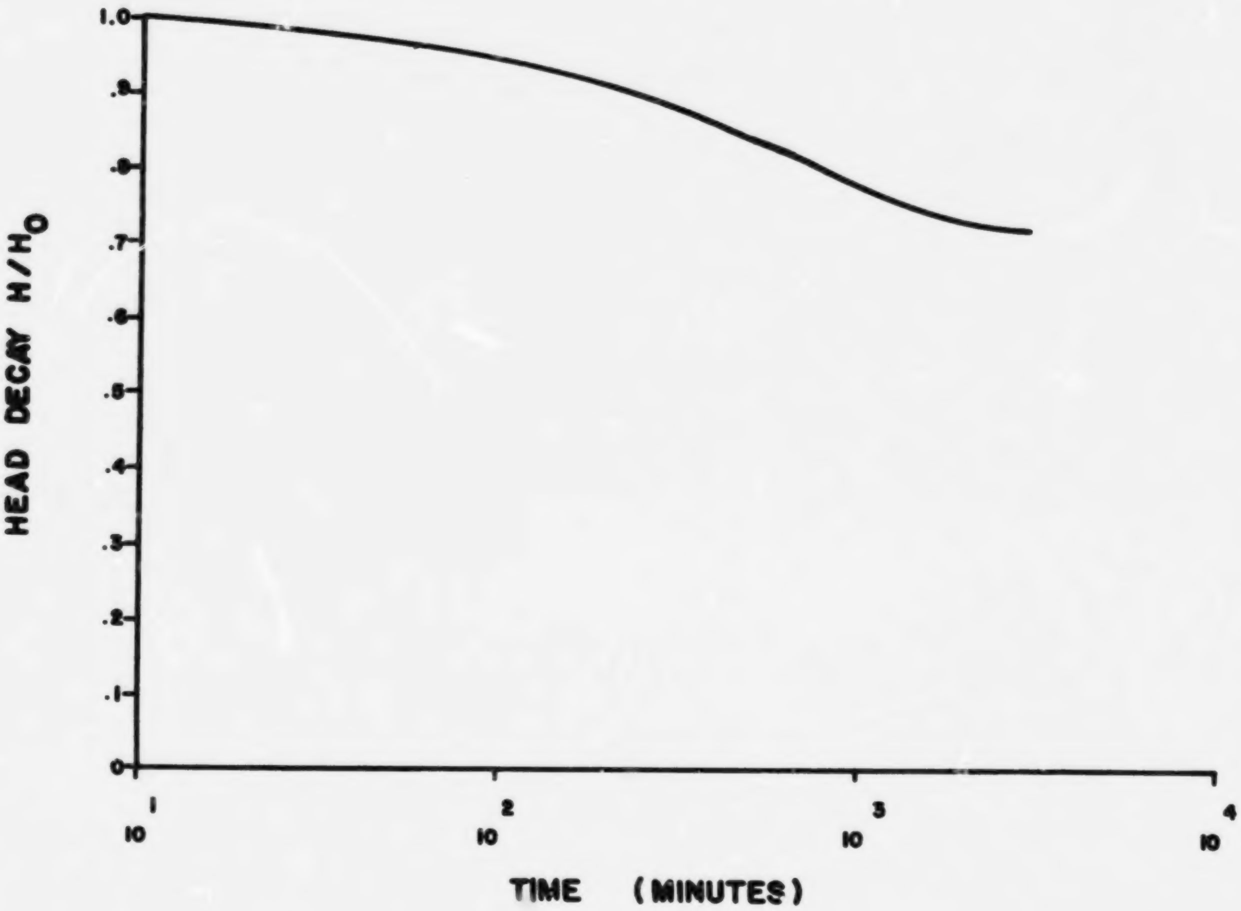

Figure 3.24 Pressure decay curve measured in borehole CCR/C-2. H/H_o is the relative (dimensionless) head monitored in the test section, expressed as a fraction of the suddenly applied H_o head.

BEST COPY AVAILABLE

record of hydraulic conductivity changes. It also allows a comparison of conductivity values derived from two types of testing.

3.6.2 Constant Pressure Injection Test Procedures and Equipment

The constant pressure injection tests at Cargodera Canyon use straddle-packers to isolate a borehole test interval . Fluid is injected into the interval at a constant pressure. The volume injected is monitored to determine the hydraulic conductivity of the interval rock. This test procedure is described by Zeigler (1976, pp. 18-19, 38-79); Hsieh (1983, pp. 10-14) and Bennett and Anderson (1976, pp. 16-17). The theoretical analysis for this test is discussed in Section 3.4.5.

Figure 3.25 is a schematic of the equipment layout for constant pressure injection testing on CCR/D-4. The straddle-packer assembly used to isolate the test interval is the same as used in pressure slug testing on CCR/D-4. A small nitrogen over water pump and reservoir is used to apply pressure and monitor flow.

Packer pressures are set at 1.24 MPa (180 psi). Interval pressure is maintained at 34 kPa (5 psi) to avoid deformation of the interval associated with high interval pressures in shallow boreholes. Zeigler (1976, pp. 39-40) quotes, as a rule of thumb, using only 1 psi of injection pressure for each foot of depth (23 kPa/m) if the interval is above the water table and .57 psi for each foot of depth (13 kPa/m) when the test interval is below the water table.

3.6.3 Results and Analysis of Constant Pressure Injection Test

The results of the constant pressure injection test in CCR/D-4 cover approximately 20 days. During this time testing was stopped repeatedly to make equipment adjustments. Injection pressure varied from 48 to 31 kPa (7 to 4.5 psi).

Table 3.7 presents the volume injected over time as well as the hydraulic conductivity. Hydraulic conductivity is calculated using the analysis presented in Section 3.4.5. Figure 3.26 graphs the hydraulic conductivity over time. Early time values must be treated as approximations since equipment problems and down time for the system may have influenced measured injected volumes. Late time values agree within an order of magnitude with pressure slug test results reported in Section 3.5.6 for borehole CCR/D-4.

The steep drop in hydraulic conductivity over time may result from a number of factors. Bouwer (1978, Section 5.5) states that injection testing in an unsaturated medium involves an artificial wetting of the test zone. Since this wetting entraps air in the voids, measured hydraulic conductivities will be less than if the medium was saturated. The small volumes injected may indicate that an extended time may be required to reach local saturation.

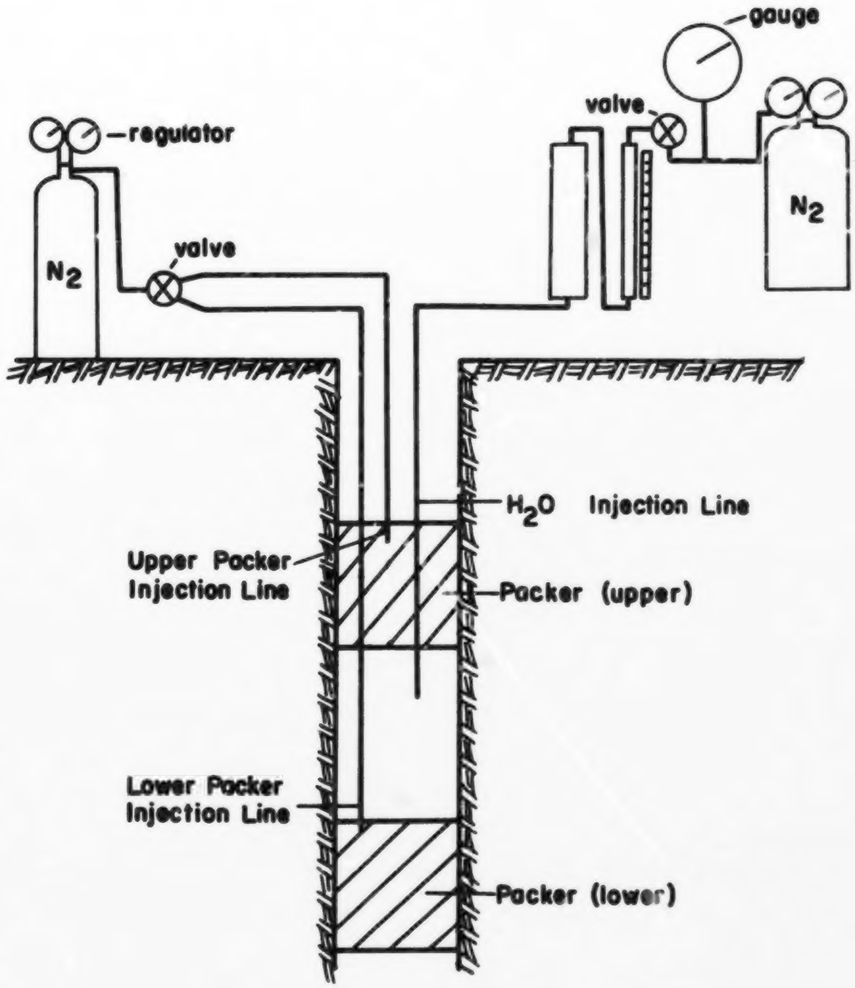
gauge
valve
regulator
N_2
N_2
valve
H_2O Injection Line
Upper Packer Injection Line
Packer (upper)
Lower Packer Injection Line
Packer (lower)

Figure 3.25 Field arrangement for constant pressure injection test.

BEST COPY AVAILABLE

Table 3.7 Constant Pressure Injection Test Results, Borehole CCR/D-4

Date	Time	Pressure (psi)	Volume Water Injected (cm^3)	Hydraulic Conductivity (cm/s)
7/31	1000	5	-	-
8/31	1010	5	5.47	1.09×10^{-9}
8/3	1100	5	0.9653	9.51×10^{-11}
8/4	1300	5	1.93	3.57×10^{-10}
8/4	1426	5	-	-
8/6	1021	5	-	-
8/7	1130	7	1.29	1.78×10^{-10}
8/8	1030	7	1.93	2.65×10^{-10}
8/8	1315	5	-	-
8/9	1030	5	0.6435	1.46×10^{-10}
8/12	1035	5	1.29	8.61×10^{-14}
8/15	1140	5	-	-
8/16	0800	5	-	-
8/20	0745	4.7	1.29	6.89×10^{-11}

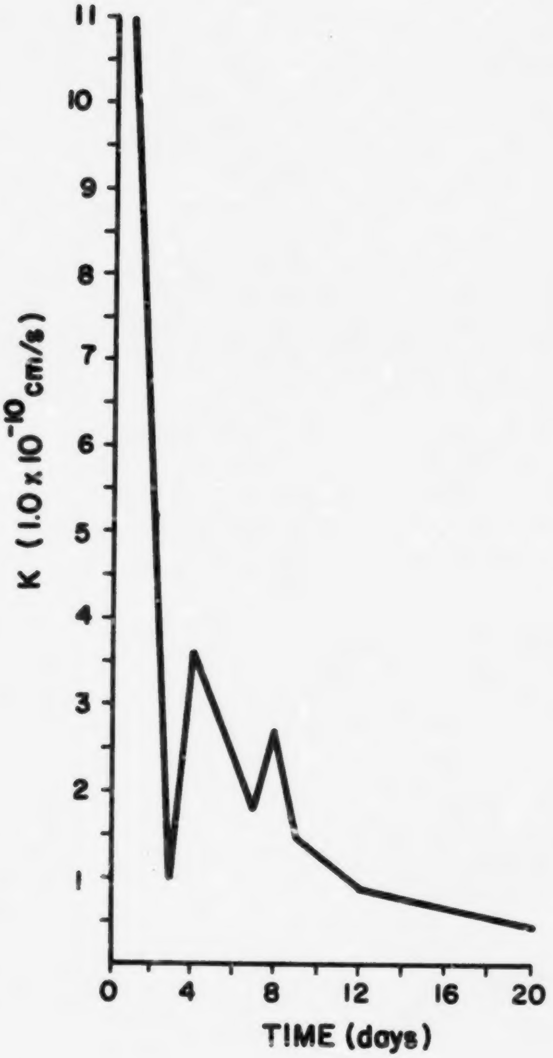

Figure 3.26 Hydraulic conductivity K determined from constant pressure injection test in borehole CCR/D-4.

BEST COPY AVAILABLE

No effort was made to monitor the consistency of injection pressures between the times when measurements were taken. Temperature effects at the surface, as discussed in Section 4.10 may have increased injection pressures during unobserved testing time. This would induce higher injection rates and result in high values of calculated hydraulic conductivity.

3.7 Neutron Probe Measurements

3.7.1 Introduction

The hydrologic characterization of unsaturated, fractured, crystalline rocks is complicated by the necessity of determining the water content of the rock. Many of the parameters in the governing equations for flow through unsaturated media are functions of water content.

Field testing at Cargodera Canyon takes place in an initially unsaturated environment. As injection proceeds, local regions within the outcrop may approach saturation. The observed water table has fluctuated from 2.4 to 4.8 m (8 to 16 ft) from the surface over the time of this study. In addition, a number of larger fracture systems may act as recharge conduits. In this case, the rock around the immediate area of the fracture should have a higher moisture content than the rock in the rest of the outcrop.

Neutron logging has been used by soil scientists to measure the water content of soils and by geophysicists to measure the saturated porosity of oil bearing formations and other rocks. The procedures are relatively simple, the equipment is portable and recommends itself to the type of field problems associated with Cargodera Canyon. The use of neutron probe measurements in unsaturated rock to determine changes in moisture content is reviewed by Tittman (1956) and McHenry (1962). A more recent discussion, with particular reference to high level radioactive waste disposal, is offered by Andrews (1983). A Swedish experience with this type of neutron probe measurement is described by Nelson et al. (1979).

3.7.2 Theory of Neutron Moisture Probe Operations

A neutron is an uncharged subatomic particle with a mass nearly equal to the hydrogen nucleus. A fast neutron has an energy level greater than one million electron-volts (eV). A slow neutron is one whose energy level is less than one thousand eV. Certain elements emit fast neutrons when they are bombarded by alpha particles. Two neutron sources are radium-beryllium and americium-beryllium. The number of neutrons emitted per second is a function of the rate of disintegration of the alpha particle provider (radium or americium). The target material that emits the neutrons is usually beryllium in commercially available probes. Before they can be detected, the fast neutrons must be slowed down. They are slowed each time they collide with atomic nuclei. Actually, several hundred richochets or collisions occur before a neutron slows to the point where it can be detected.

One exception to this are hydrogen atoms. They have approximately the same mass as the neutrons. When neutrons collide with hydrogen atoms, a tremendous loss of energy occurs. This loss of energy is so great that only 20 collisions are required to slow the neutron to a speed where it can be detected.

The only major source of hydrogen in most soils and rocks is water. If no water is present, the fast neutrons emitted from the probe will bounce away at high speeds and probably will not be detected. If water is present, it will moderate the speed of emitted neutrons. The neutrons will slow down quickly with few collisions and the collisions will have a high probability of being detected.

It is significant that the neutron moisture probe detects any source of hydrogen, not just water. The neutron moisture probe is a hydrogen analyzer and measures moisture only when no other source of hydrogen is present. If other sources of hydrogen are present, the probe reading needs to be adjusted using appropriate calibration.

A significant hydrogen source when determining the water content of low porosity crystalline rock is structural hydrogen. In most porous media, the percent hydrogen structurally bound within the material matrix is small compared to the percent of hydrogen in the water. In low porosity, crystalline rock, the percent bound water often exceeds the maximum saturated porosity of the rock. Nelson and Glenn (1975) report structural hydrogen values of 4.7-8.1 percent by volume from andesite with a porosity of 2.35 percent. Nelson et al. (1979, pp. 136-7) describe a quartz monzonite with structural water of 1.72 percent by volume to a porosity of 0.68 percent.

Standard calibration curves for neutron probe measurements are developed by using the probe in dry and saturated sands. If the saturated porosity of the sand is 30%, the presence of a small quantity of structural hydrogen will result in only a small error. However, for low porosity rock the error would be so great that the standard calibration curves would be meaningless. Since no proper bound water calibrations have been developed for crystalline rock, the neutron probe measurements can only indicate relative changes in moisture content. Andrews (1983) recommends a short spacing between source and detector to compensate for the sensitivity of the radius of influence to small changes in moisture content.

3.7.3 Neutron Moisture Probe Equipment and Procedures

The neutron moisture probe used for field testing at Cargodera Canyon is a CPN 503 Hydroprobe manufactured in 1983 by Campbell Pacific Nuclear Corporation. It is designed to measure the moisture content at depths from 15 cm (6 inches) to 150 m (500 feet) using a radioactive source and internal detection and analysis electronics. Fast neutrons are emitted from the Americium 241/Beryllium source. The detector tube contains boron tri-fluoride. The effective volume for most measurements is an oblong shape with an approximately 15 cm (6 inch) radius from the center of the measurement groove of the probe. This volume increases slightly as the moisture content of the material tested drops. This volume is estimated to encompass 90 percent of the thermalized or slowed neutrons.

Figure 3.27 shows the neutron moisture probe inserted into a standard calibration barrel. Initial calibration of the probe is accomplished in dry sand and then in saturated sand. Water calibration is performed before each field application of the probe. This is accomplished in a barrel filled with water. A final calibration is performed in the field. The probe is read exposed to the atmosphere. This is considered the "standard" count and is used to compute the actual test reading ratios.

Field procedure for the neutron moisture probe begins with the standard count calibration. This involves ten readings of 1 minute duration each while the probe is on the surface but still in its shield. The probe is then fitted over the borehole to be tested. A leveling platform is used to keep the probe centered as it is lowered down the borehole. Figure 3.28 shows the probe container and shield on the leveling platform with the probe downhole. Two readings of one minute each are taken at every foot (30 cm) of depth, beginning at the lowest point to be tested and coming up 30 cm (one foot) for each new set of readings. The shallowest reading is never less than 60 cm (two feet) to avoid exposing probe operators to the unshielded neutron source.

Data reduction involves averaging each set of two readings from each 30 cm (1 foot) depth interval. The high and low standard counts are recorded and the standard deviation is determined using the square root of the average standard count. This standard deviation is added to the average and subtracted to produce the limits within which 68 percent of the standard count readings should fall. This will confirm that the probe is operating properly. Finally, for each depth's average reading, the ratio of the average field count to the average standard count is recorded. This ratio is used to plot the moisture content change over time.

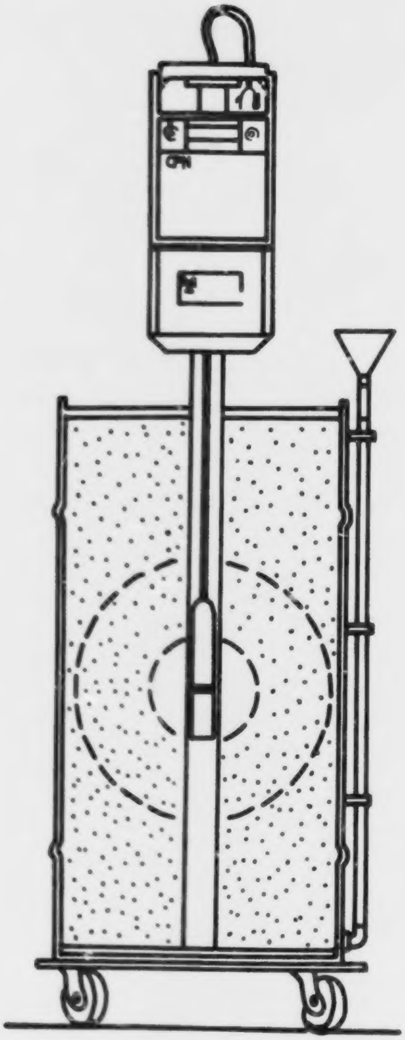

Figure 3.27 Neutron moisture probe inserted in a standard calibration barrel.

BEST COPY AVAILABLE

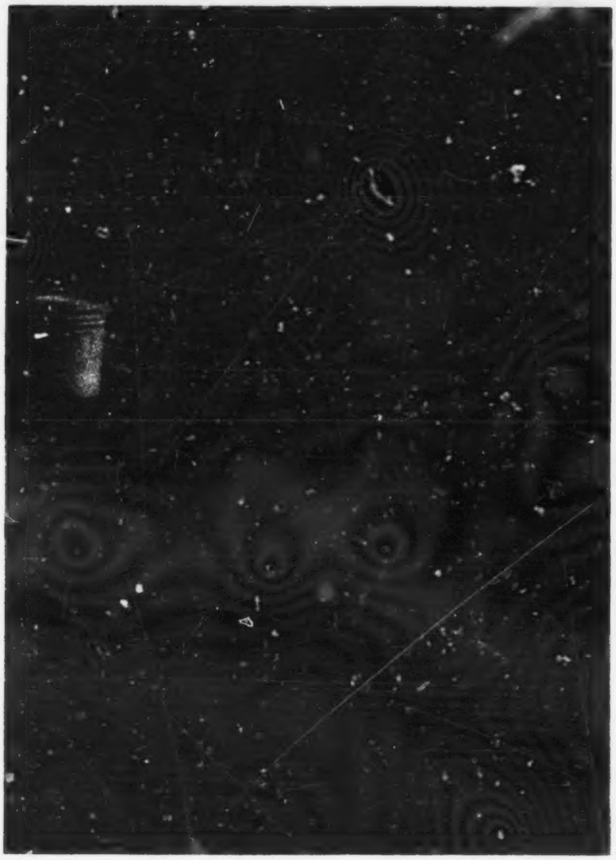

Figure 3.28 Neutron moisture probe container and shield on leveling platform above a hole.

BEST COPY AVAILABLE

CHAPTER FOUR

IN-SITU TESTING OF BOREHOLE PLUGS

4.1 Introduction

This in-situ testing phase has as objectives the emplacement of bentonite plugs and testing their performance. This assessment requires long-term testing over a range of pressure and saturation conditions. Two bunkers were constructed at the lower site to secure the equipment and instrumentation from human or animal interference and to protect it from the elements. Plugs were emplaced using methods and equipment developed in laboratory prototype studies (Section 5.10). Transient pulse testing was used to determine if the plug injection and collection structures are ready for performance testing. Long-term testing was initiated.

The assessment of the sealing performance characteristics of plugs placed in situ in a granitic rock mass is the ultimate goal of this investigation. To do this, several obstacles had to be overcome. Earlier field borehole plug studies were conducted in boreholes that penetrated an aquifer (e.g. Daemen et al., 1985, Chapter 2). Aquifer pressure induced flow through the plug. These conditions enabled permeability assessments to be performed by pressure build-up tests, volume build-up tests and tracer tests. The Oracle Ridge Mine study used a borehole (e.g. Daemen et al., 1985, Ch. 2) that penetrated two drifts, enabling access above and below the plug. This allowed injection of water above the plug and collecting it on the other side (e.g. Daemen et al., 1983, Ch. 2).

Cargodera Canyon only has single-end access boreholes. No aquifer pressure can be utilized. The solution, tubes through the plugs, proved to be the greatest weakness in the plug design and installation.

4.2 Site Preparation

The proximity of the Cargodera Canyon study area to metropolitan Tucson and the location of the lower drill site adjacent to a well-travelled off-road trail mandated the construction of secure bunkers for any long-term testing.

Two bunkers were constructed on the lower site (Figure 4.1). Figure 2.8 shows the design of the larger bunker which enclosed boreholes CCR/C-1 and CCR/C-3. A similar bunker, with the same length and width, but with a sloping floor that reduced available height at one end, encloses CCR/C-2 and CCR/D-4. Both bunkers were fitted with double-lidded steel doors that lock at each end (Figure 4.2). Figure 4.3 shows both bunkers with the bunker enclosing CCR/C-1 and CCR/C-3 in the foreground.

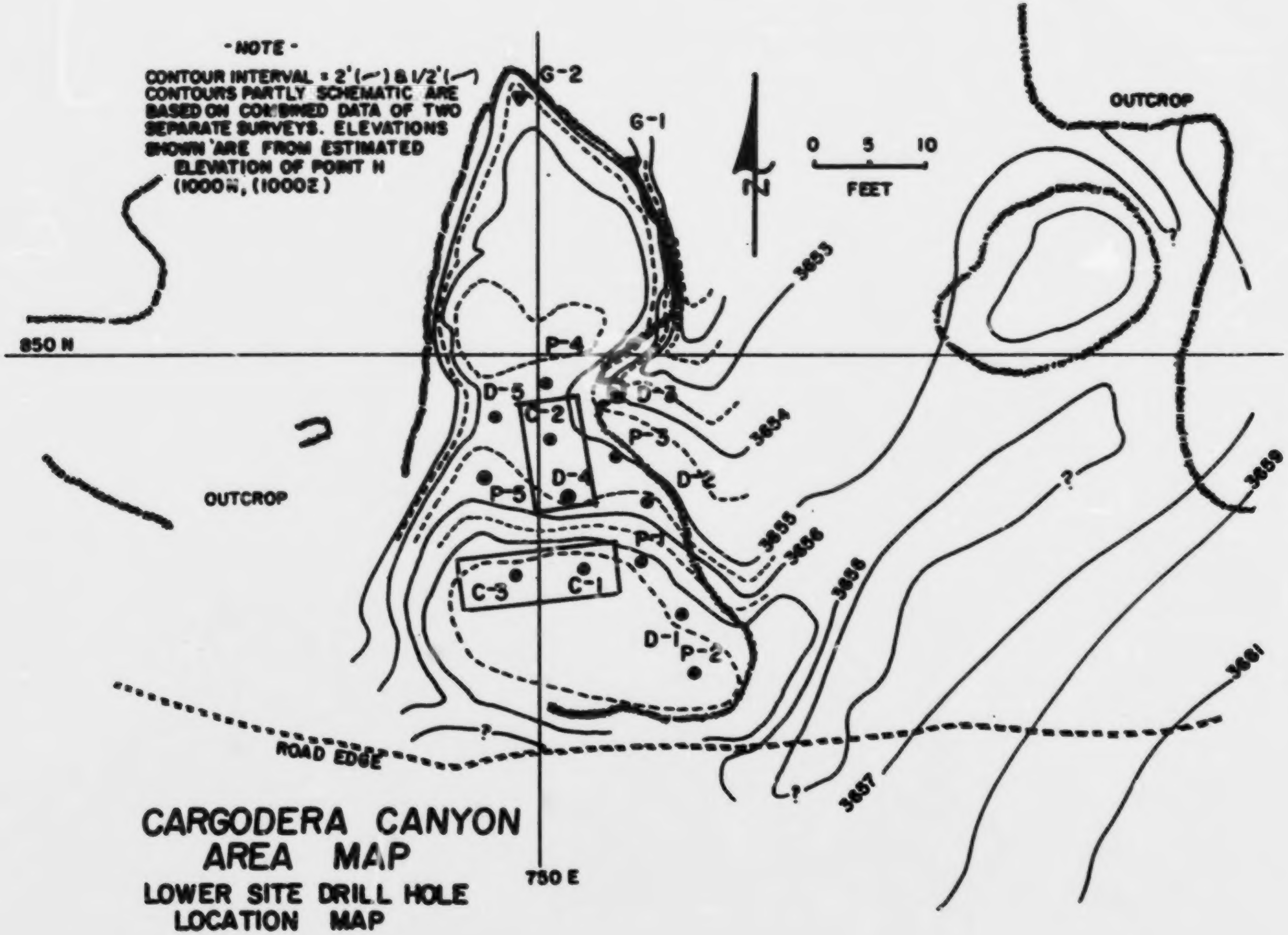
-NOTE-
CONTOUR INTERVAL = 2'(—) & 1/2'(--)
CONTOURS PARTLY SCHEMATIC ARE BASED ON COMBINED DATA OF TWO SEPARATE SURVEYS. ELEVATIONS SHOWN ARE FROM ESTIMATED ELEVATION OF POINT H (1000N, (1000E)
G-2
G-1
N
0 5 10
FEET
OUTCROP
850 N
P-4
D-5
C-2
D-3
P-3
D-4
D-2
P-5
P-1
C-3
C-1
D-1
P-2
OUTCROP
3653
3654
3655
3656
3658
3659
3657
3661
?
ROAD EDGE
750 E
CARGODERA CANYON
AREA MAP
LOWER SITE DRILL HOLE
LOCATION MAP

Figure 4.1 Lower drill site, showing location of bunkers used to protect instrumentation, enclosing boreholes CCR/C-1, C-3 and CCR/C-2, D-4, respectively.

BEST COPY AVAILABLE

Figure 4.2 Inside view of instrument protection bunker.

Figure 4.3 Protective bunkers.

BEST COPY AVAILABLE

4.3 Plug Design

The boreholes tested at the Cargodera Canyon study area are single-access holes in an unsaturated rock. Meaningful performance assessment requires long-term injection testing to determine the hydraulic conductivity of the seal and the seal interface. This estimates conductivity on the basis of measured flow through the plug. Plug design for the boreholes at Cargodera Canyon is based on the desirability to determine the mass balance for the plug-rock seal system under injection pressure.

Plugs with tubes through them provide access to the bottom of the plug. Concern existed regarding the possibility that the interface between the plug and the tube could provide a preferential flow path for the injected water. Such a preferential flow path would "short circuit" the plug-rock system and make any test performed worthless, except as an assessment of the flow conditions existing between a cement plug with a small tube through it. Laboratory tests on a plug with a tube through it were conducted. The results are reported in Chapters 5, 6 and 7.

Figure 4.4 shows the double-plug and collection/tracer system. The system uses two plugs to enclose an injection zone. Collection occurs below the lower plug and above the upper plug. The lower collection system is sealed at the bottom with a 16.3 cm (6.5 inch) diameter PVC cap glued to a fixed wooden disk. The upper collection interval is sealed with a cement plug. The collector and injector systems are connected to the surface with 6 mm (1/4 in) O.D. stainless steel tubing. Tubing for the lower collection interval passes through both lower and upper seals. Tubing for the injection interval passes through the upper seal. Inside the 6 mm (1/4 in) stainless steel tubing is a 3 mm (1/8 in) O.D. stainless steel tube. This double tube arrangement is illustrated in Figure 4.5. Collection or injection occurs through the two lines running parallel to the base of the plug. These are 14 cm (5.5 in) diameter spirals of 6 mm (1/4 in) O.D. copper tubing perforated on both sides to optimize fluid circulation. The collector system operates as a conduit for fluid in the collection interval displaced by flow through the seal or seal-rock interface. The double-tube system can also circulate tracer in any of the three isolated zones until a desired concentration is reached. Figure 4.6 details the installation of the PVC cap that forms the sealed base for the entire plug system. The injection and collection intervals are filled with sand.

4.4 Injection Test Equipment

Injection equipment for plug testing at Cargodera Canyon is designed to provide a range of controlled injection pressures to the borehole seals and to measure the inflow and outflow through the seals and seal rock interfaces. Figure 4.4 is a schematic of the injection apparatus connected to the down-hole apparatus.

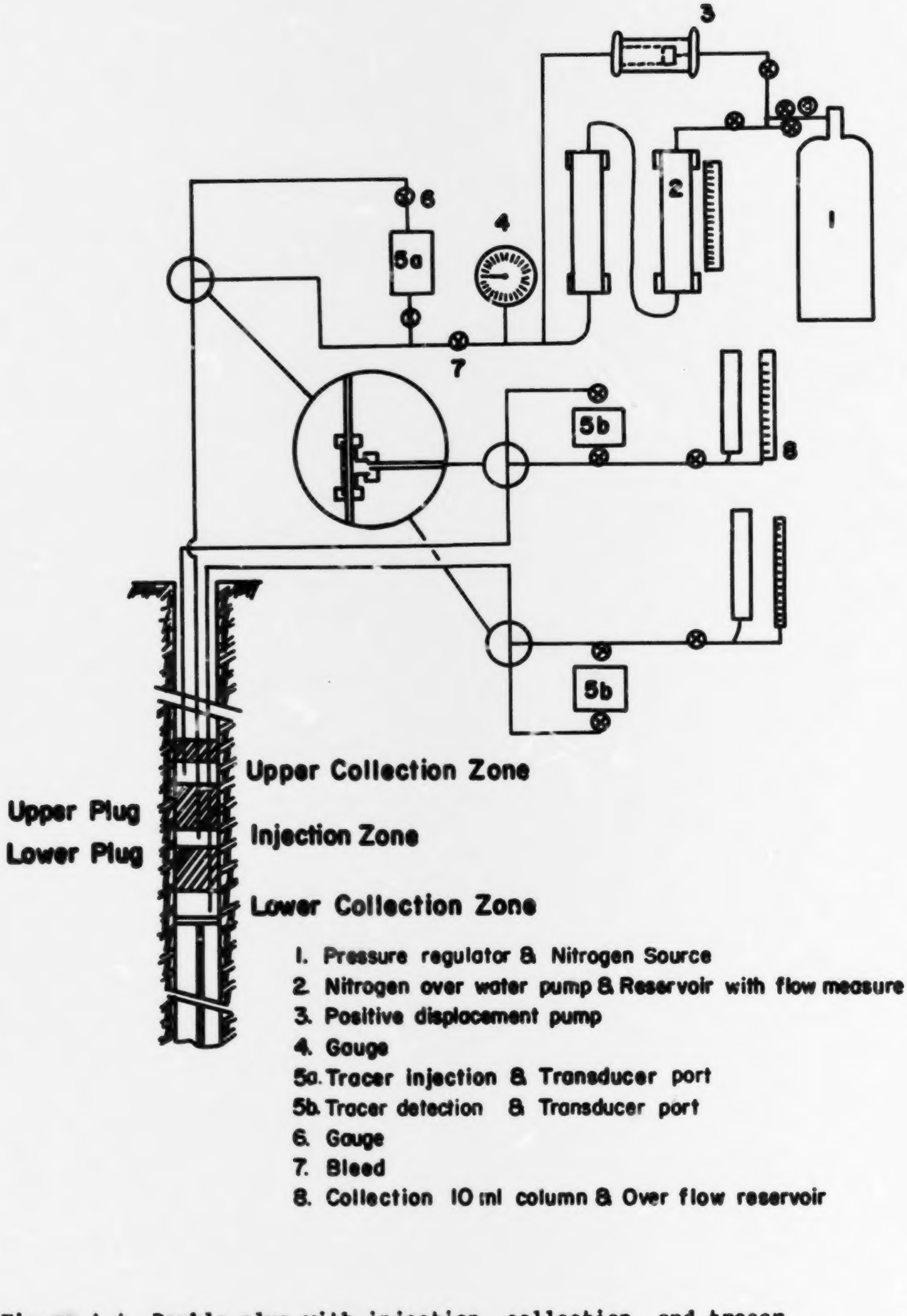
3
6
4
2
1
5a
7
5b
8
5b
Upper Collection Zone
Upper Plug
Injection Zone
Lower Plug
Lower Collection Zone
1. Pressure regulator & Nitrogen Source
2. Nitrogen over water pump & Reservoir with flow measure
3. Positive displacement pump
4. Gauge
5a. Tracer injection & Transducer port
5b. Tracer detection & Transducer port
6. Gauge
7. Bleed
8. Collection 10 ml column & Over flow reservoir

Figure 4.4 Double plug with injection, collection, and tracer monitoring system. Borehole CCR/C-1.

BEST COPY AVAILABLE

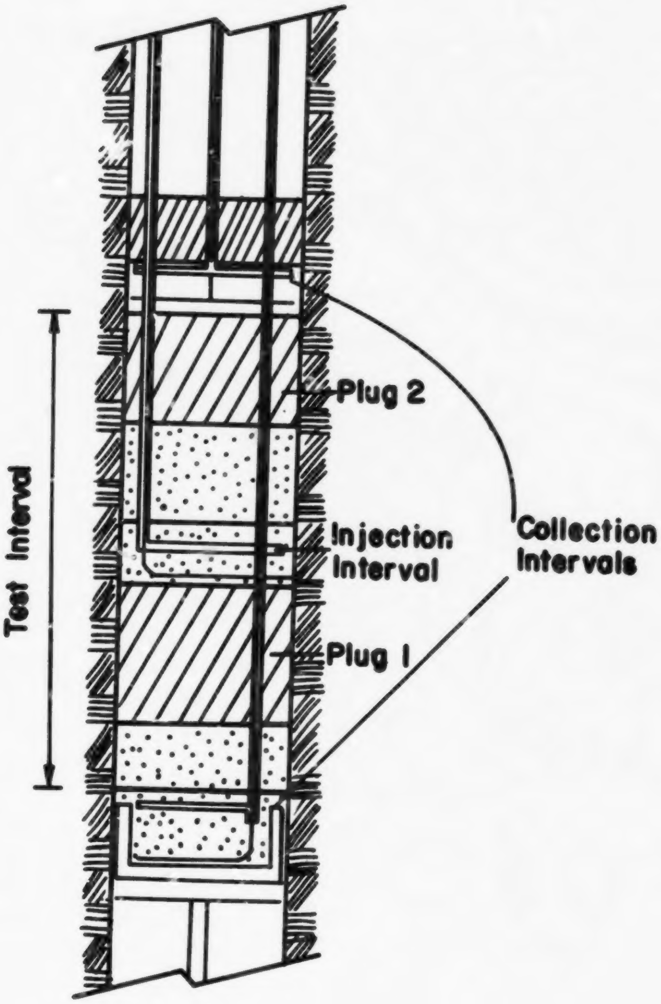
Plug 2
Injection Interval
Collection Intervals
Test Interval
Plug 1

Figure 4.5 Twin-plug bentonite test arrangement with concentric penetrating tubing.

BEST COPY AVAILABLE

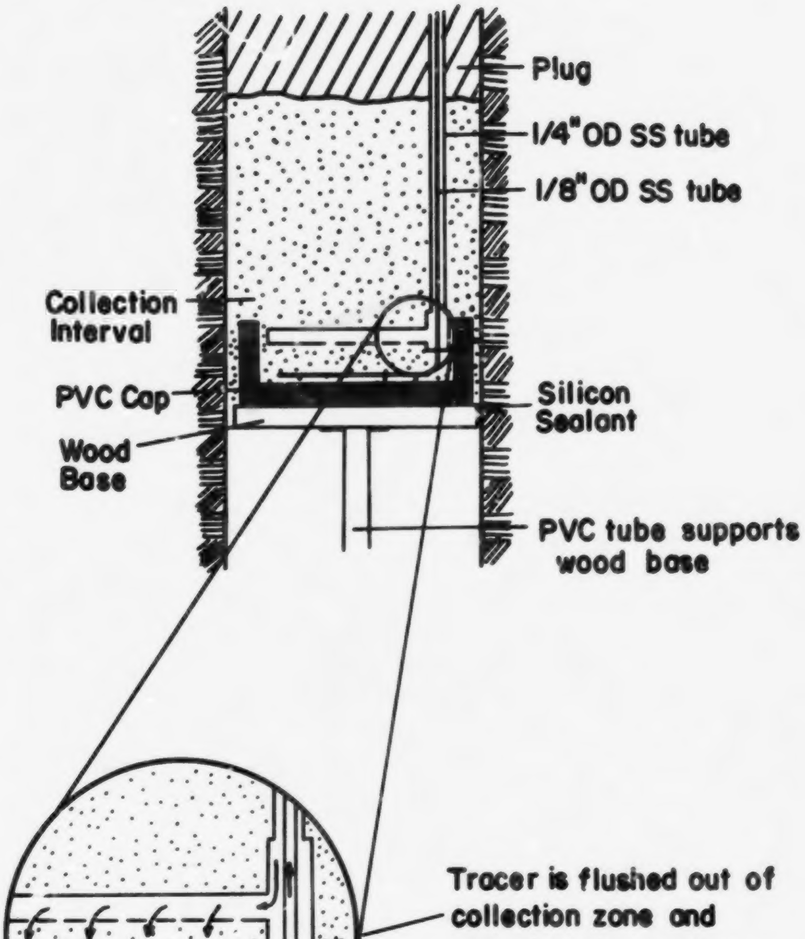
Plug
1/4"OD SS tube
1/8"OD SS tube
Collection Interval
PVC Cap
Silicon Sealant
Wood Base
PVC tube supports wood base
Tracer is flushed out of collection zone and moved to the surface.

Figure 4.6 Bottom collection zone with tracer collection system and bottom seal.

BEST COPY AVAILABLE

Two injection systems are available. The first is a stainless steel pump 30 cm (12 in) long with an inside diameter of 6.25 cm (2.5 inches). A piston inside the pump is driven by nitrogen pressure. The piston displaces water into the injection system. Attached to the piston is a rod that extends outside the cylinder. By precisely measuring the rod displacement, the volume of the injected water can be determined accurately. This system can also be connected to electronic monitoring devices. A linear voltage displacement transducer (LVDT) can be attached to the rod, and can be connected to a data acquisition computer. The pressure of the injected water can be monitored by a pressure transducer connected to the injection line. This data can also be fed into the data logger. The second system utilizes nitrogen over water and contains a large water reservoir to prevent evacuation of all the water, which would allow the nitrogen to interact with the plug.

The system is designed so that pressure can be maintained on the injection interval while the pressure pump system is refilled. Transducers can be mounted on all three interval lines without losing system pressure.

Collection is accomplished using 10 ml capacity pipettes mounted in parallel with 2.5 cm (1-inch) diameter overflow tubes. Figure 4.7 shows the injection and monitoring apparatus installed over borehole CCR/C-1. High negative flows (into the collection zone) were anticipated, based on laboratory experience. The attached tube was installed to prevent overflows or to prevent negative flows from draining the system of water. While the system is not very accurate, it may give a good assessment as to the long-term gross performance of the collection interval. Negative flow is a condition that may only last for a year or so. For long-term assessments of the plug performance, the collection system should be modified to provide greater measurement accuracy. The overflow tube would be disconnected and a sensitive pressure transducer attached to the bottom of the pipette. The pressure transducer would read the head of the water column above it. The transducer can be calibrated to determine the equivalent increase or decrease in water volume in the pipette from the pressure changes.

4.5 Plug Installation

4.5.1 Bentonite Plug Installation in Borehole CCR/C-1

Borehole CCR/C-1 was sealed using two plugs of American Colloid 1/2-inch (1.25 cm) diameter Volclay bentonite tablets. Plug emplacement started in May of 1985 and continued for approximately one month. The interval selected for testing extends from 105 cm (42 inches) to 193 cm (77 inches) below the surface. Plug emplacement was initiated with the installation of the PVC base as outlined in Section 4.3. Great care was taken in emplacing the PVC cap to establish an effective silicone seal around the full contact surface between the PVC cap and the borehole wall. This seal was given 24 hours to cure. The lower collection interval of saturated sand was poured in two steps to allow emplacement of the bottom collection apparatus. The

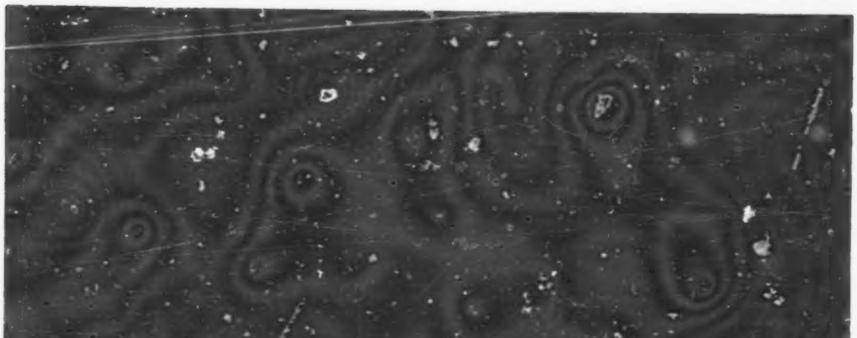

Figure 4.7 Injection test apparatus for borehole CCR/C-1.

BEST COPY AVAILABLE

lower plug was formed by dropping tablets of bentonite through water at a ratio of 1 tablet to 4 cc of water. Initially, 200 bentonite tablets were dropped. Approximately 48 hours later, 600 more tablets were dropped. The last 200 tablets were dropped 48 hours later. One week later the plug was measured as approximately 15 cm (6 inches) long. At that time, the injection interval was emplaced with saturated sand sufficient to form a column 15 cm (6 inches) high. Again, this was done in two steps to allow the installation of injection apparatus in the center of the interval.

The upper plug was formed by dropping 1000 bentonite tablets through water. One week later, plug height was measured as approximately 12.5 cm (5 inches). Another 200 tablets of bentonite were dropped through water to bring the plug length to the desired 15 cm (6 inches). Approximately 72 hours later, the plug was measured at 15 cm (6 inches) of height. The upper collection interval was formed by pouring a volume of saturated sand sufficient to create a 15 cm (6 inch) column. This was done in two steps to allow the emplacement of the upper collection apparatus. Finally, 5 cm (2 inches) of additional sand were poured. This layer was designed to act as a buffer between the upper collection interval and the cement cap to be poured above it. Pouring cement on wet sand can induce piping in the cement (e.g. Daemen et al., 1983, Fig. 3.20; Daemen et al., 1985, Figs. 2.33, 2.34, 2.37) as well as differential penetration of the sand column by stringers of the denser cement (Ch. 7). The cement cap was poured using Dowell System 1 cement prepared as follows:

1) 555 grams of cement,
2) 250 ml of water, and
3) 16 to 18 drops of D-47 antifoaming agent.

This constitutes the ingredients of one batch. Nine batches were prepared and poured. Each batch was mixed using procedures established for Cement System 1 by Daemen et al. (1983, Ch. 9, according to American Petroleum Institute (1977) standards). After a batch was prepared, it was poured into a rubber bucket and stirred while the next batch was prepared. The batches were emplaced three at a time using a bailer. Three days after emplacement the cement cap was measured as 20 cm (8 inches) high. Approximately 2.5 cm (one inch) of standing water is kept above the cement cap at all times to avoid it drying and cracking.

Figure 4.8 shows the actual plug dimensions superimposed on the core log of the test interval in CCR/C-1. Plug emplacement experience suggests that dropping the bentonite tablets in layers creates a more uniformly swelled and longer plug than dropping all pellets for the entire plug at one time. For this reason the lower plug was built with 1000 tablets while the upper plug required 1200 tablets for the same dimensions. Section 6.2 discusses the influence of the injection and collection apparatus on the competence of the bentonite plugs. An effort was made during field plug construction to secure the tubing associated with this apparatus so that minimum movement of the tubing occurred while the plugs were swelling.

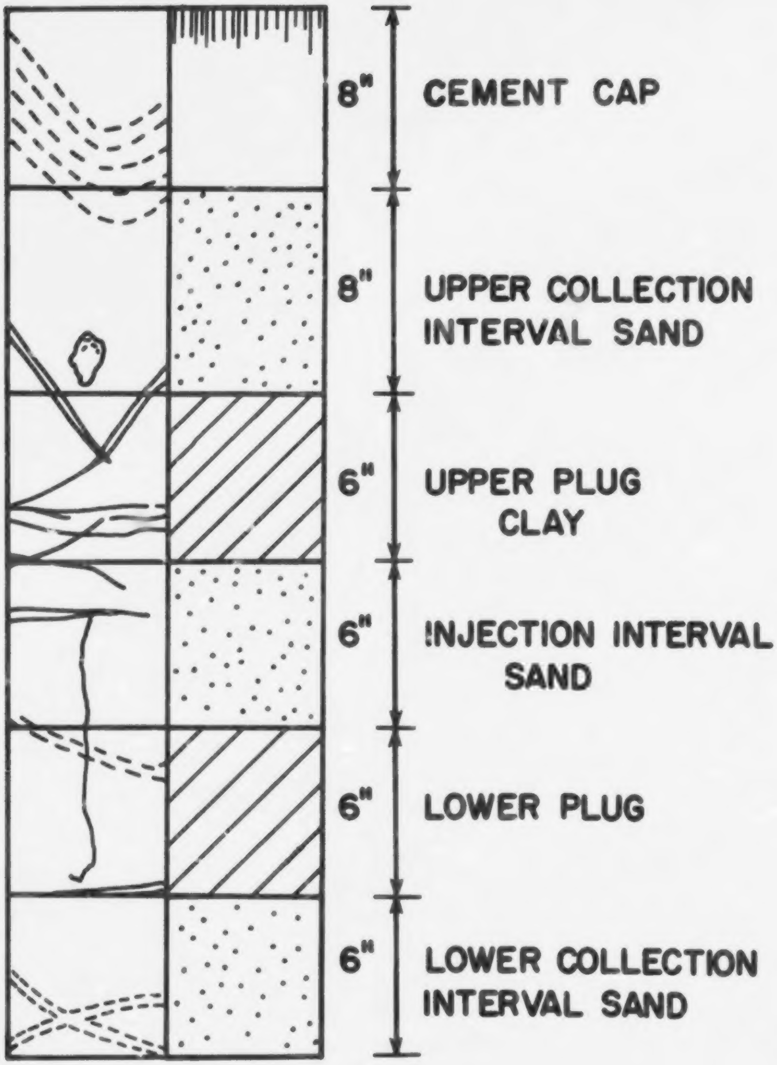

8"
CEMENT CAP
8"
UPPER COLLECTION INTERVAL SAND
6"
UPPER PLUG CLAY
6"
INJECTION INTERVAL SAND
6"
LOWER PLUG
6"
LOWER COLLECTION INTERVAL SAND

Figure 4.8 Bentonite plugs and sand-filled collection intervals in Borehole CCR/C-1 test interval. Lengths measured after installation. Core log map is included on the left side.

BEST COPY AVAILABLE

Table 4.1 lists the borehole sealing bentonite quantities recommended by the manufacturer. For a 16.3 cm (6 1/2 inch) diameter borehole, the recommendation for a 15 cm (6 inch) plug would be 4.275 kg (9 1/2 lbs). Laboratory testing in this study determined the average weight for ten 1.25 cm (1/2 inch) diameter Volclay bentonite tablets as 20.24 grams (0.045 lbs). Using the manufacturer's recommended weight, approximately 2000 tablets would be required to construct the desired seal. This is twice the number of tablets used in this study. Several factors are involved in the difference. The moisture content used in field testing was designed to maximize the swelling of the plug throughout its volume and to create as uniform a plug as possible. This may not be the most effective seal, but to infer performance of the plug as a whole from test results it is important to be able to assume some uniformity of the material tested. It is likely the manufacturer's recommended weight is based on a significantly lower moisture content. The manufacturer does not relate its recommendation to swelling times. The clay tablets swell slowly, especially if they are dropped through water all at once. Field experience suggests that at least 6 to 7 days are required for the plug to reach a final volume if it is allowed to swell freely in the axial direction. If a commercial user needs a given seal volume in a shorter time period, a larger number of tablets would be required.

4.5.2 Cement Plug Installation in Borehole CCR/C-3

Since no valid data existed for the permeability of the rock surrounding the borehole, and hence no hydraulic information regarding fractures, it did not seem desirable to plug the borehole according to the original design. If a fracture existed in the injection zone interval, water would be injected into the fracture and not into the plugs. To a lesser extent, a fracture in either of the collection zone intervals would result in faulty mass balance measurements.

The plug design for borehole CCR/C-3 would have to incorporate a way to inject water into the plugs, and not into an unknown fracture. The solution was to case the injection interval. A 10 cm long, 17.5 cm diameter piece of pvc tubing was used for casing. After the lower plug was poured, the pvc was lowered down the hole on a cord. The cord was attached to the casing through two holes drilled .5 cm from the top of the casing. The casing was lowered until its lower 1 cm was covered in wet cement. The cord was secured at the surface to keep the casing in place as the cement hardened. The following day, the cord was removed from the casing and work on the top plug commenced.

Before pouring the top plug, the injection apparatus was placed inside the casing. The casing was filled to within 2 cm of its top with sand. The upper plug was poured on top of the cased-off injection interval (Figure 4.9). Problems later arose when it was discovered that the upper plug had invaded most of the sand in the injection interval, making it impossible under the present conditions to conduct tracer tests in this hole.

Table 4.1 Weight of Bentonite Tablets Required for Borehole Seal with A Depth of 30 cm (1 ft) (American Colloid Company Volclay Tablets)

Hole Diameter (inches)	Weight of Tablets* (lbs)
2	1.77
3	4
4	7.11
5	11.11
6	16
7	21.77
8	28.44

*The manufacturer notes that swelling characteristics of clay can be affected by water quality.

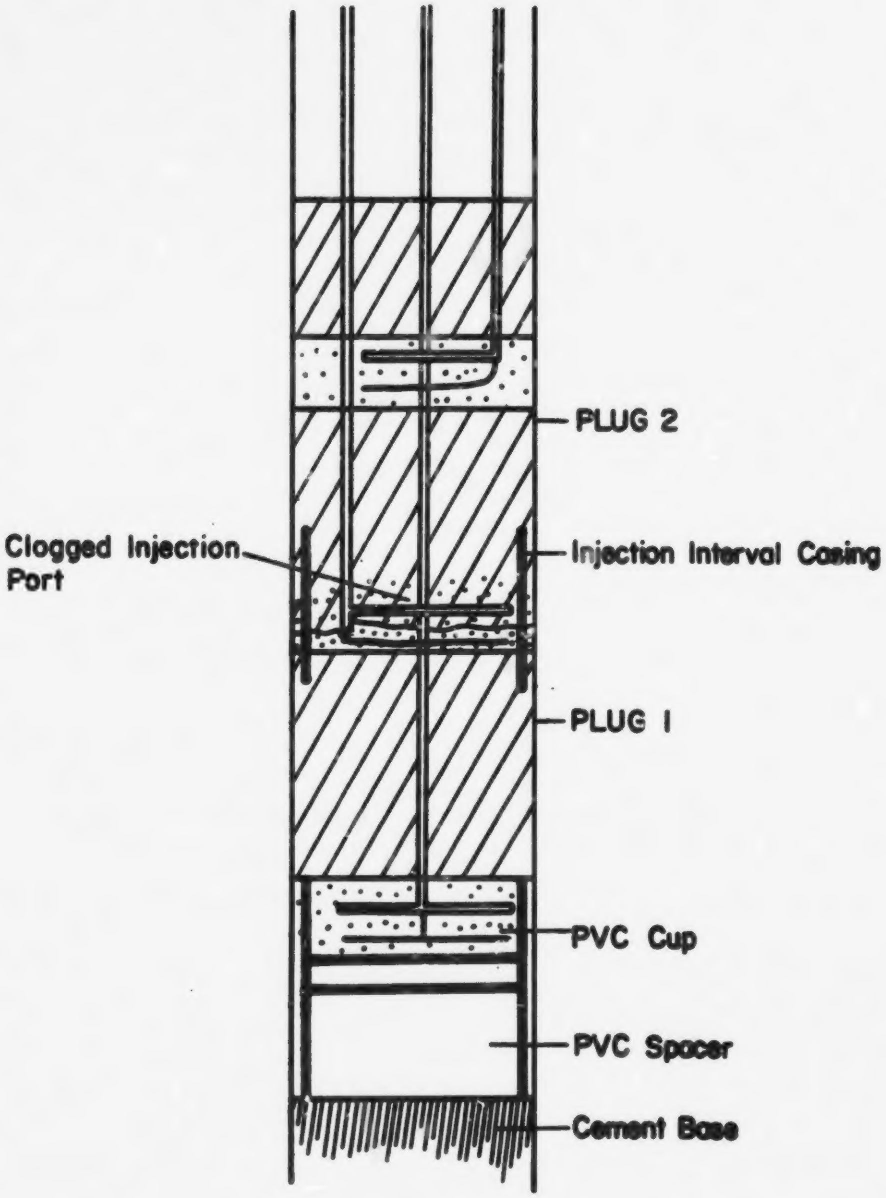
PLUG 2
Clogged Injection Port
Injection Interval Casing
PLUG I
PVC Cup
PVC Spacer
Cement Base

Figure 4.9 Cement plug in borehole CCR/C-3.

BEST COPY AVAILABLE

4.5.2.1 Plug Emplacement Procedure. The bottom of hole C-3 is quite shallow, and near the target depth for plug emplacement. An 18 cm high base was made of 17.5 cm diameter PVC tubing and was capped at the top with a 1.25 cm thick PVC disk. A ring with an inside diameter of 10 cm and an outside diameter of 17.5 cm was made of the same material and was glued on top of the cap. The cap had a 2.5 cm (1 in) NPT hole in the center. The threading enabled the base to be attached to a pipe which lowers the base into position. Once the base is on the bottom of the hole, the pipe is unscrewed from the base and lifted out of the hole.

The collector cup fit on top of the base (Figure 4.10). The cup was also constructed of 17.5 cm PVC pipe. The cup was 10 cm long and was capped on the bottom by 1.25 cm thick PVC. A disk 9.75 cm x 1.25 cm was centered on the bottom of the cap. A 2.5 cm (1 in) NPT flange was mounted in the center of the cap on the interior of the cup. The cup was lowered in the same manner as the base. Before lowering the cup, the annulus outside the disk was heavily coated with silicon seal. As the cup lowers on top of the base, the ring on the base and the disk on the cup forces the silicon outside along the edges of the borehole, sealing the collector from the bottom. Once the base/collection cup system was in place, the cup was filled to 1 cm past its top with sand.

The cement plug was made of nine standard batches of System 1 cement (Daemen et al., 1983, Table 9.1) that were mixed separately then together before being placed in the bailer. The bailer was a 1.2 m long, 10 cm diameter PVC pipe capped on one end. Several 1 cm diameter holes were drilled along the bottom edge of the bailer, in hopes that the side release would be less violent than a bottom release. The upper plug was also made of nine batches of System 1 cement and was poured with the bailer.

Following the installation of the top plug, the collection system for it was installed. The collection tubing with circulation ports was lowered into the hole, covered with 6 cm of sand and a final 15 cm cap of cement was poured.

4.5.2.2 Post-Installation Work. Sorted, dry Ottowa sand is used in this test. Wet sand could not be used due to problems encountered when cement was poured on top of it (Chapter 7). Before the test could be started the sand had to be saturated. Saturation of the sand was achieved by attaching a vacuum pump to one of the two output lines from the collection or injection system, while the other line was shut off. A vacuum was applied for five minutes. At the end of this time, a valve between the vacuum and the sand interval was closed and a valve on the other line to the interval was opened with the end of the line immersed in water. Water was allowed to flow into the interval until equilibrium was attained.

The cement invasion of the sand layer was first noticed during the saturation of the injection interval. The vacuum built up immediately on the line to the upper injection port, indicating that it had been clogged with cement. The vacuum in the lower interval built up

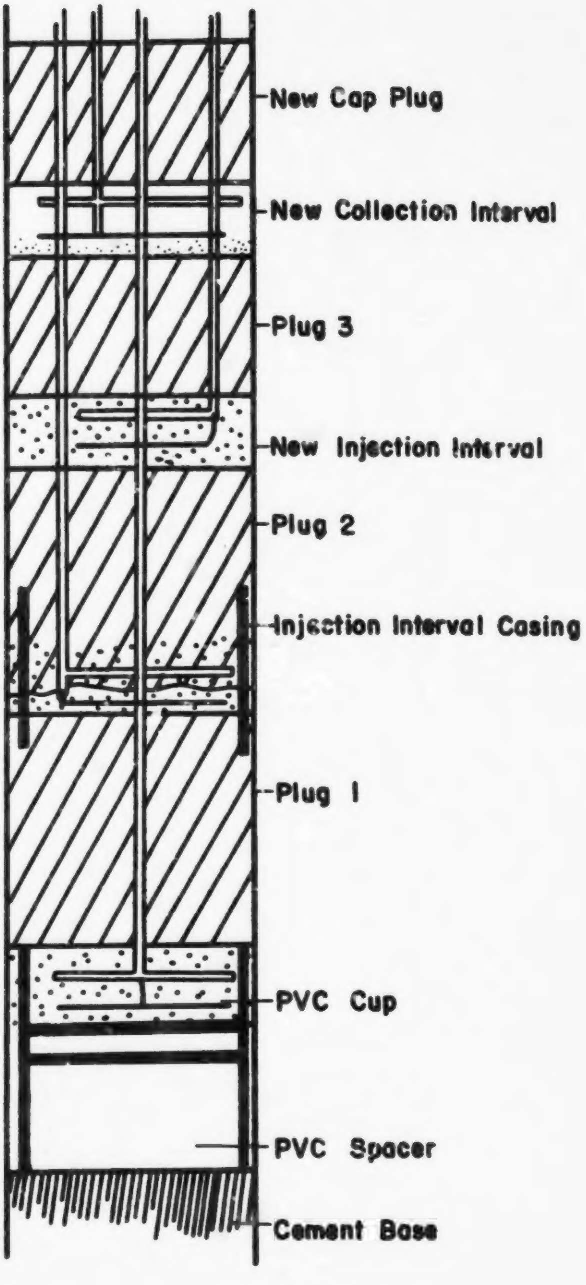
New Cap Plug
New Collection Interval
Plug 3
New Injection Interval
Plug 2
Injection Interval Casing
Plug 1
PVC Cup
PVC Spacer
Cement Base

Figure 4.10 Schematic for borehole CCR/C-3 with new top plug.

BEST COPY AVAILABLE

slower, indicating that the cement had not completely invaded the injection interval. Another reassurance that the cement had not completely filled the injection interval was that over 100 cc of water was taken from one tube, indicating that there was void space in the sand around the lower injection port.

It was most unfortunate that the injection interval had to be cased. Casing the interval isolated the cement. Hydraulic conductivity measurements assessed the quality of the cement only and not its overall performance as a sealant within the rock. However, the flexibility of the design enables any interval to act in either a collection or injection capacity. As such, another collection interval was placed on top of the cap plug after approximately 90 days of constant head tests, and an additional cap plug was poured over it. The old upper injection interval was connected to the injection pump and the old injection interval became the lower collection interval (Figure 4.10). A new test was started, this time enabling the granite, plug and interface to be tested.

4.5.3 Cement Plug Installation in Borehole CCR/C-2

The experience gained in plugging CCR/C-3 proved valuable when plugs were placed in CCR/C-2. Minor changes were made in the plug design to improve the performance of the testing equipment. The first change was to place the bottom collection interval on a cement base. The performance of the bottom collector in CCR/C-3 has shown that the silicone seal is not effective in sealing the interval from the bottom. The second change was to use approximately 2.5 cm (one inch) more sand in each interval. The clogged injection port in CCR/C-3, even though it occurred under special circumstances, warranted the avoidance of a similar incident.

The installation proceeded by placing the lower collection tubing down the borehole and pouring 2 liters of sand on top of it. A plug was placed on top of the lower collection interval by bailer. The plug is made from 9 batches of System 1 cement, as before. The following day the plug had hardened, allowing the injection interval to be placed. The injection tubing was lowered, covered with 2.5 liters of sand, and the top plug poured on top of it. The top plug is 9 batches of System 1 cement, also bailer placed. The same procedure was repeated for the top collection interval. However, the cap plug was only 7 batches of System 1 cement.

A new problem identified itself upon placement of the cap plug. After the bailer was emptied, it caught on one of the tube assemblies down the hole as it was raised. The bailer was lowered down, then gently pulled upwards in an attempt to free it. The bailer did free itself, but not until it had raised the upper collection tubing several inches. It was not discovered until later that the collection apparatus had been raised and that the top coil had become covered with cement. However, during saturation of that interval, the interval took a large quantity of water, allaying any fears that this interval would not perform as well as the others. The only restriction imposed by the clogged port was the inability to sample for tracer in that interval.

The last problem noticed with the system arose when the intervals were being saturated. The injection interval never built up sufficient vacuum to draw water into it. The vacuum pump was disconnected. A line from the interval was connected to a nitrogen bottle. A small pressure increment was applied to the line. After a few seconds a hissing sound was heard coming from the borehole. Water was trickled down the hole onto the fittings. The TEE on the 2.5 cm (1/4 in) tube was observed to be bubbling. Apparently, a fitting on the TEE had not been tightened sufficiently before it was lowered down the borehole and cemented in place.

The leaky fitting was sealed by pouring a cement plug around it. Sand was poured down the hole on top of the cap plug until it was 20 cm (8 inches) below the fitting. Fifteen batches of cement were placed on top of the sand. The top of the cement plug was 20 cm (8 inches) above the fitting. This was decided to be the best solution to the leaky fitting. The leak was small enough that cement would not invade the tubing. It was hoped that water from the tubing would not be absorbed by the cement plug in appreciable quantities.

4.6 Transient Testing of Bentonite Seals

4.6.1 Introduction

The objective of transient testing of bentonite seals is to assess the effectiveness of the seals before long-term testing is initiated. The hydraulic conductivity of soils is a function of the degree of saturation (e.g. Hillel, 1971, pp. 106-9; Lambe and Whitman, 1979, p. 292). This is important in the seal environment where achieving complete saturation may require an extended injection time. Actual flow through the plugs may not be measured for a long time as the bentonite slowly achieves saturation. In addition, the collection system on the outflow side of each plug also functions as a drain, allowing the bentonite plugs to consolidate to some degree under injection pressure. This suggests that at least part of any initial outflow may be the result of consolidation and not flow through the plugs. These factors make analysis of long-term flow through the seals and seal-rock interfaces difficult. Transient testing provides a means of approximating the competence of the plugs and of the entire tested interval, i.e. the plug-rock sealing system, in a short period of time.

4.6.2 Equipment and Procedures

The injection system designed and installed for long-term testing of bentonite seals in CCR/C-1 is equally suited for short-term transient pulse testing. A pressure pulse is generated by the pressure system and isolated between valves while it is bled to an appropriate level. By connecting the injection line to the line leading to the collection interval, the pressure pulse can be delivered to collection intervals as well as to the injection interval. Decay of the pressure pulse is monitored by a 172 kPa (25 psi) Dynisco transducer mounted on the appropriate interval line. A continuous record is maintained by the three-channel strip chart recorder used previously in borehole pressure slug testing. Intervals are tested individually and, initially, one at a time to avoid interference from pressure leaking from other intervals.

4.6.3 Analysis of the Hydraulic Conductivity of Bentonite Plugs

Analysis of the results of pressure decay tests of borehole intervals sealed with bentonite plugs is complicated by the flow assumptions that underly existing methods of treating pressure slug data. The Cooper et al. (1967), Papadopulos et al. (1973), and Bredehoeft and Papadopulos (1980) methods discussed in Section 3.5 treat all flow in the borehole as perpendicular to the axis of the test interval. Hsieh et al. (1981) developed a method for analyzing pressure decay through a "plug" tested in the laboratory. This method is discussed in Chapter 5. It assumes all flow in the test interval is through the plug, parallel to the axis of the interval.

The pressure slug tests of in-situ bentonite plugs at Cargodera Canyon take place in intervals where water flows in two directions (Figure 4.11). Developing an analytical solution for the unique and complex boundary conditions that characterize this type of flow regime is beyond the scope of this study. South and Daemen (1986) present numerical sensitivity analyses for various configurations and plug-rock relative permeabilities. Existing solutions do suggest an analytical method for approximating the hydraulic conductivity performance of the plugs in the test interval.

The Bredehoeft and Papadopulos (1980) solution described in Section 3.5 includes a term (S_w) that takes into account the compliance of the packers, as well as the compressibility of water. This term is used when the hydraulic conductivity of the test interval is calculated. The term is used as follows:

$$\beta = \frac{\pi K L t}{S_w} \tag{4.1}$$

where K is the hydraulic conductivity, L is the length of the borehole interval tested, t is time, and β is the value taken from the type curve solution after curve matching, and

$$S_w = V_w \gamma_w Cps \tag{4.2}$$

where V_w is the volume of water in the test interval, γ_w is the specific weight of water, and Cps is a pseudo-compressibility term that represents the combined effects of water compressibility and equipment compliance.

The approximation method suggested in this analysis requires that the plugs themselves be treated as packers are treated in the Bredehoeft and Papadopulos (1980) solution, i.e. as complying seals at the ends of the test interval. Packer compliance describes the deformation of

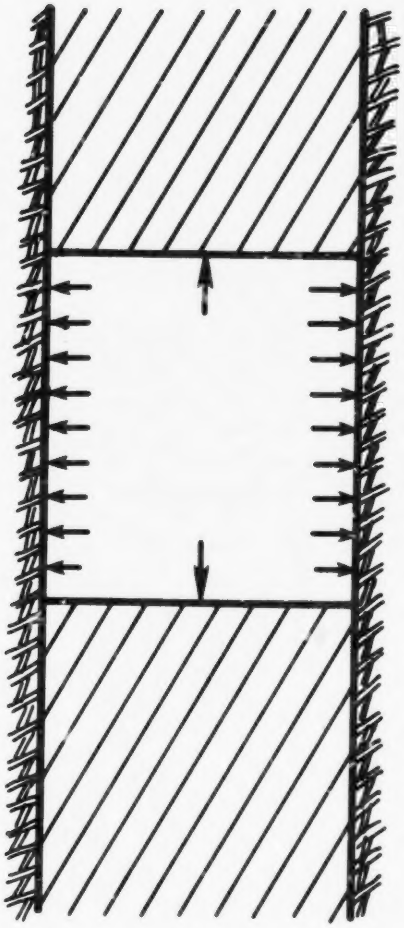

Figure 4.11 Axial and radial flow from an injection section between two plugs.

BEST COPY AVAILABLE

packers when subjected to pressure. Bentonite seals can be treated as compliant seals, deforming when subjected to pressure in the borehole interval. Packers comply by retreating to release pressure. Bentonite seals can be expected to consolidate to some degree and to allow some pressure release in the form of fluid passing through the plugs.

The hydraulic conductivity of the interval is already known from previous field testing. The Cps term can be found by rewriting equation (4.1) as:

$$S_w = \frac{\pi KLt}{\beta} \tag{4.3}$$

K and L are known. β and t are found by matching a curve of pressure decay in the plugged test interval to type curves developed from the Bredehoeft and Papadopulos solution (1980) as described in Section 3.5.

The compressibility term can be found by rewriting equation (4.2) as:

$$Cps = \frac{S_w}{V_w \gamma_w} \tag{4.4}$$

where S_w is known and V_w is the volume of water in the test interval.

Cps is normally found by preliminary calibration of field equipment as described by Hsieh (1983). Hsieh (1983, p. 87) gives the equation:

$$Cps = \frac{1}{V_w} \frac{\Delta V}{\Delta P} \tag{4.5}$$

where V_w is the water volume in the test interval and ΔV is the water volume used to induce the pressure increase ΔP.

If Cps is known and V_w is the water volume in the test interval, then

$$\frac{\Delta V}{\Delta P} = V_w \, Cps \tag{4.6}$$

This expression describes the volume ΔV that needs to be injected to induce a pressure increase ΔP when deformable packers (seals) isolate the test interval.

An empirical description of one-dimensional flow is given by Darcy's Law which states that the flow rate, Q, is proportional to the cross-sectional area, A, of the sample tested, proportional to the change in head, Δh, and inversely proportional to the length, L, of the sample tested. The coefficient of proportionality for this relationship is K, the hydraulic conductivity of the sample. Then

$$K = \frac{QL}{A\Delta h} \tag{4.7}$$

where $Q = \Delta V/t$ is the flow rate. Plug hydraulic conductivity can be approximated from

$$K = \frac{\Delta VL}{A\Delta Pt} \tag{4.8}$$

where L is the length of the plugs, A is their cross-sectional area, t is the test duration, and ΔV the cumulative flow through the plugs over the time t.

The hydraulic conductivity thus calculated should be considered a conservative estimate. The ΔV/ΔP value used assumes that the entire plug compliance is expressed in flow through the plugs. Laboratory observations (Chapters 5 and 6) show that plugs do consolidate initially under the induced pressure in the interval. L is not constant. This means that only a portion of the volume used to estimate the hydraulic conductivity of the plugs actually passes into the plugs.

It should be noted that the initial hydraulic conductivity K used to calculate S_w is obtained from the response of the entire borehole test interval. Local conductivities for individual injection or collection intervals may differ from the overall conductivity.

4.6.4 Analysis of Bentonite Plug Storativity

Analysis of field tests for the hydraulic conductivity of the borehole interval selected for sealing did not include any analysis of the specific storage of the host rock. The storage coefficient (or storativity) is defined as the volume of water stored or released by an aquifer per unit surface area per unit change in the head normal to the surface area (e.g. Todd, 1976, p. 45; Freeze and Cherry, 1979, p. 60). Crystalline rocks are expected to have low storage coefficients, 10^{-4} to 10^{-6} (Kruseman and de Ridder, 1970). Bear (1979, p. 89) lists the same range as representative for confined aquifers in general. Hsieh (1983, p. 23) references the limitations of the Cooper et al. (1967), Papadopulos et al. (1973), and Bredehoeft and Papadopulos (1980) solutions for calculating the value of storage coefficients.

When α (equation 3.27, Section 3.5.2) is smaller than 10^{-5}, the shapes of the type curves are very similar and the curves are close to each other. The solutions involved in determining the hydraulic conductivity of borehole intervals before they were sealed use α

values smaller than 10^{-5}. For this reason, no effort is made to estimate the storage coefficient of the rock.

Large α values are more likely to occur in materials with high storage coefficient values, such as unconsolidated clays (Hsieh, 1983, p. 23). The solutions and type curves appropriate to analyzing pressure decay in the plugged intervals involve larger α values, with type curves spaced more widely (Appendix B). Specific storage values can then be computed with more confidence.

The type curves used in analyzing pressure decay in plugged test intervals assume all flow occurs normal to the axis of the test interval. The storage coefficient is considered to be a property of the host rock that receives flow though the borehole wall. In the case of the intervals plugged with bentonite at Cargodera Canyon, however, the storativity of the rock is small compared to the assumed storativity of the clay, differing by several orders of magnitude. If the solution involves a large α, the storativity could be considered primarily a function of the plug storativity, where α is defined by equations 3.13 and 3.27.

$$\alpha = \frac{r_w^2 S}{S_w} \qquad (4.9)$$

and S is the storage coefficient (Papadopulos et al., 1973).

Bredehoeft and Papadopulos (1980) note that for α values greater than 0.1 the type curves plotting F(α,β) against β are similar in shape and spaced significantly apart. Matching these curves could involve significant errors in calculating hydraulic conductivity. They suggest, instead, that curves be used plotting F(α,β) against the product of αβ, where αβ is:

$$\alpha\beta = \frac{\pi r_w^2 SKLt}{S_w^2} \qquad (4.10)$$

This solution only allows the calculation of the product of hydraulic conductivity and the storage coefficient.

4.6.5 Results of Transient Pulse Testing of Bentonite Seals

Four pressure decay tests were performed on the sealed intervals in borehole CCR/C-1. Table 4.2 presents the results of the first test. The injection pressure was set at 48 kPa (7 psi) and the test was started when interval pressure was 47 kPa (6.8 psi). Table 4.3 shows the results of the second pressure decay test performed on the injection interval in CCR/C-1. Testing was initiated with an interval

Table 4.2 Borehole CCR/C-1 Injection Interval Pressure Decay Test #1 (Bentonite Plugs)

Time (min)	Pressure (psi)	H/H_o * (%)
0	6.8	100
45	6	88.2
105	5.78	85
165	5.56	81.7
225	5.41	79.6
285	5.31	78.1
345	5.25	77.2
405	5.10	75
465	5.05	74.3
525	4.94	72.8
585	4.88	71.8
645	4.82	70.9
705	4.69	69
765	4.63	68.1
825	4.54	66.8
885	4.47	65.7
945	4.46	65.6
1005	4.5	66.2
1065	4.45	65.4
1125	4.32	63.5
1185	4.26	62.6
1245	4.2	61.8
1305	4.16	61.2
1365	4.01	59
1425	3.94	57.9
1485	3.94	57.9
1545	3.94	57.9
1605	3.88	57.1
1665	3.69	54.3
1725	3.67	54
1785	3.57	52.5
1845	3.48	51.2
1905	3.38	49.7
1965	3.32	48.8
2025	3.26	47.9
2085	3.25	47.8
2145	3.2	47.1
2205	3.11	45.7
2265	3.07	45.1
2325	3.06	45
2385	3.09	45.4
2445	3.1	45.6
2505	3.13	46
2565	2.95	43.4
2625	2.92	42.9

---

*Pressure H as a percent of initial pressure H_o.

Table 4.3 Borehole CCR/C-1 Injection Interval Pressure Decay Test #2 (Bentonite Plugs)

Time (min)	Pressure (psi)	H/H_o * (%)
0	7.78	100
60	7.68	99
120	7.28	94
180	7.07	91
240	6.77	87
300	6.64	85
360	6.51	84
420	6.23	80
480	6.07	78
540	5.94	76
600	5.75	74
660	5.54	71
720	5.47	70
780	5.34	69
840	5.21	67
900	5.06	65
960	4.9	63
1020	4.87	63
1080	4.68	60
1140	4.59	59
1200	4.49	58
1260	4.39	56
1320	4.27	55
1380	4.27	55
1440	4.18	54
1500	4.05	52
1560	4.01	52
1620	3.93	51
1680	3.80	49
1740	3.69	47
1800	3.6	46
1860	3.43	44
1920	3.34	43
1980	3.24	42
2040	3.12	40
2100	3.02	39
2160	2.92	38
2220	2.75	35
2280	2.70	35
2340	2.60	33
2400	2.41	31
2460	2.30	30
2520	2.24	29
2580	2.14	28
2640	2.04	26
2700	1.95	25

Table 4.3 Borehole CCR/C-1 Injection Interval Pressure Decay Test #2--Continued

Time (min)	Pressure (psi)	H/H_o * (%)
2760	1.84	24
2820	1.75	23
2880	1.7	22
2940	1.66	21
3000	1.63	21
3060	1.53	20
3120	1.13	15
3180	1.01	13
3240	.89	11
3300	.76	10
3360	.51	7
3420	.47	6
3480	.35	5
3540	.23	3
3600	.19	2
3660	.14	2
3720	.09	1
3780	0	0

*Pressure H as a percent of initial pressure H_o.

pressure of just under 55 kPa (8 psi). Table 4.4 presents the results of the pressure decay test on the upper collection interval with an injection pressure set at 38 kPa (5.5 psi). Table 4.5 gives the results of the decay test performed on the lower collection interval. Testing was initiated when interval pressure was approximately 55 kPa (8 psi).

The analysis of these tests utilizes the methods discussed in Sections 3.5.2 and 4.6.3. For each test, a curve was prepared of dimensionless pressure decay against the log of time in minutes (Figures 4.12 through 4.15).

Curve matching was accomplished using the type curves discussed in Section 3.5.6 and plotted in Appendix B. Measured curves are superimposed on the type curves and moved horizontally, keeping the abscissa coincident, until a match with a type curve is achieved. For the first injection interval test, a match with the $\alpha = 0.1$ curve gives a time of 520 minutes for a β of 0.1. The second test in the injection interval matches with the $\alpha = 10^{-5}$ curve and at $\beta = 1$ gives a time of 720 minutes. The upper collection interval test matches the $\alpha = 0.5$ curve and at a β of 0.01 gives a time of 140 minutes. The lower collection interval test matches the curve of $\alpha = 1$ and for a β of 0.01 gives a time of 110 minutes. These results are summarized in Table 4.6.

The hydraulic conductivities listed in Table 4.6 are for the seals and the seal-rock interface, as described in Section 4.6.3. The values calculated for the injection interval actually represent two plugs, one on each end of the interval. The storativity coefficients are calculated using the method described in Section 4.6.4. Equation (4.9) relates α to storativity, S. S_w is treated as the compressibility of the water in the volume tested, to isolate the contribution of the storativity of the seals themselves.

The best method for judging the significance of the hydraulic conductivities calculated for the bentonite seals and seal-rock interfaces is to compare them to values established by laboratory testing reported in Sections 6.2, 6.3, 6.8 and 6.9. The values calculated from field tests are higher than those determined in the laboratory, but close to the values for the interval in CCR/C-1 determined in Section 3.5.6. The field test values can be expected to be higher given that they measure not only the hydraulic conductivity of the plug but also the effectiveness of the plug-rock interface. In addition, the method used to calculate field hydraulic conductivities is conservative as it does not take into account the actual compliance of the plugs when subjected to a pressure pulse. No effort was made to estimate the rate at which the plugs tested in-situ consolidate under pressure. This would be difficult to do as they drain into large reservoirs that are constantly losing water to the swelling plugs. Nevertheless, the values calculated for plug performance in the field seem to meet the standard of conductivity determined by the hydraulic conductivity of the borehole interval itself. Finally, the

Table 4.4 Borehole CCR/C-1 Upper Collection Interval Pressure Decay (Bentonite Plugs)

Time (min)	Pressure (psi)	H/H_o * (%)
0	5.42	100
60	4.92	90.8
120	4.74	87.5
180	4.57	84.3
240	4.42	81.5
300	4.29	79.2
360	4.22	77.9
420	4.15	76.6
480	4.03	74.4
540	3.96	73.1
600	3.91	72.1
660	3.85	71.0
720	3.74	69.0
780	3.61	66.6
840	3.58	66.1
900	3.55	65.5
960	3.46	63.9
1020	3.41	62.9
1080	3.33	61.4
1140	3.28	60.5
1200	3.13	57.7
1245	3.10	57.2

*Pressure H as a percent of initial pressure H_o.

Table 4.5 Borehole CCR/C-1 Lower Collection Interval Pressure Decay (Bentonite Plugs)

Time (min)	Pressure (psi)	H/H_o * (%)
0	7.9	100
60	6.77	85.7
120	6.23	78.9
180	6.10	77.2
240	5.97	75.6
300	5.72	72.4
360	5.47	69.2
420	5.22	66.1
480	4.99	63.2
540	4.87	61.7
600	4.74	60
660	4.58	57
720	4.49	56.8
780	4.33	54.8
840	4.27	54.1
900	4.14	52.4
960	4.08	51.7
1020	4.01	50.8
1080	4.00	50.6

*Pressure H as a percent of initial pressure H_o.

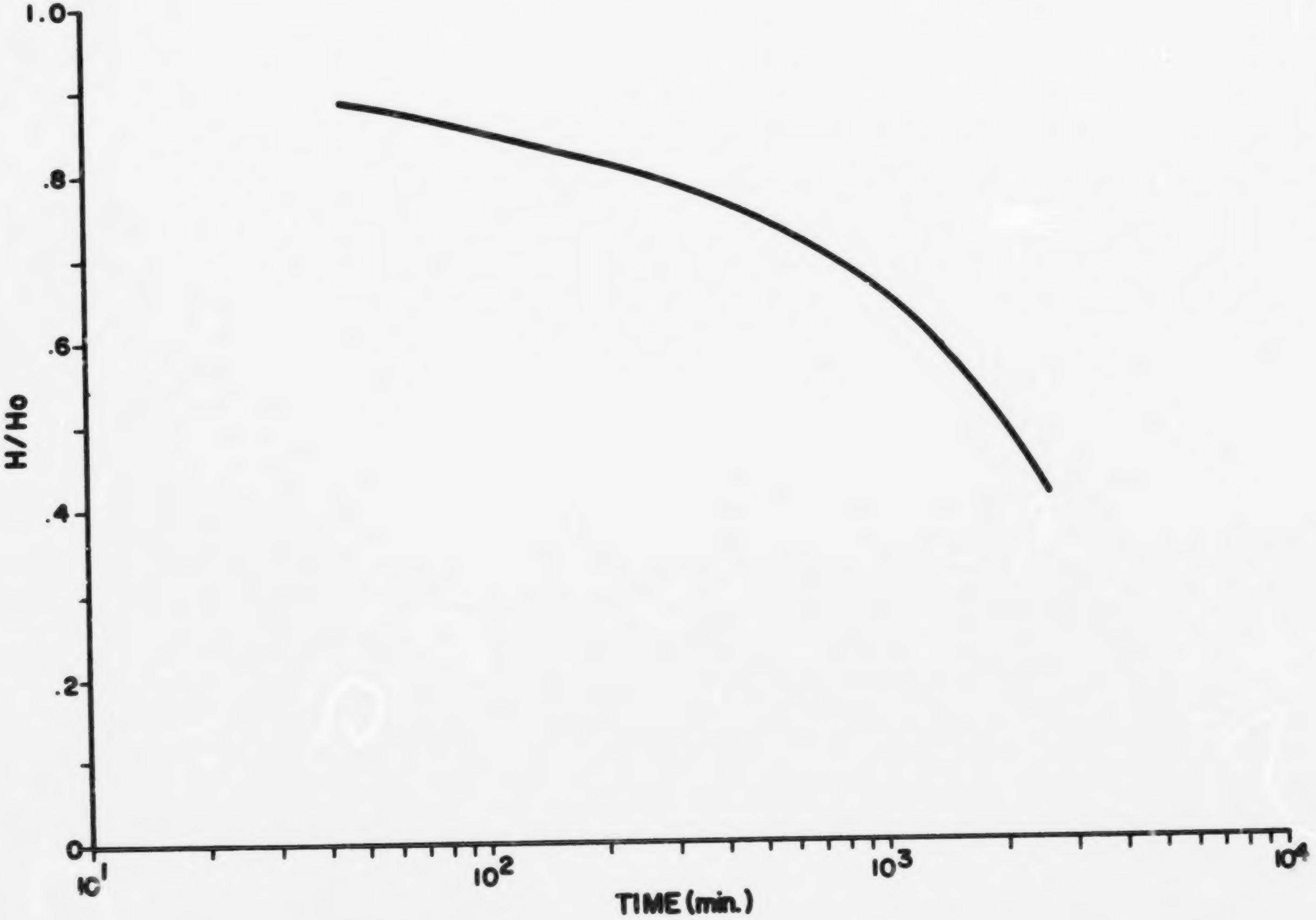

Figure 4.12 Pressure decay test, bentonite plugs in borehole CCR/C-1 - injection interval, Test 1 (Table 4.2).

BEST COPY AVAILABLE

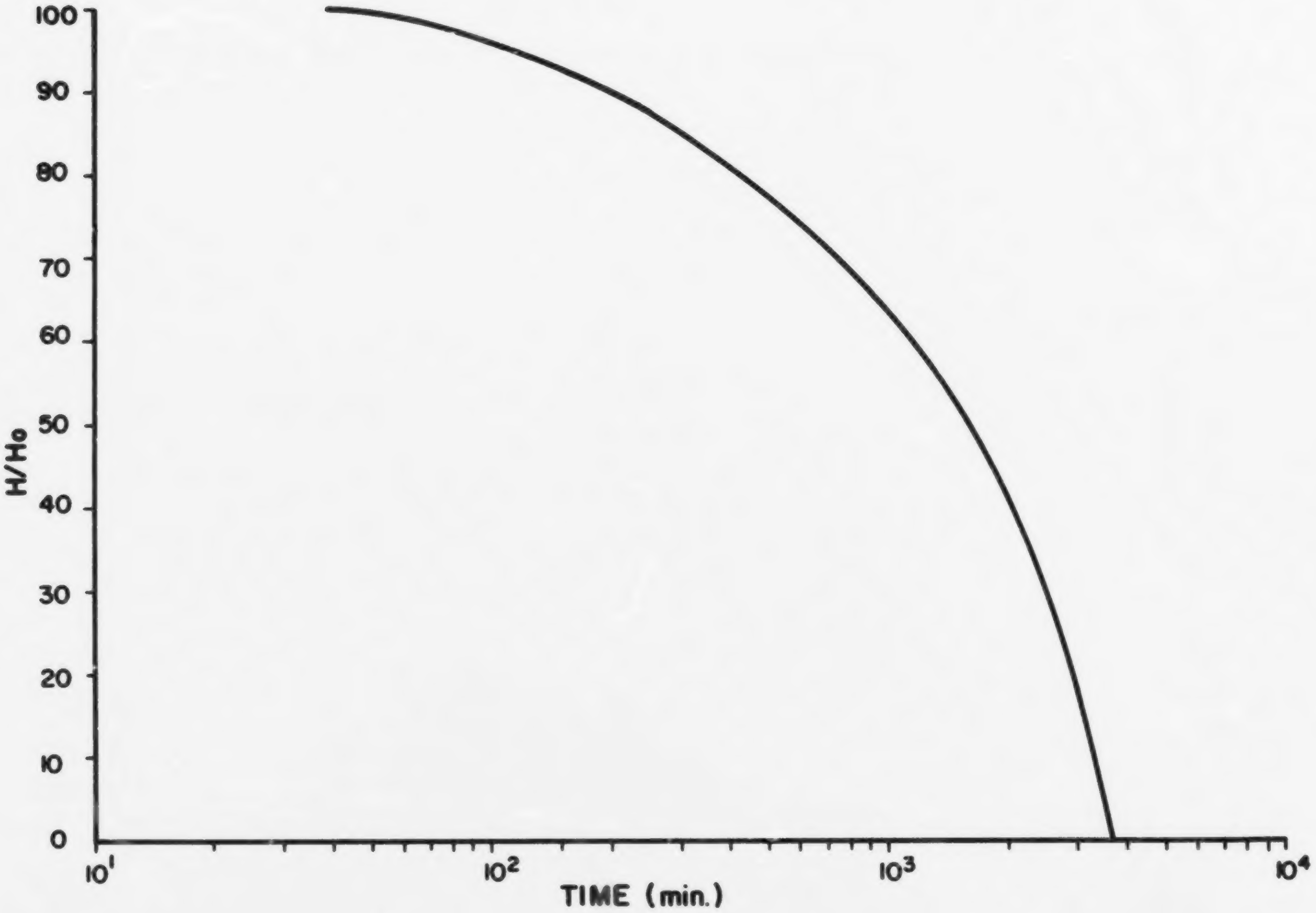

Figure 4.13 Pressure decay test, bentonite plugs in borehole CCR/C-1 - injection interval, Test 2 (Table 4.3).

BEST COPY AVAILABLE

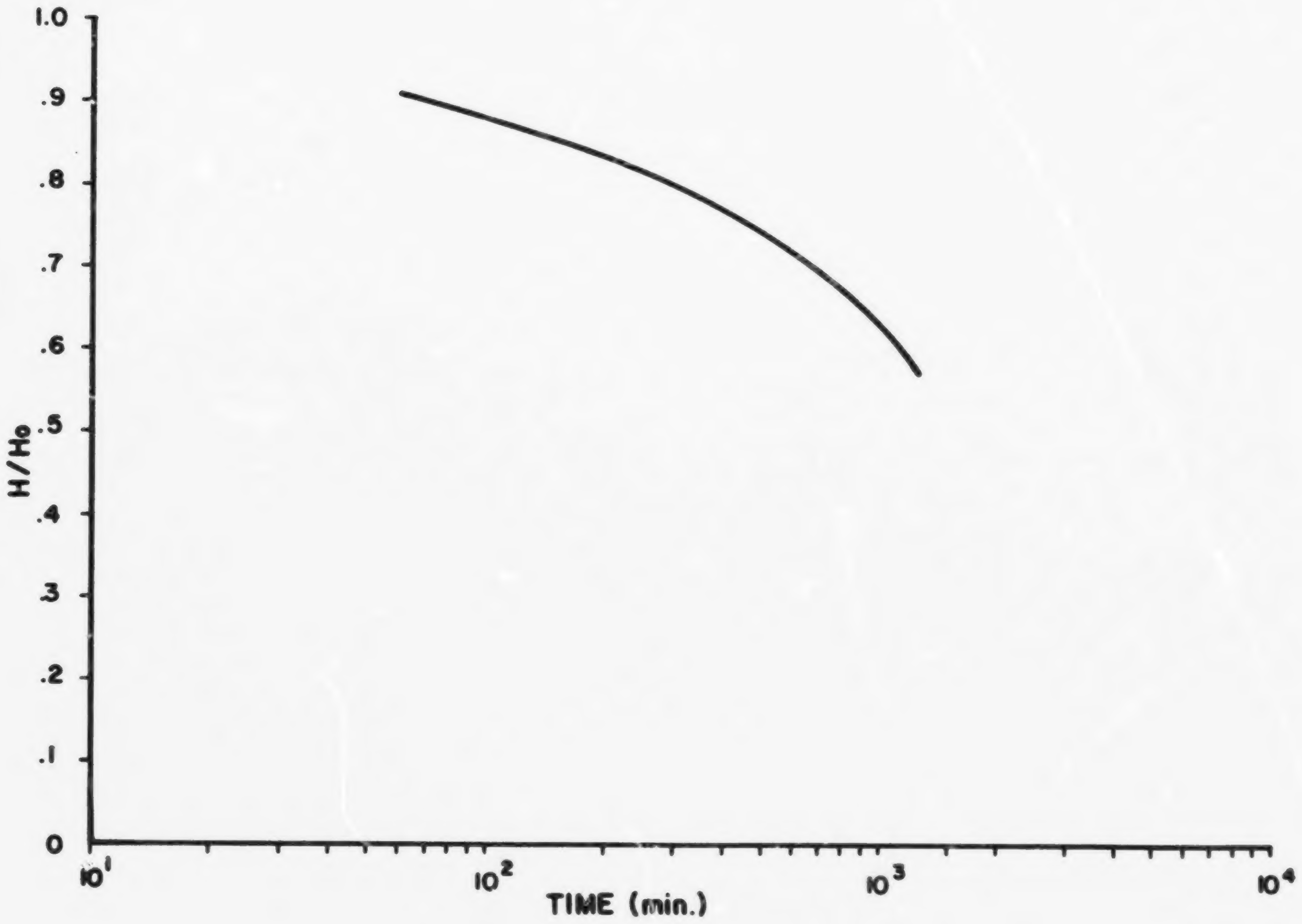

Figure 4.14 Pressure decay in upper collection interval, Borehole CCR/C-1 (Table 4.4).

BEST COPY AVAILABLE

BLANK PAGE

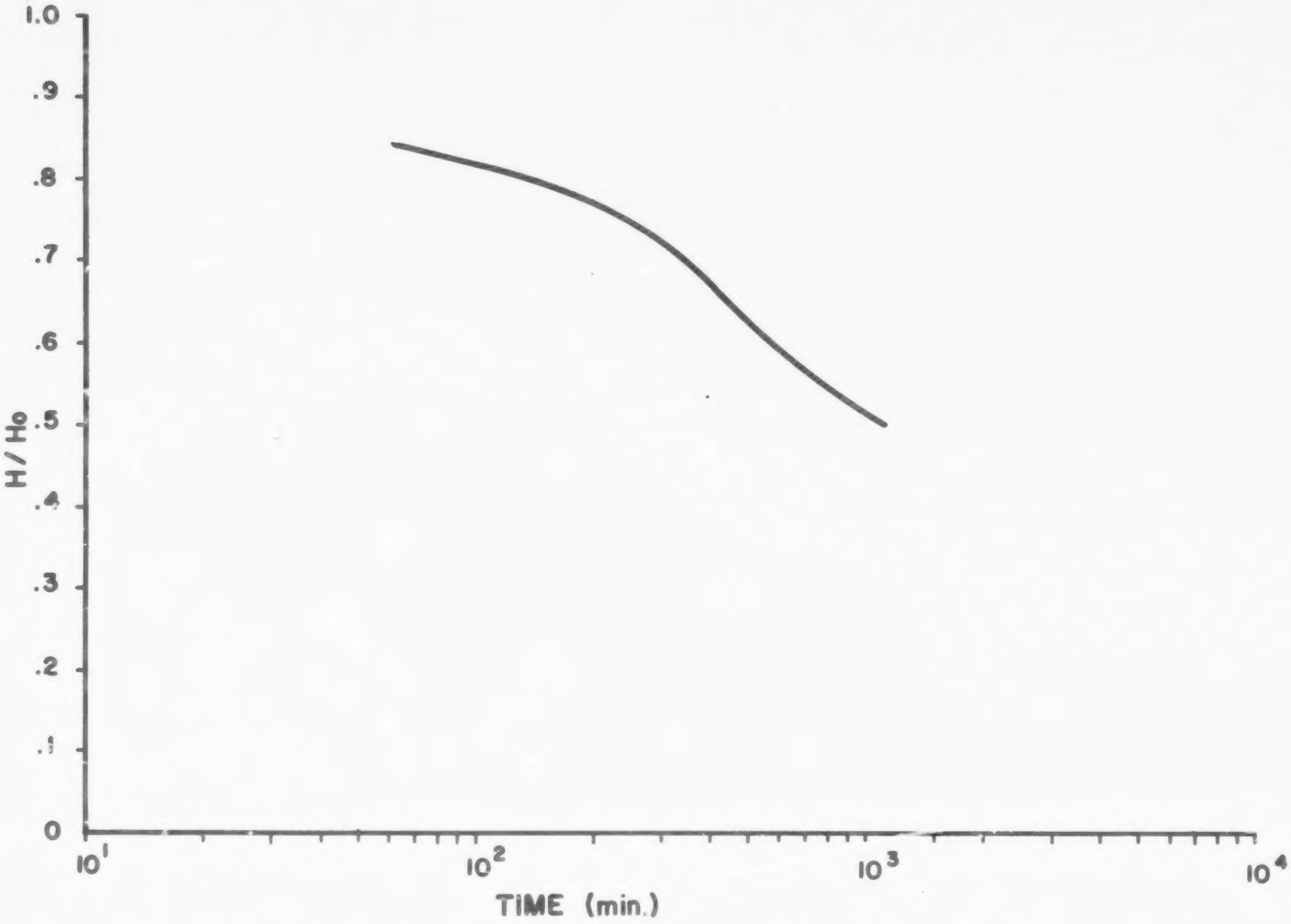

Figure 4.15 Pressure decay in lower collection interval, borehole CCR/C-1 (Table 4.5).

BEST COPY AVAILABLE

Table 4.6 Results of Pressure Slug Testing of Bentonite Seals

Test	Interval	α	β	t (min)	K (cm/s $\times 10^{-7}$)	S ($\times 10^{-5}$)
1	Injection	.1	.1	520	.342	.144
2	Injection	10^{-5}	1	720	.0341	-
3	Upper Collection	.5	.01	140	3.40	1.93
4	Lower Collection	1	.01	110	4.35	3.88

K: hydraulic conductivity

S: storage coefficient of the tested interval shape of the curves developed from the decay tests suggests that all the intervals tested are competent and enclose no major fractures or flowpaths. Any such major conduit would have resulted in an obvious drop in pressure away from the stable and shallow fall of the curves corresponding to pressure dissipation.

4.7 Long-term In-situ Performance Testing of Bentonite Plugs

Long-term in-situ testing of bentonite plugs involves injection under constant pressure into the interval between the two bentonite plugs and collection on the downstream side of each plug. Injection pressure is kept low (69 kPa; 10 psi) to avoid deformation in the test interval associated with higher injection pressures (Zeigler, 1976, pp. 39, 61, 71).

Testing began in June 1985. The injection interval has continued to take water under pressure at a rate that has declined slowly. Figure 4.16 is a plot of volume injected at approximately 69 kPa (10 psi). Both collection intervals also have continued to take water under the small head induced by the difference in height between the intervals and the collection reservoirs at the surface. Figure 4.17 is a plot of the flow into each collection interval. Both figures show that the system is reaching a state of equilibrium with no flow into the collection intervals and small flows into the injection interval.

Two factors are important in reviewing the results of constant injection testing of bentonite plugs to date. The large volumes of water injected seem problematic given that the plugs are confined on each side by presumed incompressible sand columns. This implies that the plugs can not swell. However, laboratory studies (Sections 6.2 and 6.9) suggest that the bentonite plugs draw a large quantity of water from the sand columns as they slowly saturate. Saturation involves replacing the air-filled voids with water and, therefore, does not necessitate an increase in volume. Lambe and Whitman (1979, p. 251) suggest that all pore spaces in clay are interconnected, and no pore space is truly isolated from the influence of water. This influence acts in two ways. When the effective stress on the clay reaches a certain point, the air in the voids dissolves into the water. The clay also draws water into itself through capillarity. Both these factors are treated in Chapter 6.

A number of authors have commented on the non-Darcian flow behavior apparently observed in clays, especially sodium montmorillonite bentonites of the type used here (Oakes, 1960; Mitchell, 1976, pp. 349-351, discusses several additional references as well as the likely mechanisms involved). Several reasons have been advanced for this flow behavior and resolving the issue is beyond the scope of this study. It should be noted, however, that inducing flow through bentonite plugs with low pressure gradients is difficult and probably requires extended duration for obtaining meaningful test results.

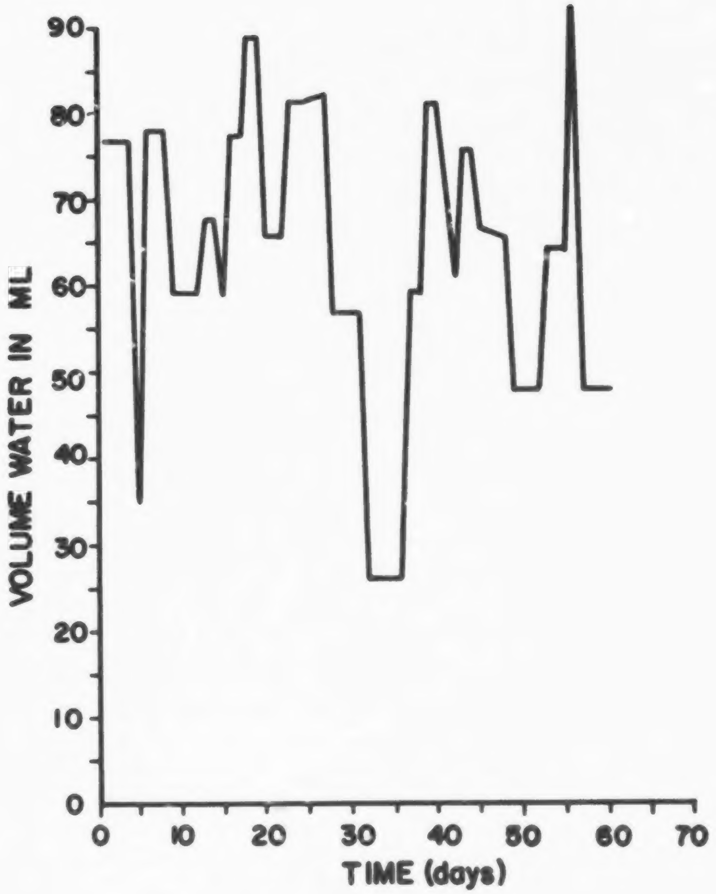

Figure 4.16 Water injected during long-term constant pressure bentonite plug testing in borehole CCR/C-1.

BEST COPY AVAILABLE

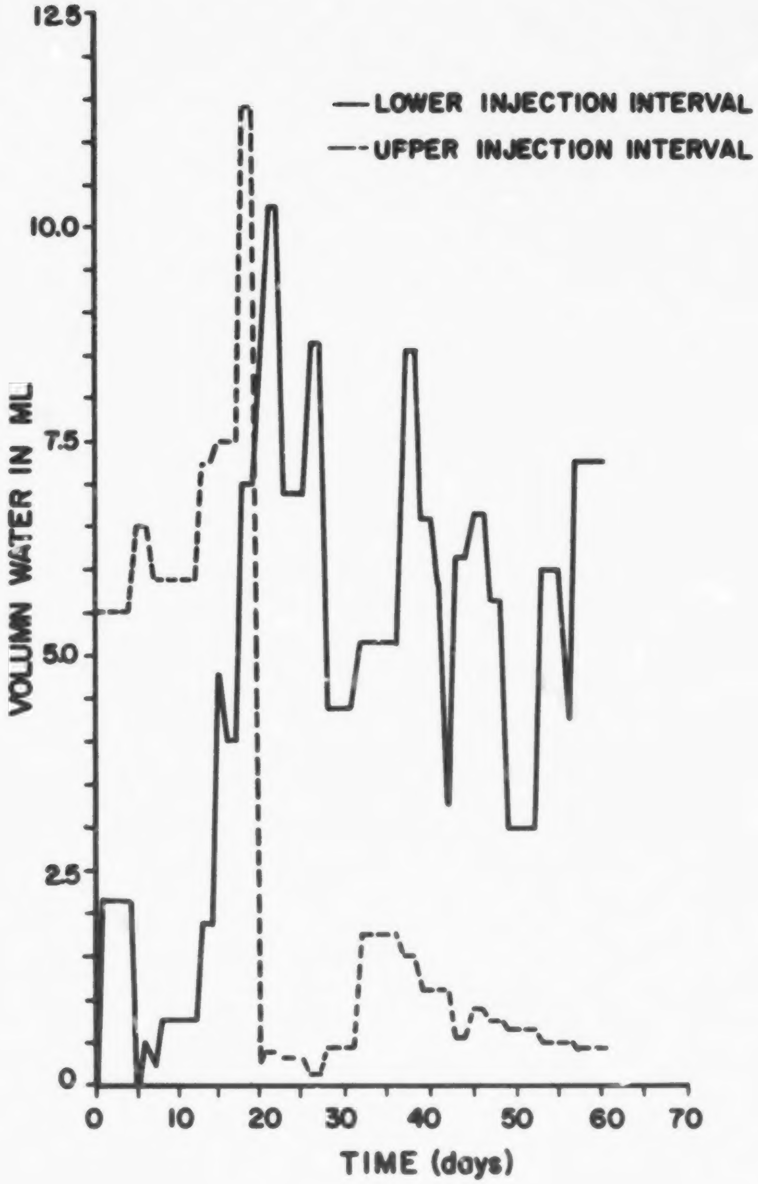

Figure 4.17 Water flow into the collection intervals during long-term constant pressure bentonite plug testing in borehole CCR/C-1.

BEST COPY AVAILABLE

4.8 Constant Head Injection Tests on Cement Plugs

The initial test performed on the plugs in borehole CCR/C-3 was a constant head injection test. The test was conducted by applying a pressure to the injection pump that produced the desired water injection pressure. The piston inside the pump fits tightly, which requires a driving pressure above that of the desired injection pressure. The pump was tested in the lab to determine the resistance of the piston to pressure applied.

Once the desired injection pressure is attained, the time, date, pressure and position of the piston monitoring rod are recorded, as well as the water levels in the collection tubes. Visits to the site are made regularly to record data and to inspect the system.

The data analysis from the constant head injection tests is simple, however not entirely correct. The analysis assumes Darcian flow conditions (equations 4.7 and 4.8). Darcy's law assumes steady-state saturated conditions and assumes that Q is the flow through the plug. Q is obtained from the inflow volume.

The results of the first constant head test performed in CCR/C-3 are listed in Table 4.7. The hydraulic conductivity of the cement plug ranges from 1.18×10^{-8} cm/s to 3.31×10^{-11} c/ms. The readings 3.21×10^{-11} through 2.10×10^{-10} are suspect. On one trip to the field a valve between the pump and injection interval was noticed to be shut. The valve was opened and a greater quantity of water was injected into the interval over the next few days. The increased flow rate is evident by the 4.86×10^{-9} cm/s value for the hydraulic conductivity, calculated for that period. The hydraulic conductivity quickly dropped back to between 5.16×10^{-10} cm/s and 6.59×10^{-11} cm/s.

The next constant head test performed in CCR/C-3 was on the new injection interval. This interval was not cased, allowing water to be injected into the borehole as well as plugs. Table 4.8 lists the results of this test. The results are very similar to those from the cased interval, ranging between 4.60×10^{-9} and 6.81×10^{-11} cm/s.

4.9 Transient Flow Testing of Cement Plugs

The method best suited for determining the hydraulic conductivity of the rock mass and that of the borehole plug/rock system was developed by Cooper et al. (1967), Papadopulos et al. (1973), and Bredehoeft and Papadopulos (1980). The pressure decay or slug test used at Cargodera Canyon is similar to the conventional slug test. The conventional slug test is conducted by creating an instantaneous head change in an open pipe in the test well. The decay of the slug is monitored. The pressure decay test used at Cargodera Canyon is performed by increasing the pressure in the test interval. The pressure decay is then monitored at the surface with a transducer and strip-chart recorder.

Table 4.7 Constant Head Injection Test #1, Borehole CCR/C-3 (Cement Plugs)

Injection Pressure (psi)	Time (min)	Flow In (cc)	Hydraulic Conductivity (cm/s)
10.0	1500	8.85	1.18×10^{-8}
12.0	4270	2.41	9.41×10^{-10}
20.0	1250	1.60	1.28×10^{-9}
25.0	4230	7.24	1.37×10^{-9}
27.6	6060	3.22	3.85×10^{-10}
29.6	10200	4.02	2.66×10^{-10}
48.8	2550	2.41	3.87×10^{-10}
47.0	20160	4.83	1.02×10^{-10}
45.0	9965	4.02	1.79×10^{-10}
53.0	37820	3.22	3.21×10^{-11} *
48.2	20140	1.60	3.33×10^{-11} *
53.2	9900	.80	3.35×10^{-11} *
51.2	7200	.80	4.34×10^{-11} *
38.8	11460	4.82	2.10×10^{-10} *
39.4	2915	2.41	4.86×10^{-9} *
39.8	5820	2.41	2.08×10^{-10}
41.6	1500	1.61	5.16×10^{-10}
42.5	1560	.80	2.41×10^{-10}
39.8	8460	1.61	9.56×10^{-11}
38.6	2610	80	2.41×10^{-10}
54.0	1620	1.61	3.68×10^{-10}
53.2	5760	2.41	1.57×10^{-10}
54.0	17280	7.24	1.53×10^{-10}
52.7	2820	1.61	2.14×10^{-10}
55.2	8730	1.61	6.59×10^{-11}

*Questionable results (See Section 4.8).

Table 4.8 Constant Head Injection Test #2, Borehole CCR/C-3 (Cement Plugs)

Injection Pressure (psi)	Time (min)	Flow In (cc)	Hydraulic Conductivity (cm/s)
25.0	1260	7.24	4.60×10^{-9}
26.0	5850	0.80	1.05×10^{-10}
28.0	13080	8.04	4.39×10^{-10}
27.2	10200	4.02	2.90×10^{-10}
26.2	7080	0.80	8.63×10^{-11}
29.8	2970	3.22	7.28×10^{-10}
28.6	20070	4.02	1.40×10^{-10}
27.2	10080	2.42	1.77×10^{-10}
27.4	4440	0.80	1.31×10^{-10}
25.8	5700	0.80	1.09×10^{-10}
26.2	14460	5.64	2.98×10^{-10}
23.0	7200	0.80	6.81×10^{-11}
26.7	10008	2.42	1.28×10^{-10}
27.5	10038	4.83	2.47×10^{-10}

The conventional analysis of the decay test assumes radial flow in a saturated medium (Bredehoeft and Papadopulos, 1980). The assumptions may not be valid for a pressure decay test performed in an interval isolated by borehole plugs. Flow occurs through the plugs, as well as through the rock. The magnitude of the plug flow will be a function of the plug hydraulic conductivity relative to that of the rock (South and Daemen, 1986, Ch. 5). A plug with a hydraulic conductivity significantly less than that of the borehole rock might have an identical decay curve as that originally obtained by the initial packer tests. A plug with a higher hydraulic conductivity than the borehole rock would increase the rate of pressure decay over the initial decay test.

The pressure decay test provides a qualitative assessment of plug performance. A comparison between the borehole pre-plugged and plugged decay curves will, to a large degree, determine if the plug is performing as desired. One problem with using such a comparison, however, is that the length of the borehole wall exposed in the plugged interval is much less than that originally used to determine the hydraulic conductivity of the rock. The interval, if suitable, is assumed to be homogeneous. When performing a decay test once the plugs are installed, the length of the borehole wall exposed is decreased by as much as an order of magnitude. The small zone between the borehole plugs may not be representative of the overall hydraulic conductivity measured during the initial decay test.

During the decay test, air was discovered in the intervals. The analysis of a two-phase test is difficult and was not conducted. The decay curve for a test conducted with gas will be more gradual than a decay test conducted with water (e.g. Hvorslev, 1951, pp. 6-7, 26-28). A combination of gas and water would yield a curve somewhere between these two curves. A comparison between the decay test conducted on the plugs and the one initially conducted to determine the hydraulic conductivity of the borehole wall was not attempted.

4.10 Influence of Temperature on In-Situ Testing

The temperatures at the Cargodera Canyon site, especially during the summer, can be extreme. To determine the influence of temperature on the instruments used to test in the field, a two-day test was run on the injection interval in CCR/C-1. A transducer was mounted to the injection line and a strip chart recorder monitored the changes in injection pressures. The pressure was set to remain "constant" at 34 kPa (5 psi). Table 4.9 lists the results. Figure 4.18 shows the change in pressure in the injection line over the same time. Surface temperatures at the site varied during this period from late afternoon highs of over 38°C (100°F) to early morning lows of 21°C (70°F). The experiment shows an increase in pressure during the hotter part of the day of approximately 5 kPa (.75 psi). This increase could be the result of actual pressure changes in the injection line or of drift in the transducer induced by the heat. Akgun and Daemen (1986, Appendix F) present a simple analysis illustrating the significant influence of temperature on pressures within fluid filled closed containers, e.g. steel pipe, and hence on transient pulse tests.

Table 4.9 Temperature Effect Test - Injection Interval CCR/C-1

Time	Pressure* (psi)
11:44 am	5.00
12:44 pm	5.05
1:44 pm	4.98
2:44 pm	4.98
3:44 pm	4.98
4:44 pm	4.94
5.44 pm	4.90
6:44 pm	4.60
7:44 pm	4.86
8:44 pm	4.93
9:44 pm	4.92
10:44 pm	5.00
11:44 pm	5.03
12:44 am	5.06
1:44 am	5.03
2:44 am	5.05
3:44 am	4.94
4:44 am	4.99
5:44 am	5.03
6:44 am	5.07
7:44 am	5.11
8:44 am	5.28
9:44 am	5.32
10:44 am	5.33
11:44 am	5.45
12:44 pm	5.68
1:44 pm	5.72
2:44 pm	5.73
3:44 pm	5.77
4:44 pm	5.79
5:44 pm	5.79
6:44 pm	5.77
7:44 pm	5.67
8:44 pm	5.53
9:44 pm	5.47
10:44 pm	5.46
11:44 pm	5.38
12:44 am	5.32
1:44 am	5.29
2:44 am	5.21
3:44 am	5.13
4:44 am	5.09
5:44 am	5.07
6:44 am	5.07
7:44 am	5.11
8:44 am	5.30
9:44 am	5.48

*Initial pressure set at 5 psi.

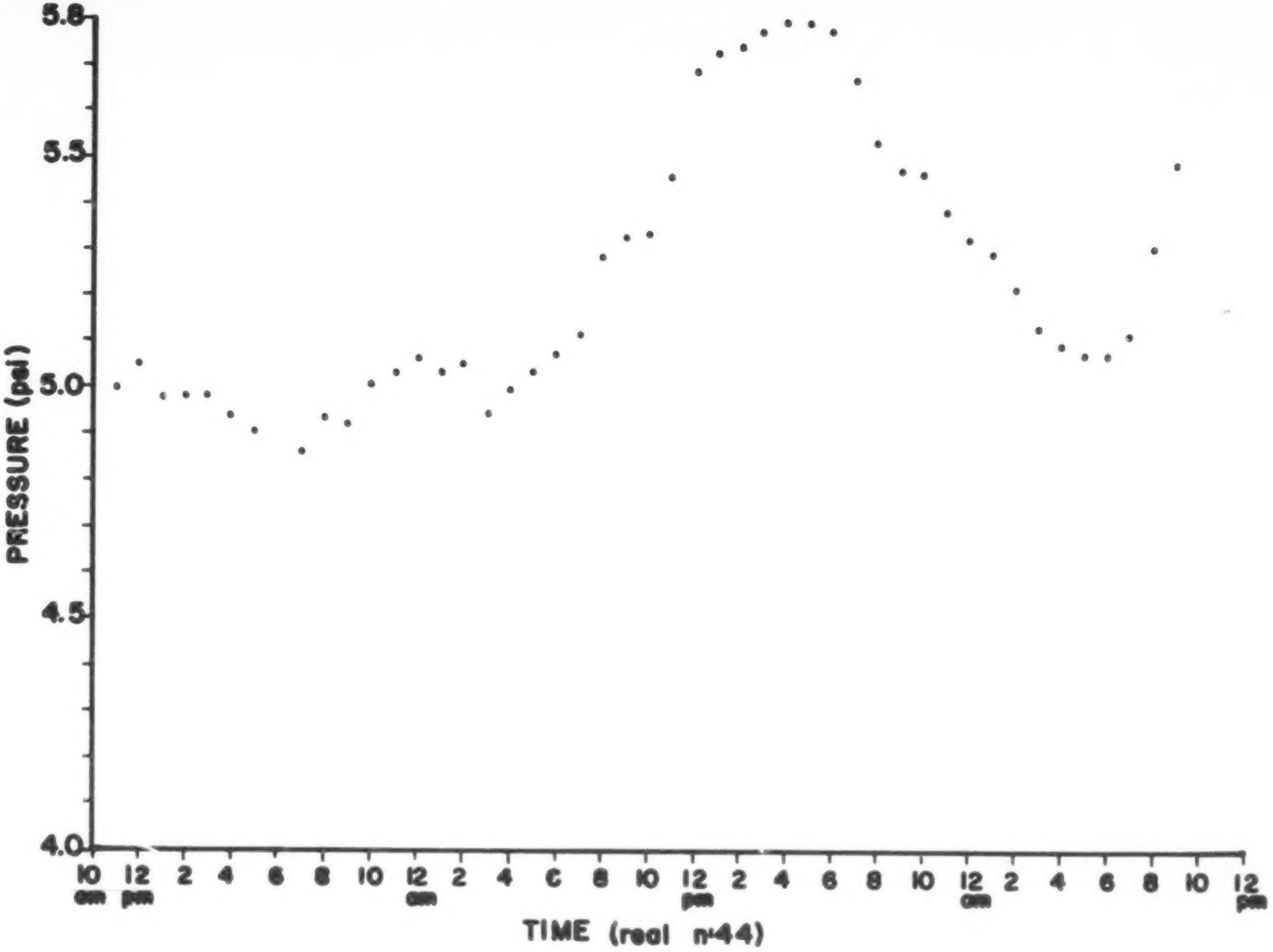

Figure 4.18 Change in pressure over a two-day period, presumably as a result of thermal effects (Section 4.8).

BEST COPY AVAILABLE

CHAPTER FIVE

LABORATORY INVESTIGATION OF BENTONITE BOREHOLE PLUGS

5.1 Introduction

This laboratory study has three principal areas of investigation, each related to in-situ testing. Field conditions are reproduced whenever possible. The three areas include (1) the study of prototype bentonite plugs at field scale and under simulated field conditions; (2) the determination of plug permeability isolated from the influence of in-situ placement and the permeability characteristics of the host rock; and (3) the establishment of reference values for the clay tested to contribute to the prediction of plug performance under field conditions. In addition, equipment calibration and performance testing is conducted at field scale to provide the appropriate values for the analysis of field results.

The study of prototype bentonite plugs in the laboratory has as objective determining the behavior of plugs as constructed and once they are subjected to injection pressure. Visual inspection of the plugs provides insight into the behavior of the plugs in the field. Subjecting the plugs and sand intervals to water under pressure and measuring the flow rates while observing changes in the test column provides information about the behavior of the plugs tested in-situ under similar conditions.

The hydraulic conductivity of bentonites used in this study when measured in the laboratory under controlled conditions provides important criteria for determining the effectiveness of plugs tested in-situ. This is especially true given the difficulty involved in precise analysis of the field test results, where available theory does not yet provide a totally adequate framework for estimating key values. Laboratory hydraulic conductivity testing includes constant pressure injection as well as pressure decay, transient analysis. The significance of consolidation and swelling to the test procedures, the clay behavior and the analysis of results is investigated. The role of moisture content and degree of saturation in hydraulic conductivity is estimated using samples similar in content and construction to the in-situ plugs.

Reference testing of bentonites has as objective determining significant engineering characteristics. These include liquid and plastic limits, optimum water content, and unconfined and confined swelling characteristics. These values provide a basis for estimating improved plug construction methods as well as judging the effectiveness of the methods used for plug construction and emplacement.

5.2 Characteristics of Bentonite Used in Seal Testing

The bentonite tablets used in this study are American Colloid Company Volclay Tablets, manufactured and distributed from Skokie, Illinois. The tablets are 1.25 cm (1/2 inch) in diameter and come in 9 to 22.5 kg (20 to 50 lb) containers. The manufacturer describes the product bentonite as a hydrous silicate of alumina comprised essentially of the clay mineral montmorillonite. Montmorillonite should represent a minimum of 90 percent of the content of the clay product. Other minerals present include feldspar, biotite and selenite. The pH of the clay should range from 8.5 to 10.5. The dry bulk density as delivered averages 2,050 kg/m^3 (128 lb/ft^3). Individual tablet density averages 2.066 g/cm^3 (129 lb/ft^3). Specific gravity varies from 2.3 to 2.5, which suggests that actual grain density ranges from 2.3 g/cm^3 (143.5 lb/ft^3) to 2.5 g/cm^3 (156 lb/ft^3).

Experiments at American Colloid established that for their 6.35 mm (1/4 inch) diameter tablets, for a number of tablets with a weight equal to 90.6 grams, total volume of the tablets is 83.9 cubic centimeters, while the pore volume is 41 cc. Similar tests with 12.7 mm (1/2 inch) diameter tablets show that for tablets equal in weight to 72 grams, total volume is 83.4 cc, pore volume is 49.9 cc, and the volume of solids is 33.5 cc. This suggests an individual tablet density of approximately 2.15 g/cm^3 (134.2 lb/ft^3).

A comparison of the indicated individual tablet density with a grain density calculated from the specific gravity range as listed by the manufacturer suggests a probable individual tablet porosity ranging from 10 to 17 percent by volume. Using the relationship $e = n/(1 - n)$, where n is porosity and e is void ratio, a void ratio of from .11 to .20 is calculated for the individual tablets.

Two 22.5 kg (50 lb) bentonite tablet containers were ordered from the manufacturer. A whole rock analysis was performed by Copper State Analytical Lab, Inc., of Tucson, Arizona on two samples. Sample one is from the most recently received and opened container. Sample two was from the container received and opened approximately eleven months earlier. Table 5.1 lists the results of this analysis. SiO_2 values were determined gravimetrically, the remaining assays by atomic absorption. The results suggest that the chemical and mineral composition of commercial bentonites, even when supplied under the same brand name, may vary significantly from batch to batch. Some of the difference in composition may be the result of alteration of minerals in the older sample. Nevertheless, differences in the quantities of major mineral assemblages suggest that any uniformity in sealing material components using commercial bentonites of the type reviewed in this study would require a compositional criterion other than brand name or commercial trademark.

Most clay minerals are phyllosilicates or layer silicates (e.g. Mitchell, 1976, p. 27). They are composed of sheets of linked silica tetrahedra and of oxygen or hydroxyl octahedra (e.g. Grimm, 1968, p.

Table 5.1 Whole Rock Analysis of Samples from Two Batches of Bentonite Ordered for This Sealing Study

	Sample 1 (% of total)	Sample 2 (% of total)
SiO_2	69.80	76.20
Al_2O_3	15.90	8.10
CaO	0.21	0.40
MgO	1.96	3.42
K_2O	1.06	0.84
Na_2O	3.30	3.6
Fe_2O_3	5.29	4.58
TiO_2	0.19	0.19
P_2O_5	0.068	0.080
MnO	0.12	0.14
LiO	1.86	2.10

51). How these sheets combine into layers is what distinguishes the major clay assemblages from each other. The layer configuration that identifies smectites is one octahedral sheet intercalated between two tetrahedral sheets, with each clay layer bounded by basal tetrahedral planes which combine to form a network of vacant hexagonal sites (e.g. Meyer and Howard, 1983, p. 15). A tetrahedral sheet consists of linked oriented silica tetrahedra sharing three basal oxygens and with apical oxygens all pointed in the same direction. Octahedral sheets are composed of linked octahedral coordination groups in which divalent and trivalent cations are enclosed by an octahedral network of oxygen and hydroxides. Both octahedral and tetrahedral sheets allow some substitution by cations of similar charge, as well as cations of similar size and different charges. This latter type of substitution produces a charge imbalance which is usually a deficiency in the positive charge in the structure. Electroneutrality is replaced when cations are adsorbed onto the basal surface in interlayer sites. These interlayer cations help determine the significant properties of clay.

The smectite family, which includes montmorillonite bentonites, allows a limited amount of solid substitution so that the excess negative charge is approximately .33 equivalents per unit cell.

Montmorillonites create this excess charge by substituting Mg^{2+} for Al^{3+} (Meyer and Howard, 1983, p. 16; Mitchell, 1976, p. 38). The engineering significance of these compositional characteristics is that the relatively low layer charge in smectites allow hydration and solvation of the interlayer cations and a reversible intracrystalline swelling created by the uptake of water. Critical to the ease and extent of the exchange and hydration is the type of interlayer cation involved. Interlayer Na is responsible for adsorbing many layers of water while Ca as the interlayer cation will only adsorb two layers of water molecules.

Table 5.1 shows that the bentonite used in this study is a Na-rich clay, with Na values significantly higher than Ca values. The significance of the predominance of Na cations over Ca cations is not limited to the swelling characteristics of the clay. The clay's permeability is also influenced by the dissolved cations and the cations in the interlayer sites. The thickness of the adsorbed water layers on the clay surface is a function of the size and valence of the adsorbed cations. The thickness of the double layer determines whether attractive forces or repulsive forces dominate. Attractive forces contribute to the formation of clay aggregates. Repulsive forces tend to create dispersed, homogeneous mixtures. Clay aggregates are responsible for large pore spaces with corresponding higher permeabilities. A homogeneous, dispersed clay has a smaller porosity and a lower permeability.

Monovalent cations, such as Na^{+}, tend to form thicker double layers and adsorb more water than polyvalent cations such as Ca^{2+} (Meyer and Howard, 1983, pp. 40-41; Grim, 1968, p. 260; Van Olphen, 1977, Ch. 7). Fluid flow is reduced near clay particles by the thicker double layer. Figure 5.1 shows that Na-saturated clays tend to have lower hydraulic conductivities than equivalent Ca-saturated clays.

The presence of Na cations influences the plastic behavior of bentonites. Smectites with Na and Li as exchangable cations are able to adsorb large amounts of water before exhibiting plastic behavior and losing their strength. This is a result of the ability of smectites to disperse as fine particles which maximizes the amount of water adsorbed. This reduces the lubricating influence of water on the individual clay particles. Na as an interlayer or exchangable cation tends to maximize the dispersion of individual clay particles (Meyer and Howard, 1983, p. 44).

Other engineering properties of clay influenced by the chemical composition include shear strength, erodability and thermal characteristics.

5.3 Constant Injection Hydraulic Conductivity Test

5.3.1 Test Objectives

Laboratory hydraulic conductivity testing using constant pressure water injection has as primary objective determining the influence of pipes penetrating the seal on the hydraulic conductivity of the bentonite seal. In-situ plug design, described in Section 4.3, uses stainless steel 3.2 mm (1/8 inch) and 6.35 mm (1/4 inch) diameter pipes to inject and collect water during plug testing. The steel pipes penetrate the bentonite plugs through their entire length. An important criterion for determining the effectiveness of this in-situ testing system is an assessment of its impact on the plugs it is designed to test. The most significant effect of the pipes would be any change they induce in the hydraulic conductivity of the plugs.

Constant injection testing also provides long-term information on the hydraulic conductivities of the plugs when they experience injection pressures similar to in-situ conditions. An in-depth assessment of the performance of bentonite plugs emplaced in the field and tested in-situ requires that the hydraulic conductivity of bentonite be isolated from the influence of the host rock and field environment. This value can then be used to judge the impact of emplacement methods and field experimental procedures on the hydraulic conductivity of the plugs.

The hydraulic conductivity of bentonite is a function of a number of parameters. These include:

(a) mineralogy of the bentonite;
(b) mineral content of the clay;
(c) clay fabric;
(d) degree of compaction or consolidation of the clay; and
(e) molding water content of the clay (Meyer and Howard, 1983, Section 2.1.1)

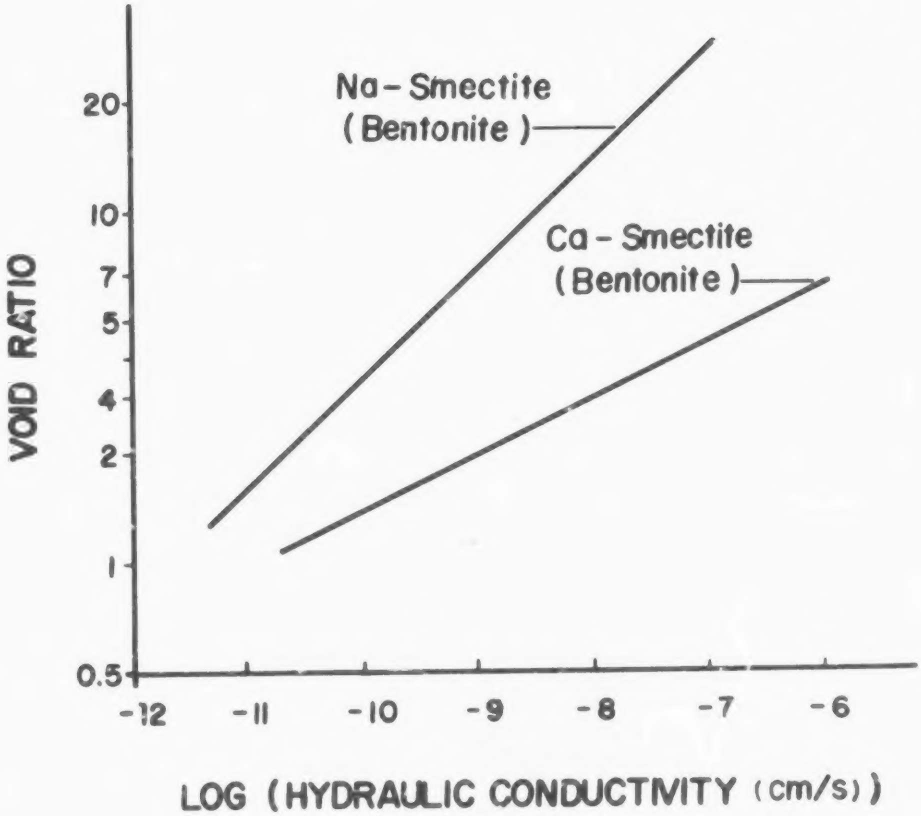

Figure 5.1 Hydraulic conductivity of bentonite as a function of void ratio and of water chemistry. (Simplified from Meyer and Howard, 1983, Figure 2-1, based on data by Mesri and Olson, 1971).

BEST COPY AVAILABLE

In addition, the hydraulic gradient and the bonding between the seal and what holds it should affect the hydraulic conductivity. These factors are more readily controlled and measured in the laboratory than in-situ.

When bentonite seals are subjected to injection pressures, they can consolidate. Since any measurement of hydraulic conductivity under these conditions requires measuring flow through the plug, the test can function as a drained consolidation test with outflow a function of consolidation as well as of flow through the plug. If measurement of flow into the plugs is used, the propensity of bentonite to take up water must be considered. These processes are important in the analysis of hydraulic conductivity testing conducted on Na bentonites.

5.3.2 Constant Injection Pressure Test Theory

Several methods are used in standard laboratory practice to determine the hydraulic conductivity of soils and clays. These include the falling or variable head test, the constant head test and tests that use the rate of consolidation of the soil (e.g. Lambe and Whitman, 1979, p. 281). In soils engineering practice, hydraulic conductivity is frequently referred to as the "coefficient of permeability" or "permeability" (Lambe, 1950, p. 52). Lambe and Whitman (1979, Section 19.1) recommend the constant head test for determining the hydraulic conductivity of low permeability, cohesive soils such as clays. The test is based on the empirical relationship between fluid flow velocity in soil and hydraulic gradient known as Darcy's law. Using the experimental apparatus shown in Figure 5.2, Darcy concluded that the rate of fluid flow, Q can be expressed as

$$Q = KA(h_1 - h_2)/L \tag{5.1}$$

$h_1 - h_2$ is the difference in piezometric head across the sample of length L. Piezometric head describes the sum of pressure and potential energies of the fluid per unit weight. K is the proportionality factor.

Relation (5.1) assumes that the material can be considered a porous medium. Flow is laminar, with small flow velocities and water molecules traveling in smooth paths approximately parallel to the boundaries of the pore spaces. This type of flow is a function of the viscous forces acting on the fluid. As long as flow is laminar, the loss of head will vary linearly with the fluid velocity. Two types of flow may vary from these conditions. At high velocities, the inertial forces in the fluid begin to dominate, until the flow can be described as turbulent and head loss will vary exponentially with velocity. The ratio between viscous and inertial forces is expressed by the Reynolds number, N_R:

$$N_R = \rho v D/\mu \tag{5.2}$$

where v is the velocity of flow, D is the characteristic dimension of the conduit. For granular material, D can be taken as the average

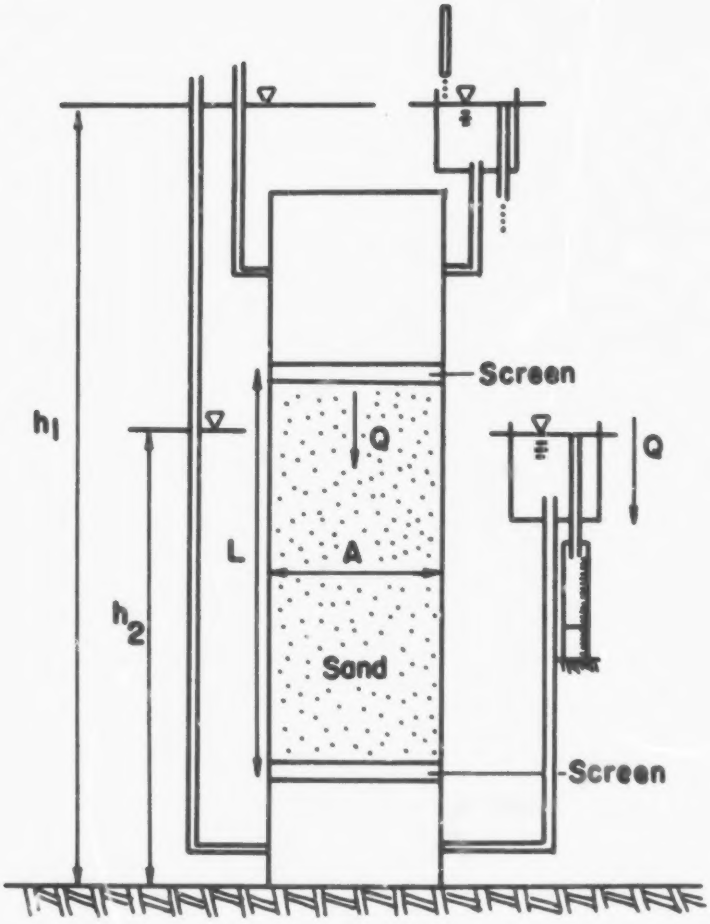
Screen
h1
Q
Q
L
A
h2
Sand
Screen

Figure 5.2 Schematic of constant head permeability test arrangement.

A: Sample cross-sectional area
L: Sample length
Q: Volumetric flowrate
$h_1 - h_2$: Driving head difference

BEST COPY AVAILABLE

particle size, D_{50} (e.g. Bouwer, 1978, p. 42), although sometimes D_{10} is used (e.g. Bear, 1979, p. 64). ρ is the fluid density, and μ is the viscosity of the fluid. The ratio of μ/ρ is the kinematic viscosity. Flow can be considered laminar as long as N_R is less than 2100 (Bouwer, 1978, p. 42). However, turbulent flow has been detected at much lower Reynolds numbers and Bear (1979) suggests that Darcy's law is valid for Reyonlds between numbers 1 and 10.

The permeability of porous media can also be described by the Kozeny-Carman equation, proposed by Kozeny and improved by Carman:

$$K = \frac{1}{K_0 S_p^2} \frac{\gamma}{\mu} \frac{e^3}{(1 + e)} \tag{5.3}$$

where K_0 is a factor depending on pore shape and ratio of the length of the actual flow path to the sample thickness, S_p is the specific surface area, μ is the viscosity of the permeant, γ is the unit weight of the permeant, and e is the void ratio. Lambe and Whitman (1979) recommend this equation for analysis of fluid flow because it takes into account not only the properties of the permeant but also the particle size and void ratio of the medium being tested. However, it does not account for the electrical layer forces acting in clays.

The application of Darcy's law to fluid flow in bentonites is problematic. Nevertheless, standard current laboratory testing practice continues to use applications of Darcy's law in determining the hydraulic conductivity of clays (Holtz and Kovacs, 1981). Mitchell (1976, pp. 349-351), after summarizing and reviewing the evidence, concludes that "...all other factors held constant, Darcy's law is valid." Pusch and associates repeatedly and forcefully state that Darcy's law is not valid for densily compacted bentonite (e.g. Pusch, 1979; Pusch et al., 1979; Pusch and Carlsson, 1985), and justify this conclusion by reporting results of the sensitivity of hydraulic conductivity to hydraulic gradient. There is no agreement on which test is most appropriate for low-permeability clays. Lambe and Whitman (1979, pp. 281-3) recommend the constant head test. Winterkorn and Fang (1975, p. 106) recommend the falling head test. Experience at the University of Arizona suggest that the falling head test using low pressure gradients is difficult to perform successfully on bentonites of the type used in this study (Sawyer and Daemen, 1987).

Darcy's law can be written as

$$Q = KiA \tag{5.4}$$

where i is the gradient of piezometric head. If V is the volume of water collected in time t, then Q = V/t. The value of the gradient i can be replaced by h/L where h is the head maintained over the test. Then

$$K = \frac{VL}{Aht} \tag{5.5}$$

This equation is used to analyze constant pressure test results.

5.3.3 Constant Injection Pressure Testing Equipment and Procedures

Constant pressure testing of bentonite plugs is conducted in the laboratory using the apparatus illustrated in Figure 5.3. Nitrogen over water maintains a constant head over the clay samples. The plugs were built over columns of sand, each 1000 cc in volume and saturated before the clay was added. 1.25 cm (1/2-inch) diameter American Colloid Volclay bentonite tablets were used to seal the tubes. Each plug was constructed by dropping 200 tablets through 800 ml of water standing above the sand column. Tubes 2 and 3 include 3.14 cm (1/8-inch) diameter stainless steel pipe sealed at the top and bottom. The clay plugs for 2 and 3 were built around these steel pipes. The plugs were allowed to saturate and swell for 14 days before the tubes were sealed and testing was begun. The PVC tubes have a diameter of 10 cm (4 inches) and are 30 cm (12 inches) long. The PVC caps used to seal them are 6.25 cm (2 1/2 inches) high. All fittings and tubing for pressure injection and drainage are 6.25 mm (1/4 inch).

The tubes were capped and sealed after plug construction was completed. Unfortunately, this apparatus requires that tubes and seals be pressurized after plug construction as tube capping is accomplished using epoxy. This means that the plugs experience some pressure and movement while the tubes are tested. Pressure testing was done to a maximum of 620 kPa (90 psi) over a period of 24 hours, while allowing no drainage. In this way, once the pressure slug was induced into the tube and isolated from its source, all decay was either through the plug or as a result of leaks. Several leaks were found and the tubes were resealed.

Water is provided with two reservoirs mounted above the apparatus. Figure 5.4 shows the equipment. A scale on the smaller diameter reservoir allows calculation of total flow into all four tubes. 5 ml capacity pipettes collect any outflow. Procedure requires taking readings every 24 hours or less.

Initial injection pressure was set at 34 kPa (5 psi). The injection pressure was raised 69 kPa (10 psi) after 3 months of essentially no-flow conditions in all four tubes suggested that a higher pressure gradient might be needed to induce measurable flow. This is discussed in Section 6.2.

Nitrogen over water provides the injection pressure. Nitrogen is soluble in water, and the solubility is a function of pressure and temperature. Care must be taken to avoid introducing nitrogen into the plugs. Distilled water is used. The sand columns were saturated and the plugs constructed with distilled water. Testing takes place

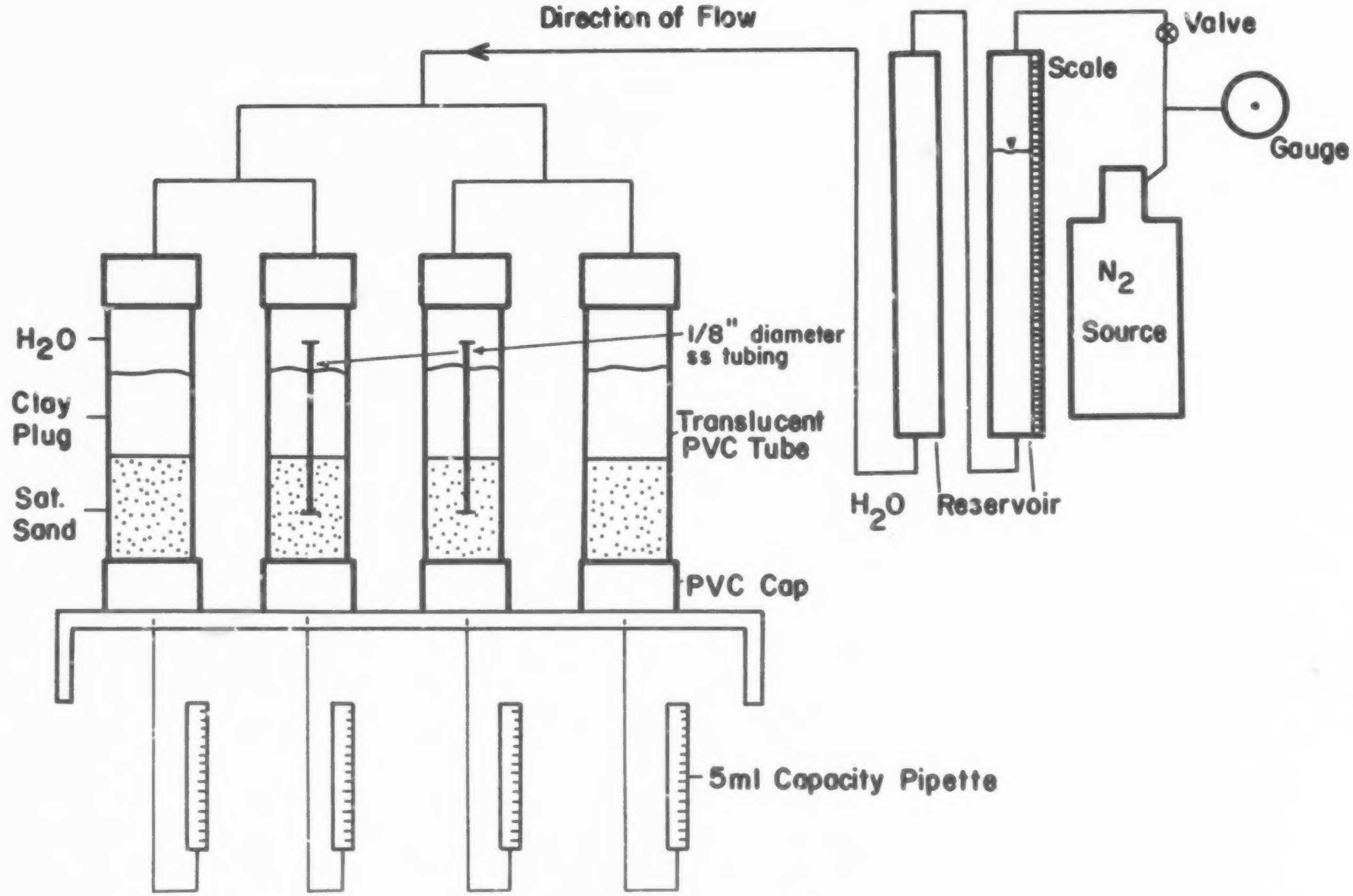
Direction of Flow
Valve
Scale
Gauge
N_2
Source
H_2O
1/8" diameter ss tubing
Clay Plug
Translucent PVC Tube
Sat. Sand
H_2O
Reservoir
PVC Cap
5ml Capacity Pipette

Figure 5.3 Experimental arrangement for laboratory constant pressure testing of bentonite plugs. PVC test tubes are numbered 1 through 4 from left to right.

BEST COPY AVAILABLE

145

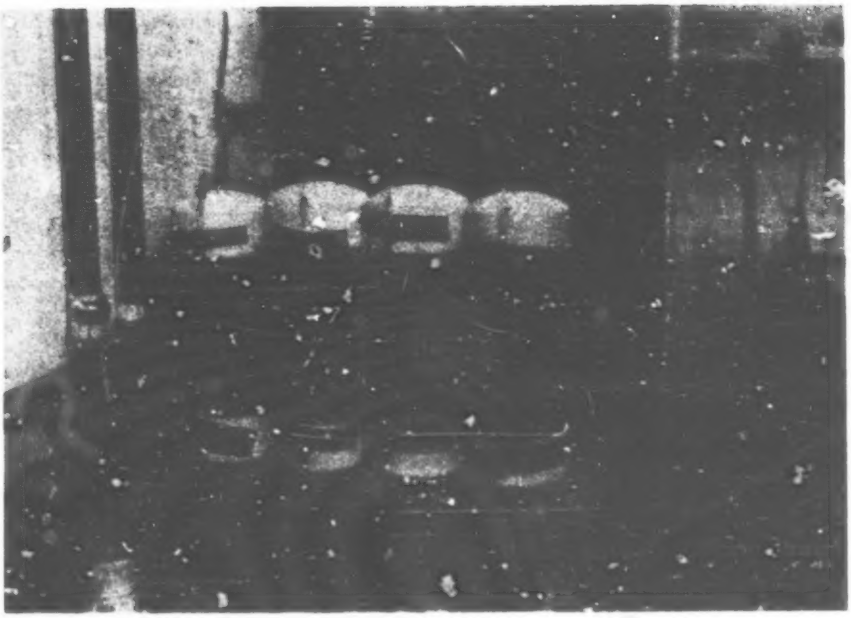

Figure 5.4 Constant pressure flow testing of bentonite plugs in PVC pipe.

BEST COPY AVAILABLE

in a laboratory environment, with monitored daily temperature variations of less than 2 to 3 degrees celsius.

5.4 Consolidation Testing

5.4.1 Introduction

Consolidation testing of bentonite plugs in the laboratory has the primary goal of determining the significance of consolidation on hydraulic conductivity measurements. In-situ performance testing of bentonite plugs involves subjecting those plugs to injection pressures over extended periods of time. Flow through the plugs is collected downstream from each plug. The plugs can drain if they consolidate under injection pressure. Hydraulic conductivity values are derived from the collected outflow. Part of this outflow may be the result of plug consolidation and not strictly of flow through the plugs.

An important issue in a performance assessment of bentonite seals is the volume stability of the seals over time. Once the plugs have been emplaced in a field environment, this stability is difficult to estimate. Laboratory testing can provide information necessary to estimate the condition of the in-situ plugs. If the bentonite consolidates under injection pressures, there will be a corresponding plug volume reduction. In the case of the plugs at the Cargodera Canyon study area, consolidation may involve separation of the plugs from the surrounding sand columns. This additional void space on the upstream side of each plug would alter the dimensions of the injection reservoir and its holding capacity.

When bentonite consolidates, its void ratio decreases. Total pore spaces available for fluid flow are reduced and there should be a corresponding decrease in hydraulic conductivity. This may be more than offset by ongoing saturation of the plugs, which is examined in the next section. There is evidence that the effect of consolidation on void ratio is not the same over the length of the plug (Hamilton and Crawford, 1959). Results from this study indicate that the same is true of saturation. Bentonite plugs, then, may develop significant non-uniformity in water content and in degree of compaction as a result of processes induced by the injection pressures.

Consolidation may also affect the strength of the plug. Decreasing void ratios are associated with increases in effective stress as the actual skeleton of the plug experiences a larger portion of the load applied (Lambe and Whitman, 1979, Ch. 21,28). This increase in effective stress is usually associated with an increase in strength (Lambe and Whitman, 1979, Ch. 21,28).

5.4.2 Consolidation Test Theory

One-dimensional hydraulic consolidation of soils is described by:

$$\pm\left(\frac{\gamma_s}{\gamma} - 1\right) \frac{d}{de}\left[\frac{K(e)}{1 + e}\right] \frac{\partial e}{\partial z} + \frac{\partial}{\partial z}\left[\frac{K(e)}{\gamma\,(1 + e)} \frac{\partial \sigma'}{\partial e} \frac{\partial e}{\partial z}\right] + \frac{\partial e}{\partial t} = 0 \qquad (5.6)$$

where z is the one-dimensional material coordinate, e is the void ratio, K(e) is the function relating permeability to void ratio, σ' is effective stress, and γ and γ_s are the unit weights of fluid and solid (Gibson et al., 1967). The first term in this equation represents the contribution of the weight of the material to its own consolidation. This term can be neglected for laboratory testing of representative samples (Znidarcic, 1982; Gibson, 1967). The governing equation then becomes

$$\frac{\partial}{\partial z}\left[\frac{K(e)}{\gamma\,(1+e)}\frac{\partial\sigma'}{\partial e}\frac{\partial e}{\partial z}\right]+\frac{\partial e}{\partial t}=0 \qquad (5.7)$$

Two fundamental properties included in this equation determine the rate of consolidation. The hydraulic conductivity K(e) determines the rate at which fluid can move through the sample and therefore the rate at which the sample can drain while loaded. The second factor is the compressibility of the soil skeleton. Consolidation is analyzed by determining these two material properties with laboratory testing.

Traditionally, the void ratio-effective stress relation and the hydraulic conductivity as a function of void ratio are determined by oedometer testing. The sample is loaded incrementally and the sample deformation is monitored. After each load increment, the hydraulic conductivity is measured using a constant or falling head test. The procedure is time consuming under ordinary conditions, and when testing bentonite clays the time involved may exceed practical laboratory limits. In addition, hydraulic conductivity testing imposes a pressure gradient across the sample which continues the consolidation process, making hydraulic conductivity measurements questionable (Znidarcic, 1982).

Other tests to estimate soil consolidation include:

(a) step loading test,
(b) constant rate of deformation;
(c) controlled gradient test;
(d) constant rate of loading test;
(e) seepage test, and
(f) relaxation test.

All tests available today involve initiating consolidation and then attempting to back-calculate the material coefficients of the governing equation (Znidarcic, 1982). The methods to solve this inversion problem involve some approximation (Lambe and Whitman, 1979, p. 411). Most test procedures, and all the common tests used commercially, utilize Terzaghi's theory of one-dimensional consolidation (Winterkorn and Fang, 1975, p. 112). The test procedures developed from this theory assume that over a reasonable testing time the excess pore pressures induced by loading dissipate (Lambe and Whitman, 1979, p. 423; Holtz and Kovacs, 1981, p. 291). The rate of dissipation is a function of permeability. Terzaghi states that "changes in water content due to changes in the state of stress take place very slowly, because the low permeability of the soil does not permit a rapid transfer of water from one part of the soil mass to another" (Terzaghi, 1942, p. 265). For clays that are, for engineering purposes, essentially impermeable, this process is too slow to measure.

Test results, discussed in Section 6.3, bear out what theory predicts with respect to the clays under study. Long-term consolidation remains constant which makes various curve-fitting approximation solutions ineffectual.

The test apparatus and procedures for consolidation testing are designed to provide long-term testing at pressures that approximate the injection pressures at Cargodera Canyon. Oedometer type devices were not employed for the reasons already discussed and because they employ continuous saturation reservoirs that can induce swelling in Na bentonites. Oedometers are also designed to reduce any friction the sample might experience as it undergoes a volume change. The smooth tubing used for testing in this study was tested for sample-wall friction by performing a push-out test on one of the plugs tested. The results of this test are reported in Section 6.3.

5.4.3 Consolidation Test Equipment and Procedures

Consolidation testing of bentonite plugs is accomplished using the apparatus illustrated in Figure 5.5. Nitrogen is the source of consolidation pressure. The system is similar to the apparatus used in constant pressure testing, described in Section 5.3.3 (Figure 5.4). No reservoir is required and compressed gas flows directly into tubes 5-8. Tube dimensions are identical with those described for constant pressure testing. Plug construction used the same specifications except that saturation was allowed to continue for 16 days until no standing water remained above the bentonite plugs. Pressure testing of the tubes after plug construction was performed using pressures less than 34 kPa (5 psi) and soap solutions at sealing edges to identify leaks. Special care was taken not to preconsolidate the plugs by draining them into imperfectly saturated sand with test pressures. Once plugs are constructed, they begin drawing water from the sand, and back pressure saturation must be continued until testing is initiated.

Collection of outflow was accomplished with four 25-ml capacity pipettes. Figure 5.6 shows the apparatus once testing had been initiated. An effort was made to estimate the height of each plug above the sand column. Irregular plug surfaces made this difficult. A reference point at the top of each plug was marked and its position measured periodically to monitor changes in the volume of the plugs.

Consolidation pressure was initially set at 34 kPa (5 psi). At that time 5 ml-capacity pipettes were used to collect outflow. Initial consolidation and pore pressure equilibration resulted in an almost instantaneous flow greater than the capacity of the pipettes. The test was stopped and the pipettes were replaced by 25 ml-capacity pipettes. When testing resumed, a consolidation pressure of 69 kPa

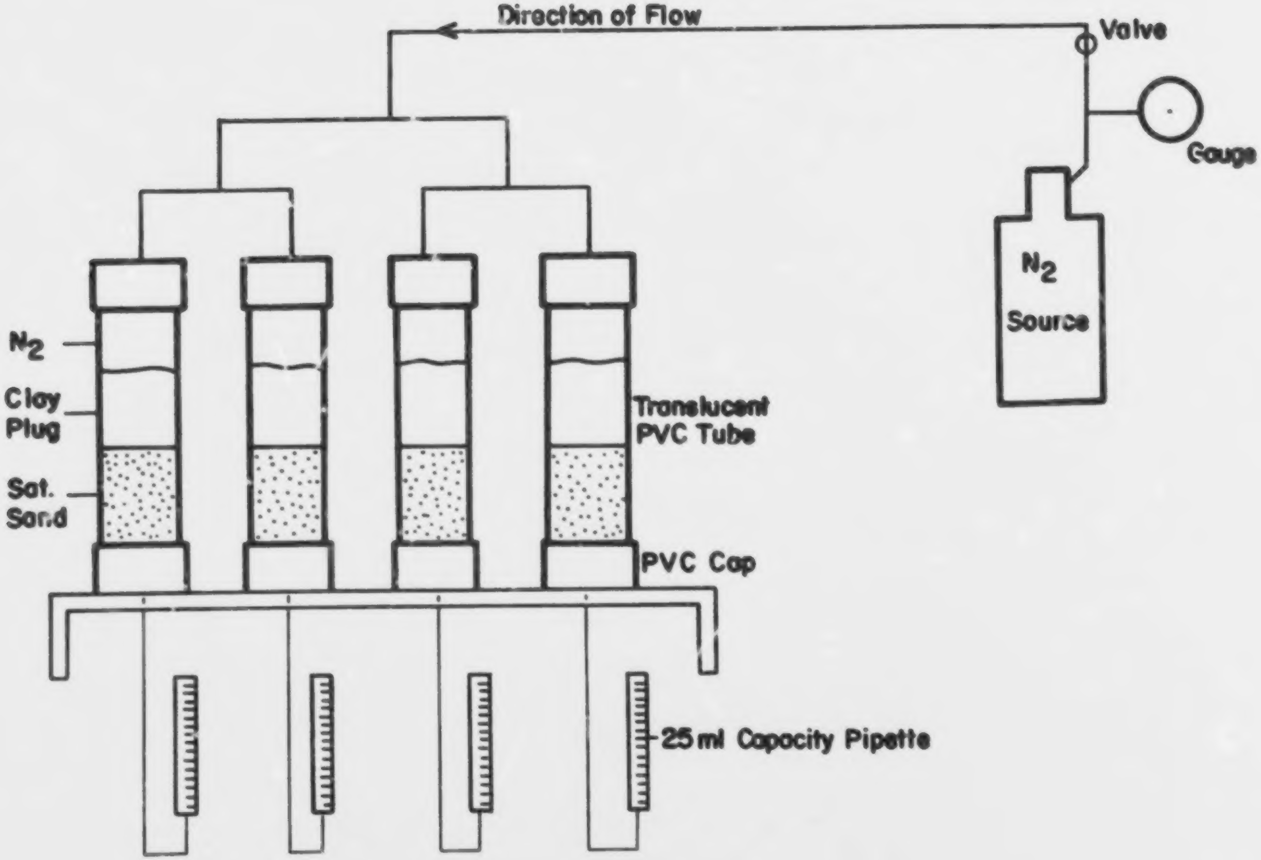
Direction of Flow
Valve
Gauge
N_2
Source
N_2
Clay Plug
Sat. Sand
Translucent PVC Tube
PVC Cap
25 ml Capacity Pipette

Figure 5.5 Schematic of apparatus for consolidation testing of bentonite plugs: tubes 5 through 8.

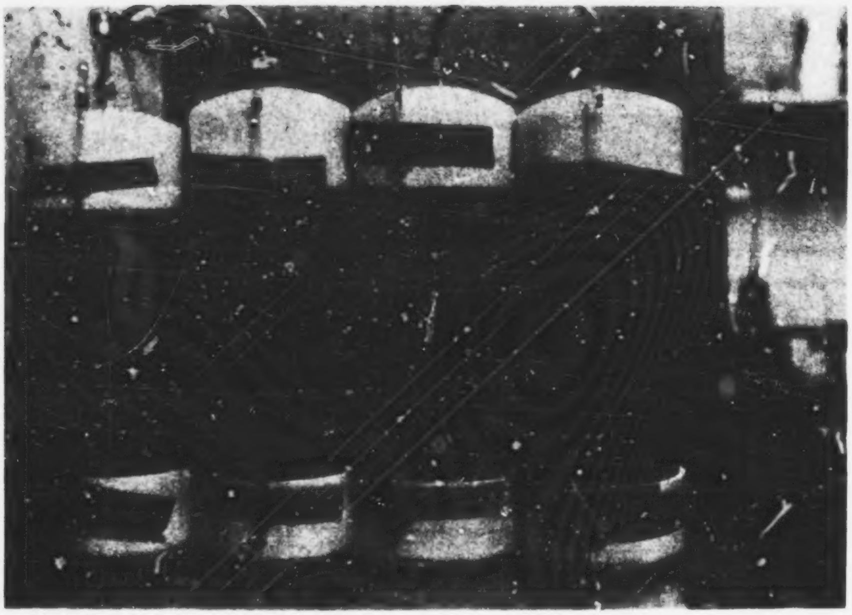

Figure 5.6 Apparatus for consolidation testing of bentonite plugs: tubes 5 through 8.

BEST COPY AVAILABLE

(10 psi) was used as the clay plugs had already experienced a 34 kPa (5 psi) stress. Later, pressure was increased to 138 and then to 207 kPa (20 and 30 psi). Each time a new pressure is used, careful early time measurements are made. Readings of outflow are taken at 30 seconds, one minute, two minutes, four minutes, eight minutes and at similar intervals for the first two hours of consolidation under a new pressure.

Consolidating with nitrogen dehydrated the surface of the plugs. After several weeks of testing, small cracks appeared in the surface of the plugs. Thes cracks deepened over time. The deepest cracks were wedge-shaped and approximately 2 cm (3/4 inch) deep. When testing at a certain pressure was completed, pressure was removed from the system. The fittings at the top of each tube were loosened and approximately 90 ml of water was added. After 24 hours, no standing water could be observed above any of the plugs, and the cracks had healed. The tubes were then closed and testing resumed.

Distilled water is used for plug construction and each time plugs are allowed to heal. Testing takes place in a laboratory with temperature variations limited to approximately 2 to 3 degrees celsius.

5.5 Swelling Rate/Moisture Content Testing

5.5.1 Introduction

Laboratory swelling rate and moisture content testing of bentonite plugs has as primary objective determining the effects of these factors on the measurement of hydraulic conductivity. In-situ testing of bentonite plugs at Cargodera Canyon involves injecting water under pressure into plugs over an extended period of time. Plug design incorporates a system for collecting the outflow. Preliminary field results, reported in Section 4.7, suggest that high inflows and low or no outflows may characterize the system for much of its testing history. If the high inflows are not a result of plug intake, they may indicate a failure in the plug system or the presence of fractures or damaged zones acting as conduits in the rock surrounding the plugs and injection interval.

Moisture content is related to permeability in most soils as a function of void ratio (e.g. Lambe and Whitman, 1979, Section 19.3). Higher moisture contents are associated with higher hydraulic conductivities. Though this relationship may hold for bentonite clays where sodium is the predominant exchangable cation, the ability of the clay to take up and hold water makes meaningful hydraulic conductivity measurements difficult. Simply achieving sample saturation presents many problems (Lowe and Johnson, 1960; Black and Lee, 1973; Brand, 1975). This is significant because all Darcian flow models assume saturation.

The ability of sodium bentonites to adsorb water and to swell can have several consequences on hydraulic conductivity of seals. Plugs that are allowed to swell freely in one direction may become more permeable through part of their volume. At the same time, swelling pressures induced at the confinement surfaces may reduce permeability along interface surfaces. Plugs that are completely confined, such as the ones tested at Cargodera Canyon, may exert swelling pressures against all confining surfaces. This may result in an overall decrease in hydraulic conductivity of the seal system over time, but could also result in an increased conductivity, especially if swelling opens up unfavorably oriented fractures in the rock.

5.5.2 Swelling Rate/Moisture Content Test Theory

The moisture content of a clay sample is the ratio of the weight of the water in the sample to the weight of the clay solids. The degree of saturation is the ratio of the volume of water in the clay to the volume of voids available. Both ratios are expressed as a percent. The swelling rate of clay can be described in a number of ways. Free swell is defined as

$$\frac{\text{final volume} - \text{initial volume}}{\text{initial volume}} \times 100$$

and is expressed as a percent. It is determined by dropping dry clay into a graduated cylinder filled with water and observing the equilibrium swelled volume (e.g. Holtz and Gibbs, 1956; Winterkorn and Fang, 1975, p. 90). Sodium bentonites have measured free-swell values as great as 1200% with this type of test (Holtz and Kovacs, 1981, p. 189). The swell index, C_s, is defined as $-\Delta e/\Delta \log \bar{\sigma}_v$ where Δe is the change in void ratio, and $\Delta \bar{\sigma}_v$ is the change in effective stress applied to the sample. It is usually measured after unloading a sample in confined compression (Lambe and Whitman, 1979, p. 321). If clays are subjected to repeated loading and unloading, the swell index and the compression index will approximately equal each other (Mitchell, 1976, p. 253; Lambe and Whitman, 1979, p. 321). The compression index has the same form as the swell index without the negative sign. Lambe and Whitman (1979, p. 322) give C_s values for a sodium montmorillonite of 9 when unloaded from 1000 to 100 kPa and 17 when unloaded from 100 to 10 kPa.

Swelling percentage is the amount of vertical swell of heave obtained when the clay is wetted at a nominal pressure, usually 6.9 kPa (1 psi). It is expressed as a percentage of the initial sample thickness (Hilf, 1975, p. 305). The testing procedure uses pressures associated with in-situ testing of bentonites to determine swelling percentages relevant to plug performance testing.

Researchers have related the swelling performance of clays to index values or reference values that can be reliably determined in the laboratory (Holtz and Gibbs, 1956; Ladd and Lambe, 1961; Kantey and Brink, 1962 - all quoted by Hilf, 1975, p. 305). Methods of identifying and classifying swelling clays are reviewed by Kassiff et al. (1969, Ch. 3). They conclude that shrinkage limit, liquid limit, plasticity index and free swell tests are useful, when used in combination, to predict swell behavior.

5.5.3 Swelling Rate/Moisture Content Testing Equipment and Procedures

Swelling rate and moisture content testing of bentonite plugs is performed using the apparatus illustrated in Figure 5.7. Water is injected under low pressure into tubes 9 through 12 using a nitrogen over water system. The effectiveness of this system depends upon nitrogen's solubility in water under given temperatures and pressures.

Tube dimensions and sealing specifications are identical to those described for tubes 1 through 8 in the preceding sections of this chapter. Plug construction proceeded as for tubes 1 through 8. Plugs saturated and swelled for 14 days before the tubes were sealed and testing was initiated. Preliminary tube test pressures were low to avoid forcing water into the plugs before inflow could be monitored. Figure 5.8 shows the apparatus configuration with testing underway.

Distilled water is used for plug construction and injection. Temperature is controlled as in the tests already described. As in the consolidation test, volume change is monitored with a reference height marked on the outside of each tube. Injection pressure was initially set at 34 kPa (5 psi) and later was increased to 69 kPa (10 psi).

5.6 Reference Testing

5.6.1 Introduction

Laboratory reference testing of the bentonite clays used for in-situ sealing has as its objective determining the significant water content values that determine the engineering properties of this clay. Water content is a critical factor in the stress-strain behavior of clay (Meyer and Howard, 1983, p. 42). The water content at which a clay is compacted influences the hydraulic conductivity of the seal (Meyer and Howard, 1983, p. 38; Holtz and Kovacs, 1981, p. 118).

Three types of tests were performed. The liquid limit test determines approximately the minimum water content at which the clay behaves as a liquid, that is, flows as a liquid and exhibits little shear strength (Lambe and Whitman, 1979, p. 33). The plastic limit test determines approximately the lower bounds of water content at which the clay behaves plastically (Holtz and Kovacs, 1981, p. 34). The moisture/density compaction test predicts the optimum water content that corresponds to the maximum degree of compaction (Meyer and Howard, 1983, p. 38).

5.6.2 Liquid Limit Tests

The liquid limit has been determined for American Colloid 1.25 cm (1/2 inch) diameter Volclay bentonite tablets using the ASTM D 423-66 test procedures and equipment, with one important modification. The procedural modification overcomes one of the basic objections raised by Holtz and Kovacs (1982, p. 38) to the standard ASTM test procedure. The procedure calls for mixing bentonite with distilled

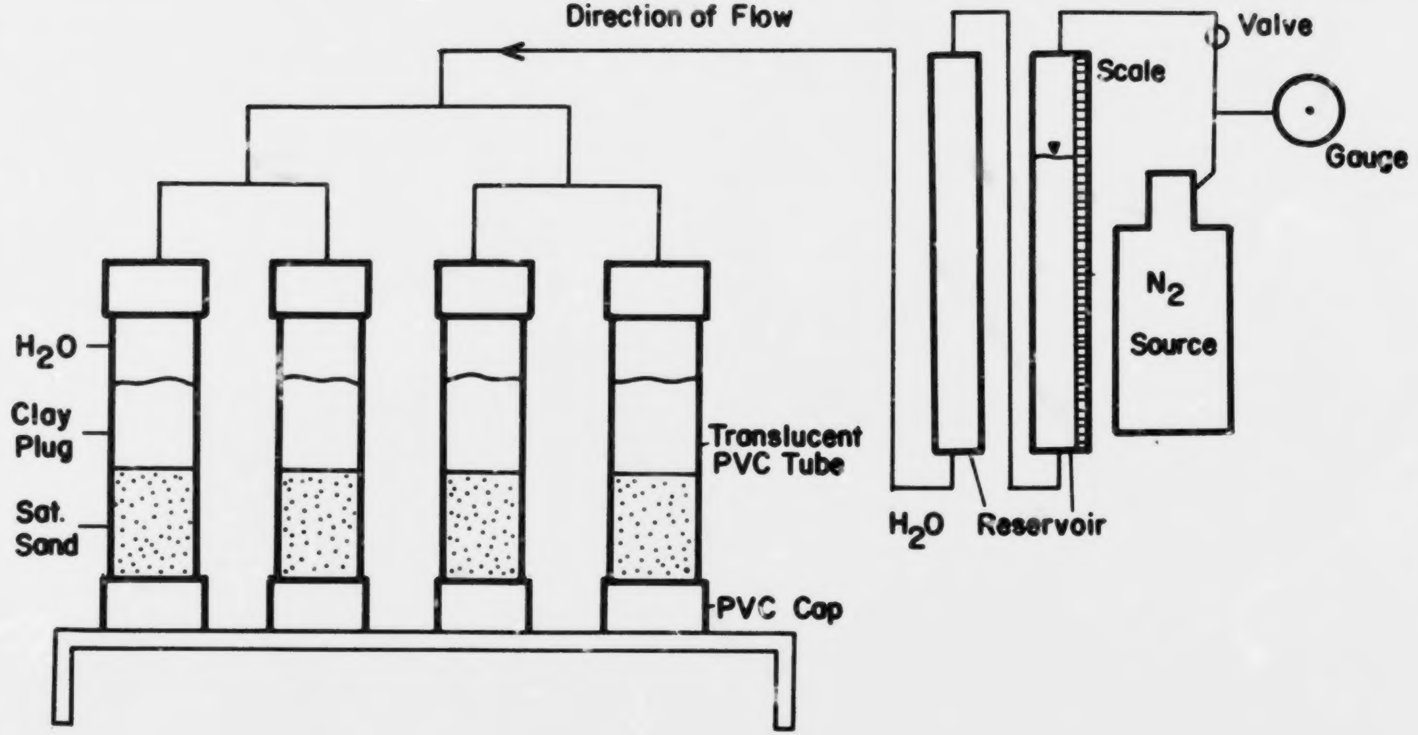
Direction of Flow
Valve
Scale
Gauge
N_2
Source
H_2O
Clay
Plug
Sat.
Sand
Translucent
PVC Tube
PVC Cap
H_2O
Reservoir

Figure 5.7 Experimental arrangement for swelling rate and moisture content experiments on bentonite plugs.

BEST COPY AVAILABLE

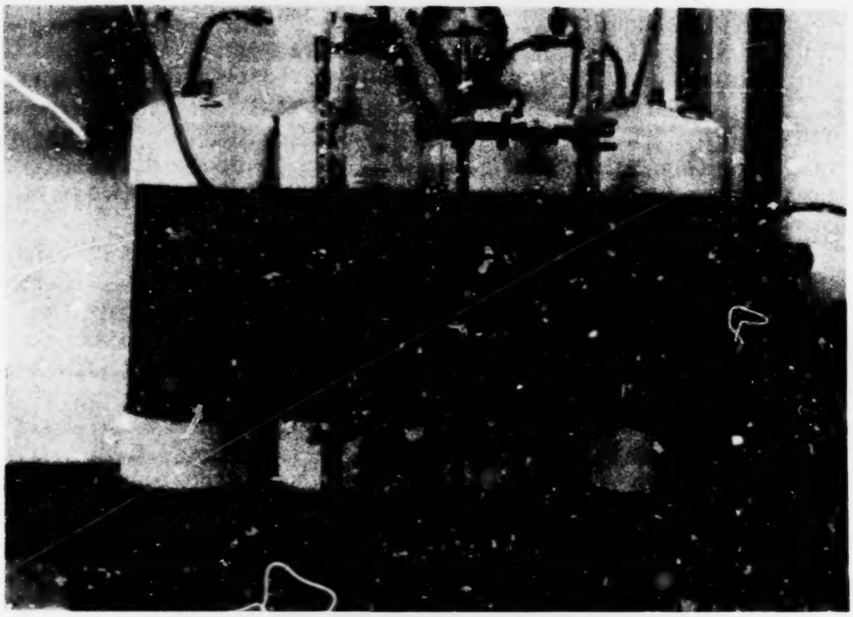

Figure 5.8 Apparatus for bentonite swelling rate and moisture content testing.

BEST COPY AVAILABLE

water and testing the resulting bentonite paste. The objective of the testing associated with this study is to determine reference values relevant to the plugs emplaced and tested at Cargodera Canyon. An effort was made in all testing to use clay produced in a manner similar to in-situ seal construction. Reference testing clay was produced by dropping tablets through the amount of water required for a given moisture content. The containers of clay and water were then sealed and left untested for 14 days. At that time the clays were inspected for homogeneity. Clays at higher water contents, greater than 200 percent, required some mixing to move the unadsorbed water into contact with all the clay. The mixed clays mixed were then resealed and left untested for 7 more days.

Liquid limit testing uses bentonite clay paste prepared at different moisture contents. A sample is prepared by placing it in the brass dish of the liquid limit device. A groove is cut in the paste using a grooving tool. The depth of the sample in the cup in the paste should be approximately 1 cm. The brass dish is then raised and dropped using the liquid limit testing device. The dish is dropped 1 cm at a rate of 2 drops per second until the bottom of the groove closes along a distance of 1.25 cm (1/2 inch). The number of drops required for closure at each moisture content is recorded.

5.6.3 Plastic Limit Test

Plastic limit testing was performed on the American Colloid 1.25 cm (1/2 inch) diameter Volclay bentonite tablets using procedures conforming to the ASTM D 424-59 standard, with the important modification in sample preparation described in Section 5.6.2. An 8 gram sample is formed into an ellipsoidal mass. It is rolled on a ground glass plate using fingers to apply pressure and rolling at a rate of 80 to 90 strokes per minute. When the diameter of the thread becomes 3 mm (1/8 inch), it is broken into 6 to 8 pieces, reshaped into an ellipsoidal mass, and rerolled. This procedure is repeated until the thread can no longer be formed as the soil crumbles under pressure. The clay is weighed and the water content determined by oven drying the sample for three days at 110°C.

5.6.4 Harvard Miniature Compaction Test

Moisture density testing was performed on American Colloid 1/2 inch diameter Volclay bentonite tablets using a Harvard Miniature Mold (Wilson, 1970) and an energy input equivalent to the ASTM Standard Proctor Test (ASTM D698-78).

Three phases are present in an unsaturated clay: solid, liquid and gas. When the clay is reduced in volume without permitting drainage, the gas phase is expelled. The void ratio decreases. The degree of saturation increases as the ratio of volume of water to the volume of voids is greater. The volume of water in the clay is constant throughout the test. The strength, permeability and swelling characteristics of the clay are affected by the compaction method, by the compaction effort, and by the moisture content of the specimen at the time of compaction. The moisture density relation established by the compaction curve describes these relationships.

The test procedure determines these relationships using a Harvard Miniature Compaction Mold and fabricated hammer as described by Sawyer and Daemen (1987). Samples with different moisture contents were prepared as described in Section 5.6.2. Six moisture contents were tested. Compaction effort conforms to the effort specified in the Standard Proctor Test (ASTM D 698-78). Five clay layers, with fifteen blows per layer, are used to achieve compaction. After compaction for each sample, dry density is determined .

5.7 Transient Hydraulic Conductivity Testing

5.7.1 Introduction

The primary objective of laboratory transient pulse testing is to determine the hydraulic conductivity of the bentonite plugs. Standard techniques for determining the hydraulic conductivity of low permeability materials are difficult or impractical. They involve long-term injection to achieve steady-state flow. Achieving steady state flow and measuring very small flow rates can make the values derived from these tests problematic. The constant injection test analysis in Section 6.2 illustrates some of these problems. Hsieh et al. (1981) review various transient pulse testing and analysis methods. They present a general solution and develop equations for limiting cases. This phase of laboratory testing attempts to employ the methods and analysis they present to determine hydraulic conductivity values for the clay used in-situ as a borehole seal.

5.7.2 Transient Hydraulic Conductivity Analysis

Transient pulse testing uses an experimental arrangement illustrated in Figure 5.9. The sample tested links two fluid reservoirs. At the start of the experiment, the fluid pressure in the upstream reservoir is suddenly increased. Pressure decay in the upstream reservoir is monitored as is the pressure build-up of the downstream reservoir. Brace et al. (1968) developed a method for analyzing the upstream decay to calculate the hydraulic conductivity of the sample. The method assumes no compressive storage in the sample. This assumption may be approximately true for crystalline rock, but is a poor one for shales, argillites and especially clays. Lin (1977) developed a model that accounts for compressive storage. However, the solution requires that the specific storage of the sample be determined from laboratory testing for porosity and bulk compressibility. The solution by Hsieh et al. (1981) accounts for specific storage without requiring that it be known.

Hsieh et al. (1981) use a mathematical model developed by Brace et al. (1968). The equation describing one-dimensional flow of a slightly compressible fluid in a saturated porous media where hydraulic conductivity, K, and specific storage, S_s, are constant is

$$\frac{\partial^2 h}{\partial x^2} - \frac{S_s \partial h}{K \partial t} = 0 \qquad (5.8)$$

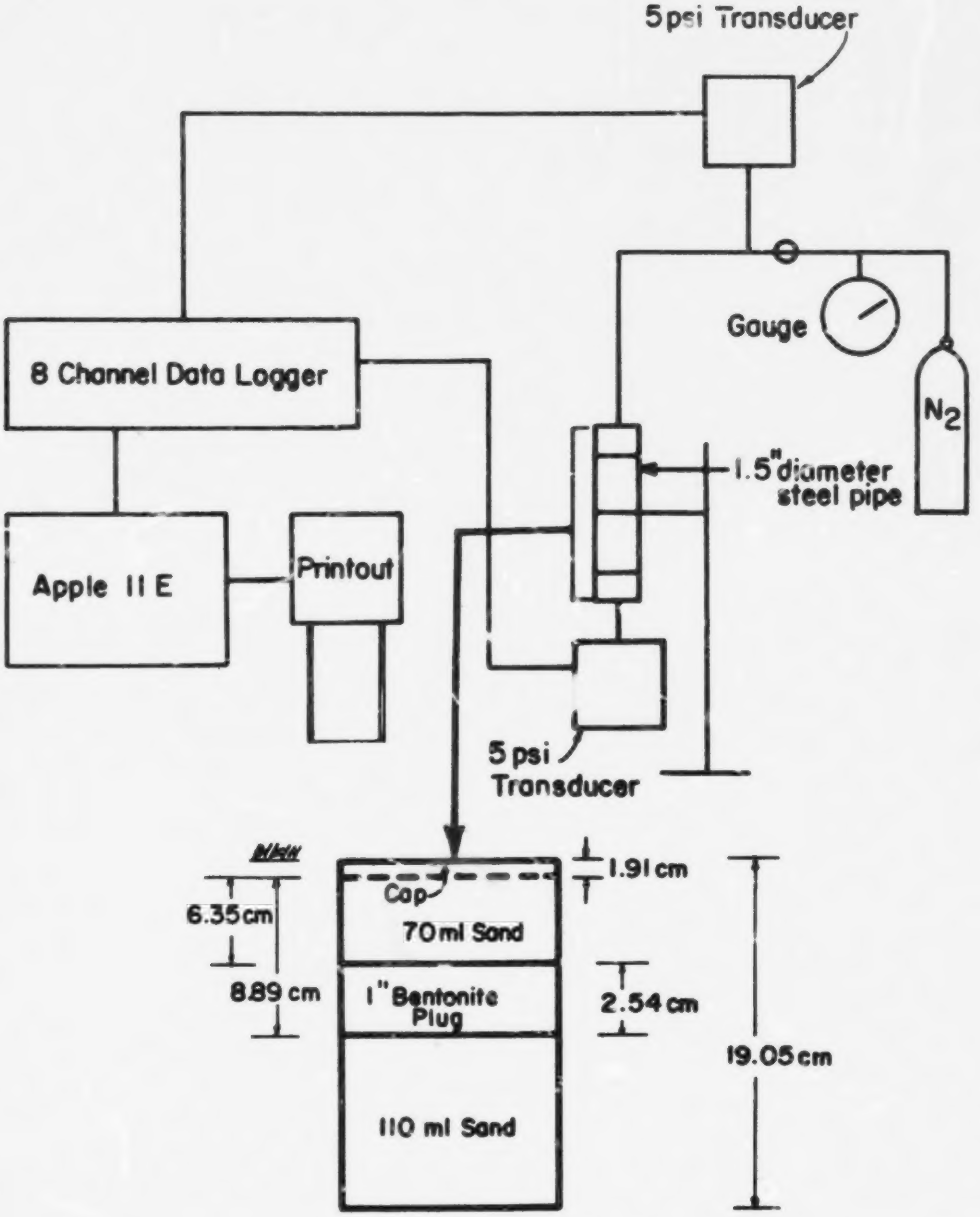
5psi Transducer
8 Channel Data Logger
Gauge
N_2
1.5" diameter steel pipe
Apple II E
Printout
5 psi Transducer
Cap
70 ml Sand
1" Bentonite Plug
110 ml Sand
6.35 cm
8.89 cm
1.91 cm
2.54 cm
19.05 cm

Figure 5.9 Apparatus and sample dimensions for laboratory transient pulse testing of bentonite plug.

BEST COPY AVAILABLE

where h is the hydraulic head, x is the distance along the sample, $x = 0$ is the downstream face, $x = L$ is the upstream face, and t is the time from the start of the experiment. At the start of the experiment, hydraulic head distribution is uniform and 0

$$h(x,0) = 0 \quad \text{for} \quad 0 < x < L \tag{5.9}$$

The upstream and downstream faces of the sample are in direct contact with the respective reservoirs and this is described by

$$h(0,t) = h_d(t) \quad \text{for} \quad t \geq 0 \tag{5.10}$$

$$h(L,t) = h_u(t) \quad \text{for} \quad t \geq 0 \tag{5.11}$$

where h_d is the hydraulic head in the downstream reservoir and h_u is the hydraulic head upstream.

Conservation of mass at the sample reservoir interfaces is expressed by

$$\frac{S_d}{KA}\frac{dh_d}{dt} - \left(\frac{\partial h}{\partial x}\right)_{x=0} = 0 \quad \text{for} \quad t > 0 \tag{5.12}$$

and

$$\frac{S_u}{KA}\frac{dh_u}{dt} + \left(\frac{\partial h}{\partial x}\right)_{x=L} = 0 \quad \text{for } t > 0 \tag{5.13}$$

where S_d is compressive storage of the downstream reservoir, S_u is compressive storage of the upstream reservoir. At the start of the test, hydraulic head in the downstream reservoir equals the head in the sample:

$$h_d(0) = 0 \tag{5.14}$$

A hydraulic head increase H is applied at the start of the test to the upstream reservoir

$$h_u(0) = H \tag{5.15}$$

The analytical solution to this problem uses the dimensionless time variable

$$\alpha = \frac{Kt}{L^2 S_s} \tag{5.16}$$

and the dimensionless parameters

$$\beta = \frac{S_s AL}{S_u} \qquad (5.17) \qquad\qquad \gamma = \frac{S_d}{S_u} \qquad (5.18)$$

where A is the cross-sectional area of the sample.

The solution, presented by Hsieh et al. (1981) for the decay of hydraulic head in the upstream reservoir is

$$\frac{h_u}{H} = \frac{1}{1 + \beta + \gamma} + 2 \sum_{m=1}^{\infty} \frac{\exp(-\alpha\phi_m^2)(\beta + \gamma^2 \phi_m^2/\beta)}{\left[\frac{\gamma^2 \phi_m^4}{\beta^2} + (\gamma^2 \beta + \gamma^2 + \gamma + \beta) \frac{\phi_m^2}{\beta} + (\beta^2 + \gamma\beta + \beta)\right]} \qquad (5.19)$$

where ϕ_m are roots of

$$\tan\phi = \frac{(1 + \gamma)\phi}{\frac{\gamma\phi^2}{\beta} - \beta} \qquad (5.20)$$

Build-up in the downstream reservoir is described by

$$\frac{h_d}{H} = \frac{1}{1 + \beta + \gamma} + 2 \sum_{m=1}^{\infty} \frac{\exp(-\alpha\phi_m^2)(\beta - \gamma \phi_m^2/\beta)}{\left[\frac{\gamma^2 \phi_m^4}{\beta^2} + (\gamma^2 \beta + \gamma^2 + \gamma + \beta) \frac{\phi_m^2}{\beta} + (\beta^2 + \gamma\beta + \beta)\right] \cos\phi_m} \qquad (5.21)$$

An approximate "early time" solution when α is small is given by

$$h_u/H = \exp(\alpha\beta^2)\ \mathrm{erfc}(\alpha\beta^2)^{1/2} \tag{5.22}$$

An approximate solution for large time, i.e. large α is

$$\frac{h_u}{H} = \frac{1}{1+\beta+\gamma} + \frac{2\exp(-\alpha\phi_1^2)(\beta + \gamma^2\phi_1^2/\beta)}{\left[\frac{\gamma^2\phi_1^4}{\beta^2} + (\gamma^2\beta + \gamma^2 + \gamma + \beta)\frac{\phi_1^2}{\beta} + (\beta^2 + \gamma\beta + \beta)\right]} \tag{5.23}$$

for the upstream reservoir and

$$\frac{h_d}{H} = \frac{1}{1+\beta+\gamma} + \frac{2\exp(-\alpha\phi_1^2)(\beta - \gamma\phi_1^2/\beta)}{\left[\frac{\gamma^2\phi_1^4}{\beta^2} + (\gamma^2\beta + \gamma^2 + \gamma + \beta)\frac{\phi_1^2}{\beta} + (\beta^2 + \gamma\beta + \beta)\right]\cos\phi_1} \tag{5.24}$$

where ϕ_1 is the first root of equation (5.20)

Another important limiting case is when $\gamma \to 0$, as the downstream face of the sample is essentially impermeable. This is described by

$$\frac{h_u}{H} = \frac{1}{1+\beta} + 2\sum_{m=1}^{\infty} \frac{\exp(-\alpha\phi_m^2)}{\phi_m^2/\beta + \beta + 1} \tag{5.25}$$

where ϕ_m are roots of

$$\tan\phi = -\phi/\beta \tag{5.26}$$

5.7.3 Transient Hydraulic Conductivity Testing Equipment and Procedures

Transient hydraulic conductivity testing of American Colloid 1.25 cm (1/2 inch) diameter Volclay bentonite tablets is performed using the apparatus illustrated in Figure 5.9. The 2.5 cm (one-inch) long clay plug is contained between two sand columns in a 1.25 cm (1/2 inch) I.D. steel pipe. Pressure is induced in the upper reservoir using a nitrogen-over-water system, the water reservoir being the small free space at the top of the upper sand column. Upper reservoir pressure is monitored by a Dynisco 34 kPa (5 psi) transducer mounted on the injection line. Downstream reservoir pressure is monitored by an identical transducer mounted directly to the bottom cap of the steel pipe. A valve between the nitrogen source and the upper reservoir allows the isolation of a pressure pulse in the test apparatus. The transducers are connected to a multi-channel data-logger. The data-logger converts the transducer signals for the Apple II-E microprocessor which outputs the reservoir pressures at 10 to 20 minute intervals.

Plug construction is accomplished with clay of a given moisture content. The clay is prepared as described in Section 5.6.1. The clay is taken from the container and placed in a mold with a 1.25 cm (1/2 inch) thickness and a diameter equal to the diameter of the steel pipe used for testing. Excess clay is removed from the mold and the clay is extruded as gently as possible and placed in the pipe above the bottom sand layer. This procedure is repeated to form a plug 2.5 cm (1 inch) long. An effort is made to avoid kneading or compacting the plug in any way. Some smearing is involved in assuring a tight fit between the plug and the steel pipe. Once the entire plug assembly is complete, the fittings in the caps of the pipe are plugged and the apparatus is left for three days to a week. This allows the plug to draw water from the sand and swell against the sides of the pipe, forming an effective seal. When testing is completed, the plug is removed and a portion is weighed and oven-dried to determine the moisture content of the tested sample.

The configuration of the upper and lower reservoir is designed to approximate optimum test design as described by Hsieh et al. (1981). The actual ratio of downstream to upstream reservoir in this test set-up is 0.87. This is the ratio of water volumes, not total volume, since the actual ratio is based on the compressibility of water and sand is assumed to be incompressible. Hsieh et al. (1981) also recommend a ratio of 1 to 10 and 10 to 1 for a test to determine the specific storage of the sample. For this study, a separate pipe was prepared with reservoir volumes equal to the ratios recommended by Hsieh. Plug construction in this pipe is accomplished using the same procedures already described.

5.8 Saturation Test

5.8.1 Introduction

The significance of degree of saturation to the hydraulic conductivity of bentonite plugs has been discussed previously in the context of both field and laboratory investigations. Degree of saturation also influences the compressibility of a clay (Lambe and Whitman, 1979, Section 28.6). Lambe and Whitman (1979, pp. 313-332) suggest that for sodium montmorillonites at low confining pressures, void ratios of more than 25 can exist. For a saturated clay, this would correspond to a moisture content of 900%. At high confining pressures, void ratios can be as low as .2 with a corresponding moisture content of 7%. The relationship of void ratio to water content to degree of saturation is also important in determining the volume stability of bentonite clays (Meyer and Howard, 1983, Section 2.1.3.1).

The objective of saturation testing is to determine the relationship of moisture content to degree of saturation at the low pressures experienced by clay seals when tested in situ at Cargodera Canyon. In this way, the moisture content of the clay as it approaches 100% saturation can be predicted.

5.8.2 Theory

The behavior of a clay sample when subjected to stress will be controlled by the effective stress the clay experiences (Lambe and Whitman, 1979, Chapter 16). Effective stress $\bar{\sigma}$ is defined as the total stress σ minus the pore water pressure p:

$$\bar{\sigma} = \sigma - p \qquad (5.27)$$

For a partially saturated clay, this can be rewritten as

$$\bar{\sigma} = \sigma - u^* \qquad (5.28)$$

where u^* is the equivalent pore pressure and is equal to

$$u^* = u_a a_a + u_w a_w \qquad (5.29)$$

where u_a is the pore pressure carried by gas; a_w is defined as the water surface area of an element divided by the total surface area of that element and a_a is the air surface area divided by the total area of that element (Lambe and Whitman, 1979, Section 16.3). In a saturated soil a_a is zero and equation (5.30) reduces to

$$u^* = u_w a_w \qquad (5.30)$$

where a_w varies between 0.97 and 1.00 and, therefore, approximates

$$u^* = p \qquad (5.31)$$

The effective stress equation can be rewritten as

$$\bar{\sigma} = \sigma - u_a + a_w(u_a - u_w) \qquad (5.32)$$

since $a_a + a_w$ is approximately equal to 1. If a_w is allowed to equal approximately 1, then the pore pressure can be expressed as

$$u_w = \sigma - \bar{\sigma} - u_a \qquad (5.33)$$

When a clay sample is loaded axially with no drainage permitted, the stress applied is experienced to a large degree by the fluids in the clay (Lambe and Whitman, 1979, p. 296). The ratio of pore pressure build-up to total stress applied is defined as the pore pressure parameter C. Lambe and Whitman (1979, Section 2.6.1) discuss this pore pressure parameter in relationship to an undrained oedometer test on a saturated soil. Figure 26.3 of Lambe and Whitman (1979, p. 393) shows the idealized result, with C as a straight line slope between applied load and pore pressure build-up. The slope of this line is approximately 45 degrees and the ratio is approximately one. In this type of test, the effective stress experienced by the clay solids is approximately zero. Then $u_w = \sigma$. However, if the soil is not saturated, then $u_w = \sigma - u_a a_a$ and the pore pressure parameter will be less than one. The closer the clay is to being saturated, the closer the value of C will be to unity.

5.8.3 Saturation Test Equipment and Procedures

Saturation testing of American Colloid 1.25 cm (1/2 inch) diameter Volclay bentonite tablets is accomplished using the same equipment and procedures as described in Section 5.7.3, with one exception: the pressure induced in the upper reservoir is kept constant over the duration of the test and the pressure build-up in the downstream reservoir is monitored.

5.9 Large-Scale Transient Testing

5.9.1 Introduction

The laboratory hydraulic conductivity testing portion of this study uses clay plugs with diameters smaller than the seals tested in-situ at Cargodera Canyon. The transient pulse test described in Section 5.7 is performed on samples with a diameter of 3.8 cm (1.5 inches) and a thickness of approximately 2.5 cm (1 inch). The objective of the large-scale transient pulse test is to determine the hydraulic conductivity and specific storage coefficient for a plug with dimensions similar to the plugs tested in the field. This provides some comparison with respect to the influence of scale on this type of testing. Conditions of testing more realistically approximate in-situ test environments without the influence of host rock characteristics. In addition, the large-scale test is conducted with higher pressures.

The influence of test pressures on results can be estimated by comparing the hydraulic conductivities calculated for different scales of testing.

5.9.2 Large-Scale Transient Test Theory

The theory of transient pulse testing of laboratory samples is discussed in Section 5.7.2.

5.9.3 Large-Scale Transient Testing Equipment and Procedures

Large-scale transient plug testing of American Colloid 1.25 cm (1/2 inch) diameter Volclay bentonite tablets is accomplished using the reservoir-plug configuration shown in Figure 5.10. The inside diameter of the steel pipe is 15 cm (6 inches). A total of 16,120 cm^3 (.59 ft^3) of sand was used to create a lower interval approximately 90 cm (36 inches) high. It was poured in two layers to allow emplacement of the lower reservoir pressure monitoring apparatus. This apparatus includes a 6 mm (1/4 inch) copper tube coiled and perforated as described in Section 4.3. The copper coil is connected to the top of the pipe by 6 mm (1/4 inch) stainless steel tubing. The bentonite plugs were formed by dropping 800 bentonite tablets through 90 cm (3 feet) of water standing above the sand. After 7 days, a plug 12.5 cm (5 inches) long had formed. The aspect ratio of this plug with respect to diameter and length is .83. The aspect ratio of plugs tested at Cargodera Canyon is .92.

Testing is accomplished using a nitrogen-over-water system. Pressure is introduced directly into the upper reservoir or into the lower reservoir via the copper coil. Pressure decay in either reservoir is monitored using a 345 kPa (50 psi) Dynisco transducer and the strip chart recorder described in Section 3.5.3. The ratio of downstream water volume to upstream water volume is .1. Testing is performed at night to minimize the influence of temperature.

5.10 Plug Prototype Study

One of the difficulties associated with in-situ testing of a material as complex in its behavior as bentonite is the necessity of inferring behavior from simple mass-balance measurements. The plug prototype was designed to overcome this difficulty by simulating field dimensions and conditions while allowing a visual inspection of changes in the plugs over an extended time of testing.

Figure 5.11 is a schematic of the plug prototype and apparatus used for testing. The test column is constructed in a clear plastic tube with an inner diameter of 15 cm (6 inches). The dimensions of the sand and clay intervals are similar to the ones used in plug construction in borehole CCR/C-1 at Cargodera Canyon. The testing system utilizes nitrogen over water to inject into either sand interval. An injection/collection assembly that duplicates the system used in in-situ testing connects the two sand intervals with the test apparatus.

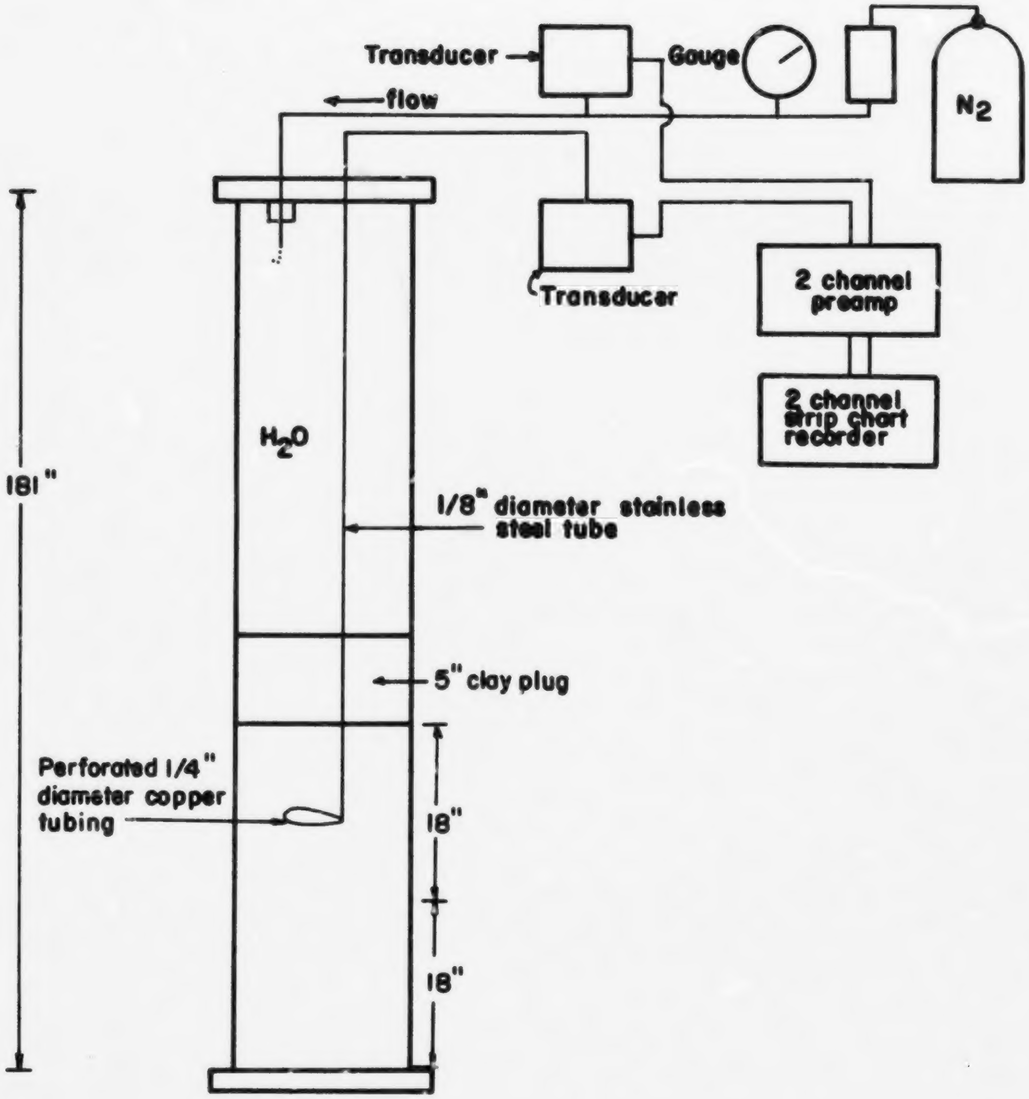
Transducer
flow
Gauge
N_2
Transducer
2 channel preamp
2 channel strip chart recorder
H_2O
181"
1/8" diameter stainless steel tube
5" clay plug
Perforated 1/4" diameter copper tubing
18"
18"

Figure 5.10 Large scale transient pulse test apparatus.

BEST COPY AVAILABLE

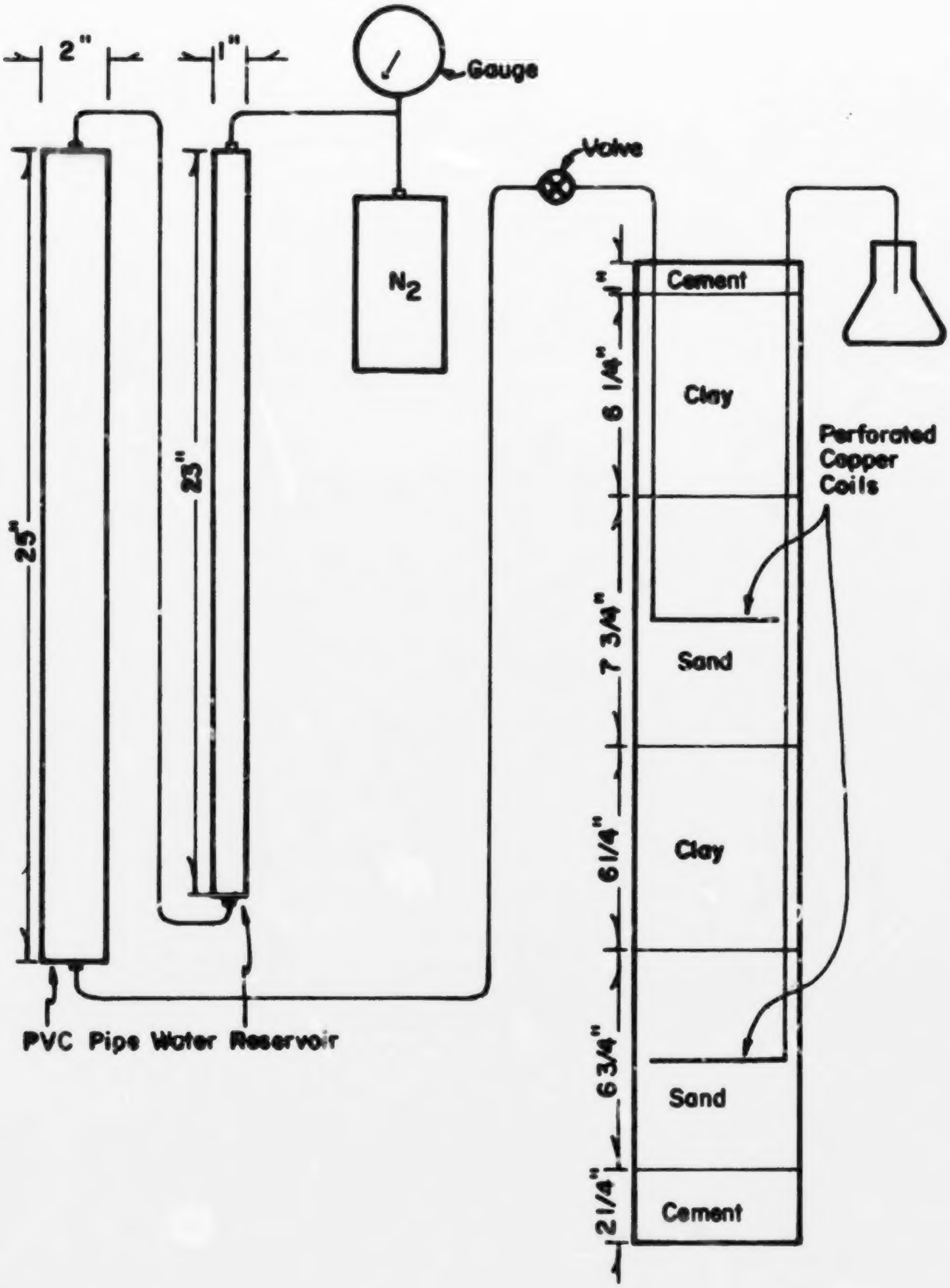

2"
1"
Gauge
Valve
N2
25"
23"
Cement
1"
6 1/4"
Clay
Perforated Copper Coils
7 3/4"
Sand
6 1/4"
Clay
6 3/4"
Sand
2 1/4"
Cement
PVC Pipe
Water Reservoir

Figure 5.11 Laboratory prototype for field bentonite plug simulation tests.

BEST COPY AVAILABLE

Plug construction in the prototype used the same procedures as in the field except that both plugs were constructed in three separate steps, dropping 300, then 400, and finally 300 tablets through water with a week between each drop.

CHAPTER SIX

RESULTS AND ANALYSIS OF LABORATORY TESTING OF BENTONITE BOREHOLE PLUGS

6.1 Introduction

The primary objective of this laboratory testing is to determine engineering properties of the bentonite clay used for field testing at Cargodera Canyon. The results and analyses in this chapter bear directly on the performance assessment of the plugs tested in situ.

The hydraulic conductivity of bentonite seals and seal rock interfaces is the critical concern in field testing. Determining an "ideal" (laboratory) performance against which real (field) performance can be measured requires hydraulic conductivity values established in controlled laboratory tests.

Two processes that affect the hydraulic conductivity of seals are consolidation and swelling. Both are difficult to assess in the field when the only measurements available are flow rates. Both processes can be quantified in the laboratory as a function of time and pressure as well as volume change. Once determined, these rate values can be used to adjust field flow measurements to reflect probable actual flow through the seal and seal-rock interface.

A comprehensive performance assessment of clay seals must judge the effectiveness of the emplacement method. The moisture content of the clay when emplaced, the degrees of compaction and saturation, and the volume and pressure of the water available for plug intake are among the variables that need to be selected. To make these decisions, the essential reference characteristics of the material must be known. They must be determined over a range of conditions similar to those experienced in the field.

In-situ testing of bentonite seals in a low-permeability rock mass involves transient analyses. Transient analysis can provide hydraulic conductivity and specific storage for both rock and clay within reasonable testing times. The effectiveness of this type of test for materials with no or little available previous testing as a reference can only be judged by laboratory comparisons. Laboratory results can be compared to laboratory steady-state test results. Similarly, the significance of test variables, such as reservoir volumes and volume ratios, as well as test pressures, can be estimated.

Scale tests and prototype observations provide a context for comparison of laboratory and in-situ testing. Large-scale laboratory experiments simulate field conditions in terms of seal size and pressures. Prototype observations provide a record of visible changes in volume and homogeneity of the seal material.

6.2 Hydraulic Conductivity: Constant Pressure Injection

Section 5.3 describes the purpose, theory, equipment and procedures used to test the hydraulic conductivity of bentonite plugs. Four plugs were tested under pressures of 34 to 69 kPa (5 to 10 psi). Appendix C includes test records over approximately 4 months. Tables C.1 and C.2 show inflow, outflow per plug, test pressure, estimated loss of saturation and hydraulic conductivity calculated for two daily measurements.

Hydraulic conductivities average approximately 10^{-8} cm/s for all four plugs. These values were determined assuming that all outflow from the plugs represented flow through the plugs. In fact, as discussed in Section 6.3, a significant portion of this flow is the result of plug consolidation. A more meaningful estimate of the hydraulic conductivity of the plugs might be made by subtracting the consolidation drainage from the outflow. This adjusted outflow is the basis for the analysis in this section.

Table 6.1 presents the results of hydraulic conductivity testing on the plugs in tubes 1 through 4 under constant pressure injection. Pressure was 34 kPa (5 psi) throughout this period. Hydraulic conductivity was calculated using the adjusted outflow discussed above. The conductivity values correspond to flow rates averaged over a twenty-four hour period during which two or three measurements were taken. These measurements, and the hydraulic conductivities calculated from the unadjusted outflow (Appendix C) were used to determine the hydraulic conductivities shown. Unadjusted hydraulic conductivity values were averaged for each twenty-four hour period and corrected using the consolidation rate discussed in Section 6.3.

Figures 6.1 and 6.2 plot the adjusted hydraulic conductivity. Dashed portions represent periods over which no measurement was made or when the measurements were considered suspect as a result of adjustments in the test equipment. These adjustments were primarily replacing the nitrogen source and refilling the water reservoirs.

The plugs in tubes 2 and 3 contain steel pipes as described in Section 5.3.3. These were designed to simulate the tubing that penetrates the plugs tested at Cargodera Canyon. A comparison of Figures 6.1 and 6.2 shows that the penetrated plugs exhibit an abrupt early time increase in hydraulic conductivity. The spike is absent in Figure 6.1. This suggests that the high conductivity in Figure 6.2 is a result of the pipes penetrating the plugs. If an experimental procedure was the cause, the anomalous values should be present in all four plugs. Both high values are approximately 6×10^{-7} cm/s, which is still low enough to approximate the hydraulic conductivity of the host rock tested at Cargodera Canyon (Sections 3.5.6 and 3.6.3). The field plug at the top of the injection interval is penetrated by two steel pipes, which may increase the penetration influence on the hydraulic conductivity of the Cargodera Canyon plug.

Table 6.1 Apparent Hydraulic Conductivity* of Tubes 1-4, May-July 1985

Date	Cumulative Time (days)	Average Hydraulic Conductivity (cm/s x 10^{-7}) Tube 1	Tube 2	Tube 3	Tube 4
May 5	0.14	-8.57	-8.75	-8.8	-8.75
6	1.45	-2.51	-2.61	-2.75	-2.58
7	2.45	-2.94	-3.12	-3.18	-3.08
8	3.32	-3.57	-3.51	-3.49	-3.49
9	4.19	-3.57	-3.51	-3.49	-3.49
10	5.21	-	-	-	-
11	-	-	-	-	
12	-	-	-	-	-
13	-	-	-	-	-
14	9.08	-3.32	+6.3	+5.79	-3.30
15	10.15	-2.97	-2.74	-2.81	-2.74
16	11.12	-3.24	-3.10	-3.11	-3.11
17	11.97	-3.06	-2.95	-2.95	-2.84
18	13.32	-2.74	-2.60	-2.62	-2.57
19	-	-	-	-	-
20	14.90	-3.0	-3.69	-3.73	-3.71
21	16.22	-2.63	-2.51	-2.55	-2.51
22	17.03	-3.61	-3.48	-3.49	-3.51
23	18.15	-2.89	2.80	-2.86	-2.86
24	19.25	-2.99	-2.89	-2.90	-2.90
25	20.16	-3.34	-3.23	-3.33	-3.33
26	-	-	-	-	-
27	-	-	-	-	-
28	-	-	-	-	-
29	24.15	-2.97	-3.32	-3.33	-3.33
30	25.13	-3.24	-3.13	-3.14	-3.15
31	26.02	-3.15	-3.11	-3.11	-3.11
June 6	32.31	+1.04	+1.83	+1.91	+1.45
7	33.18	-3.08	-3.	-2.99	-3.04
8	34.11	-3.21	-3.19	-3.33	-3.21
10	36.17	-3.10	-3.12	-3.17	-3.12
11	37.17	-3.1	-3.1	-3.21	-3.1
12	38.25	-3.09	-3..08	-3.15	-3.05
13	39.24	-3.22	-3.06	-3.01	-3.21
14	39.43	-3.97	-3.89	-3.97	-1.29
15	41.12	-2.87	-2.87	-3.04	-2.88
16	42.1	-3.22	-3.21	-3.01	-3.22
17	43.2	-2.95	-2.95	-2.9	-2.94
18	44.72	-2.61	-2.61	-2.69	-2.61
19	45.75	-2.98	-2.98	-3.14	-3.01
20	46.73	-3.17	-3.18	-3.21	-3.19
21	47.70	-3.15	-3.24	-3.05	-3.14
22	48.71	-3.15	-3.14	-3.19	-3.19
23	49.7	-3.09	-3.09	-3.18	-3.12
24	50.72	-2.94	-2.96	-3.04	-2.97

Table 6.1 Apparent Hydraulic Conductivity* of Tubes 1-4, May-July 1985 --Continued

Date	Cumulative Time (days)	Average Hydraulic Conductivity (cm/s x 10^{-7}) Tube 1	Tube 2	Tube 3	Tube 4
25	51.68	-3.14	-3.13	-3.23	-3.15
26	52.66	-3.12	-3.12	-3.18	-3.14
27	53.38	-3.8	-3.79	-3.91	-3.83
28	54.76	-2.55	-2.2	-2.44	-2.41
July 1	58.31	-3.03	-3.03	-2.42	-3.04
2	59.29	-3.07	-3.07	-3.16	-3.09
3	60.39	-2.86	-2.79	-3.01	-3.15
4	61.34	-3.14	-3.14	-3.23	-3.33
5	62.25	-3.33	-3.32	-3.4	-3.33
6	-	-	-	-	-
7	-	-	-	-	-
8	65.29	-3.49	-3.5	-3.52	-3.5
9	66.26	-3.01	-3.01	-3.07	-3.03
10	67.33	-3.06	-3.06	-3.09	-3.07
11	68.28	-3.19	-3.19	-3.19	-3.21
12	69.33	-2.97	-2.98	-2.98	-2.98
13	70.24	-3.40	-3.39	-3.39	-3.41
14	71.21	-3.20	-3.20	-3.20	-3.22
15	72.35	-2.72	-2.74	-2.76	-2.78
16	73.30	-3.38	-3.35	-3.33	-3.39
17	74.32	-2.97	-3.01	-3.02	-3.01
18	75.24	-3.29	-3.29	-3.28	-3.29
19	76.34	-2.99	-2.98	-2.98	-3.00
20	77.42	-3.07	-3.07	-3.05	-3.08
21	78.16	-2.96	-2.95	-2.94	-2.97
22	79.32	-3.00	-3.00	-2.99	-3.01
23	80.38	-3.24	-3.24	-3.22	-3.25
24	81.31	-2.99	-2.99	-2.97	-3.00
25	82.37	-3.06	-3.07	-3.05	-2.71
26	83.28	-3.26	-3.26	-3.22	-3.27
27	83.95	-4.02	-4.02	-4.00	-4.04
28	-	-	-	-	-
29	86.32	-2.91	-2.98	-2.90	-2.97
30	87.31	-3.16	-3.15	-3.13	-3.16
31	88.33	-3.09	-3.09	-3.05	-3.09

*"Hydraulic Conductivities" listed are based on measured outflow reduced by consolidation outflow (equation 6.2).

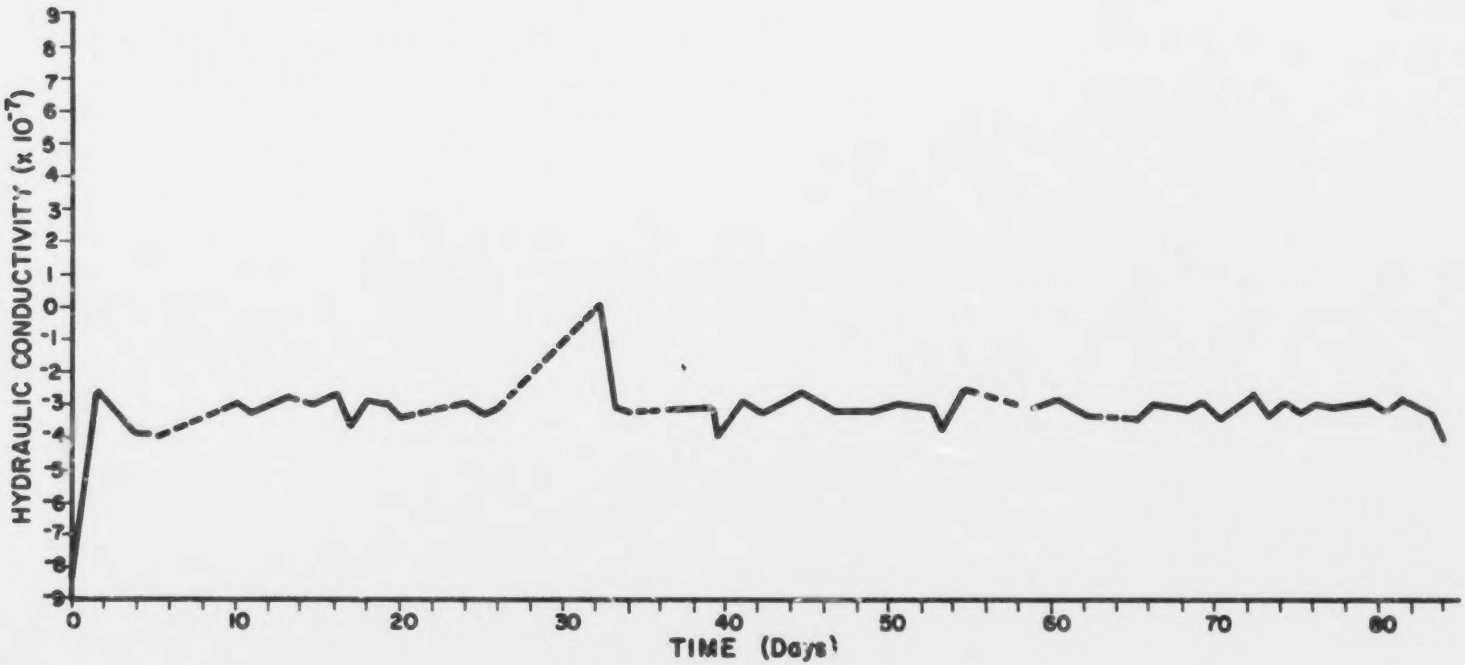

Figure 6.1 Apparent hydraulic conductivity (adjusted for consolidation) of bentonite in tubes 1 and 4. Dashed sections of the curve are uncertain or have not been measured. Injection pressure 34 kPa (5 psi).

The apparent hydraulic conductivity is based on outflow corrected for estimated consolidation outflow. The latter exceeds the former.

BEST COPY AVAILABLE

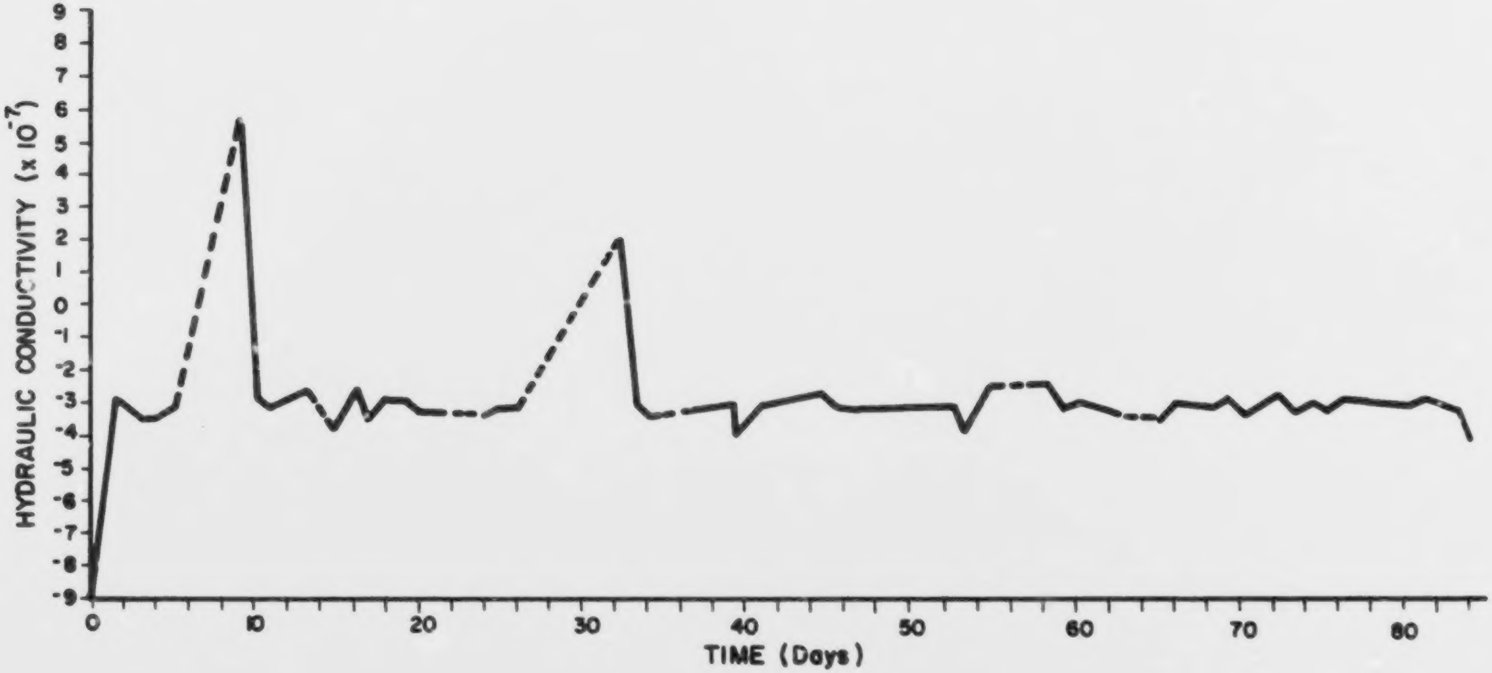

Figure 6.2 Apparent hydraulic conductivity (adjusted for consolidation) of bentonite in tubes 2 and 3. Dashed sections of the curve are uncertain or have not been measured. Injection pressure 34 kPa (5 psi).

The apparent hydraulic conductivity is based on outflow corrected for estimated consolidation outflow. The latter exceeds the former.

The high conductivity in tubes 2 and 3 drops off sharply, within 24 hours. This suggests that the bentonite plugs quickly sealed arou the penetrating pipes. The ability of the bentonite to infill voids or heal discontinuities and penetrations by swelling is one of the criteria used to evaluate the performance of seals with respect to seal functions (Meyer and Howard, 1983, p. 20, quoted from D'Appolonia, 1980a). This sealing may have been enhanced by the higher flows around the pipes. These higher flows bring more water into contact with the clay and may induce preferential swelling.

Another hydraulic conductivity spike occurs at approximately 30 days. The peak varies from plug to plug, with the highest value measured in plug 2 at approximately 2 x 10^{-7} cm/s. This spike occurs in all four plugs at the same time. It is probably the result of experimental procedure. A review of the test history suggests that in early June pressure was released from the system while reservoirs were refilled with water. Higher flows are recorded for the period immediately following the reapplication of pressure.

Flow is approximately constant for the remainder of the test. The negative hydraulic conductivity values listed in Table 6.1 and plotted in Figures 6.1 and 6.2 reflect the fact that outflow from the plugs is slightly less than predicted for consolidation alone. The consolidation factor applied to adjust the hydraulic conductivity values is an average rate calculated from approximately 3 months of consolidation testing (Section 6.3). This average rate may smooth the hydraulic conductivity over time reported here.

The results suggest that no flow occurred through the plugs except for two brief periods. Two factors should be considered with respect to this conclusion. Three months is not a long time for a test of this type. Pusch et al. (1982) report a hydraulic conductivity of 10^{-10} to 10^{-12} cm/s for Na-rich bentonites using constant head injection. Singh (1982) reports conductivities of 10^{-9} cm/s for similar natural clays. Westsik et al. (1982) used constant head tests on compacted Na and Ca-rich bentonite clays and clay sand mixtures. Their hydraulic conductivities range from 10^{-10} cm/s to 10^{-13} cm/s. Hodges et al. (1982) tested similar samples and found hydraulic conductivities ranging from 10^{-11} to 10^{-13} cm/s. Sawyer and Daemen (1987) used a falling head test on Na-rich commercial bentonite clays. They report average conductivities of 10^{-9} cm/s. If 10^{-10} cm/s can be used as an average hydraulic conductivity, the time necessary to measure an outflow of 1 ml can be calculated. Equation (5.5) for constant head testing can be solved for time. V is the desired 1 ml outflow, K is assumed to be 10^{-10} cm/s, h is the 34 kPa (5 psi) injection pressure, and A and L are the crosssectional area and length, respectively, of the plugs tested. A time of 40 days is predicted for 1 ml throughflow.

Two alternatives are available in standard soils laboratory practice to avoid the long testing time predicted for the clays used in this study. One would be to use the conventional falling head test. However, this test does not provide a mass balance. The test assumes that all flow into the plug will be equalled by outflow. The falling head test measures the fall in head of a standpipe over the sample. The flow rate, Q, into the sample equals the fall velocity, dh/dt, times the area, a, of the standpipe (e.g. Bouwer, 1978, p. 41). To solve for hydraulic conductivity, this relationship

$$q = (-dh/dt)a \qquad (6.1)$$

is set equal to the flow rate predicted by Darcy's law (equation 5.4). However, the flow predicted by Darcy's law is flow through the plug and not flow into the plug. This consideration is especially important when testing bentonite clays where a number of processes, including the swelling discussed in Section 6.4, affect flow. This problem is reported by Sawyer and Daemen (1987) for falling head tests on bentonite. They report negative outflows in every tested clay.

The second alternative is to increase the injection pressure. The low injection pressures used in this test were designed to simulate the conditions of the plugs tested in situ. Pressures used in the field are limited by the depth of test interval from the surface. The use of higher pressures is questionable, however, from the perspective of what they will do to the clay samples. Using equation (5.5), the pressure required to produce an outflow of 1 ml in one day is calculated at approximately 1.4 MPa (200 psi). Lambe and Whitman (1979, p. 77) quote a strongly qualified correlation between unconfined compressive strengths for clays (from < 24 to > 388 kPa) and resistance to penetration. Section 6.3 of this study discusses how one plug failed when penetrated by gas under 69 kPa (10 psi) pressure. When pressure is applied with fluid or gas, a weakness in the plug may be vulnerable to failure at pressures significantly lower than the overall sample strength since penetration can occur at the weakest point.

High injection pressures also affect the clay consolidation. When a clay sample is loaded axially, excess pore pressure develops at the surface where the load is applied. Normally, this pressure is dissipated through a soil and the entire sample experiences the pressure gradient imposed by the load. Low hydraulic conductivity clays will take much longer to dissipate these excess pore pressures since the rate of consolidation is a function of the hydraulic conductivity of the clay (Section 5.4). Large excess pore pressures will take longer to dissipate than small ones. High injection pressures should result in an extremely non-uniform distribution of pore pressures through the length of the sample. Darcy's law is linear (Freeze and Cherry, 1979, p. 72) and assumes a linear pressure gradient along the length of the sample. The degree to which test procedures increase the non-linearity of that gradient should affect the applicability of Darcian analysis to the results.

Constant head and falling head tests are the most commonly used laboratory methods for determining the hydraulic conductivities of soils, including clays (Holtz and Kovacs, 1981, Section 7.4). Transient pressure pulse methods, however, may prove more applicable to very low permeability materials. Results from this type of testing are discussed in Sections 6.6 and 6.8.

Pressures used for injection at Cargodera Canyon range from 34 to 69 kPa (5 to 10 psi). To determine the conductivity of laboratory samples across that range, injection pressure in the test apparatus was increased to 69 kPa (10 psi). Table 6.2 shows the results of this increase in injection pressure over four days of testing. No meaningful change in hydraulic conductivities resulted from the pressure increase.

6.3 Consolidation Test Results and Analysis

Section 5.4 describes the objectives, analysis and procedures used to determine the consolidation of bentonite plugs. Four plugs were consolidated at 69 kPa (10 psi). Three of these plugs were also consolidated at 138 and 207 kPa (20 and 30 psi). Consolidation was measured as the volume of water drained from the plugs. Outflows over time are included in Appendix D.

Consolidation is usually analyzed by plotting the sample deformation against the log of time (Casagrande, 1936; Liu and Evett, 1981, Section 4.2). Graphical methods are used to estimate the coefficient of consolidation by approximating the time required for 50 or 90 percent of total consolidation (Holtz and Kovacs, 1981, Section 9.4). These methods utilize the change in slope of the deformation versus log of time plot as primary consolidation approaches its limit. The conventional oedometer test uses a longitudinal displacement gage to measure the sample deformation. Linear displacement should be proportional to volumetric change and a similar change in slope should be observed in an outflow against the log of time plot. Figures 6.3 through 6.6 show the drained outflow plotted against the log of time for the 4 plugs used in this test. No flattening of the slope occurs. The curves represent approximately 35 days of testing.

The unusual curve in Figure 6.6 represents a plug failure after approximately 20 days of testing. The failure was expressed as nitrogen flowing through the plug and up the collection pipette. A crack at the plug surface was visible through the tube containing the plug to a depth of approximately 5 cm (2 inches), or half the length of the plug. The near-horizontal slope of the curve until failure occurs represents the fact that no flow occurred through the plug. This would seem to be the result of the failure process. Pressurized gas penetrated the plug; no consolidation took place. Over time, the penetration worked deeper into the plug until the plug was completely punctured.

Another method of analyzing consolidation is to plot the deformation of the sample against the square root of time (e.g. Lambe and Whitman,

Table 6.2 Apparent Hydraulic Conductivity* in Tubes 1 through 4. Constant Pressure at 10 psi.

Date	Time of Reading	Interval Between Readings (sec)	Hydraulic Conductivity* (cm/s x 10^{-7}) Tube 1	Tube 2	Tube 3	Tube 4
8/10	1723	4980	-6.26	-6.31	-6.20	-6.43
8/11	1416	75180	-1.61	-1.61	-1.60	-1.63
8/11	1430	840	-	-	-	-
8/12	0817	64020	-1.81	-1.81	-1.79	-1.82
8/12	1650	30780	-2.57	-2.58	-2.58	-2.58
8/13	0823	55980	-1.99	-1.99	-2.00	-1.99
8/13	0830	420	-	-	-	-
8/13	1852	37320	-2.35	-2.32	-2.37	-2.32
8/14	0809	44220	-2.26	-2.28	-2.25	-2.29

*"Hydraulic Conductivities" listed are based on measured outflow reduced by consolidation outflow (equation 6.2).

Table 6.3 Summary of Slopes, Outflow vs. Square Root of Time for Consolidation Tests

Injection Pressure kPa (psi)	Plug 5 (cc/min$^{1/2}$)	Plug 6 (cc/min$^{1/2}$)	Plug 7 (cc/min$^{1/2}$)
69 (10)	.665	.675	.737
138 (20)	.626	.625	.633
207 (30)	.611	.565	.568

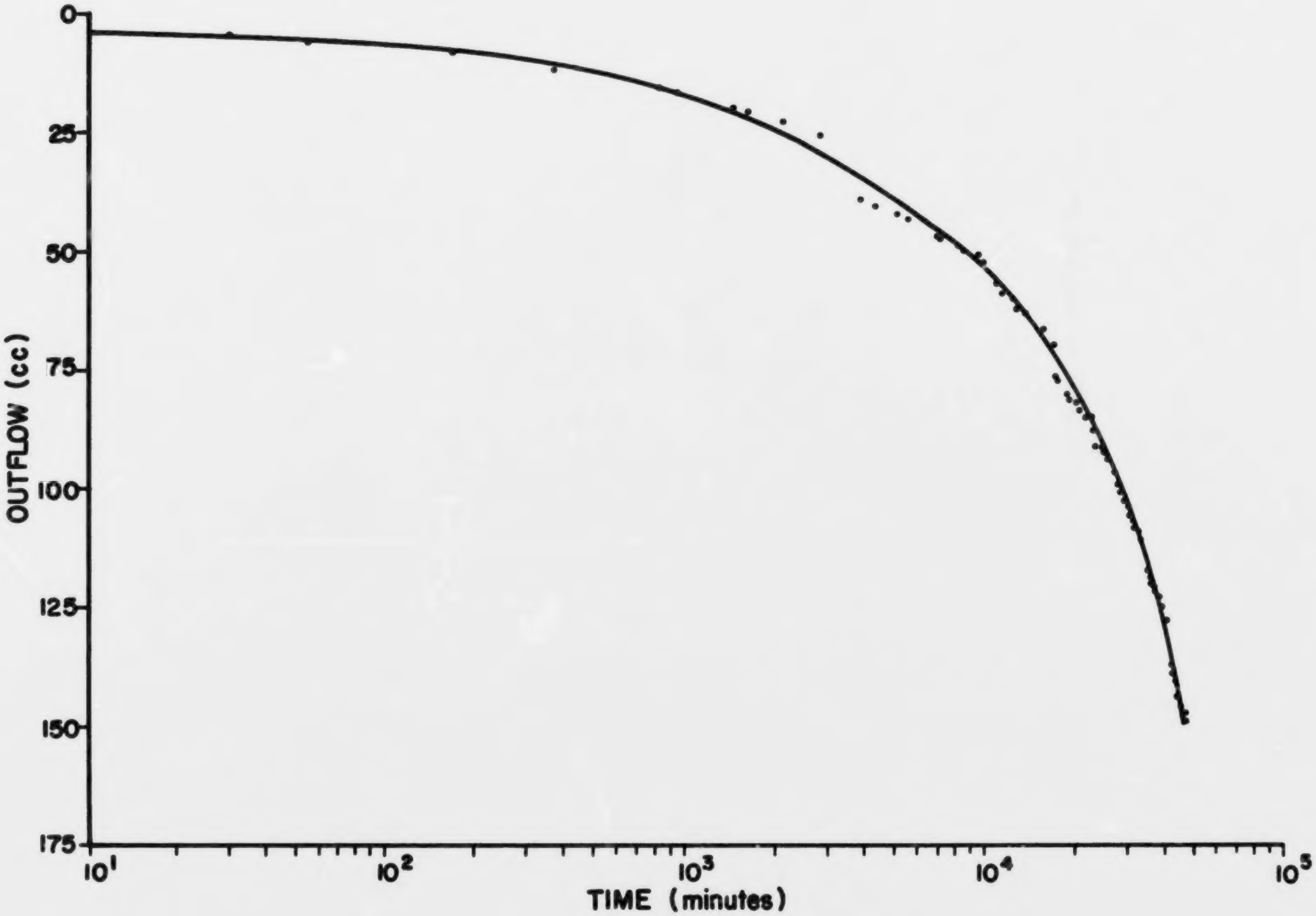

Figure 6.3 Consolidation outflow. Bentonite plug 5 at 69 kPa (10 psi).

BEST COPY AVAILABLE

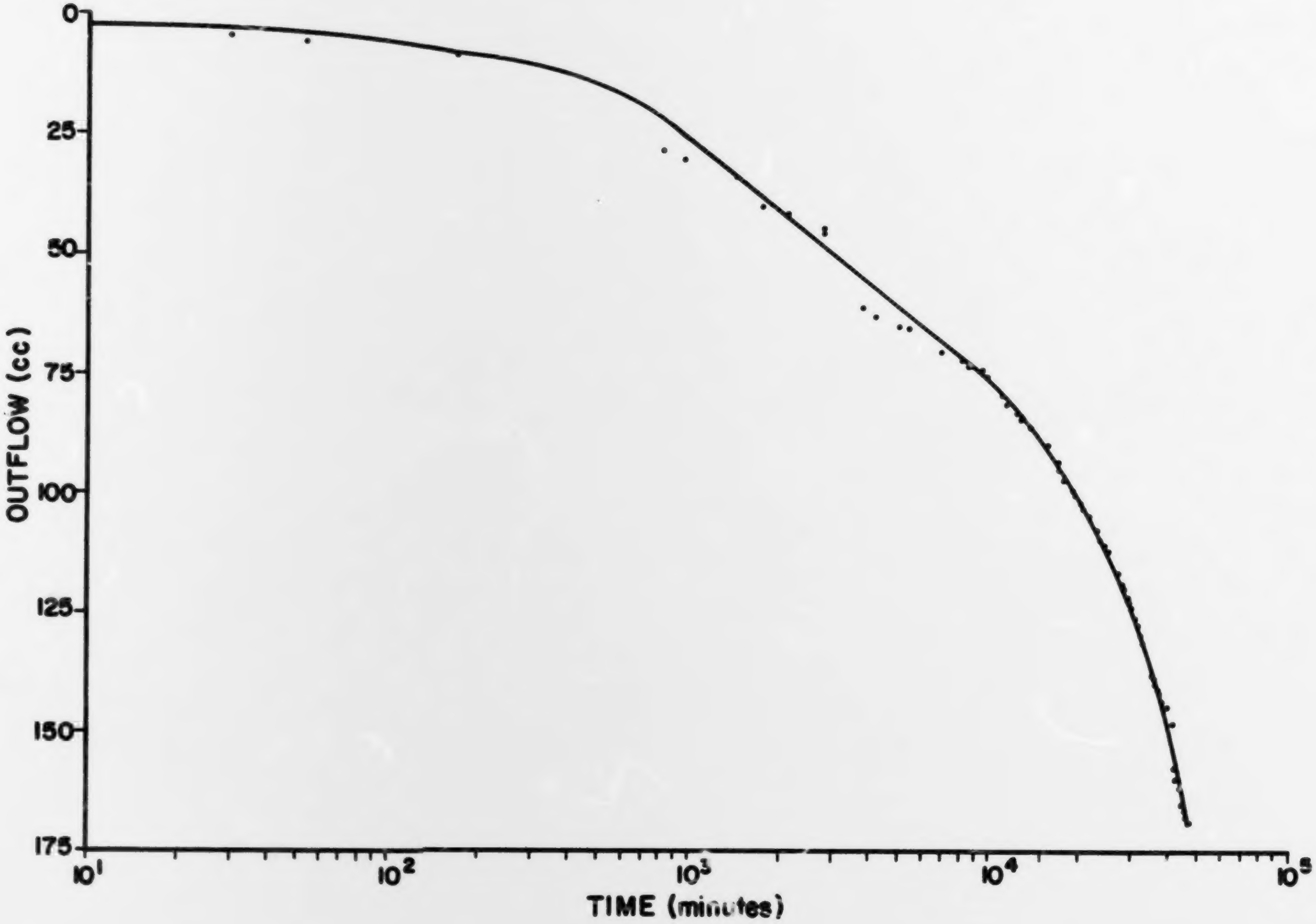

Figure 6.4 Consolidation outflow. Bentonite plug 6 at 69 kPa (10 psi).

BEST COPY AVAILABLE

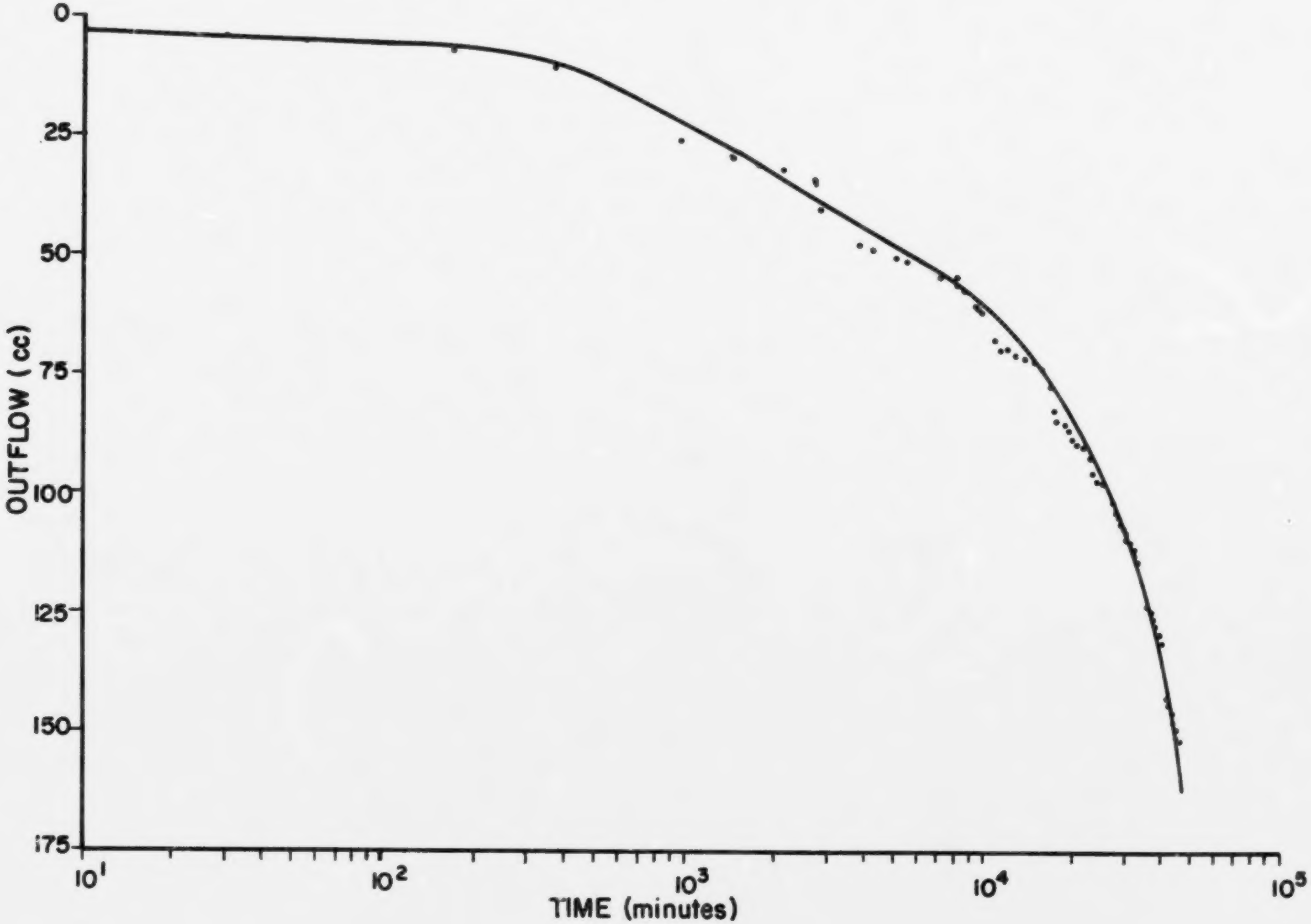

Figure 6.5 Consolidation outflow. Bentonite plug 7 at 69 kPa (10 psi).

BEST COPY AVAILABLE

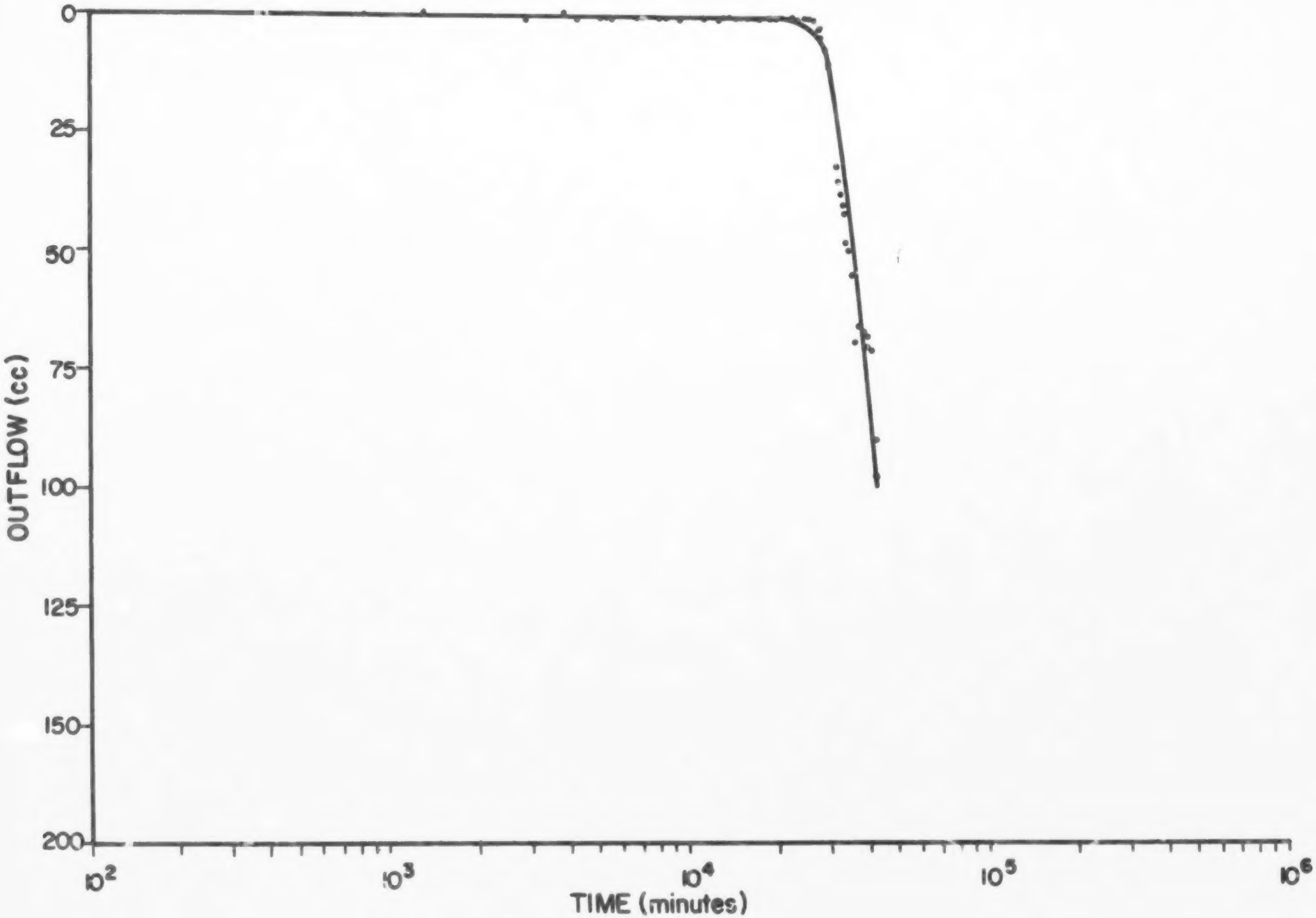

Figure 6.6 Consolidation outflow. Bentonite plug 8 at 69 kPa (10 psi).

BEST COPY AVAILABLE

1979, p. 412; Taylor, 1948; Holtz and Kovacs, 1981, p. 400). A similar flattening of the slope of the plot should allow approximating the time involved in a given percentage of consolidation. Figures 6.7 through 6.10 show outflow plotted against the square root of time for the four plugs tested. No flattening of the slopes is apparent. However, for plugs 5, 6 and 7, the plots suggest a near linear relationship between deformation and the time factor. Calculations show a correlation of better than 98 percent with a straight line slope.

The primary objective of this testing is to determine the significance of consolidation on hydraulic conductivity measurements. This involves estimating what volume of flow under a given pressure is the product of consolidation. The relationship between outflow and time expressed in Figures 6.7 through 6.10 provides a basis for making such an estimation. The slope of the straight line approximation is used to calculate the flow volume for a given time. This volume is then subtracted from the outflow measured in the conductivity test. The adjusted flow volume is used to calculate the hydraulic conductivity. The usual expression (5.5) for hydraulic conductivity under constant head conditions is

$$K = VL/Aht \tag{5.5}$$

The adjusted expression is

$$K = (V - V_c)L/Aht \tag{6.2}$$

where V_c is the outflow volume produced by consolidation.

The coefficient of consolidation as determined by conventional oedometer testing will normally vary with pressure used to achieve consolidation (Liu and Evett, 1981, p. 78). This results from the relationship between pressure and consolidation limits. The coefficient is calculated for each pressure assuming that consolidation has essentially ended (Holtz and Kovacs, 1981, Section 8.4). The consolidation in Figures 6.3 through 6.10 gives no indication of approaching a limit. The relationship between the rate of consolidation derived from the slopes in Figures 6.7 through 6.10 and the applied stress was investigated by increasing the pressure to 138 kPa (20 psi).

Figures 6.11 through 6.13 show outflow plotted against the square root of time for a consolidation pressure of 138 kPa (20 psi). These plots can also be approximated by straight-line slopes with correlations of better than 98 percent. The slopes are similar to the ones for flow at 69 kPa (10 psi). Table 6.3 (page 179) summarizes the slopes for each plug at the designated consolidation pressure as a function of outflow against the square root of time in minutes. Testing at 138 kPa (20 psi) was continued for approximately 2 weeks.

Figures 6.14 through 6.16 show the relationship of outflow to the square root of time at a consolidation pressure of 207 kPa (30 psi).

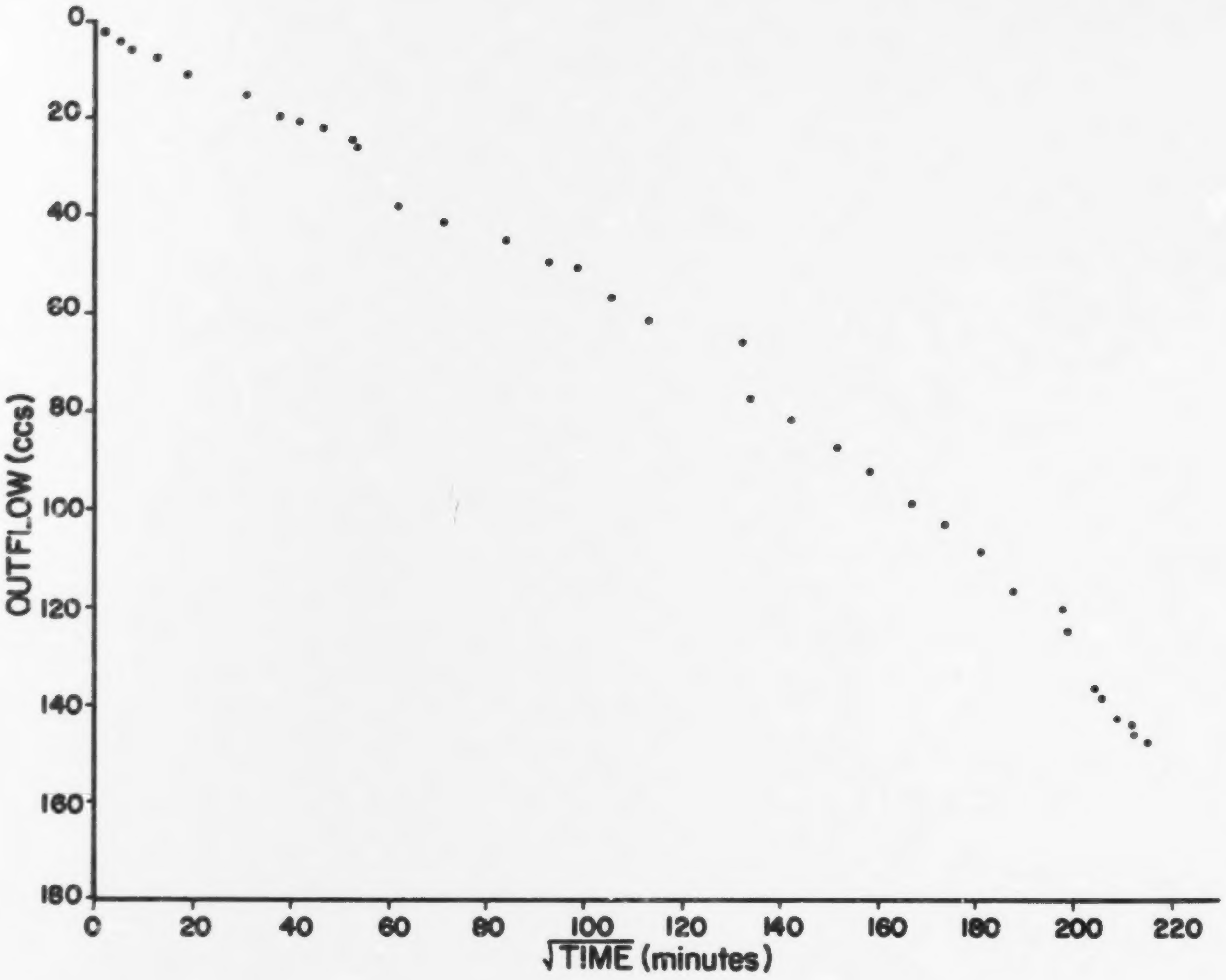

Figure 6.7 Consolidation outflow. Bentonite plug 5 at 69 kPa (10 psi).

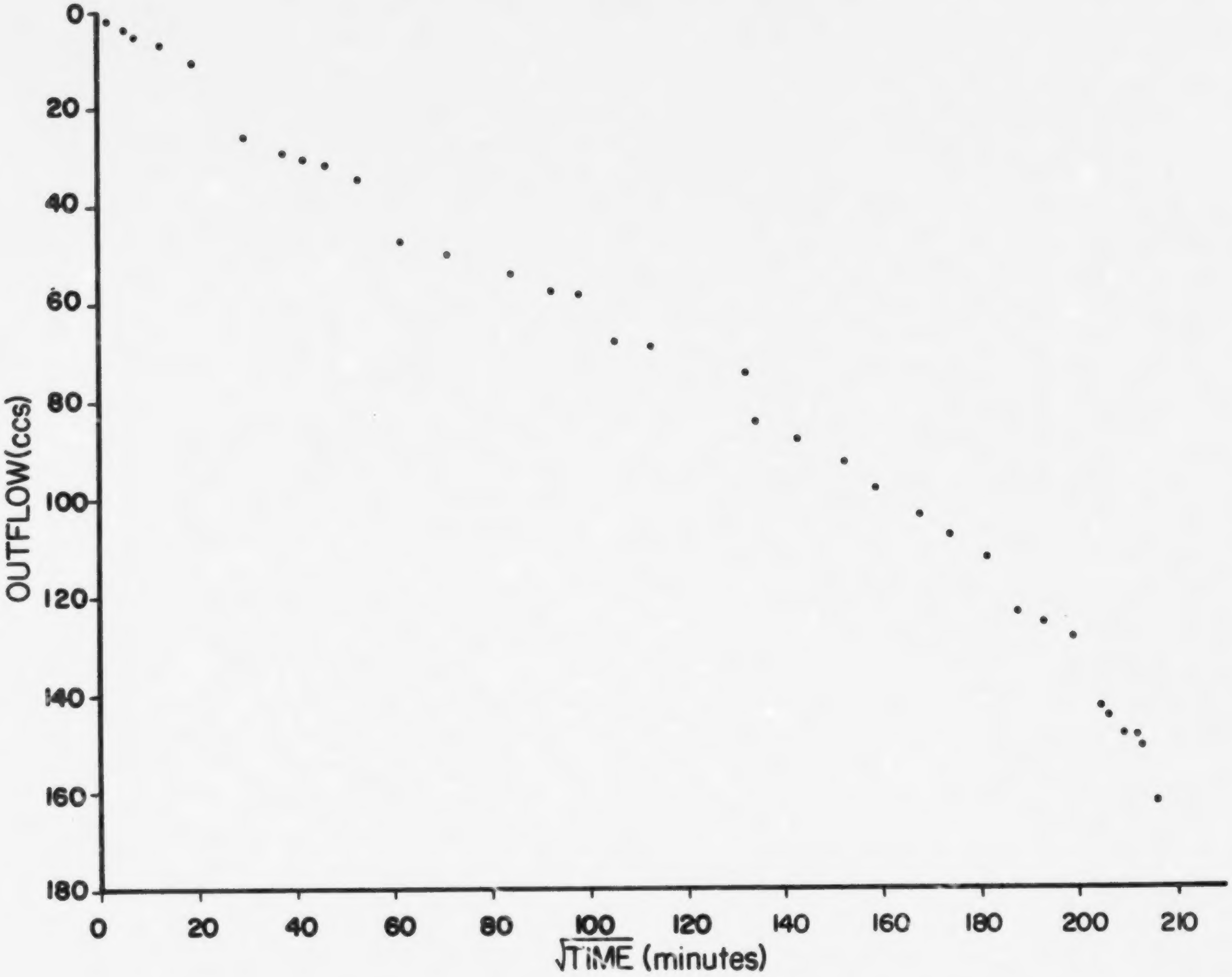

Figure 6.8 Consolidation outflow. Bentonite plug 6 at 69 kPa (10 psi).

BEST COPY AVAILABLE

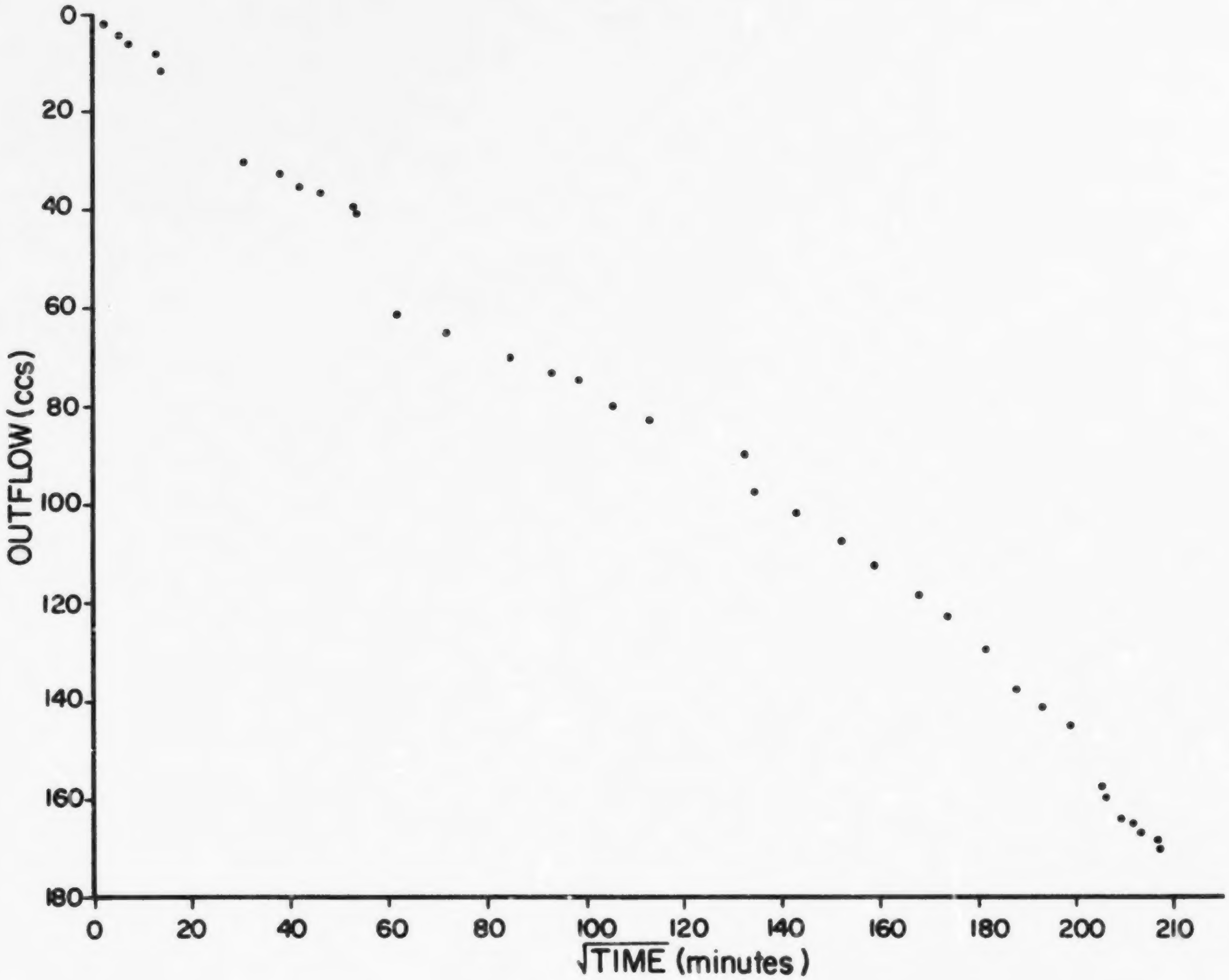

Figure 6.9 Consolidation outflow. Bentonite plug 7 at 69 kPa (10 psi).

BEST COPY AVAILABLE

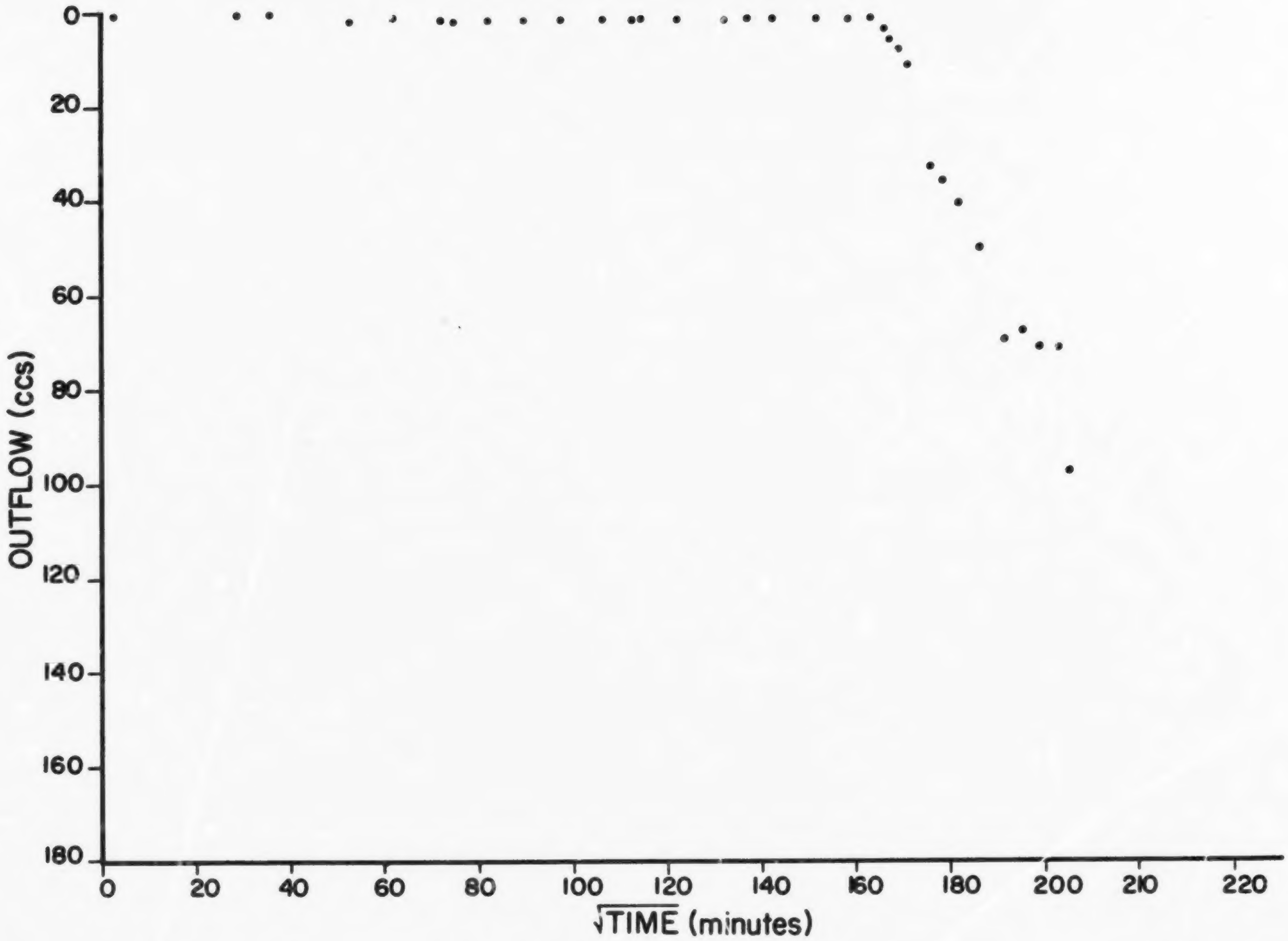

Figure 6.10 Consolidation outflow. Bentonite plug 8 at 69 kPa (10 psi).

BEST COPY AVAILABLE

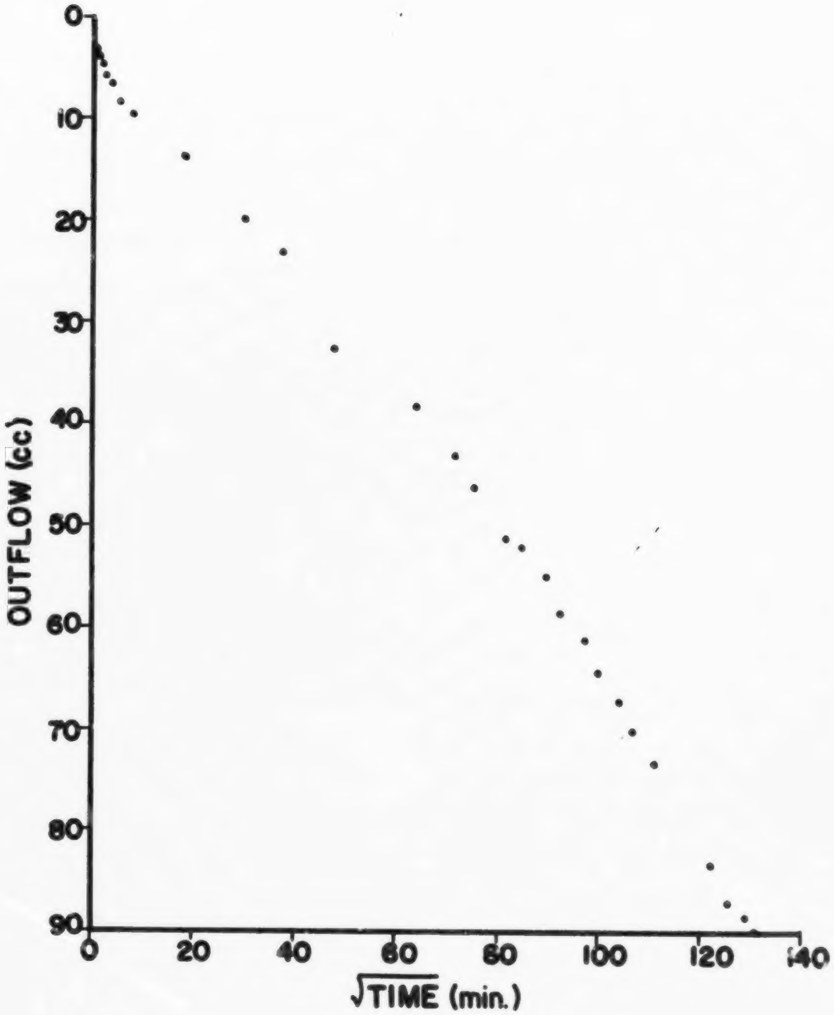

Figure 6.11 Consolidation outflow. Bentonite plug 5 at 138 kPa (20 psi).

BEST COPY AVAILABLE

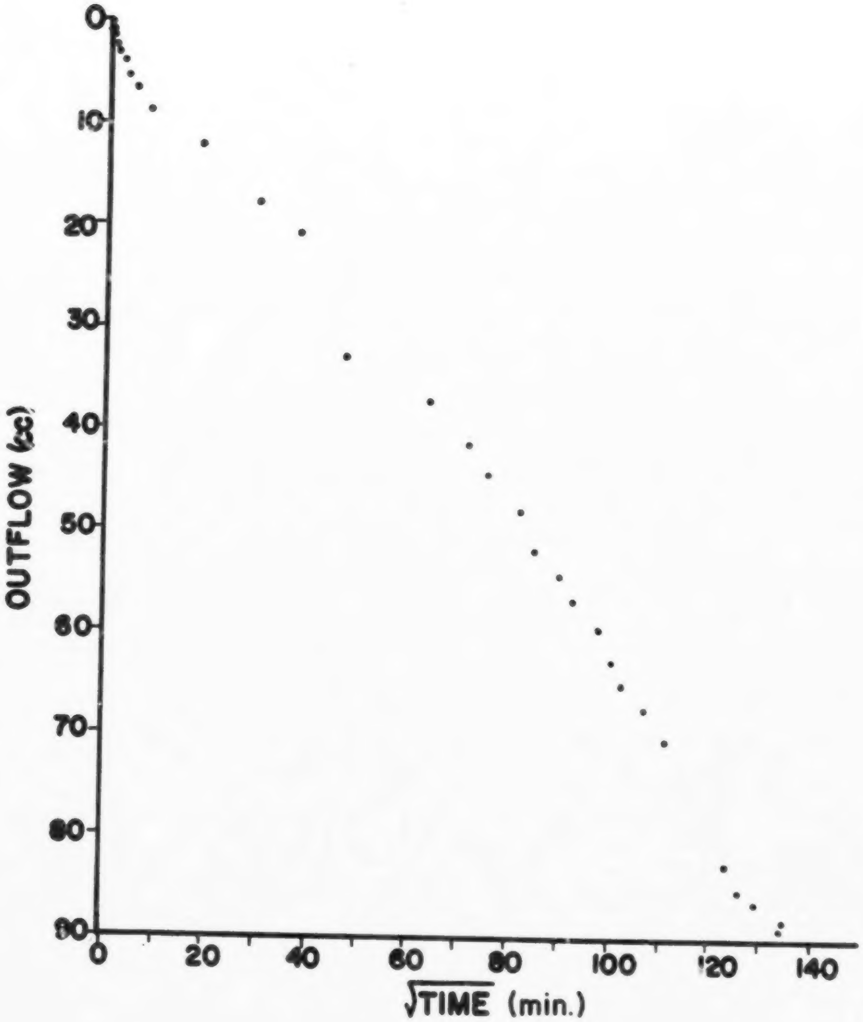

Figure 6.12 Consolidation outflow. Bentonite plug 6 at 138 kPa (20 psi).

BEST COPY AVAILABLE

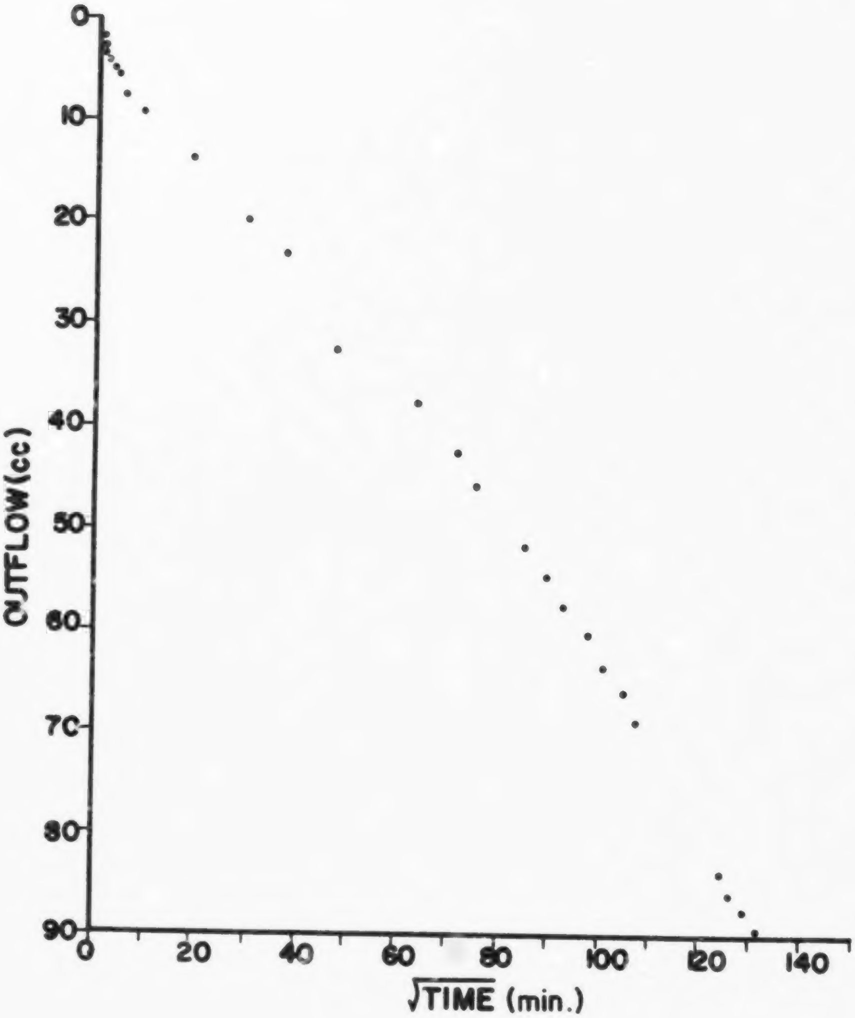

Figure 6.13 Consolidation outflow. Bentonite plug 7 at 138 kPa (20 psi).

BEST COPY AVAILABLE

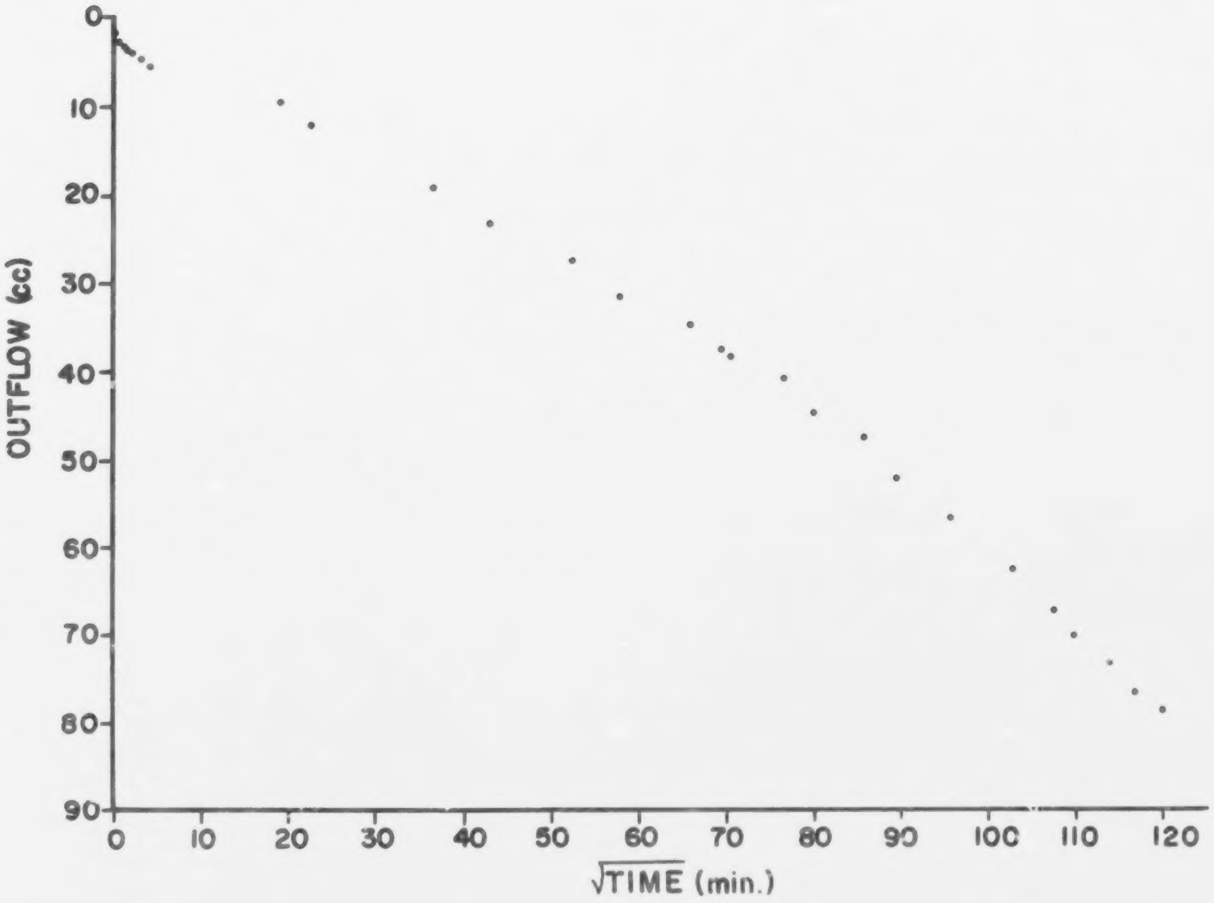

Figure 6.14 Consolidation outflow. Bentonite plug 5 at 207 kPa (30 psi).

BEST COPY AVAILABLE

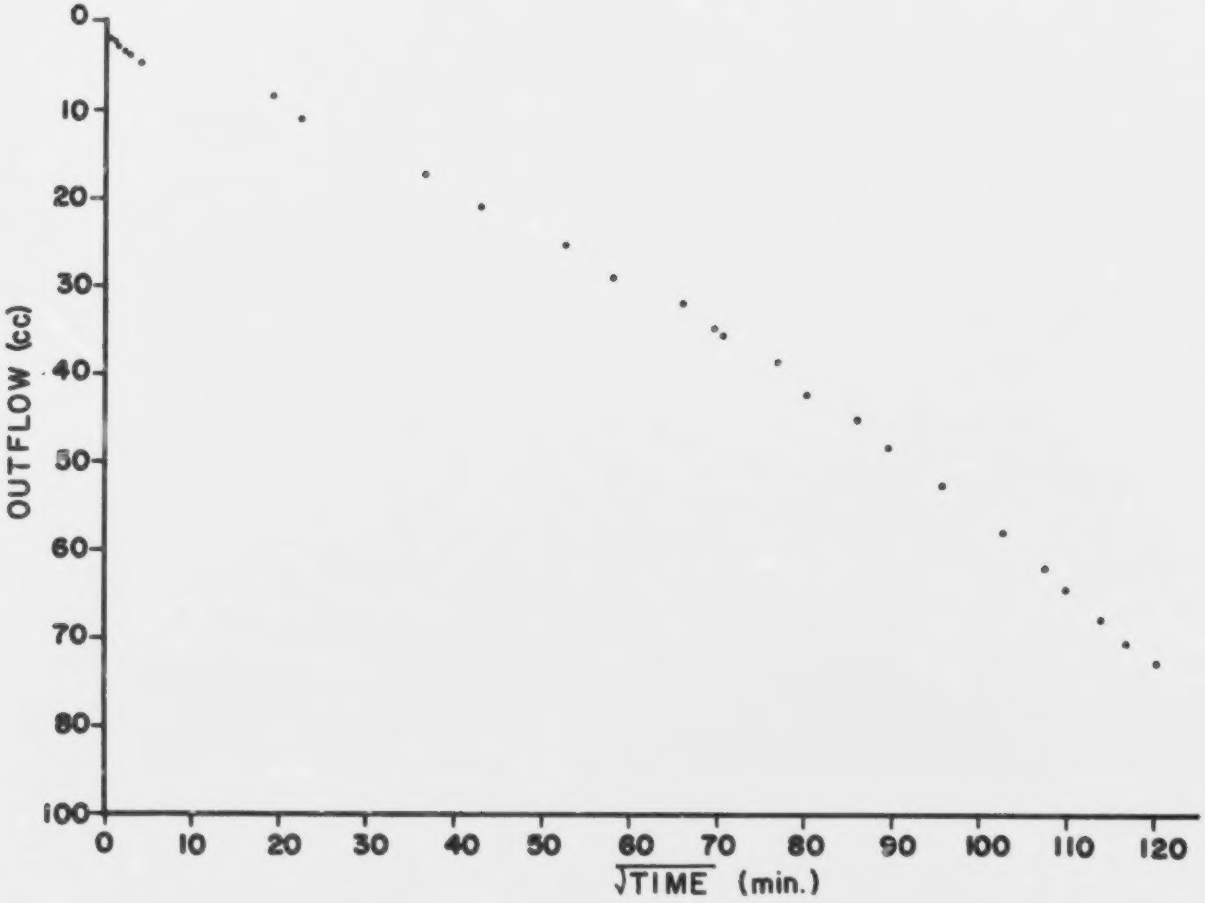

Figure 6.15 Consolidation outflow. Bentonite plug 6 at 207 kPa (30 psi).

BEST COPY AVAILABLE

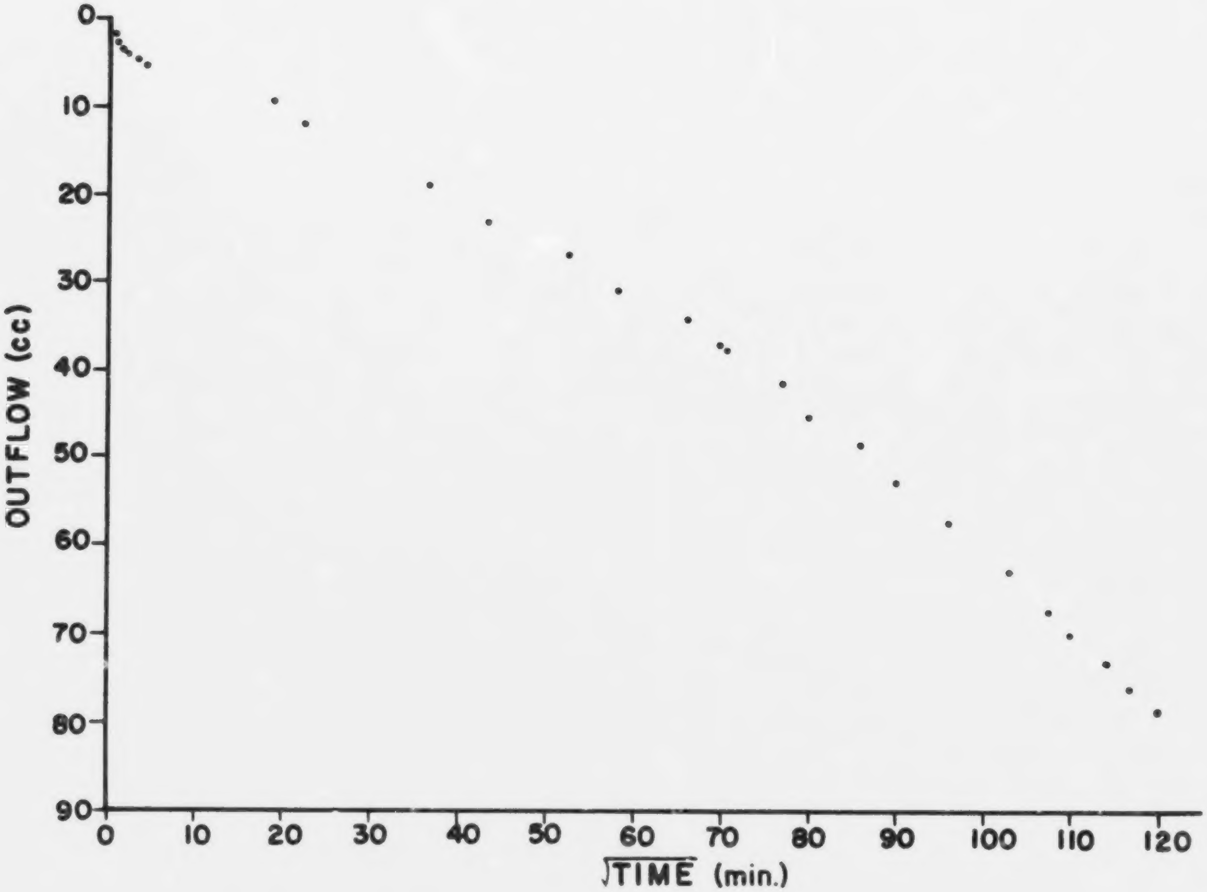

Figure 6.16 Consolidation outflow. Bentonite plug 7 at 207 kPa (30 psi).

BEST COPY AVAILABLE

Testing at this pressure was continued for approximately 12 days. Slopes from these plots are included in Table 6.3. A comparison of the slopes at all three pressures shows that the rate of consolidation as a function of time has increased consistently for plugs 5 and 6, less so for 7. The rate seems to be independent of the pressure, at least across the range of loads actually applied.

The plug consolidation over a range of pressures and an extended test period is summarized in Figure 6.17, which plots outflow against the square root of time in hours. Total time represented is approximately 54 days. It is apparent from the plot that consolidation is not approaching a limit.

The hydraulic conductivity measurements made in this study are adjusted for consolidation. However, consolidation is a finite process. Long-term plug testing in the laboratory or in situ could conceivably continue beyond the time required for 100 percent primary consolidation. It is, therefore, desirable to estimate how long consolidation could continue under the range of pressures used in this study. This time can be estimated using the relation between the coefficient of consolidation and time expressed by

$$t_D = c_v t/H^2 \tag{6.3}$$

where c_v is the coefficient of consolidation, t_D is a dimensionless time factor, t is time, and H is the length of the longest drainage path, in this case the sample length (Holtz and Kovacs, 1981, Section 9.3).

The coefficient of consolidation is defined as

$$c_v = (K/p_w)((1 + e_o)/a_v) \tag{6.4}$$

where K is hydraulic conductivity, assumed to be 10^{-9} cm/s, p_w is the unit weight of water, e_o is the original void ratio of the sample, and a_v is the coefficient of compressibility.

These equations can be combined and solved for time:

$$t = t_D H^2 a_v \rho_w g/K(1 + e_o) \tag{6.5}$$

a_v is defined as the change in void ratio divided by the change in applied stress (Lambe and Whitman, 1979, p. 155). Original void ratio for each plug can be approximated as the volume of water in the plug divided by the volume of the dry pellets. Using the description of plug construction in Section 5.3.3, a void ratio of 4 is calculated using an approximate volume of 1 cc per tablet (Section 6.4). a_v is found from the relationship (Lambe and Whitman, 1979, p. 157)

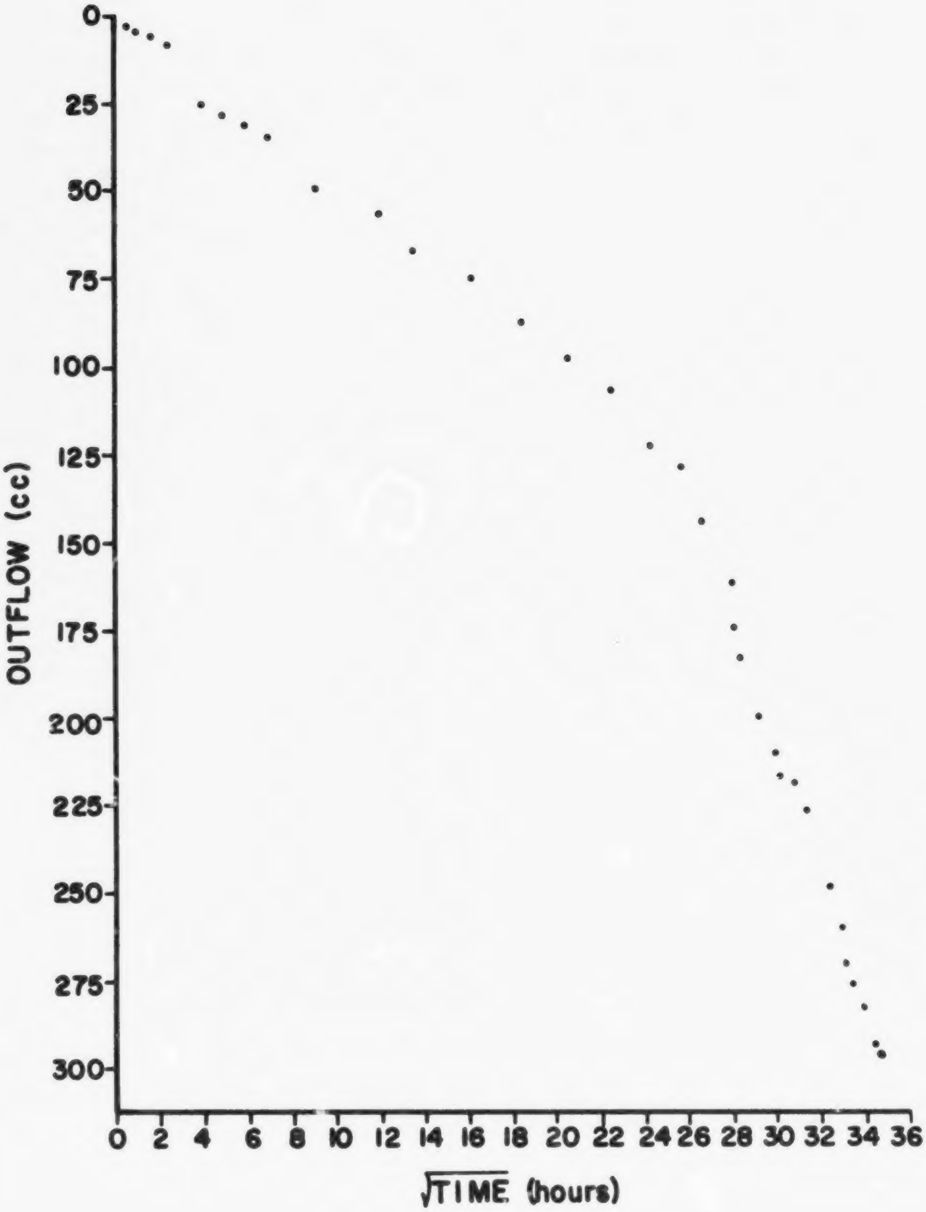

Figure 6.17 Consolidation of bentonite plug 6 at 69, 138 and 207 kPa (10, 20 and 30 psi).

BEST COPY AVAILABLE

$$a_v = 0.435C_c/\sigma_{va} \qquad (6.6)$$

where C_c is the compression index and σ_{va} is the average stress. Lambe and Whitman (1979, p. 318) offer an empirical relationship between liquid limit and C_c as C_c = 0.007 (liquid limit - 10%). Using a liquid limit of 360 (Section 6.4) a C_c of 2.45 is calculated and a_v can be estimated as .43 psi^{-1}. t_D is found using the relationship t_D = 1.781 - .933 log (100 - U%), where U is the percent consolidation desired, in this case 98%. Then t_D = 1.5. Using these values to solve for time indicates that for 98% consolidation to occur, the plugs would have to be tested for approximately 3 years at 69 kPa (10 psi). This suggests that hydraulic conductivity should be adjusted for consolidation for any test reported on here.

A visual estimate of consolidation is possible using the reference heights established for each plug at the start and end of each pressure episode. Table 6.4 compares the consolidation as measured from the length of the plugs with consolidation as measured by volume of water drained. Consolidation is expressed as percent of original height or volume. The volumetric estimate should be considered more accurate as lengths are based on only one point on the plug surface.

Lambe (1959, pp. 80-81) states that friction between the consolidating material and the testing device can affect the results of consolidation testing significantly. To determine the bond between the clay plug and the walls of the tube used for testing, a pushout test was performed on plug 8 after it failed. Water was injected into the bottom of the test apparatus and displacement of the plug was monitored. No displacement was noted at pushout pressures of 7 to 28 kPa (1 to 4 psi). At 34 kPa (5 psi) the plug moved immediately to the top of the apparatus. This test provides only a crude approximation of the bond between plug and the tube surface, but it suggests that frictional slip should be only a small component of the apparent consolidation behavior of the plug.

6.4 Swelling/Moisture Content Testing

The objectives, method of analysis and procedures for these tests are described in Section 5.5. Testing was performed on four plugs over approximately 32 days. The main test involved water injection into the plugs under low pressure and undrained conditions. The test was begun with the apparatus filled with water. All flow into the system is considered to be flow into the plugs. To determine the flow per plug, total flow is averaged over the four plugs tested. Since no drainage was permitted, no consolidation or flow through the plugs could occur.

Table 6.5 presents, over approximately 32 days, total flow into the system and average change in moisture content per plug. Injection pressure was 34 kPa (5 psi). The moisture content is the ratio of the

Table 6.4 Volumetric and Linear Deformation Measurements during Bentonite Plug Consolidation Testing

Volumetric Measurements

Pressure (psi)	Plug	Original Volume (cc)	Outflow (cc)	Consolidation (% Orig. Vol.)
10	5	500	148.05	29.6
10	6	500	162.70	32.5
10	7	500	168.65	33.7
20	5	442	90.75	20.5
20	6	427	89.00	20.8
20	7	421	91.60	21.8
30	5	441	78.60	17.8
30	6	428	72.70	17.0
30	7	419	78.7	18.8

Linear Measurements

Pressure (psi)	Plug	Original Length (in)	Final Length (in)	Consolidation (% Orig. Leng.)
10	5	4.0	3.6	10
10	6	4.0	3.5	13
10	7	4.2	3.8	10
20	5	4.0	3.8	5
20	6	3.9	3.6	8
20	7	4.2	3.7	12
30	5	4.1	3.8	7
30	6	3.8	3.7	3
30	7	4.0	3.8	5

Table 6.5 Saturation Tests on Bentonite Plugs in Tubes 9 through 12

Time (min)	Cumulative Inflow (cc)	Moisture Content (%)
0	0	235.34
6	0.3218	235.43
15	0.8044	235.57
27	0.9653	235.61
2776	12.2269	238.75
2805	12.3877	238.80
3859	14.6400	239.43
4381	15.4444	239.65
5056	16.5706	239.97
5343	17.0532	240.10
5963	17.5359	240.23
6948	18.8729	240.59
7339	19.1147	240.68
7970	19.7882	240.86
8639	19.9491	240.91
11767	21.3970	241.31
12503	21.7187	241.40
13027	21.5579	241.36
13680	21.8796	241.45
14425	21.8796	241.45
15264	21.7187	241.4
15967	22.0405	241.49
17335	22.0405	241.49
18355	22.0405	241.49
18834	22.0405	241.49
20149	22.3623	241.58
21611	22.3623	241.58
22689	22.3623	241.58
23197	22.3623	241.58
24058	22.6840	241.67
25490	21.2361	241.27
26024	24.7755	242.25
26938	25.0972	242.34
27346	25.2581	242.39
27457	25.0972	242.34
28367	25.5799	242.48
28939	25.5799	242.48
30490	25.9016	242.57
31576	26.0625	242.61
32678	26.3843	242.70
33243	26.2234	242.66
34138	26.5451	242.75
34153	26.5451	242.75
34263	26.5451	242.75
34778	26.8669	242.84
35580	27.5104	243.02
36116	27.8322	243.11

Table 6.5 Saturation in Tubes 9 through 12--Continued

Time (min)	Cumulative Loss (cc)	Moisture Content (%)
37000	28.3148	243.24
37606	28.4657	243.29
38452	28.6366	243.33
38928	28.6366	243.33
39881	28.6366	243.33
42771	29.2801	243.51
43305	29.1192	243.47
44141	29.1192	243.47
44726	28.9583	243.42
45615	29.1192	243.47
46195	29.1192	243.47
47065	29.4410	243.56

weight of water in the plug to the weight of solids that comprise the plug. The water content of the dry tablets was determined by laboratory testing. Three sets of ten tablets each were weighed, oven-dryed for three days, and weighed again. An average moisture content of 10% was determined. Todd Harriety of American Colloid , the manufacturer of the bentonite tablets used in this testing, confirmed that 10% was the manufacturer's estimate of shipped moisture content. The moisture content for the prepared plugs prior to testing was 235%. After approximately 32 days, the moisture content had increased to 243%. Figure 6.18 shows the change in moisture content over time for an average plug. Approximately 66% of the increase occurs in the first 7 days, and 50% occurs in the first three days.

The decrease in the rate of change of moisture content may be a function of two processes. When the plugs are originally constructed, they are allowed to swell freely up the tubes as they adsorb the water available. This swelling will continue until there is no more water available to the clay or until the clay has reached its free swell limit. An experiment was performed in conjunction with the swelling/moisture content tests to determine the free swell potential of bentonite tablets. Two graduated cylinders, with volumes of 250 and 1000 ml, were used. The smaller cylinders received 25 bentonite tablets dropped through 100 ml of water. The larger cylinder received 100 tablets dropped through 400 ml. The final volume in the smaller cylinder was 125 ml and in the larger the final volume was 510 ml. After approximately 30 days it was observed that swelling had essentially ended. After 40 days the free water still standing above each clay sample was removed and measured. The smaller cylinder had 13 ml of free water and the larger cylinder 142 ml. The free swell of the sodium bentonite tablets used in this study can then be calculated using (Holtz and Kovacs, 1981, p. 189):

$$\text{free swell} = (\text{final volume} - \text{initial volume})/\text{initial volume} \times 100 \tag{6.7}$$

Averaging the results of the two cylinders gives a free swell of 300%.

As a comparison, Holtz and Kovacs (1981, p. 189) suggest that sodium montmorillonites have free-swell values of 1200% and greater. The results they discuss use a powdered dry clay that has passed a No. 40 sieve. The increased surface area for powdered clay should give it a greater free swell than highly precompacted bentonite tablets.

The significance of this test is that the plugs tested had approached the limit of their free swell potential prior to testing. Their ability to freely take in available water is significantly less than hydrating tablets with a lower moisture content.

The test with the graduated cylinders had another interesting result. After 40 days of testing, the combined volumes of the clay and water were unchanged in both cylinders. The dry tablets have a measured porosity. If the clay were saturated, the total volume could be expected to decrease by the volume of voids in the clay. This suggests that even after 40 days of swelling, the clay remains

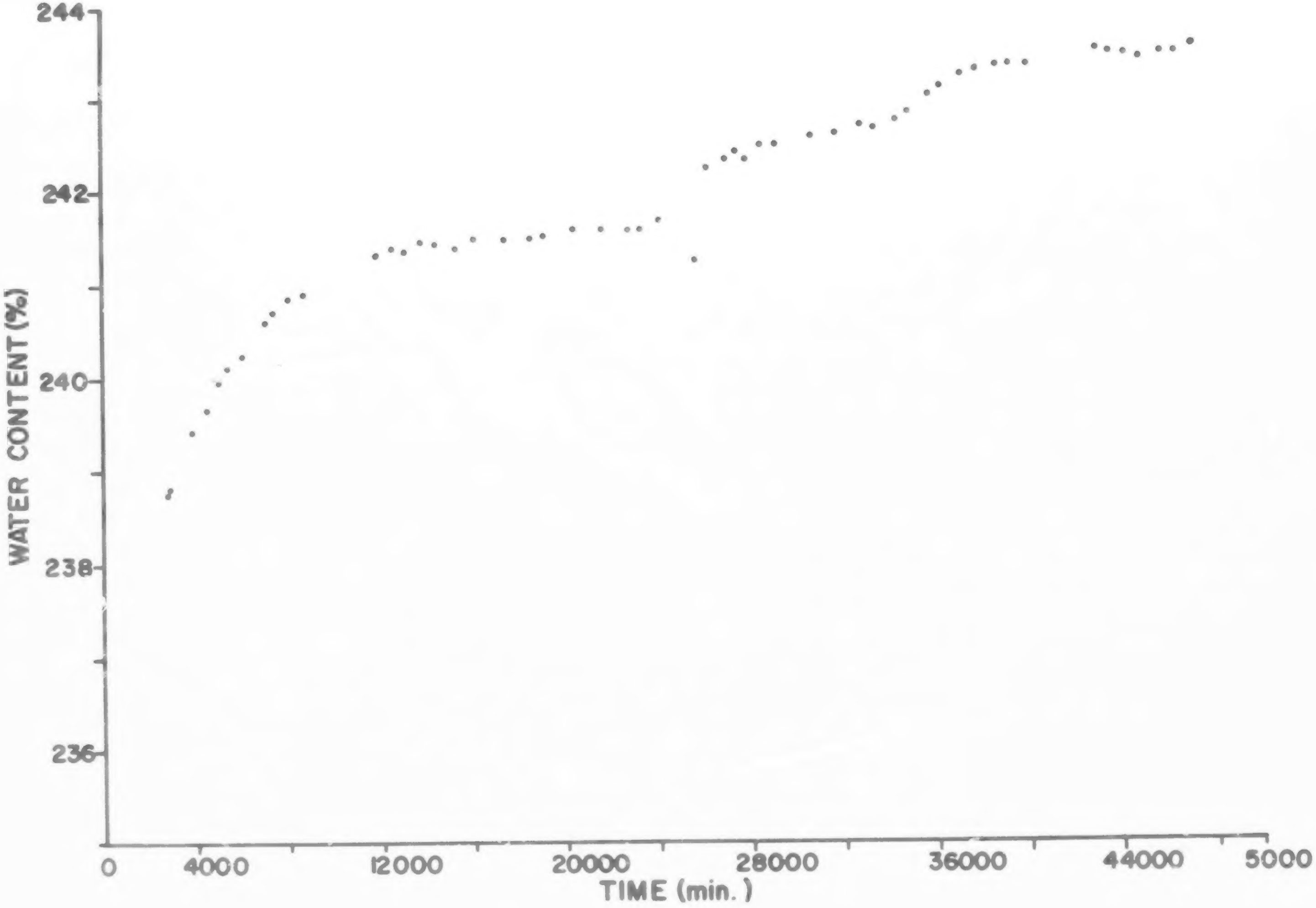

Figure 6.18 Change in water content for plugs 9 through 12 at 34 kPa (5 psi) injection pressure.

BEST COPY AVAILABLE

unsaturated. This may explain the steep initial increase in moisture content as water is pressurized on the plugs. The degree of saturation of the plugs increases as air is driven from the void spaces to be replaced by water. This process will stop when pore pressure in the clay comes into equilibrium with the applied pressure.

The primary objective of this testing is to determine the significance of swelling and change in moisture content on the hydraulic conductivity of the bentonite plugs. Table 6.6 presents the change in moisture content results from the tests described in Section 6.2. As discussed in that section, a difference in the volume of water injected into the system and the volume collected was measured. The actual volumes measured are included in Appendix C. The volume of water injected that was never collected was assumed to have been taken in by the plug, with a corresponding change in volume and moisture content. Figure 6.19 shows the change in moisture content over time.

It is instructive to compare the results in Tables 6.5 and 6.6, as well as Figures 6.17 and 6.18. After approximately 30 days, the moisture content in plugs 1 through 4 (tested for hydraulic conductivity) had increased from 235% to approximately 246%. This correlates closely with the 9% increase experienced by plugs 9 through 12. This correlation occurs despite the fact that plugs 1-4 are allowed to drain. This evidence is confirmed by visual inspection of plugs 1-4, which have increased in volume by more than 10%. No effort was made to measure the actual increase, as no increase had been expected when the testing was initiated, and no reference point had been established.. The implications for hydraulic conductivity testing of bentonite plugs of these change of moisture content/ swelling results are discussed in Section 6.2.

A final measure of swelling discussed in Section 5.5.2 is the swell index. This corresponds to the index of compressibility except that it measures the expansion of the clay upon unloading. An attempt was made to estimate a swell index for the clay used in this study. Measurements were made using the apparatus for consolidation testing described in Section 5.4.3. At the end of the 207 kPa (30 psi) test cycle, two plugs were unloaded. The collection pipettes were filled with water and the amount of water drawn up into the plug was measured. After approximately 7 days the average intake into the plugs was 17.2 ml. Using the expression $C_s = \Delta e / \log \Delta \sigma_v$, a swell index of .12 is calculated for the clay. This can be compared with swell index values of 2.5 to 17 reported by Lambe and Whitman (1979, p. 322) for sodium montmorillonites. Lambe and Whitman (1979, p. 321) note that C_s is always much smaller than C_c for virgin compression. A wide range of values seem possible, which may qualify the value of this measurement in predicting the performance of bentonite plugs.

Heights were measured for all four plugs tested for swelling and change in moisture content. Table 6.7 summarizes these results. The height measurements reflect only one point on the surface of each plug.

Table 6.6 Moisture Content of Bentonite Plugs in Tubes 1 through 4

Time (min)	Cumulative Water Uptake (cc)	Moisture Content (%)
0	0	235.34
2.45	68.19	240.1
9.08	101.85	242.48
11.97	111.73	243.14
16.22	130.09	244.42
19.25	142.42	245.28
25.13	152.45	245.98
33.18	162.11	246.65
37.17	174.26	247.50
39.43	166.10	246.93
43.20	171.39	247.30
46.73	178.51	247.80
49.70	248.06	252.64
52.66	265.55	253.86
58.31	298.83	256.19
61.34	311.24	257.05
66.26	318.46	257.55
69.33	324.36	257.97
72.35	345.12	259.41
75.24	479.11	268.76
78.16	489.99	269.52
81.31	493.48	269.76
83.28	502.43	270.39
86.32	492.86	269.71
89.36	535.13	272.67

Table 6.7 Summary of Bentonite Plug Longitudinal Expansion Measurements for Tubes 9 through 12

	Plug			
	#9	#10	#11	#12
Initial Height (in)	4.00	3.65	3.70	3.60
Final Height (in)	4.90	4.50	4.50	4.40
Expansion (% initial length)	23	23	22	22

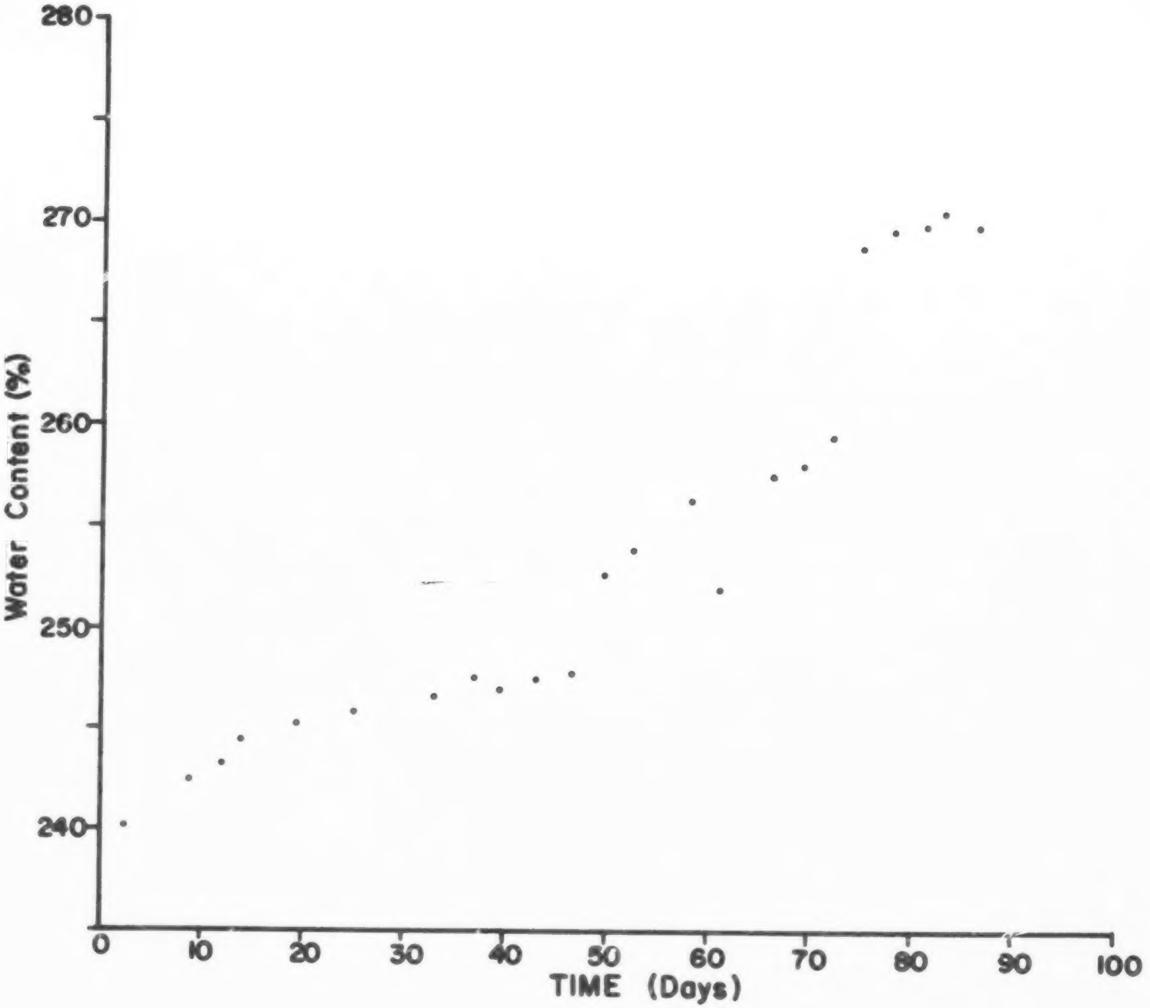

Figure 6.19 Change in water content for bentonite plugs 1 through 4 at 34 kPa (5 psi) injection pressure.

BEST COPY AVAILABLE

6.5 Reference Testing

6.5.1 Liquid Limits

The objectives and methods used for liquid limit determination are discussed in Section 5.6.2. Two liquid limit tests were conducted. The first tested samples at 16 different moisture contents. The results of the test (Table 6.8) show that control of moisture content can be difficult with this type of clay. If a large sample volume is prepared for a variety of tests, as was done in this case, it is difficult to achieve homogeneity of moisture content throughout the sample. Care must be taken with mixing to avoid altering the clay fabric. For this test, it was important that the clay fabric resemble as closely as possible that of the clay used for in-situ and laboratory experiments. At the same time, some mixing is required to assure contact of water and clay throughout the sample volume.

Samples with the same moisture content behave differently if the degree of adsorption differs from sample to sample. Adsorbed water is water bound electrically between the layers that make up the clay structure. This water is considered by some researchers to behave more viscously than free water in void spaces (Section 5.2). The degree to which available water is adsorbed is a function of time and of clay surface area in contact with water. The sample preparation method used in this test allowed samples several weeks to adsorb the water available, but the only way to make a uniform surface available throughout the sample volume would be to grind the tablets and mix them continuously. The difference of degree of adsorption may account for the anomalous performance of samples 9 and 13 in the first test.

A second liquid limit test was performed on seven samples with different moisture contents approximately one month after the first test. The results of this test are shown in Table 6.9. The intention of delaying the second test for one month was to determine how time to absorb would influence the determined liquid limit.

Figure 6.20 is a plot of moisture content against the log of the number of blows for the first test. Ideally, the results will plot in a straight line for samples with counts between 10 and 40 (Lambe, 1959, p. 25). The liquid limit is the moisture content predicted for a blow count of 25 (Lambe, 1959, p. 26). The flow curve shows that results of this test deviated slightly from the straight line approximation. Moisture content calculated from the first test as the liquid limit is approximately 360%. Figure 6.21 is the flow curve for the second test. It shows a liquid limit of approximately 362%.

These results can be compared with liquid limits for four different Na smectites quoted by Meyer and Howard (1983, p. 43). The values range from 280% to 700%, with an average of 440%. Liquid limits quoted by Lambe and Whitman (1979) for similar bentonites are significantly higher, including 710% (p. 33), and ranging from 494 to 710%. (p. 322) The results reported from this test fall at the low end of the expected range for clays of similar composition. The differences may

Table 6.8 Results of Bentonite Liquid Limit Test 1

	Moisture Content (%)	Drops
1	40.19	over 200
2	68.23	over 200
3	96.27	over 200
4	124.31	over 200
5	152.34	over 200
6	180.38	over 200
7	236.46	a) 137 b) over 200 c) over 200
8	259.0	a) 105 b) over 250 c) over 200
9*	260.0	a) 140 b) 133 c) 105 Average: 126
10	270.0	a) 128 b) 165 c) over 200
11	280.0	a) 142 b) over 200 c) over 2000
12	292.54	a) 7 b) 7 c) 6 Average: 18 2/3
13*	343.59	a) 32 b) 32 c) 50 Average: 38
14	348.61	a) 4 b) 4 c) 3 Average: 3 2/3
15*	418.37	a) 4 b) 4 c) 7 Average: 5
16	460.76	too liquidy to test

* ?

Table 6.9 Results of Bentonite Liquid Limit Test 2

Moisture Content (%)	Drops
182.4	a) way over 250
258.9	a) over 250 b) over 250
261.2	a) over 250 b) over 250 c) over 250
271.2	a) 254 b) over 250 c) over 250
321.1	a) 37 b) 59 c) 38 Average: 44 2/3
358.9	a) 15 b) 19 c) 36 Average: 23 1/3
409.2	a) 10 b) 9 c) 41 Average: 20

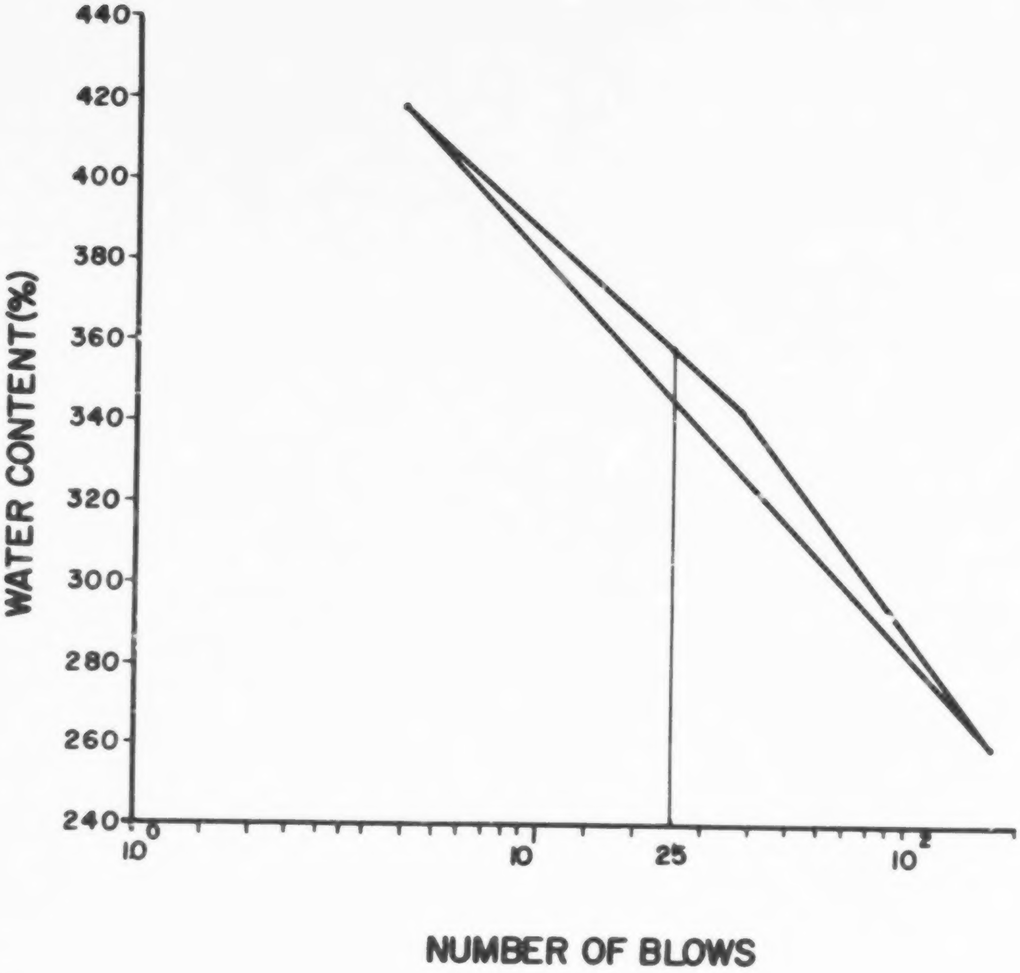

Figure 6.20 Results of bentonite liquid limit determination, Test 1.

BEST COPY AVAILABLE

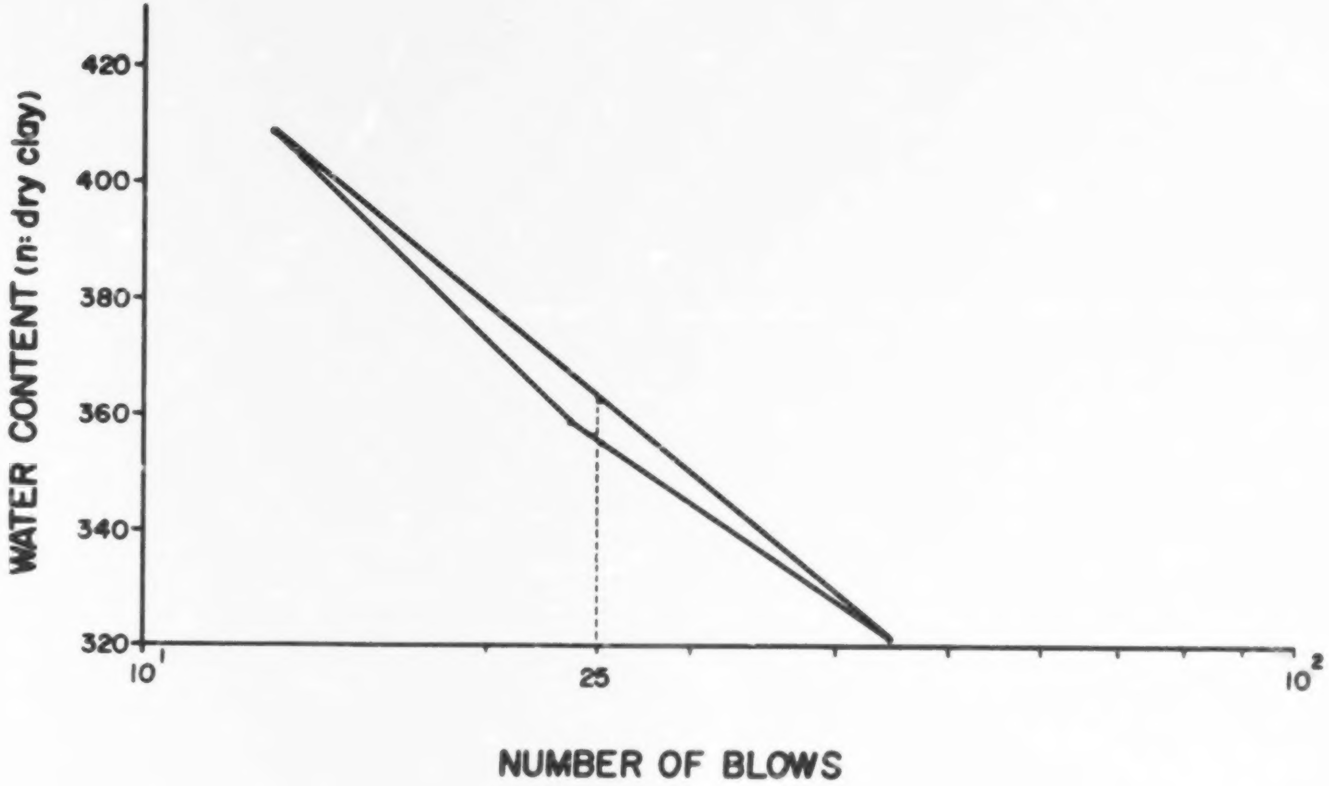

Figure 6.21 Results of bentonite liquid limit determination, Test 2.

BEST COPY AVAILABLE

result from the differences in available surface areas and rates of absorption between powdered and tablet forms of the same clay.

6.5.2 Plastic Limit Test

The objective and procedures used in determining the plastic limit for the clays used in this study are described in Section 5.6.3. Four samples with moisture contents of 68.36% were tested. The samples were prepared using the procedures described in Section 5.6.3. The results are presented in Table 6.10. The samples weighed approximately 8 grams at the beginning of the test. End moisture contents varied from 20.30 to 54.85%. The plastic limit was determined as the average end moisture content of 37.51%..

This value is significantly lower than reported plastic limits for similar clays. Meyer and Howard (1983, p. 43) list plastic limits of 86 to 97% for 4 Na-smectites. Lambe and Whitman (1979, p. 33, 322) quote 54% for Na-montmorillonite. Mitchell (1976, Sections 9.6 and 9.7) suggests values from 50 to 100%, with the higher values for Na-montmorillonites, and with even considerably higher values for very small particle size mixes. There are a number of possible causes for this discrepancy. The clay used for testing is extremely sticky at low water contents. Each test involved the loss of some clay to the test surface. This made an accurate accounting of weight difficult. More significant is the fact that samples at this water content are very difficult to mix. They retain, to a certain degree, the structure of the tablets. This structure should influence the plastic limit by reducing the water content at which the clay still retains some molding strength.

6.5.3 Harvard Miniature Compaction Test

The objectives, equipment and procedures used for the Harvard Miniature Compaction test are described in Section 5.6.4. Seven samples with different moisture contents were tested. Samples were prepared using the procedure described in Section 5.6.2. Tables 6.11 and 6.12 present the results. The compaction curve is shown in Figure 6.22. The curve conforms to a general paraboloid which increases to a maximum dry unit weight at an optimum moisture content and then decreases with increasing moisture content. The curve suggests an optimum moisture content of approximately 45%. Maximum dry density is between 17 and 18 grams/in^3 or 1.04 to 1.10 g/cm^3.

Sawyer and Daemen (1987) report results from a test by American Colloid on a granular bentonite of similar composition to the clay used in this study. The optimum dry density is 1,346 kg/m^3 (84 lb/ft^3), which is greater than the 1,025 to 1,090 kg/m^3 (64 to 68 lb/ft^3) of this study. The optimum moisture content found by the manufacturer is 13% significantly less than the results of this test. Sawyer and Daemen (1987) also tested seven commercial bentonites with a Harvard Miniature Mold compaction test. Dry densities range from 1,090 to 1,460 kg/m^3 (68 to 91 lb/ft^3). Optimum

Table 6.10 Bentonite Plastic Limit Test Results

Sample	Initial Water Content (%)	Initial Weight (g)	End Weight (g)	Estimated Loss of Clay (g)	Water Loss (g)	Final Clay Solids Weight (g)	End Water Content (%)
1	68.36	8.08	5.11	1.5	1.47	3.34	53.90
2	68.36	8.30	4.74	1.0	2.56	3.91	20.45
3	68.36	8.02	5.49	1.0	1.53	3.75	45.77
4	68.36	8.02	5.15	0.8	2.07	3.93	29.93
					Average = Plastic Limit =		37.51

Table 6.11 Harvard Miniature Compaction Test Results

Trial #	Weight of Compacted Soil and Mold (g)	Weight of Mold (g)	Weight of Soil (g)	Wet Density g/cm^3	Dry Density g/cm^3
1 a	491.6				
b	502.88				
c	502.34				
Average:	498.94	408.63	90.31	1.45	1.04
2 a	503.77				
b	502.54				
c	504.03				
Average:	503.45	408.63	94.82	1.52	.879
3 a	488.46				
b	493.68				
Average:	491.07	408.63	82.44	1.32	1.00
4 a	506.61				
b	507.72				
c	509.56				
Average:	507.96	408.63	99.33	1.60	.947
5 a	503.98				
b	506.26				
c	506.76				
Average:	505.67	408.63	97.04	1.56	.927
6 a	502.6				
b	502.13				
c	503.64				
Average:	502.79	408.63	94.16	1.51	.819
7 a	511.16				
b	506.73				
Average:	508.945	408.63	100.315	1.61	1.05

Table 6.12 Harvard Miniature Compaction Test - Water Content

Trial #	Can	Weight of Can (g)	Weight of Wet Soil and Can (g)	Weight of dry Soil and Can (g)	Weight of Water (g)	Weight of Dry Soil (g)	Water Content (%)
1	21T	13.84	40.48	33.03	7.45	19.19	38.82
	26T	15.44	53.62	42.9	10.72	27.46	39.04
						Average:	38.93
2	12T	14.7	58.98	39.98	19.0	25.81	73.61
	33T	15.28	57.49	40.24	17.25	24.96	69.11
						Average:	71.36
3	-	117.34	439.9	43.005	102.215	160.345	32.44
4		177.34	572.12	290.405	281.715	113.065	68.45
5	-	177.34	568.7	289.43	279.27	112.09	68.12
6		13.41	395.30	72.22	323.08	58.81	84.6
7	A23	21.96	70.54	53.48	17.06	31.52	54.13

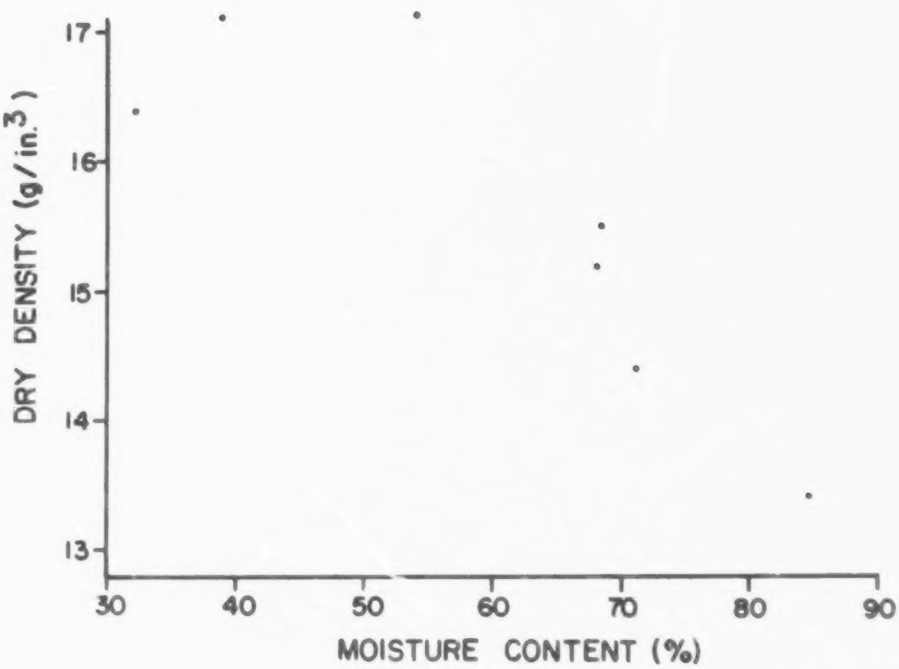

Figure 6.22 Harvard Miniature Compaction Mold Test curve for bentonite used in sealing experiments.

BEST COPY AVAILABLE

water contents vary from 8 to 26%. The apparently low dry densities and high moisture content determined in the test reported here may be the result of too low a compactive effort. Lambe and Whitman (1979, p. 515) suggest that for a given type of compaction, the higher the compactive effort, the higher the dry density and the lower the optimum moisture content. Another explanation, however, may be more relevant to the type of clay tested in this study. Hilf (1975, p. 248) discusses the effects of increasing moisture content on the behavior of the soil as compacted. Once the soil has been compacted to near saturation, additional moisture content will only decrease the density achieved by compaction. The optimum moisture content, as determined by compaction testing, will be a function of the void space that survives compaction. The clay used in this test has a porosity of about 20% in tablet form. The voids locked in the tablets may only be able to communicate with the voids in the overall hydrated clay when the tablets have sufficiently hydrated to open the tablet structure. This suggests that, for this clay, increasing the moisture content will allow greater densification as it makes available the trapped void spaces in the tablets to compaction. Simply increasing the compactive effort would not produce an accurate measure of the potential for densification of the clay.

6.6 Transient Hydraulic Conductivity Testing

Small-scale transient pulse testing was performed on three clay samples using the procedures and equipment discussed in Sections 5.7.2 and 5.7.3. Figures 6.23 through 6.25 present results of transient tests. Both upstream pressure decay and downstream pressure increase are plotted. Each sample was weighed and oven-dried for three days at the end of each test to determine moisture content.

The pressure plots are analyzed to determine hydraulic conductivity using the theory discussed in Section 5.7.2. Late time approximations were used to provide the necessary $\alpha\beta$ values. Late time approximation values for different β values are included in Appendix E. Type curves developed from the approximate solution are presented in Appendix F.

The results of small-scale transient pulse testing are presented in Table 6.13. The table includes the ratio of downstream to upstream volumes γ. The $\alpha\beta$ match point is described with the equivalent time value in minutes taken from the actual test curve.

A comparison of the hydraulic conductivity values determined for these samples with the results discussed in Section 6.8 for large-scale testing shows a significant difference. Small-scale plug hydraulic conductivities are much lower than large-scale values. There are a number of explanations for these differences in addition to the scale aspect. The small samples had lower moisture contents than the large-scale sample. Small samples were taken from pre-mixed and saturated clay. The large-scale plug was formed by dropping bentonite tablets through water to simulate field conditions. Large-scale sample density can be assumed to be non-uniform over the length of the sample, as suggested by the observations on prototype plug behavior in Section 6.9. Finally, the large-scale plug was able to drain into the

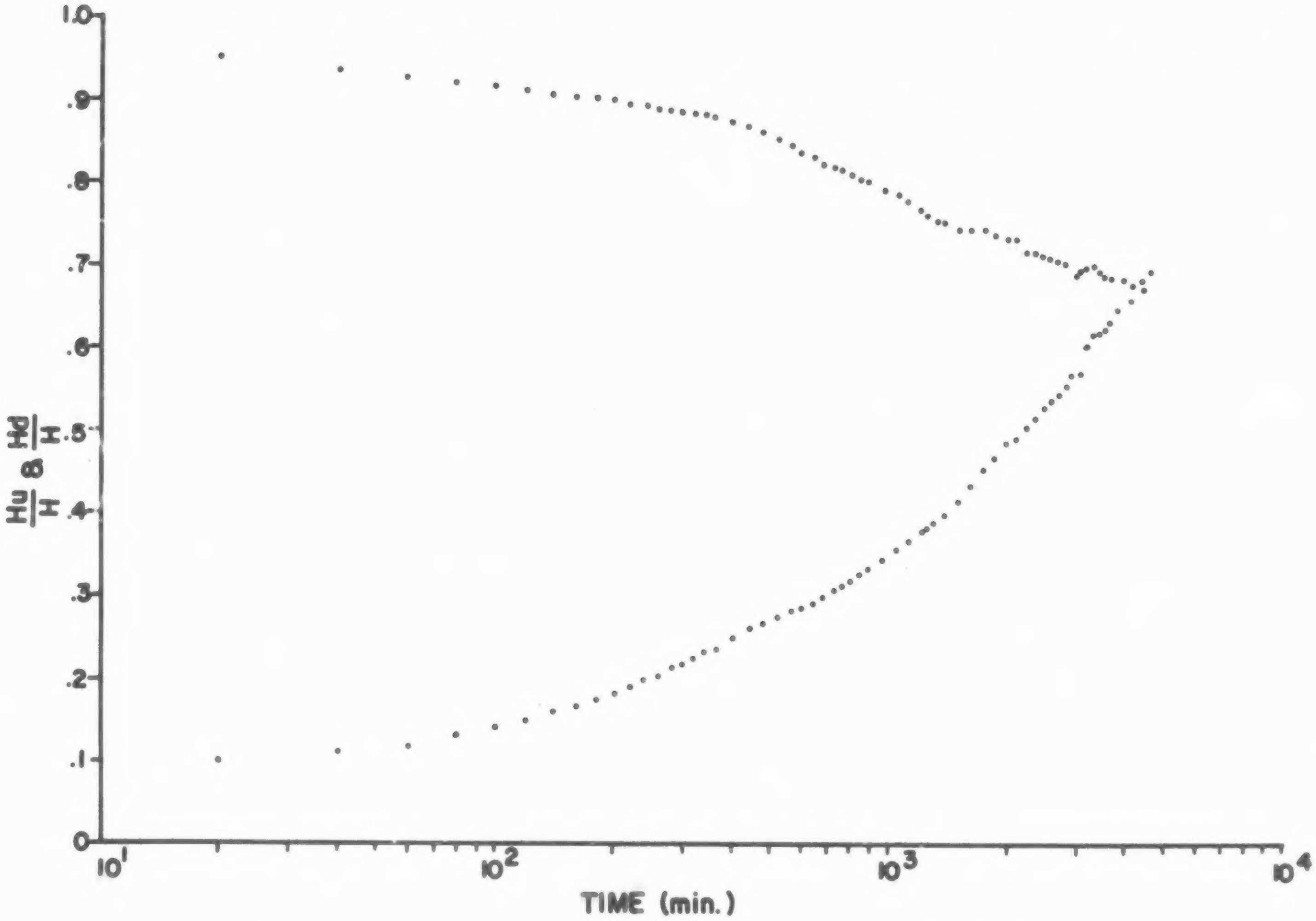

Figure 6.23 Transient pulse test. Sample with 168% final water content. H_u: upstream reservoir pressure decay. H_d: downstream reservoir pressure (head) build-up

BEST COPY AVAILABLE

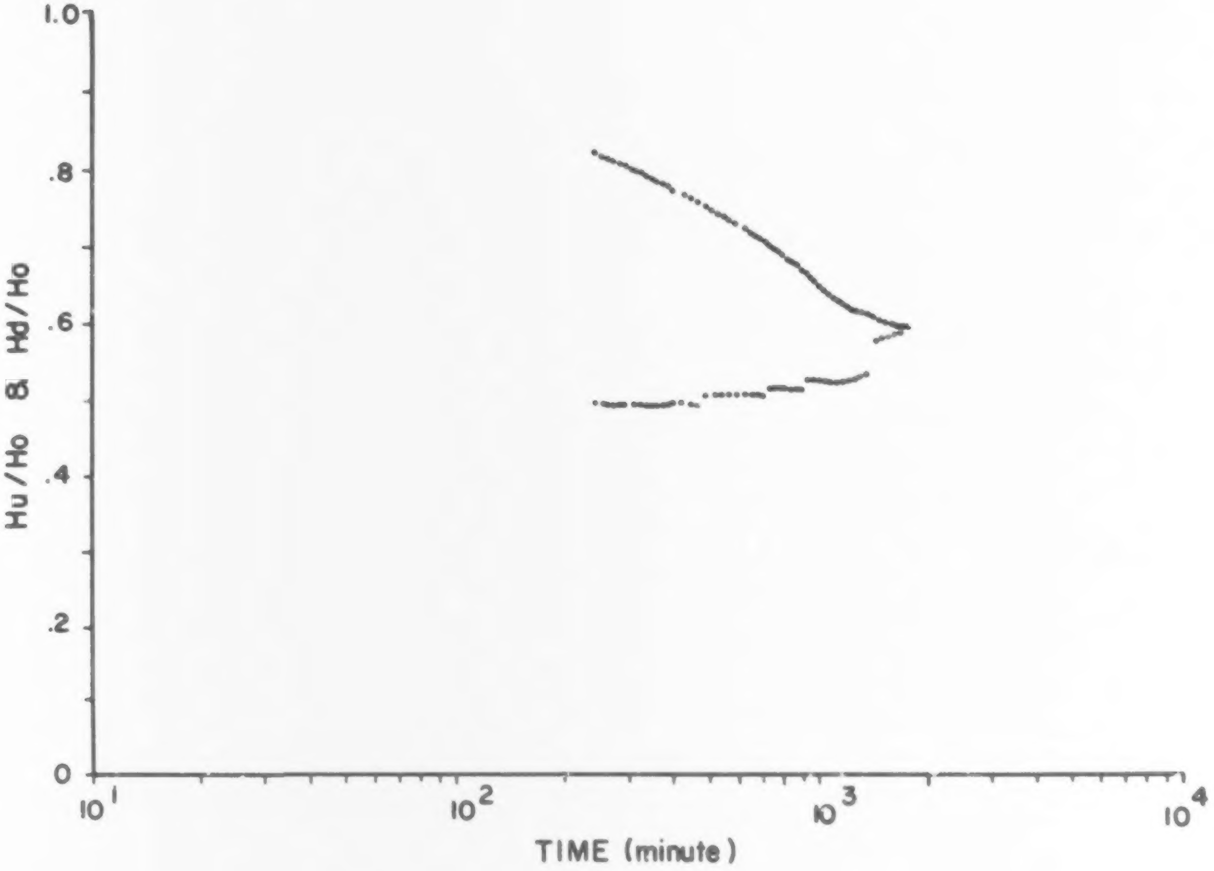

Figure 6.24 Transient pulse testing on bentonite plug. H_u: upstream reservoir pressure decay. H_d: downstream reservoir pressure build-up.

BEST COPY AVAILABLE

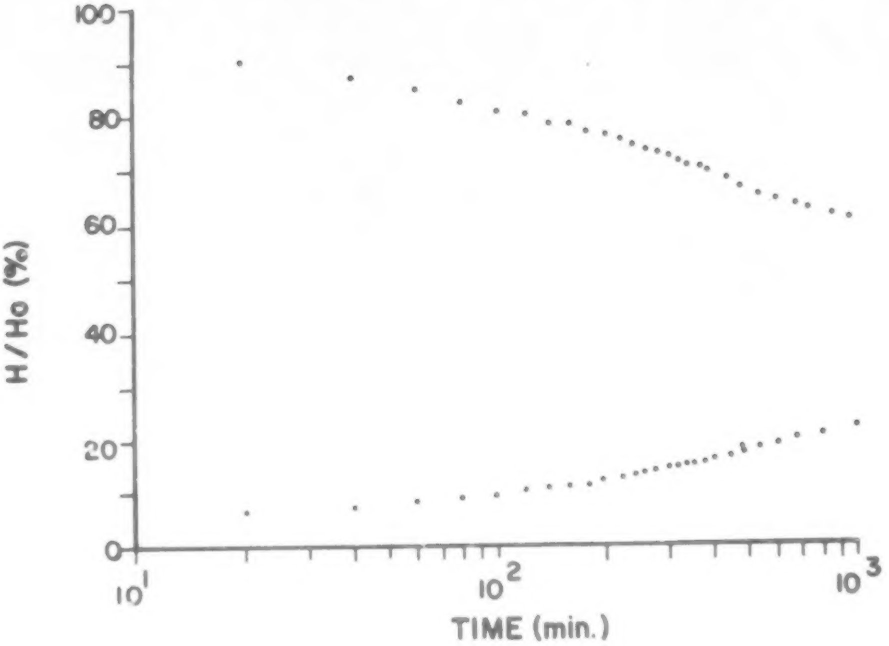

Figure 6.25 Transient pulse testing on bentonite plug.
H_u: upstream reservoir pressure decay.
H_d: downstream reservoir pressure build-up.

Table 6.13 Results of Small-Scale Transient Pulse Testing on Bentonite Plugs

Initial Sample Moisture Content (%)	Final Moisture Content (%)	γ	β	$\alpha\beta$	Time (min)	S_s (cm^{-1})	K (cm/s)
≈75	104	.87	0.1	1	1550	7.35×10^{-9}	5.2×10^{-12}
≈100	168	.87	0.1	1	1200	7.35×10^{-9}	4.8×10^{-12}
≈125	204	.87	0.1	1	1600	7.35×10^{-9}	5.1×10^{-12}

γ: ratio of downstream to upstream reservoir volumes

S_s: specific storage

K: hydraulic conductivity

lower reservoir while tested. The samples tested in the small-scale test had controlled volumes. No drainage was allowed and sand columns at both ends of each small plug prevented swelling.

A review of these differences in test procedure combined with the testing experience suggests that the method of plug construction is the most significant factor involved in the differences in observed hydraulic conductivity. The low moisture contents and confined volume of the pre-mixed, small-scale samples should contribute to lower hydraulic conductivity for these samples. The lower moisture contents are indicative of plugs not completely saturated. It should be noted that the recorded moisture content for each sample is the moisture content measured at the end of the test. Initial moisture content was much lower. Initial moisture for the large-scale sample is probably in excess of 250%, as indicated in the discussion of swelling in Section 6.4. Meyer and Howard (1983, p. 38) suggest that lower moisture contents provide lower hydraulic conductivity as long as the moisture content is wetter than optimum as determined by compaction testing (see also Section 6.5.3). The confined volume of the small-scale samples results in the full swelling pressure being directed against the wall of the test cylinder. This should provide a less permeable sample-wall interface than the free-swelling environment of the large-scale plug.

The results of this test provided some difficulty in curve matching. At the beginning of each test it is necessary to remove all reservoir pressure. Ideally, the pressure in each reservoir begins at zero. However, the soft clay allows some initial displacement downstream as soon as it experiences pressure. This results in a sudden increase in downstream reservoir pressure at the very beginning of the test. This displacement also results in a sudden loss of pressure in the upper reservoir. Testing was initiated after this adjustment was complete and the entire system had equilibrated. Nevertheless, early time portions of the curve were suspect because of this change in pressure conditions. In addition, pressure curves tend to be flatter than type curves predict because the range of pressure change is smaller. Curve matching was accomplished using type curves developed from the late-time approximation. All three tests were analyzed primarily with the decay curves and using the late-time portion of each test. Pressure increase curves were disregarded in the test of the 168% water content sample and only used for adjustment in the other two tests.

6.7 Saturation Test

The objectives and procedures for this test are described in Section 5.8. The test was performed in conjunction with the transient pulse test described in Section 6.6. After each sample was tested for hydraulic conductivity by observing the pressure changes in both reservoirs, the reservoir pressures were removed. The upper reservoir then received a constant pressure pulse and the pressure increase in the lower reservoir was monitored. Figures 6.26 and 6.27 illustrate the response. Each figure also shows the upper reservoir pressure pulse. The relationship of moisture content to percent of upper reservoir pressure achieved is illustrated in Figure 6.28. For this

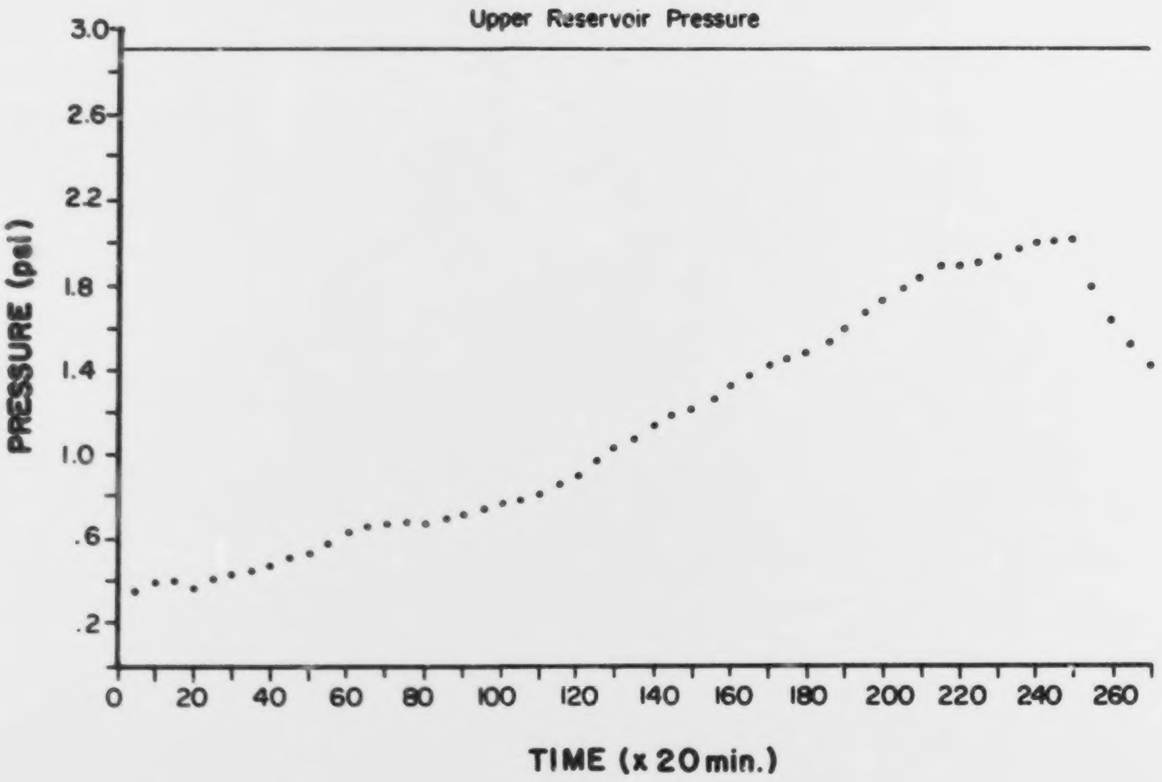

Figure 6.26 Lower reservoir pressure build-up as a result of upper reservoir pressure during bentonite saturation test.

BEST COPY AVAILABLE

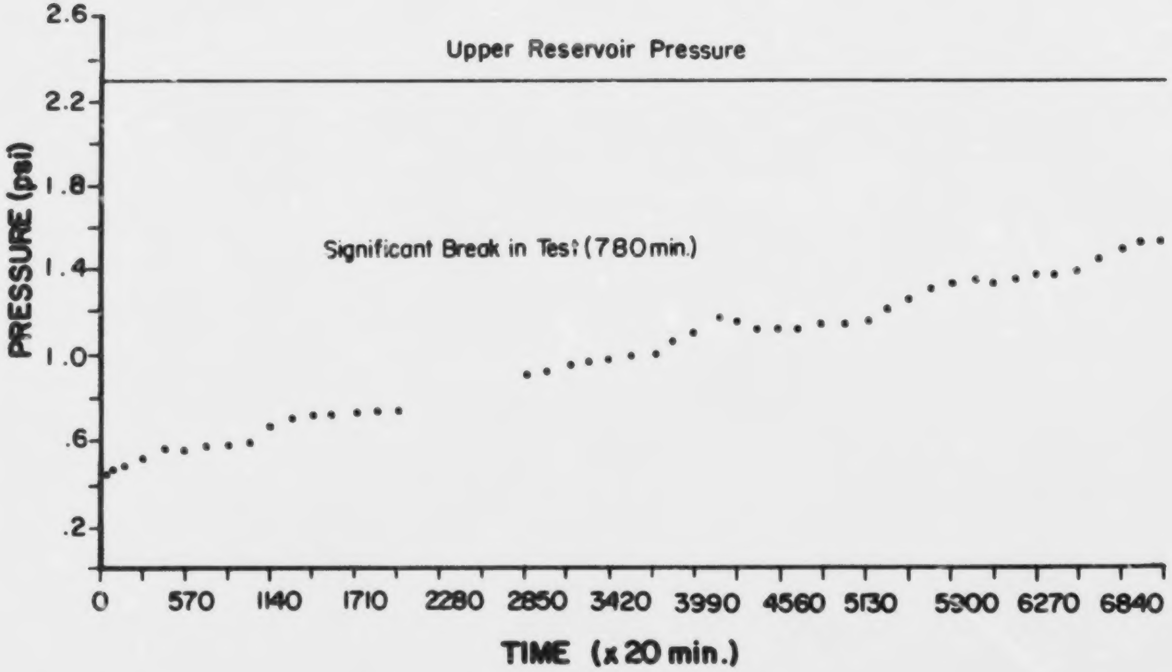

Figure 6.27 Lower reservoir pressure build-up as a result of upper reservoir pressure during bentonite saturation test.

BEST COPY AVAILABLE

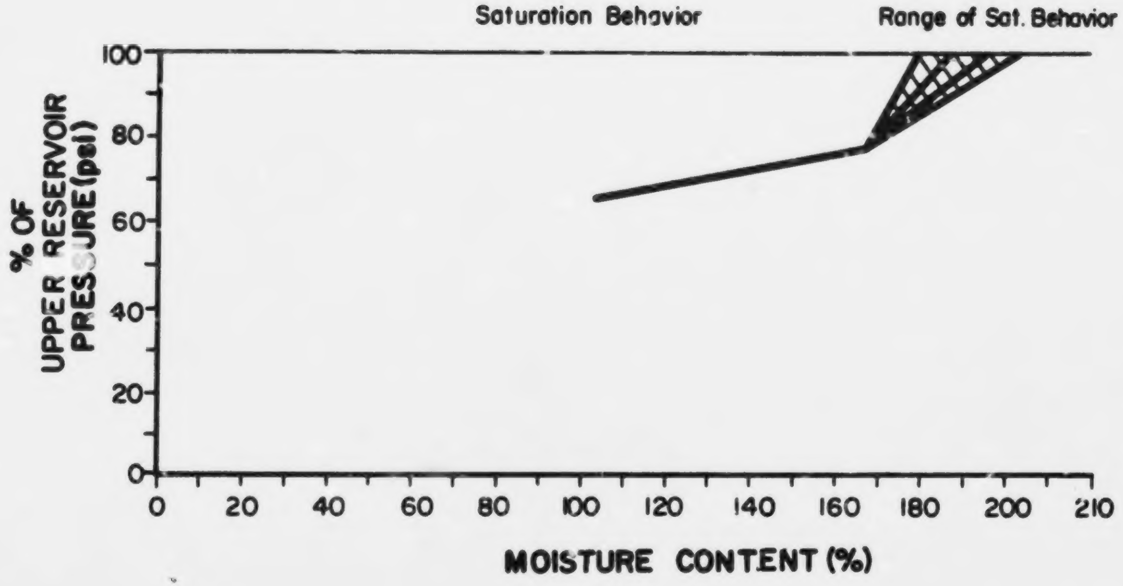

Figure 6.28 Relation between lower reservoir pressure (as a percent of upper reservoir pressure) and moisture content for bentonite saturation tests.

BEST COPY AVAILABLE

test, 100% represents a saturated response. As the graph suggests, saturation should fall between 180% and 200% moisture content.

This test illustrates the relationship between moisture content and saturated behavior. It is not clear that at the higher moisture contents described the sample is actually saturated. The test only measures the behavior of the sample with respect to its ability to respond to a constant pressure head. There does seem to be a correspondence between increasing moisture contents and the ability of the sample to behave as if it was saturated . However, the test does not provide an estimate of void volumes still filled with gas. The fluidized character of the clay at higher moisture contents may disguise the presence of unhydrated void spaces.

The difficulty of saturating low permeability clays in the laboratory has been demonstrated (e.g. Brand, 1975). Even with an extensive effort, using high backpressures, the degree of saturation achieved is difficult to estimate (Sawyer and Daemen, 1987). The procedures and results of this test suggest that saturated performance may be achieved with appropriate moisture contents. This behavior may correspond to the behavior of clays that are actually saturated.

6.8 Large Scale Transient Tests

The objectives, procedures and equipment of this test are discussed in Section 5.9. The ratio of downstream to upstream reservoir volume for this test is 0.1. Three tests were performed using the 0.1 reservoir ratio. The last three tests were performed by injecting into the downstream reservoir. The reservoir ratio γ for these tests is 10.

The results are similar in early time and only diverge in the late time slopes when the pressure decay is plotted against the log of time. Analysis was accomplished using the error function solution described in Section 5.9.2. The error function solution is represented by a single type curve included in Appendix F.

The error function solution is appropriate for situations where the hydraulic conductivity of the sample is small, the time involved in the test is relatively short, and the specific storage of the sample is large. Under these conditions, the decay in the upstream reservoir behaves as if the downstream reservoir is an infinite distance away. As section 5.9.2 shows, the error function curve plots the product $\alpha\beta^2$ against dimensionless pressure decay. This means that only the product of hydraulic conductivity and specific storage, KS_s, can be calculated from this solution. To arrive at a value of hydraulic conductivity, the specific storage of the plug must first be estimated. This was accomplished for these tests by matching the test curves to the type curve and noting that all three tests diverge from the type curve at a dimensionless pressure decay value of approximately 70%. A plot of $\alpha\beta^2$ curves diverging from the error function solution curve provided by Hsieh et al. (1981) suggests a β for these tests of 0.01. The specific storage can be calculated from

$$S_s = \beta S_u / AL \qquad (6.7)$$

where S_u is the compressive storage of the upstream reservoir, A is the cross-sectional area of the plug, and L is the length of the plug.

Table 6.14 presents the results. Specific storage is estimated as 7.86×10^{-7} cm^{-1}. Hydraulic conductivities are approximately 1×10^{-9} cm/s.

The second set of three tests, accomplished by injecting and monitoring pressure in the lower reservoir, was analyzed using type curves developed from the late time approximation given by Hsieh et al. (1981). These type curves plot the product $\alpha\beta$ against dimensionless pressure decay. Hydraulic conductivity can be calculated using

$$K = \alpha\beta S_u L/At \qquad (6.8)$$

Specific storage is calculated using the β value for the type curve used in each solution. The results of these three tests are shown in Table 6.14.

Table 6.14 shows that both hydraulic conductivity and specific storage values of the two sets of tests differ by less than one order of magnitude. The difference may be a function of the assumptions underlying each solution used. The error function solution depends on the magnitude of specific storage assumed. Large specific storage values result in low hydraulic conductivities. The late time approximation assumes that the influence of specific storage is negligible (Hsieh et al., 1981). Low specific storage values result in low hydraulic conductivities, as the value of β, and therefore of $\alpha\beta$, is low with respect to time.

The results of the large scale tests suggest that increasing the plug size does not significantly affect the hydraulic conductivity values developed for the respective samples. The results appear to be more sensitive to the types of solutions used to analyze the tests.

6.9 Plug Prototype

The objectives and design of the plug prototype constructed in the laboratory are discussed in Section 5.10. The prototype was built at the same time as the seals were emplaced in situ in Cargodera Canyon. After approximately one month, testing was begun on the prototype.

The sand intervals between the bentonite plugs were observed to have lost a significant amount of water to the hydrating clay. They were visibly drier to a distance of two to three inches from the sand-clay interface than the wet sand away from the clay (Figure 6.29). To saturate the sand and back pressure the clay plugs, water was injected into both sand intervals at 34 kPa (5 psi) pressure. Over approximately one week, the upper sand interval with one clay-sand interface,

Table 6.14 Results of Large Scale Bentonite Plug Transient Pulse Tests

Test No.	Ratio of Downstream to Upstream Reservoirs (γ)	Solution Approximation	β	$\alpha\beta^2$	S_s ($cm^{-1} \times 10^{-7}$)	K ($cm/s \times 10^{-9}$)
1	.1	erfc	.01	.01	7.86	1.14
2	.1	erfc	.01	.01	7.86	1.07
3	.1	erfc	0.1	0.1	7.86	1.00
				$\underline{\alpha\beta}$		
4	10	late time	1	.1	1.21	.560
5	10	late time	.3	1	.363	.217
6	10	late time	.65	.1	.786	.275

S_s: specific storage

K: hydraulic conductivity

BLANK PAGE

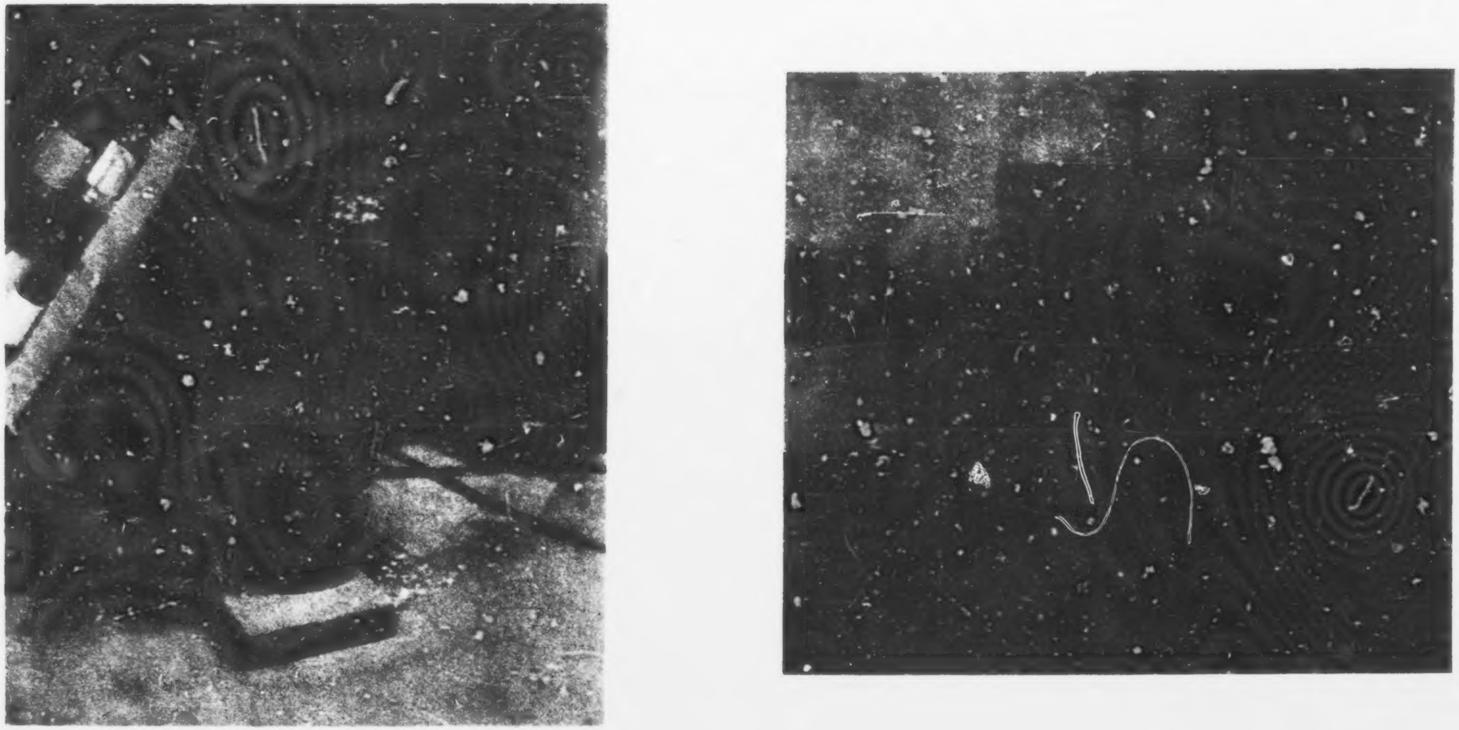

Figure 6.29 Sand drying adjacent to bentonite plugs, presumably due to water adsorption by bentonite from sand.

BEST COPY AVAILABLE

took 1200 ml of water. During the same period, the lower interval required 4200 ml. The lower interval has two sand-clay interfaces. At the end of this injection period, both sand intervals appeared to be saturated.

A 2 cm (3/4 inch) wide crack appeared between the sand and clay when one interval was pressurized and the other was not. This crack is shown in Figure 6.30. When pressure was moved to the other interval, the crack healed in the unpressurized interval and opened up on the other side of the plug. The fact that the crack moved as pressure direction was changed suggests the clay-tube interface bond was not strong enough to resist the injection pressure. This was confirmed by the push-out test described in Section 6.3. Nevertheless, the only possible explanation for the crack itself is consolidation and compliance of the clay seal. It is interesting that the crack itself is filled with air as well as water. The source of the air is probably the collection-injection apparatus installed in the plug. The open ends of these lines were left open during the plug hydration period. As water was drawn from the sand by the clay, air was probably drawn into the sand from outside the system via the tubing penetrating the plugs.

A constant injection test was initiated when the sand intervals appeared to be saturated. Approximately twice as much volume is injected in either interval as is collected on the other side of the plug. Most of the flow out of the collection interval is probably the result of the plug moving into the collection interval and forcing excess water out. For this reason, the outflow is not used to calculate a hydraulic conductivity value.

Prototype observations bear directly on the record of plug testing at Cargodera Canyon. The high inflows observed during in-situ testing are similar to the inflows recorded for the prototype test. The absence of observable outflows in the field would seem to be a result of the fact that the plug-rock interface should form a stronger bond than the plug-tube interface. This means the plugs won't slide in the borehole.

The loss of water in the sand intervals should have occurred in the field as well. The unsaturated character of the injection and collection intervals may explain the relatively high apparent permeabilities calculated for the plugs during transient testing in the field (Section 4.9). These tests would be sensitive to any loss of water and pressure to resaturate the sand.

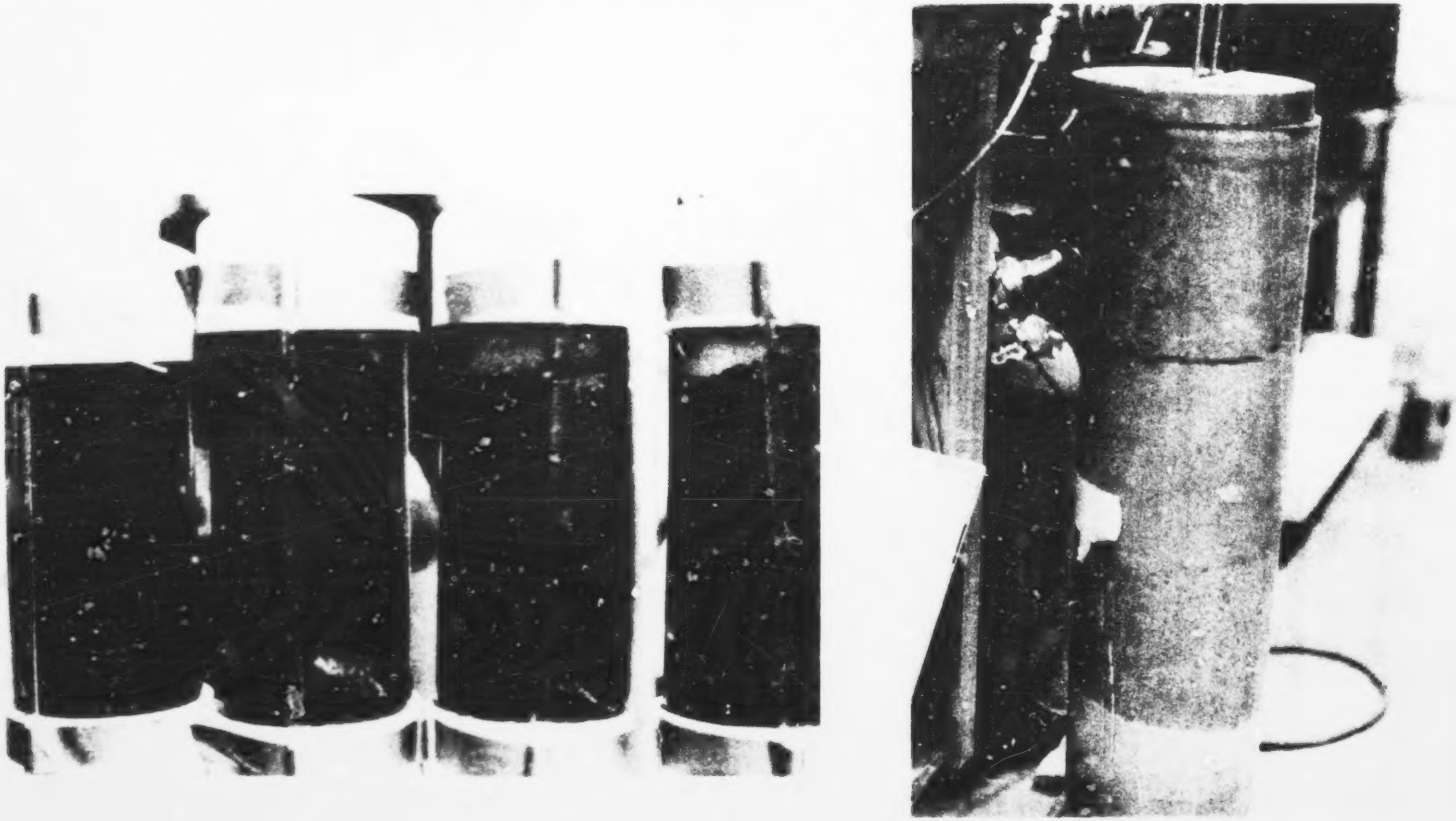

Figure 6.30 Separation between bentonite plugs and sand-filled adjacent reservoirs. Also note large void spaces visible at clay-pipe interface.

BEST COPY AVAILABLE

CHAPTER SEVEN

LABORATORY TESTING OF CEMENT PLUGS

7.1 Introduction

The objective of this laboratory testing was to determine whether certain procedures, equipment designs, and plug emplacement techniques would prove worthy in a field environment. Three main experiments were conducted in the laboratory. A prototype of the plug system was built to scale and was used for tests and for equipment evaluations. The second set of tests had the objective of assessing the influence of penetrating tubes on the sealing characteristics of cement plugs. The third set of tests was conducted to assess the effects of water channeling through cement plugs.

7.2 Plug Prototype

The plug prototype was constructed to give a physical representation of the proposed plug design. The construction of the plug also provided valuable experience in plug emplacement procedures. The plug prototype proved useful in testing procedures to be implemented in the field. Field instrumentation was tested and calibrated on the prototype.

7.2.1 Prototype Construction

The plug prototype was constructed in a 17.5 cm (7 inch) O.D. clear acrylic tube 75 cm (30 inches) high. A PVC sewer cap was lowered to the bottom of the pipe and sealed to a disk on the bottom with silicone seal, as was done at Cargodera Canyon. The collection tubing was lowered to the bottom of the tube and covered with sand. The first cement plug, a mix made of nine batches of System 1, was then bailer placed on top of the sand layer. Bailer placement of the plugs in the prototype would determine the turbulence of the cement release. If the turbulence is too great, the cement could invade the injection/collection intervals and clog the tubing. The modified bailer used for plug emplacement proved quite effective in reducing turbulence during cement release.

The next test performed on the prototype was to assess the method designed to saturate the sand after the plugs had hardened. The plugs were not poured on saturated sand because past tests (Daemen et al., 1983, Section 3.4; 1986, Section 2.5) had shown that the water in the sand could be forced up through the cement plug, sometimes with detrimental effects. At that time it was believed that the sand intervals could be saturated from the surface.

The method for resaturating the sand was relatively simple. A vacuum was applied to one line leading to the interval, with the other line to the interval closed off. The vacuum was applied for approximately

5 minutes, after which it was shut off and a valve between the vacuum and the interval was closed. The valve on the other line was then opened while the line was immersed in water. The vacuum in the interval drew water into the interval. From these laboratory tests it was concluded that the saturation procedure worked acceptably.

7.2.2 Equipment Calibration

For long term testing at Cargodera Canyon, a data logging system on site was desired. The data logging system is designed around an Apple IIE computer. The computer records digital inputs from pressure transducers, linear voltage displacement transducers (LVDTs), and thermocouples. Prior to installing the equipment in the field, it was connected to the prototype and testing of the plugs was conducted. The prototype enabled an accurate performance assessment of the data logging system hardware and software.

7.3 Effects of Pipe Penetrating Through Plugs

The installation of borehole plugs with pipes through them generated concern that the interface between the pipe and plug might be a preferential flow path. If it is, tests performed would not be a true assessment of plug sealing performance. Laboratory tests simulating the situation were conducted, to determine the effect tubes would have.

A similarity exists between a pipe through a plug and a sealed shaft. A shaft liner could be considered a large pipe in a borehole. The laboratory test designed to assess the effect of a 6.3 mm (1/4 inch) pipe through a plug was altered to accommodate testing of larger pipes.

7.3.1 Test Equipment and Procedure

A 10 cm (4 inch) I.D. clear acrylic tubing 37.5 cm (15 inches) long simulates the borehole. The ends of the tubes are capped. Each cap has two holes drilled in it. A center hole allows access to the pipe inside the tubing. The second hole is for the injection line on the top cap and collection line on the bottom cap. The pipes inside the tubes are 6.3 mm (1/4 inch)stainless steel tubes, which simulate the conditions of Cargodera Canyon, and 3.8, 5, and 7.5 cm (1 1/2, 2 and 3 inch) O.D. mild steel pipes. Two of each size were tested for a total of 8 tests (Figure 7.1).

The top cap of each tube is connected to the same reservoir. The reservoir is a nitrogen over water type pump made from 2.5 cm (1 inch) I.D. clear acrylic tubing. A ruler attached to the side of the reservoir enables reading the water height. The bottom cap on each tube connects to pipets mounted on the side of the acrylic tubing. The pipets have 5 ml capacity for the tubes which exhibit high flow rates and 1 ml capacity for the tubes with low flow rates. The height of the water in each pipet, as well as the reservoir height and pressure, is read and recorded once a day or every other day. The pipets are either drained or filled if the flow of water into or out of the bottom of the plug necessitates it. A constant head pressure test was conducted on the plugs for approximately four months.

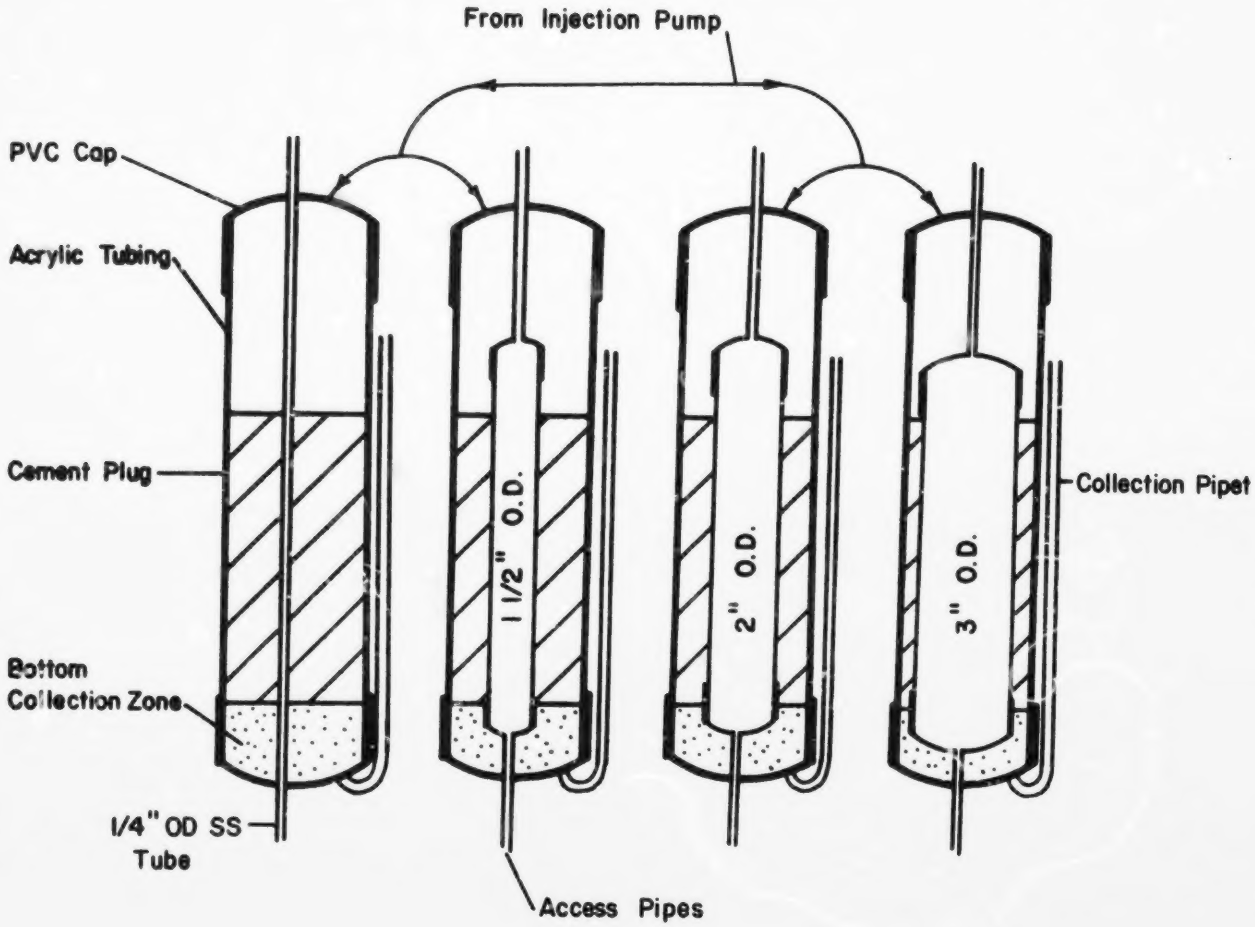
From Injection Pump
PVC Cap
Acrylic Tubing
Cement Plug
Bottom Collection Zone
1/4" OD SS Tube
Access Pipes
1 1/2" O.D.
2" O.D.
3" O.D.
Collection Pipet

Figure 7.1 Schematic of pipe through plug test. Two tests were performed for each pipe size. Steel pipes (6.3 mm, 3.8 cm, 5 cm, and 7.5 cm) are embedded in cement plugs.

BEST COPY AVAILABLE

7.3.2 Analysis

The constant head test analysis uses a weighted average to calculate inflow. Since all tubes are connected to the same reservoir, separate inflow for each tube is unobtainable. The weighted average analysis assumes the flow of water into each plug to be proportional to the area of that plug divided by the sum of the areas of all plugs. Prior to calculating the inflow, however, water that flows out of the plugs is subtracted from the total inflow:

$$Q_i = (a_i/A)(Q_T - \Sigma Q_O) \tag{7.1}$$

where Q_i = inflow for plug i

a_i = area of plug i

A = total area of all plugs

Q_T = total inflow

ΣQ_O = sum of all the outflow values.

7.3.3 Results of Constant Head Tests

Figure 7.2 is the calculated inflow curve for the tube tests. The inflow volumes are much greater than anticipated; those at Cargodera Canyon have been considerably less. The hydraulic conductivity of the plugs calculated from inflow is on the order of 2×10^{-9} cm/s - high for cement. No significant steady state outflow has been observed. Longer term tests may result in steady-state flow, and are needed. Figures 7.3 through 7.9 show the outflow for the pipe tests. The plugs can be grouped into four categories, determined by the net outflow sequence for the plug.

The first category is characterized by inflow into the plug from the outflow side. Tubes 1 and 2 are in this category. Tube 1 absorbed 8.3 cc of water during the test; Tube 2 absorbed 6.5 cc. Both tubes have a 6.3 mm (1/4 inch) stainless steel tube through the cement plug. The negative flow, or inflow, is due, perhaps, to the hydrating cement absorbing small quantities of water and to capillary suction.

The second category is characterized by a period of inflow followed by no flow. Tubes 3 and 6 exhibited this pattern. Tube 3 absorbed 4.4 cc of water over 90 days and then showed neither inflow nor outflow for the remaining 30 days. Tube 6 absorbed 2.9 cc of water over 70 days and showed no measurable outflow or inflow for the remaining 50 days. Tube 3 has a 3.8 cm (1 1/2 inch) diameter mild steel pipe through it; tube 6 has a 5 cm (2 inch) one. This category perhaps is developed by a cessation of the hydration which caused the inflow and by an approaching saturation. These tubes may have imbibed less water than the first two because they have less exposed cement surface area.

The third category plugs have inflow followed by no flow followed by outflow. Tubes 5 and 8 are in this category. Tube 5 absorbed 1.4 cc of water during the first 30 days, stopped for 30 days, and then

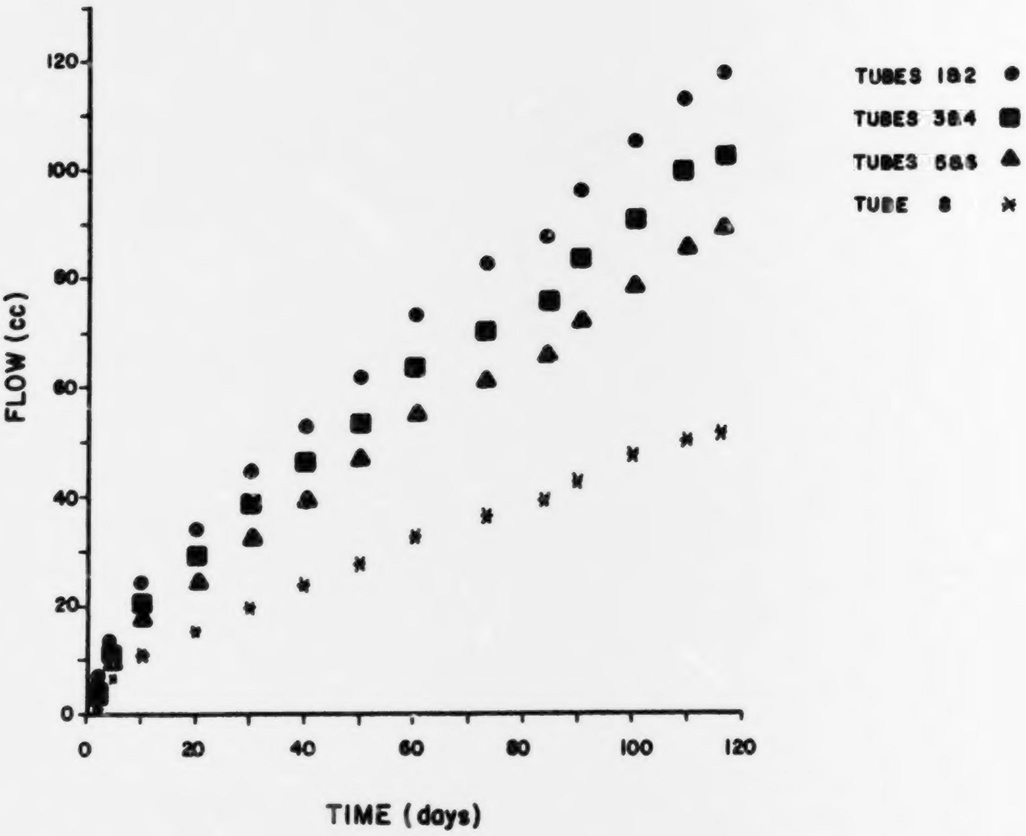

Figure 7.2 Cumulative inflow for tests on cement plugs with embedded steel pipes.

BEST COPY AVAILABLE

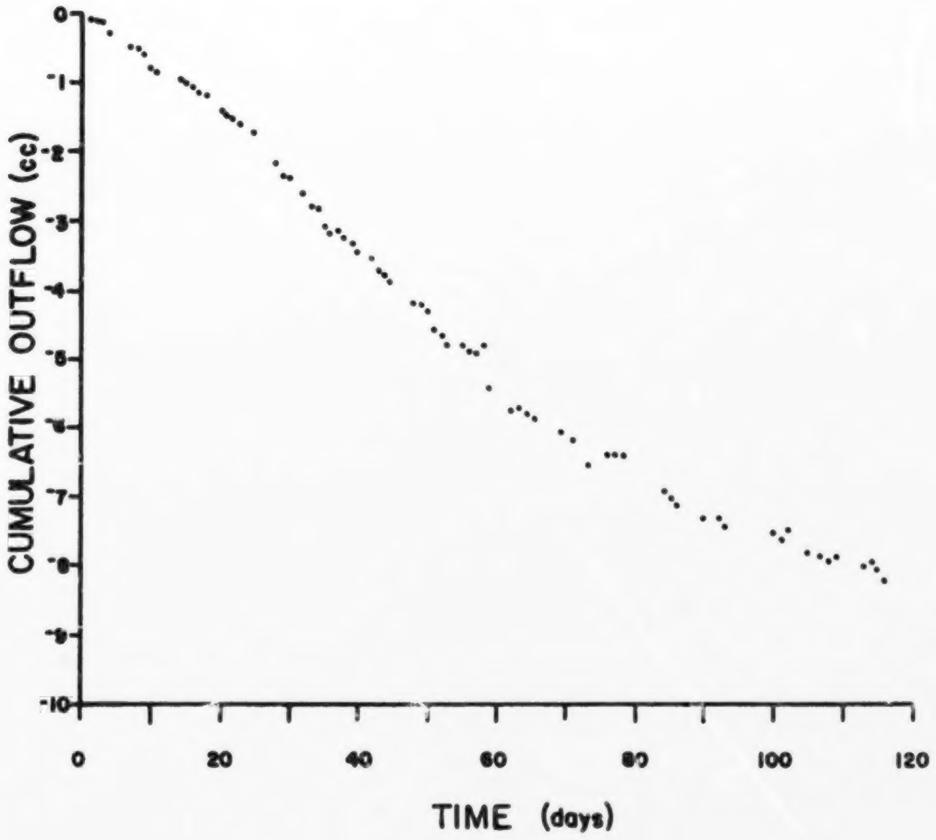

Figure 7.3 Outflow from tube 1. The cement plug in this tube is penetrated by a 6.3 mm (1/4 inch) stainless steel pipe.

BEST COPY AVAILABLE

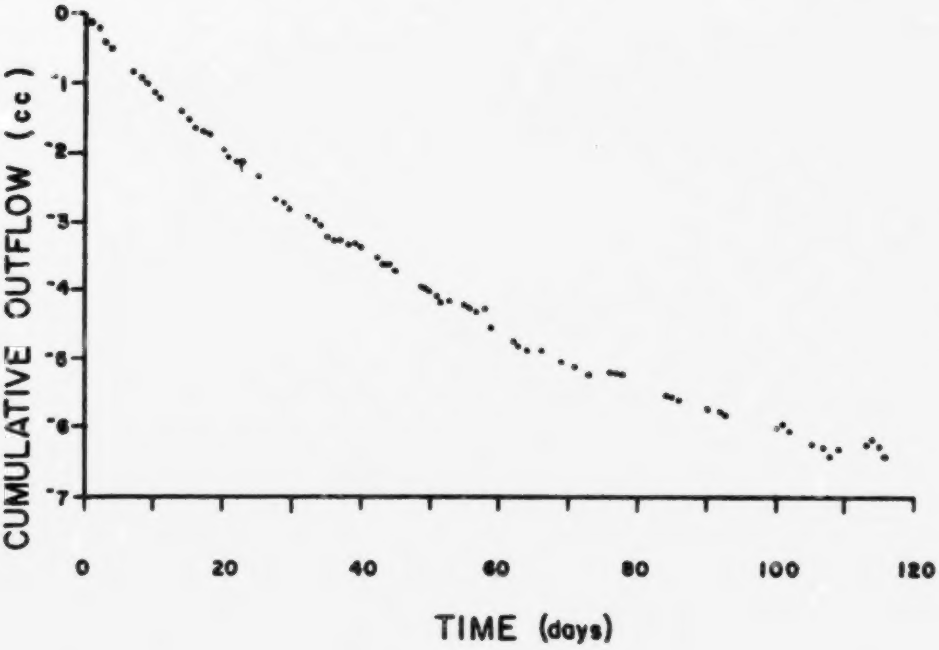

Figure 7.4 Outflow from tube 2. The cement plug in this tube is penetrated by a 6.3 mm (1/4 inch) stainless steel pipe.

BEST COPY AVAILABLE

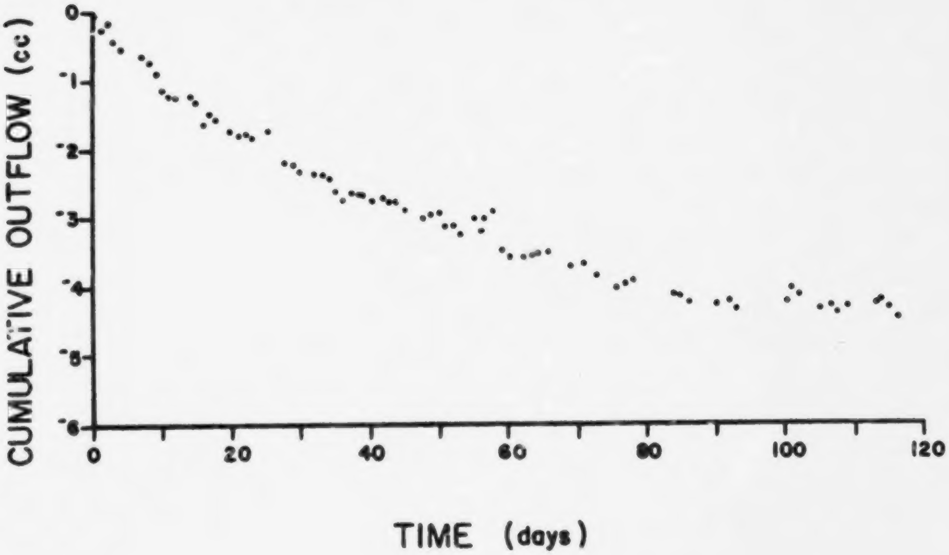

Figure 7.5 Outflow from tube 3. The cement plug in this tube is penetrated by a 3.8 cm (1 1/2 inch) mild steel pipe.

BEST COPY AVAILABLE

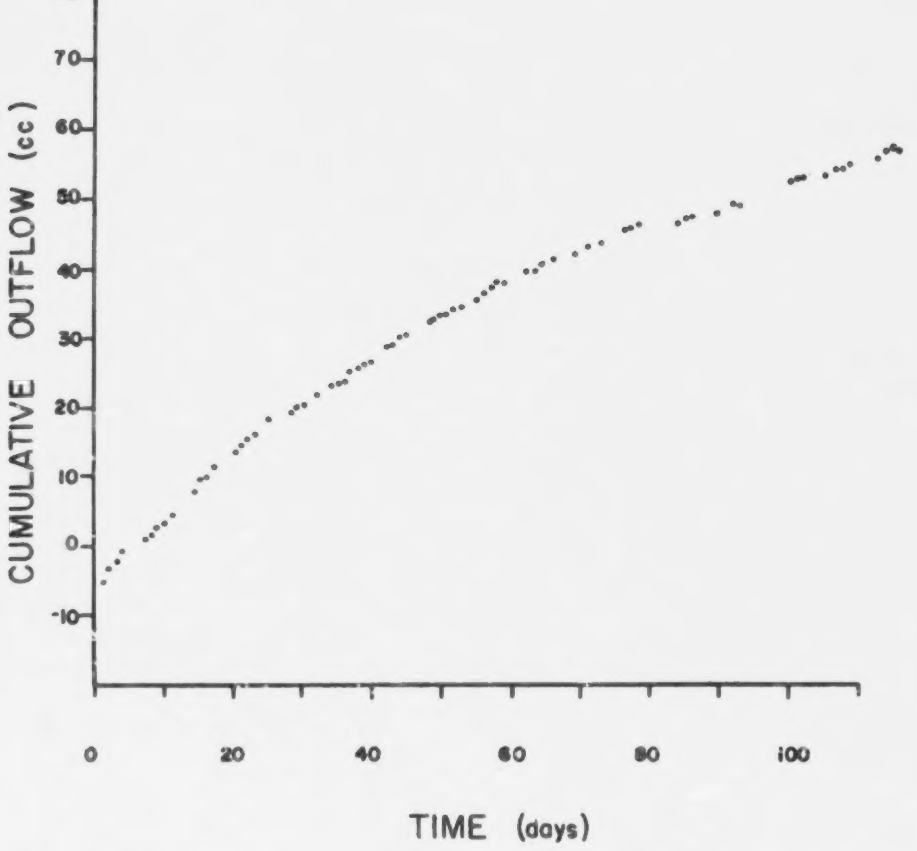

Figure 7.6 Outflow from tube 4. The cement plug in this tube is penetrated by a 3.8 cm (1 1/2 inch) mild steel pipe.

BEST COPY AVAILABLE

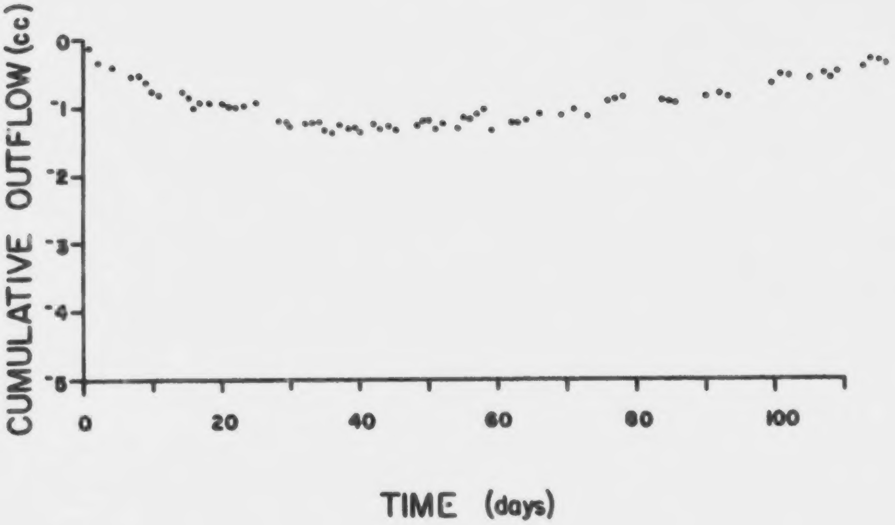

Figure 7.7 Outflow from tube 5. The cement plug in this tube is penetrated by a 5 cm (2 inch) mild steel pipe.

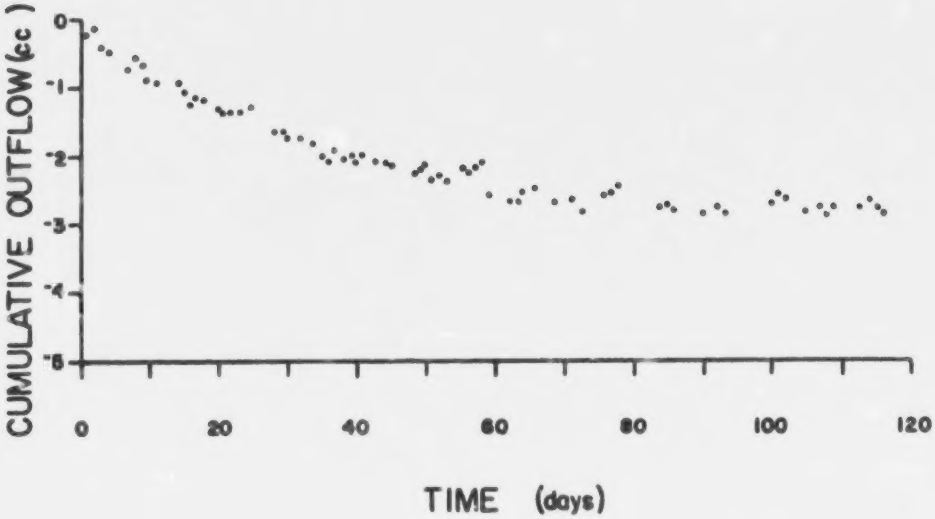

Figure 7.8 Outflow from tube 6. The cement plug in this tube is penetrated by a 5 cm (2 inch) mild steel pipe.

BEST COPY AVAILABLE

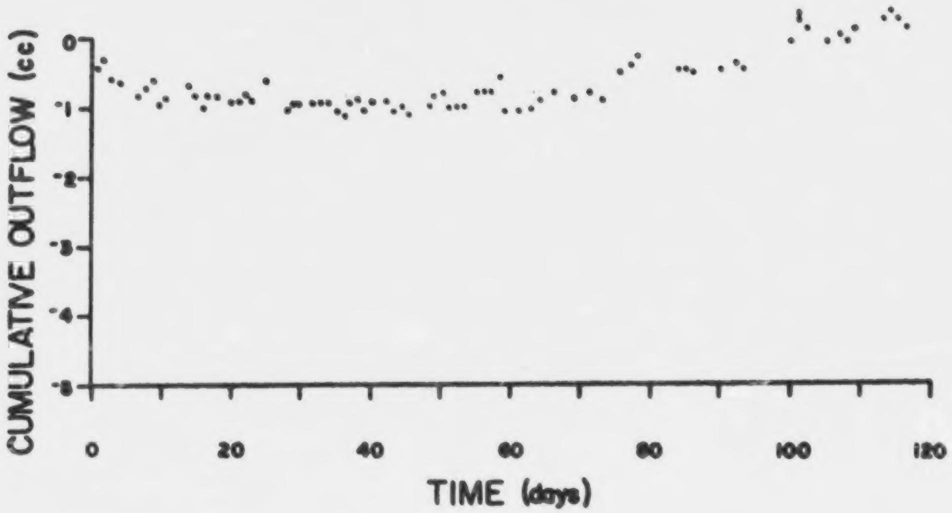

Figure 7.9 Outflow from tube 8. The cement plug in this tube is penetrated by a 7.5 cm (3 inch) mild steel pipe.

BEST COPY AVAILABLE

ejected 1.0 cc during the last 60 days. Tube 8 absorbed 1.0 cc of water in the first 10 days of testing; the flow stopped for approximately 52 days. The tube then ejected a little more than 1 cc over the remaining 60 days. The outflow is either due to water flowing through the cement or through the interface between the cement and the pipe. Tube 5 has a 5 cm (2 inch) diameter mild steel pipe through the plug; the tube 8 plug is penetrated by a 7.5 cm (3 inch) pipe.

The fourth category, Tube 4, has a consistent net outflow. 6 cc of water were absorbed into the plug during the first day. The flow rapidly reversed, and 63 cc flowed out of the plug during the rest of the test. Tube 4 has a 3.8 cm (1 1/2 inch) mild steel pipe through the plug. The flow through the tube occurred through the cement, or, more likely, through a gap between the pipe and plug. If the flow occurred through the cement, Darcy's equation would yield a hydraulic conductivity of 1.3×10^{-9} cm/s.

The flow through the category 3 and 4 plugs may be flow along an interface between the cement and pipe. The interface can be modelled as two parallel plates. The hydraulic conductivity K_j of a channel between two parallel plates is related to the aperture a by (Zeigler, 1976, p. 10):

$$K_j = (\gamma/12\mu)a^2 \qquad (7.2)$$

where γ = unit weight of fluid
μ = fluid viscosity

The steady-state flow rate per head change can be described as (Witherspoon et al., 1980):

$$Q/\Delta h = c(a^3) \qquad (7.3)$$

The constant c takes into account fluid properties and flow geometries. For a rectangular flow path of wdith W_f and length L_f:

$$c = \frac{W_f}{L_f}\frac{\gamma}{12\mu} \qquad (7.4)$$

The cubic law was first determined to be valid for rock fracture apertures above 20 μm by Iwai (1976, p. 3). Witherspoon et al. (1980) reanalyzed Iwai's data and concluded that the cubic law is valid down to 4 μm.

Applying the cubic law to tube 4, a fracture aperture of 28 μm with a hydraulic conductivity of 6.5×10^{-5} cm/sec is calculated. Applying the cubic law to the outflow from tubes 5 and 8 yields aperture hydraulic conductivities of 6.4×10^{-7} cm/s and 5.4×10^{-7} cm/s, respectively, for apertures of 2.6 μm and 2.7 μm. As quoted above, experimental work has not shown that the cubic law is valid for these small apertures.

7.3.4 Conclusion

The primary objective of this test was to determine the effect a penetrating 6.3 mm (1/4 inch) diameter stainless steel pipe would have on the sealing performance of a cement plug. Two plugs with such pipes through them were tested under constant head conditions for approximately four months. The results indicate that the pipes have a negligible effect on the sealing performance of the plugs.

This test also focused attention on the sealing performance of cement plugs with larger diameter pipes through them. A trend was observed of increasing hydraulic conductivity with pipe diameter increases. These results are based on a small sample population. To further investigate the size effects, more tests should be conducted to enable a statistical comparison between pipe size and sealing performance.

7.4 Thermal Contraction Test

Thermal contraction of a pipe through a plug could cause the interface to open. Flow of cold air or water through the pipe could cause enough contraction of the pipe to pull it away from the plug. To investigate this possibility, a scouting test was conducted.

7.4.1 Procedure

The thermal contraction test was conducted by connecting the access tube in tube 1 through silicon tubing to a cold water bath. A pump circulates cold water through the pipe. Readings of temperature, outflow volumes and inflow volumes are made periodically.

7.4.2 Results

The results of the thermal contraction test are plotted in Figure 7.10. The test was conducted for approximately 4 days. The results are the opposite of what was expected: as the pipe and plug cooled, water was taken into the cement plug in the tube, not expelled from it. Air in the bottom sand interval is suspected as a possible cause of the reverse flow. As the water cooled the tube and cement, the air bubble also cooled and contracted. The expansion and contraction of the bubble would match the temperature increases and decreases. Figures 7.3 through 7.9 also suggest the possibility of the presence of air in the collection system. The small variations in the outflow of the tubes correlate with each other. Fluctuations in atmospheric pressure cause the bubble to expand and contract, expelling or absorbing water, thus directly impacting on outflow. No attempt has been made to calculate either water or air volume changes resulting from the temperature changes.

No detectable outflow occured during the first three days of the pipe contraction flow test. As the circulating water returned to room

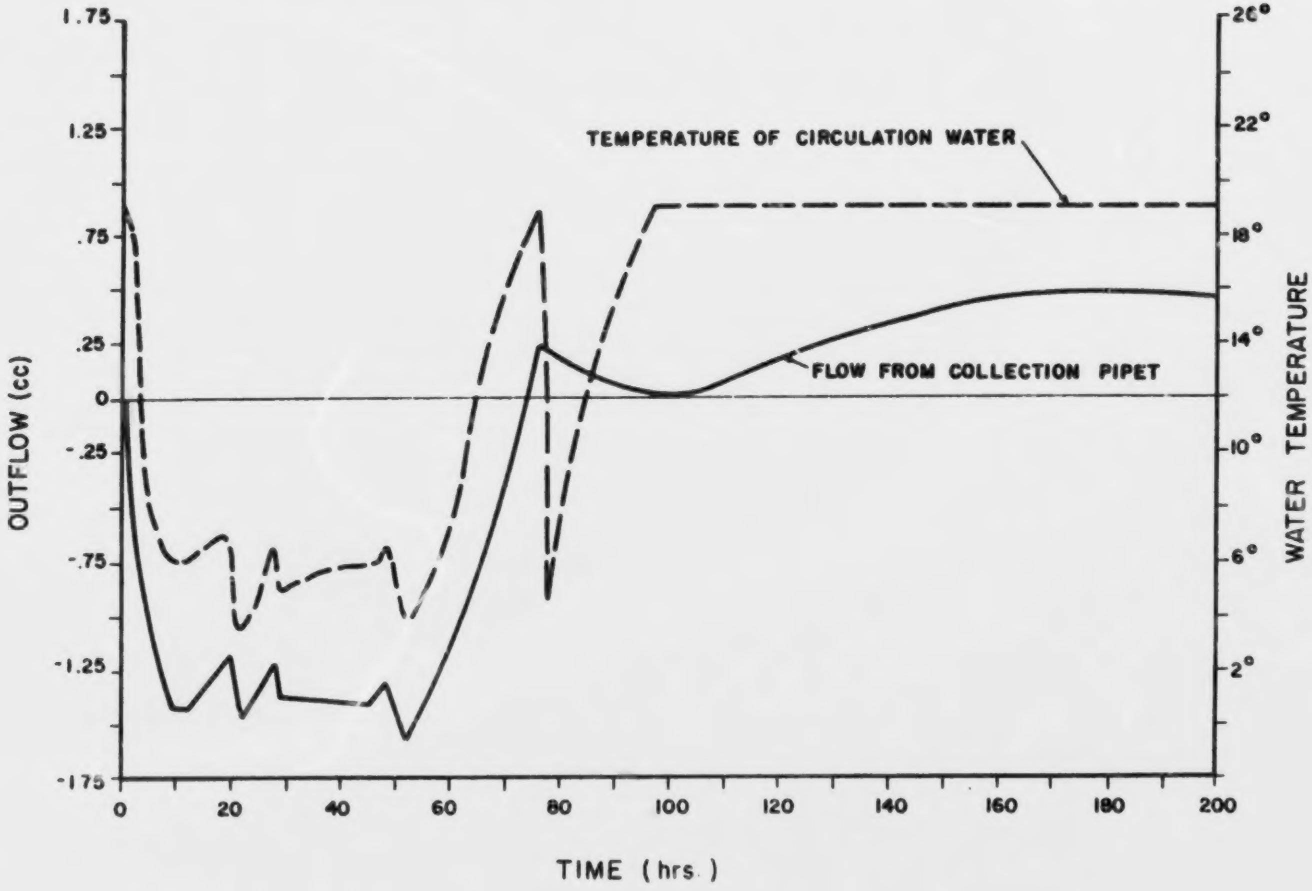

Figure 7.10 Cement plug outflow for pipe thermal contraction test. Water temperature is given in centigrade.

BEST COPY AVAILABLE

temperature, water was expelled from the plug. Up to this time the plug had not exhibited any outflow (Figure 7.4). Ice was again added to the bath, and a flow reversal was observed. The water temperature was allowed to return to room temperature. More water was expelled. The temperature of the water thereafter was kept constant to determine if the outflow would continue. No new outflow has been detected.

7.4.3 Conclusions

The objective of this test was to determine if thermal contraction of the pipe in the plug would open an interface large enough to cause flow. The test results indicated that the cold water that circulated through the tube had a minor effect on the sealing performance of the plug. A net outflow appears to have been induced, but it was small and did not persist.

This single and short term test obviously is not sufficient to warrant drawing broad conclusions. It does suggest that the phenomena occurring during a pipe (liner, casing) cooling event might be more complicated that anticipated. Clearly, further testing should be accompanied by thermal analysis, notably of pipe, cement, water and air (i.e. pore fluid) thermal contractions. In all probability the tests should be run for a considerably longer period, and, preferably, more comprehensive temperature monitoring should be incorporated.

7.5 Piping Test

Borehole plugging obtains much of its technology from oil well cementing practices. With the technology, it also shares some of the problems. The most predominant cause of oil well cementing failure appears to be channeling of gelled mud in the annulus between the casing and borehole wall (Moore, 1974, p. 430; 1986, p. 437). The mud channels form in the cement when the cement is pumped down the drill stem and up through the annulus. Some of the mud is not displaced upwards by the cement. The channels then permit gases or fluids to leak into and through them once the cement hardens.

Channeling of water in borehole and shaft plugs has been a major concern throughout this study. Early lab tests conducted prior to placement of plugs at McNary Dam in Washington first recognized this problem (Daemen et al., 1983, Section 3.4; 1985, Section 2.4). When cement was poured on top of a saturated granular material, i.e. sand, the cement caused some of the pore water to flow up through the plug. The cement hardened with some of the channels remaining open. On a larger scale, a 5 m shaft plug in rock salt had channels or pipes form up to .6 m in diameter. Figure 2.37 of Daemen et al. (1984) is an illustration cited from Sitz (1981, Fig. 2) of the failed shaft plug with the channels mapped along the plug-rock interface.

The objective of this preliminary study is to identify parameters governing the piping phenomenon. Perhaps the most important factor is the head of water required to cause piping in cement. Another important factor is the volume of water that flows through the pipe or channel formed in the cement paste. This investigation has as objective the determination of the lowest head of water at which piping will occur. The volumetric effects of piping will then be assessed at the lowest head.

Other parameters or variables affecting piping are the viscosity, density and height of the cement column. Trying to accurately determine how each of these parameters affects piping would be a project well beyond the bounds of this one. This preliminary scouting investigation has dealt only with the height of cement column poured. The initial viscosity and density of cement were kept constant.

7.5.1 Procedure

The tests are performed in various lengths of 5 cm (2 inch) O.D. clear plastic tubing. PVC bases are glued onto one end of the tubing. 1.3 mm (1/8 inch) O.D. clear nylon tubing, a valve and a 2.5 cm (1 inch) O.D. tube are connected to the base (Figure 7.11).

The test procedure is to mix a batch of cement, Dowell System 1, and pour the cement into the 5 cm (2 inch) diameter tube. The valve between the reservoir and the cement sample is opened. The water level in the reservoir at the start of the test is level with the top of the cement. The water level is slowly raised until channels or pipes of water occur in the cement. The valve is closed and the height of the water in the reservoir is measured and recorded. The following day, a falling head test is performed on the cement sample. The test is continued until it is decided that a) the permeability has remained constant, b) the permeability is very low, or c) the permeability decreases and approaches a constant value.

7.5.2 Results

The objective of determining the lowest head required to induce piping was not obtained in this test. Some technical problems were solved over the course of the experiments. The main conceptual problem, however, was not overcome.

An early problem was cement flow into the injection pipe when the valve was opened between the cement sample and the water reservoir. The cement in the pipe increased the head of water required to cause piping. This problem was alleviated by placing a piece of nylon stocking over the end of the fitting on the base of the cement sample holder.

The main problem with this test procedure was that it did not account for the time dependency of piping. The head of water was increased until piping occurred. Piping was noticed at lower heads when the water level in the reservoir was raised at a slower rate. The time effects of piping were not fully realized during the testing phase of this study, which accounts for the erratic data collected. Thus, the lowest head at which piping occurs was never determined.

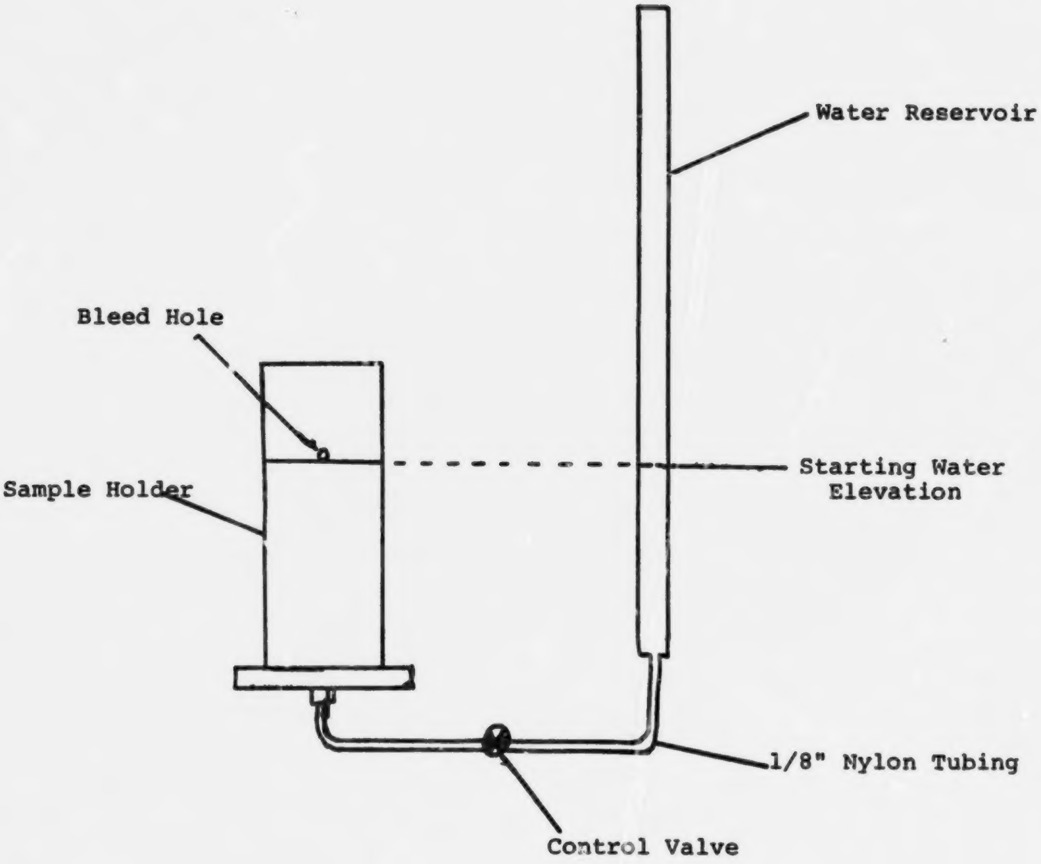
Water Reservoir
Bleed Hole
Sample Holder
Starting Water Elevation
1/8" Nylon Tubing
Control Valve

Figure 7.11 Cement plug piping test apparatus.

BEST COPY AVAILABLE

7.5.3 Recommendations

Minor changes in the test procedure might determine the lowest head required to cause piping. Rather than raising the head of water until piping occurs, the test should be conducted by applying a specific head to the cement sample and recording the time required to cause piping, if it occurs at all. Once the lowest head required for piping is determined, then different volumes of water could be piped through samples at this head. The volume of water piped should be decreased until the permeability of the piped sample approaches that of unpiped cement. Other heads should be used and the procedure repeated.

Other tests could be conducted in the same manner as described above, but with sand or gravel on the bottom of the cement holder. The initial piping test forces a single jet of water through the cement. Sand or gravel on the bottom of the sample might distribute the pressure along the bottom of the sample, thereby increasing the pressure and/or volume of water required to induce and leave permanent channels. This might also be a more realistic piping model.

CHAPTER EIGHT

SUMMARY, CONCLUSIONS, AND RECOMMENDATIONS FOR FURTHER RESEARCH

8.1 Summary

A two-phase program for the study of bentonite and cement borehole seals in granitic rock has been initiated. The first phase involves in-situ emplacement and testing of seals as well as characterization of the hydrogeologic properties of the host rock. Several long-term investigations of the impact of seal testing on the character of the host rock also have been started. The second phase is composed of laboratory tests designed to investigate the engineering characteristics of the bentonite and cement used for sealing. These experiments also examine the suitability of various testing methods for providing a performance assessment of the candidate material.

The following investigations, experiments and analysis are included:

(1) The Cargodera Canyon study area is characterized with a review of geologic investigations and the borehole drilling history. A chemical analysis of the host rock is included.

(2) The methods available for the determination of the hydrogeologic characteristics of low permeability rocks are reviewed and compared with respect to the specific requirements of this study.

(3) Available boreholes are studied using core logs, photologging and videologging. Suitable intervals are selected for testing and sealing.

(4) Pressure slug tests are performed on intervals in four 16.315 cm (6 1/2 inch) diameter boreholes.

(5) A long-term constant injection test is initiated in a 6.315 cm (2.5 inch) diameter borehole.

(6) Two slump block and mortar bunkers are constructed to enclose and secure boreholes chosen for sealing.

(7) Two bentonite seals are emplaced in a 16.315 cm (6 1/2 inch) diameter borehole. Injection/collection apparatus is installed.

(8) Cement seals are emplaced by bailer in two 16.315 cm (6 1/2 inch) diameter holes. Injection/collection instrumentation is installed.

(9) Pressure slug tests are performed on sealed intervals to determine the competence of the seals.

(10) Long-term low pressure constant injection testing of the emplaced bentonite seals is initiated.

(11) Neutron probe measurements are initiated to monitor changes in the degree of saturation of the host rock around the test holes.

(12) Four bentonite plugs are tested in the laboratory to determine hydraulic conductivity using constant pressure injection.

(13) Four bentonite plugs are tested in the laboratory for consolidation performance testing under nitrogen pressure.

(14) Four bentonite plugs are tested in the laboratory to determine swelling and moisture content changes under pressure.

(15) Liquid limits, plastic limits and optimum water content reference testing is conducted on representative samples of the bentonite clay.

(16) Transient pulse testing is performed on small (3.75 cm (1 1/2 inch) diameter) and large (15 cm (6 inch) diameter) plugs to determine hydraulic conductivity and storativity of the clay.

(17) Saturation of the bentonite is estimated using a constant pressure test.

(18) Laboratory prototypes of the plugs emplaced in-situ are constructed and tested to observe and explain behavior of the plugs tested in the field.

(19) Laboratory flow tests are performed on cement plugs penetrated by steel pipes of various diameters.

(20) Thermal contraction tests are performed on steel pipes penetrating cement plugs.

(21) Piping (channeling) experiments are performed on cement plugs.

8.2 Conclusions

The investigations and experiments have been completed or have progressed sufficiently to provide an initial basis for discussing the plug properties and the methods used in determining them. This discussion must be viewed as specific to the results described in this study. All the testing was conducted with the local conditions of the Cargodera Canyon study area as the reference model. Many decisions made during the field testing were a function of the remoteness of the site, access problems and the physical limits imposed by the character of the outcrop chosen for testing. Equipment design and procedures were equally specific to the problems encountered during in-situ work. Laboratory tests have as primary objective clarifying or predicting aspects of in-situ plug performance. No effort was made to design them as a standard for laboratory research in this area. They do suggest, however, that a variety of field conditions can be isolated and effectively simulated in the laboratory.

The site characterization established the geologic suitability of the Cargodera Canyon site for in-situ study of seal performance. The rock is a relatively young and undeformed quartz monzonite. Drill holes have sufficient unfractured and slightly fractured intervals appropriate for testing. The diameters of the boreholes, 6.25 and 16.315 cm (2 1/2 and 6 1/2 inches), are large enough to allow testing and fracture mapping. Year-round access, though difficult and time-consuming, is possible. Building and testing materials can be transported to the site with 4-wheel drive vehicles.

A comparison of available methods for testing the hydraulic conductivity of low permeability rock suggests the pressure slug method described by Cooper et al. (1967), Bredehoeft and Papadopulos (1976), and Hsieh et al. (1981) as most suitable. Three boreholes were tested using this method. Hydraulic conductivities ranged from 10^{-8} to 10^{-10} cm/s, depending on the fracture density in the test interval. These values were within the range suggested by other researchers for this type of rock. Once the equipment was assembled at the site, the testing was not difficult to perform, though the experience of this study was limited to boreholes of shallow depths. The dependence of the testing on the effectiveness of packers and transducers suggests that this equipment should be tested extensively before it is used in the field.

Bentonite plug construction consisted of dropping bentonite tablets through water. This method is used widely for sealing wells, for example specifically for the installation of piezometers. Though it seems to provide an adequate seal, it does not allow much control of the composition of the plug in terms of density and homogeneity. Plug volumes can only be estimated before actual seal emplacement and final volume is a function of how long the plugs are allowed to swell. If the plugs are constrained at either end, e.g. by sand columns or any saturated medium, they will continue to draw water in quantities significant enough to make testing difficult. The tablets used in this study retain their air-filled void spaces even when hydrated and are, therefore, not saturated. These void spaces may provide a flow path that reduces the seal effectiveness if they ever become fully saturated. The test method used at Cargodera Canyon allows the plugs to drain as they are pressurized by injection water. Laboratory results suggest they will consolidate under this pressure even as they swell through adsorption of available water. This makes volume control of the plugs difficult.

The sealed intervals were tested using the pressure slug method. The pressure decay results are analyzed in terms of two-dimensional flow in the test interval. The method of analysis is empirical and approximate. It suggests the hydraulic conductivity of the seals and seal-rock interfaces range from 10^{-8} cm/s to 10^{-9} cm/s. These values are considered to be conservative and represent an upper bound of actual seal performance. The results indicate that the seals perform at a hydraulic conductivity close to that of the host rock. The testing is relatively simple once the apparatus is assembled in the sealed intervals.

The seals were also tested using constant pressure injection. The evidence of this study suggests that this test type requires an extended time, possibly more than a year, before meaningful hydraulic conductivity values can be determined. Laboratory results indicate that the plugs continue to draw water from the adjacent sand intervals for several months. Large quantities of water have been injected or allowed to flow into the test intervals. A small decrease in the flow rate has been observed for all the intervals.

Constant injection testing has been more successful in an adjacent unsealed borehole. This test serves to monitor changes in the hydraulic conductivity of the rock as injection testing continues. The hydraulic conductivities of this test interval have fallen over a period of less than a month from 10^{-9} to 10^{-11} cm/s. Flow rates are so low that it is difficult to measure the actual volume injected over time periods of less than three or four days.

Neutron moisture probe measurements are taken once a week in nearby unsealed boreholes. No appreciable change in the moisture content of the unsaturated rock has been observed. The low porosity of the quartz monzonite suggests that any such change may be difficult to measure even if it does occur.

Hydraulic conductivity determinations of bentonite plugs, especially when tested with constant pressure injection, i.e. over prolonged periods of time, have to consider the complications arising from consolidation and swelling. Laboratory tests have been performed to determine the significance of these processes. When their results are applied to the hydraulic conductivity measurements, the plugs are considered to have allowed no flow at all over the time tested. The low permeabilities suggested for the clays used in this study by other researchers, ranging from 10^{-9} to 10^{-13} cm/s, tend to confirm this observation.

The consolidation testing of four plugs in the laboratory suggests that consolidation can be expected to continue for a long time, long enough to be a factor over the span of the field tests. Laboratory results indicate that the swelling rate is more controlled and limited in time. Testing, however, was performed under pressure injection conditions. A short experiment with two plugs suggests that if the seals are unloaded, they will swell again.

The liquid limits established for the bentonite fall within the range of expected values. The plastic limit and the maximum dry density are unusually low. The optimum moisture content is higher than predicted. Observation of the clay while it was prepared for testing suggests that the tablet structure of the bentonite may significantly affect its engineering properties. This structure imposes certain sample preparation requirements that differ from ASTM standards for soils in general.

Transient pulse testing of bentonite samples to determine reference hydraulic conductivity values was accomplished using a method designed for low permeability rock. The method was successfully applied to most clay samples. The exceptions were samples with water contents approaching the liquid limit. The hydraulic conductivities calculated from test results range from 10^{-9} cm/s to 10^{-10} cm/s. These values recommend the bentonite as a potential seal on the basis of its permeability. Storativity values range from 10^{-7} cm^{-1} to 10^{-8} cm^{-1}. These values are high compared to the rocks for which the testing method was designed. They do, however, fall within the range experimentally determined for clays of this type.

Laboratory plug prototype observations have proved very helpful in understanding the performance of plugs in the field. They show significant void spaces in the hydrated plugs. The voids survive substantial injection volumes and prevent saturation. In addition, visual observations indicate that the plugs and sand columns can separate as the clay consolidates under injection pressure. This provides a free space that eventually fills with water. The plug prototype also provides visual evidence of differences in density and hydration along the plug length. Even when the plugs are constructed in three separate drops, with 7-day swelling intervals between, some tablets retain their tablet structure and never entirely swell.

The plug design at Cargodera Canyon has not been used in earlier borehole plugging studies. The design enabled two plugs to be tested simultaneously. This was accomplished by straddling an injection zone on top and bottom with plugs. Located on each end of the plug system are collection intervals. The injection and collection intervals are saturated sand layers connected to the surface with stainless steel tubes through the plugs.

Tests were conducted in the lab to determine the effect a tube penetrating a plug has on the sealing characteristics of the plug. Other lab tests were conducted to determine when and how water channelling adversely affects the sealing performance of a cement plug.

The plug design enabled three methods of assessing the plug's hydraulic conductivity to be used: constant head, pressure slug and tracer tests. The constant head tests have been the easiest to perform and their results the most reliable. The hydraulic conductivity of the cement plug/rock system has been determined, by constant head testing, to be in the order of 10^{-10} to 10^{-11} cm/sec. Pressure slug tests have been conducted on the cement plug collection and injection intervals, but the results were not used because of air trapped in the intervals. Tracer tests can be performed in only two of the collection zones. Since one port on two of the water circulating tubes has been clogged, no meaningful tracer tests can be performed on their respective plugs. Tracer tests could be run on the other two plugs, but were never performed because there had been no flow through the plugs up to the point of termination of the field experiments.

The low hydraulic conductivity of the cement plugs as evidenced by constant head tests has shown that the sealing requirement can be met by bailer placement procedures in a dry, vertical hole in granite. Other factors outside the scope of this study may negate the previous statement. These factors, such as conditions of the rock mass, inclination of the borehole, ease with which a bailer will work, etc., must be investigated.

The methods used for assessing the sealing performance characteristics of the cement plugs at Cargodera Canyon produced adequate results. The constant head test was the most reliable and the simplest to perform. However, several months of testing are required to obtain an accurate assessment of the plug hydraulic conductivity. Tracer tests would have been beneficial if the tests could have been continued until steady-state flow was obtained. Pressure slug testing is desirable because a test can be run in just a few days.

The presence of stainless steel pipes through laboratory cement plugs did not adversely affect their sealing performance. No outflow was detected from such cement plugs during four months of testing. The thermal contraction test did not open a gap between the pipe and the plug through which water could flow. The results of these tests could be applied to the field testing at Cargodera Canyon with the conclusion that the pipes through the plugs there did not adversely affect the plugs. Penetrating pipes had a temporary negative influence on bentonite plugs.

8.3 Recommendations for Further Research

The emplacement of bentonite seals to be tested in-situ at Cargodera Canyon utilized a tablet dropped through water method commonly used to seal boreholes. Preliminary testing suggests that this emplacement method provides an effective hydraulic seal. The plug that results is difficult to characterize. Laboratory observations suggest that such plugs are significantly non-homogeneous. This makes analysis of test results difficult. It also complicates the issue of long-term seal behavior. An alternative method of seal design would use clay precompacted to a given density and compacted at a carefully chosen water content. Testing of these types of seals might allow a more rigorous analysis of seal performance as a certain plug uniformity could be expected. In addition, critical design parameters, such as water content, degree of saturation, and dry and wet density, could be controlled more closely and tested over a range of values.

The measurement of hydraulic conductivity in low permeability rocks is facilitated by available sophisticated transient and steady-state analysis methods. This is not the case with bentonite seals. Traditional soil mechanics views these clays as essentially impermeable. Methods designed for rock testing have few provisions for a material as porous, compressible and weak as these clays. Nevertheless, their candidate status as potential repository sealants suggests that further research consider the issue of how to test them. The tentative success of transient pulse testing recommends this method as one area of further experimentation, as well as the development of more comprehensive and realistic analysis procedures designed specifically for soft clay, e.g. taking into account water adsorption, draining, swelling and consolidation.

The strength of bentonite clays when used to seal boreholes is of concern. Testing in this area could clarify some of the issues left unresolved in this study. The ability of the clays when compacted to resist penetration would allow hydraulic conductivity testing with high injection pressures. If swelling is allowed to occur, is the strength of the seal-rock interface enhanced? Equally critical is the issue of swelling pressures induced by confined compacted and uncompacted bentonite seals exposed to water. If bentonites are used to seal fractured borehole intervals, it is important to be able to predict whether they will migrate into the fractures, thus sealing fractures, or, conversely, propagating fractures and enlarging fracture apertures. Another strength aspect of these clays that needs to be addressed is their erodability, e.g. resistance to piping.

All the testing done in this study used distilled water. No effort was made to determine intrinsic permeability values for the clay seals. The hydraulic conductivity of the seal may vary significantly with permeant chemistry. This area of testing could utilize existing test designs, procedures and equipment and should involve a range of chemical alternatives. The results could be compared to the values obtained from this study to determine the effect of the composition of the permeant on the behavior of plugs.

The results of the tests performed on bailer placed cement plugs in dry holes in granite indicate that the plugs perform as well as the rock in preventing fluid flow. If the current approach is to be used for other borehole plug assessments, some system design changes are recommended. These will not affect the plug performance, but will improve the techniques for assessing their performance. Improvements include increasing the length of the injection interval and saturating the sand prior to placing the plugs.

To facilitate the use of pressure decay tests for assessing the performance of borehole plugs, the interval length tested during the initial packer testing and that tested when plugs are installed should be the same. Therefore, a shorter packer interval and a longer plug injection interval should be used. A direct comparison between the pre-plug and post-plug decay tests could then be made. The difference between the two tests should be a function of plug performance. A small change can be expected in the decay curves due to the presence of sand in the injection interval. The sand will decrease the volume of water in the interval; the decay of the pressure slug is a function of the volume and compressibility of water.

A problem with the slug tests performed on the cement plugs is the presence of air in the intervals. The procedure for de-airing and saturating the intervals was not effective. To avoid future problems with air in the intervals it is suggested that the plugs be poured on saturated sand. Piping or channelling of water may occur, and their effects need not be investigated, as well as potential remedial measures to preclude such occurrences.

The information obtained regarding the performance of bailer placed cement plugs in an unsaturated (dry at installation) granite is only a small sample of the many field environment possibilities. The boreholes at Cargodera Canyon are a relatively benign environment for plugs. This may in fact be the actual environment for an eventual granite repository. However, there may be areas near a repository that are not so favorable to borehole plugs. The following is a list of recommendations for other borehole tests.

(1) Perform the tests in a saturated granite. The presence of water when plugging with cement has been shown deliterious to plug performance, at least with some installation procedures (e.g. Daemen et al., 1985, Section 2.4).

(2) Test longer plugs. A 17.5 cm (seven inch) plug may not be representative of actual borehole plugs.

(3) Test boreholes that allow access to both ends. A borehole plug that is accessible from the top and the bottom can be tested with greater ease and confidence in the results.

(4) Test boreholes penetrating an aquifer. Placing plugs in this type of environment presents a greater challenge to successful borehole plugging.

(5) Test different permeants on the plugs. The permeant used in this study was distilled water. Water of different pH, Eh, chemical and organic/biological contents simulating ground water conditions likely to exist at a repository site could yield interesting and important results.

(6) Install the plugs in dry boreholes. Leave the plugs for a given length of time and then test them. One of the most important aspects involving borehole plugging with cement is drying shrinkage. Plugs left dry for long periods of time may shrink and pull away from the borehole wall. However, it is unclear how long such drying might take for long plugs, and how far it might propogate along the plug.

(7) Test plugs in horizontal or near-horizontal boreholes. The plug emplacement procedures required would be different than those for vertical boreholes.

(8) Plug a borehole that is in the vicinity of an advancing tunnel or drift. Test the borehole plug prior to, during, and after excavation of the drift. Changes in hydraulic conductivity values will reflect mechanical properties of the plug as the stress and displacement environment changes.

(9) As a general recommendation regarding borehole plugging, a borehole, perhaps, should not be sealed in a single lift. Several lifts may prove to be a better barrier. If conditions exist in the

borehole that give a high probability of plug failure in the short term, several separate plugs may decrease the probability of complete failure of the borehole seal.

(10) Testing of sanded cement plugs, i.e. plugs less susceptible to shrinkage, in dry conditions.

A number of generic issues that deserve attention should be studied in more detail in the laboratory. This includes, in particular, conditions under which piping develops, both for cementitious and for earthen plugs. Of specific interest in this regard would be a systematic investigation of water pressures and flows, cement viscosity (or rehology) and piping.

Of a more specialized interest would be the study of the influence of penetrations (e.g. tubing) through plugs on plug performance. The thermal effect experiments reported on suggest a need for a more detailed and careful investigation, experimental and analytical, of the effects of penetrations on plug performance. Such configurations are highly likely to be encountered, e.g. in cased boreholes and lined shafts.

BLANK PAGE

REFERENCES

Akgun, H., and J.J.K. Daemen, 1986, "Size Influence on the Sealing Performance of Cementitious Borehole Plugs," NUREG/CR-4738. Prepared for Division of Engineering Safety, Office of Nuclear Regulatory Research, U.S. Nuclear Regulatory Commission, by the Department of Mining and Geological Engineering, University of Arizona, Tucson.

American Geological Institute, 1974, Glossary of Geology, M. Gary, R. McAfee, Jr., and C.L. Wolf, editors, Washington, DC.

American Petroleum Institute, 1977, Testing Oil-Well Cements and Cement Additives, Spec-10B, Twentieth Edition, American Petroleum Institute, Dallas, Texas, April.

Andrews, J.W., 1983, "Water Content of Unsaturated, Fractured, Crystalline Rocks from Electrical Resistivity and Neutron Logging," Masters Thesis, Department of Hydrology and Water Resources, University of Arizona, Tucson.

Arnett, R.C., R.G. Baca, J.A. Caggiano, and D.J. Carrell, 1980, "Radionuclide Release Scenario Selection Process for a Possible Basalt Repository," pp. 131-140, Radioactive Release Scenarios for Geologic Repositories, Proceedings of the NEA Workshop, Paris, September 1980. Published by The OECD Nuclear Energy Agency, Paris, 1981.

ASTM D423-66 (Reapproved 1972), "Standard Test Method for Liquid Limit of Soils," American Society for Testing and Materials, Philadelphia.

ASTM D424-59 (Reapproved 1971), "Standard Test Method for Plastic Limit and Plasticity Index of Soils," American Society for Testing and Materials, Philadelphia.

ASTM D698-78, "Standard Test Methods for Moisture-Density Relations of Soils and Soil-Aggregate Mixtures using 5.5-lb (2.49 kg) Rammer and 12-in. (305-mm) Drop," Annual Book of ASTM Standards, Volume 04.08, Soil and Rock; Building Stones. American Society for Testing and Materials, Philadelphia.

Atomic Energy of Canada Limited, 1978, Management of Radioactive Fuel Wastes: the Canadian Disposal Program, AECL-6314, J. Boulton (ed.), Atomic Energy of Canada Research Company, Whiteshell Nuclear Research Establishment, Pinawa, Manitoba, Canada, Oct.

Banks, N.G., 1980, "Geology of a Zone of Metamorphic Core Complexes in Southeastern Arizona," Geological Society of America Memoir 153, Cordilleran Metamorphic Core Complexes, pp. 177-217.

Barbreau, A., R. Heremans, and B. Skytte Jensen, 1980, "Radionuclide Migration in Geological Formations," pp. 515-530, Radioactive Waste Management and Disposal, Proceedings of the First European Community Conference, Luxemburg, May 20-23. R. Simon and S. Orlowski, Editors. Harwood Academic Publishers.

Bear, J., 1979, Hydraulics of Groundwater, McGraw-Hill, Inc., New York.

Bennett, R.D. and R.F. Anderson, 1982, "New Pressure Test for Determining Coefficient of Permeability of Rock Masses," Technical Report GL-82-3, U.S. Army Engineer Waterways Experiment Station, Vicksburg, Mississippi.

Black, D.K. and K.L. Lee, 1973, "Saturating Laboratory Samples by Back Pressure," Journal of The Soil Mechanics and Foundations Division, Proceedings of the American Society of Civil Engineers, Vol. 99, No. SM1, pp. 75-93.

Bouwer, H., 1978, Groundwater Hydrology, McGraw-Hill, Inc., 480 pp.

Bouwer, H. and R.C. Rice, 1976, "A Slug Test for Determining Hydraulic Conductivity of Unconfined Aquifers with Completely or Partially Penetrating Wells," Water Resources Research, Vol. 12, No. 3, pp. 423-428.

Brace, W.F., J.B. Walsh, and W.T. Frangos, 1968, "Permeability of Granite Under High Pressure," Journal of Geophysical Research, 73, pp. 2225-2236.

Brand, E.W., 1975, "Back Pressure Effects on the Undrained Strength Characteristics of Soft Clay, Soils and Foundations," Japanese Society of Soil Mechanics and Foundation Engineering, Vol. 15, no. 2, pp. 1-16, 1975.

Bredehoeft, J.D., A.F. England, D.B. Stewart, N.J. Trask, and I.J. Winograd, 1978, "Geologic Disposal of High-Level Radioactive Wastes - Earth-Science Perspectives," Geological Survey Circular 779, 15 + v pp., U.S. Geological Survey.

Bredehoeft, J.D. and S.S. Papadopulos, 1980, "A Method for Determining the Hydraulic Properties of Tight Formations," Water Resources Research, Vol. 16, no. 1, pp. 233-238.

Burkholder, H.C., 1980, "The Development of Release Scenarios for Geologic Nuclear Waste Repositories," pp. 13-26, Radionuclide Release Scenarios for Geologic Repositories, Proceedings of the NEA Workshop, Paris, Sept. 1980. Published by The OECD Nuclear Energy Agency, Paris, 1981.

Carslaw, H.S. and J.C. Jaeger, 1959, Conduction of Heat in Solids, Oxford University Press, London.

Casagrande, A., 1936, "The Determination of the Pre-Consolidation Load and its Practical Significance," discussion D-34, Proceedings of the First International Conference on Soil Mechanics and Foundation Engineering, Cambridge, Mass., Vol. III, pp. 60-64.

Committee on Radioactive Waste Management, 1978, "Geologic Criteria for Repositories for High-Level Radioactive Wastes," 19 + vii pp., National Academy of Sciences, Washington, DC, August 3.

Cooper, H.H., Jr., J.D. Bredehoeft, and I.S. Papadopulos, 1967, "Response of a Finite-Diameter Well to an Instantaneous Charge of Water," Water Resources Research, Vol. 3, no. 1, pp. 263-269.

Daemen, J.J.K., D.L. South, W.B. Greer, N.I. Colburn, S.L. Cobb, B. Kousari, S.P. Mathis, R.G. Jeffrey, and C.A. Wakely, 1982, "Annual Report, Rock Mass Sealing, June 1, 1981 - May 31, 1982," prepared for U.S. Nuclear Regulatory Commission, SAFER Division, by the Department of Mining and Geological Engineering, University of Arizona, Tucson.

Daemen, J.J.K., D.L. South, W.B. Greer, J.C. Stormont, S.A. Dischler, G.S. Adisoma, K. Fuenkajorn, D.E. Miles, B. Kousari, and J. Bertuca, 1983, "Annual Report, Rock Mass Sealing, June 1, 1982 - May 31, 1983," NUREG/CR-3473, prepared for the U.S. Nuclear Regulatory Commission, Division of Health, Siting and Waste Management, by the Department of Mining and Geological Engineering, University of Arizona, Tucson.

Daemen, J.J.K., W.B. Greer, G.S. Adisoma, K. Fuenkajorn, W.D. Sawyer, Jr., A. Yazdandoost, H. Akgun, and B. Kousari, 1985, "Annual Report, Rock Mass Sealing, June 1, 1983 - May 31, 1984," NUREG/CR-4174, prepared for the U.S. Nuclear Regulatory Commission, Office of Nuclear Regulatory Research, Division of Radiation Programs and Earth Sciences, by the Department of Mining and Geological Engineering, University of Arizona, Tucson.

Daemen, J.J.K., W.B. Greer, K. Fuenkajorn, A. Yazdandoost, H. Akgun, A. Schaffer, A.F. Kimbrell, T.S. Avery, J.R. Williams, B. Kousari, and R.O. Roko, 1986, "Annual Report, Rock Mass Sealing, June 1, 1984 - May 31, 1985," NUREG/CR-4642, prepared for the U.S. Nuclear Regulatory Commission, Office of Nuclear Regulatory Research, Division of Health, Siting and Waste Management, by the Department of Mining and Geological Engineering, University of Arizona, Tucson.

D'Appolonia Consulting Engineers, 1980a, "Repository Sealing Evaluations of Materials Research Objectives and Requirements," Technical Report ONWI-108, Office of Nuclear Waste Isolation, Battelle Memorial Institute, Columbus, Ohio.

D'Appolonia Consulting Engineers, 1980b, "Repository Sealing Design Approach - 1979," Technical Report ONWI-55, Office of Nuclear Waste Isolation, Battelle Memorial Institute, Columbus, Ohio 43201.

Davis, G.H., 1980, "Structural Characteristics of Metamorphic Core Complexes, Southern Arizona," Geological Society of America Memoir 153, Cordilleran Metamorphic Core Complexes, pp. 35-77.

Deju, R.A., 1983, Testimony by Dr. Raul A. Deju, Basalt Waste Isolation Project, before the Subcommittee on Energy Research and Production, Committee on Science and Technology, United States House of Representatives, Washington, DC, March 2, 9:30 am. RHO-BW-SA-293 P, Rockwell Hanford Operations, Hanford, Washington.

Department of Energy, 1982, "NWTS Program Criteria for Mined Geologic Disposal of Nuclear Waste Repository Performance and Development Criteria," DOE/NWTS-33(3), Office of NWTS Integration, Battelle Memorial Institute, Columbus, Ohio, July Public Draft.

Department of Energy, 1984, "Yucca Mountain Site, Nevada Research and Development Area, Nevada, Draft Environmental Assessment," DOE/ew-0012.

DOE/NWTS-30, 1982, "Proceedings of the 1982 National Waste Terminal Storage Program Information Meeting," prepared by the Office of NWTS Integration, Battelle Project Management Division, Columbus, Ohio 43201.

Earlougher, R.C., Jr., 1977, "Advances in Well Test Analysis," American Institute of Mining, Metallurgical and Petroleum Engineers, Inc.

Ehlers, E.G. and H. Blatt, 1980, Petrology - Igneous, Sedimentary, and Metamorphic, W.H. Freeman and Company, San Francisco.

Engineering News Record, 1985, "Nuclear Waste Burial at Sea Feasible, Economical," October 10, Vol. 215, pp. 17-18.

Evans, D.D., 1983, "Unsaturated Flow and Transport Through Fractured Rock-Related to High-Level Waste Repositories," NUREG/CR-3206, prepared by the Department of Hydrology and Water Resources, University of Arizona, Tucson.

Fagerstrom, H. and B.L. Lundahl, 1977, Handling of Buffer Material Quartz - Bentonite, KBS Teknisk Rapport 37, Karnbranslesakerhet, Stockholm.

Fernandez, J.A. and M.D. Freshley, 1984, "Repository Sealing Concepts for the Nevada Nuclear Waste Storage Investigations Project," Sandia Report SAND 83-1778. Prepared by Sandia National Laboratories, Albuquerque, New Mexico, for the U.S. Department of Energy under contract DE-AC04-76P00789.

Ferris, J.G. and D.B. Knowles, 1954, "The Slug Test for Estimating Transmissibility," U.S. Geological Survey Ground Water Note 26, pp. 1-7.

Ferris, J.G. and D.B. Knowles, 1963, "The Slug-Injection Test for Estimating the Coefficient of Transmissibility of an Aquifer," pp. 299-304, Geological Survey Water Supply Paper 1536-I, Methods of Determining Permeability, Transmissibility and Drawdown, compiled by R. Bentall, U.S. Government Printing Office, Washington, DC.

Ferris, J.G., D.B. Knowles, R.H. Brown, and R.W. Stallman, 1962, "Theory of Aquifer Tests," Geological Survey Water-Supply Paper 1536-E. U.S. Government Printing Office, Washington.

Forster, C.B. and J.E. Gale, 1980, "A Laboratory Assessment of the Use of Borehole Pressure Transients to Measure the Permeability of Fractured Rock Masses," Lawrence Berkeley Laboratory, report LBL-8674 (SAC-28, UC-70).

Freeze, R.A. and J.A. Cherry, 1979, Groundwater, Prentice-Hall, Inc., Englewood Cliffs, New Jersey, 604 pp.

Gibson, R.E., G.L. England and M.J.L. Husey, 1967, "The Theory of One-Dimensional Consolidation of Saturated Clays. I. Finite Non-Linear Consolidation of Thin Homogeneous Layers," Geotechnique, Vol. 17, pp. 261-273.

Grim, Ralph E. 1968, Clay Mineralogy, Second Edition, McGraw-Hill Book Company, New York, 596 pp.

Gulick, C.W., J.A. Boa, and A.D. Buck, 1980, "Bell Canyon Test (BCT) Cement Grout," Development Report, Sandia National Laboratories, Albuquerque, New Mexico.

Heineman, R.E., W.A. Carbiener, and S.J. Basham, 1978, "The Technical Program for Establishing the Scientific Basis for Geologic Disposal," DOE Environmental Control Symposium, Washington, DC, Nov. 28-30.

Hilf, J., 1975, "Compacted Fill," Ch. 7, pp. 244-311, Foundation Engineering Handbook, H.F. Winterkorn and H-Y Fang, Editors, Van Nostrand Reinhold Company, New York.

Hillel, D., 1971, Soil and Water - Physical Principles and Processes, Academic Press, New York.

Hodges, F.N., J.H. Westsik, Jr., and L.A. Bray, 1982, "Development of a Backfill for Containment of High-Level Nuclear Waste," in Scientific Basis for Nuclear Waste Management V, Proceedings of the Materials Research Society Fifth International Symposium on the Scientific Basis for Nuclear Waste Management, June 7-10, 1982, Berlin, Germany, W. Lutze, editor, Vol. 11, pp. 641-648, North-Holland, New York.

Holtz, R.D. and W.D. Kovacs, 1981, An Introduction to Geotechnical Engineering, Prentice-Hall, Inc., Englewood Cliffs, New Jersey, 732 pp.

Holtz, W.G. and H.J. Gibbs, 1956, "Engineering Properties of Expansive Clays," Transactions, Paper No. 2814, ASCE, Vol. 121, pp. 641-677.

Hsieh, P.A., J.V. Tracy, C.E. Neuzil, J.D. Bredehoeft, and S.E. Silliman, 1981, "A Transient Laboratory Method for Determining the Hydraulic Properties of 'Tight' Rocks - I. Theory," International Journal of Rock Mechanics, Mineral Science and Geomechanical Abstracts, Vol. 18, pp. 245-252.

Hsieh, P.A., 1983, "Theoretical and Field Studies of Fluid Flow in Fractured Rocks," Ph.D. Dissertation, Department of Hydrology and Water Resources, University of Arizona, Tucson.

Hvorslev, M.J., 1951, "Time Lag and Soil Permeability in Groundwater Observations," Bulletin No. 36, U.S. Army Engineer Waterways Experiment Station, Vicksburg, Mississippi.

Intera Environmental Consultants, Inc., 1981, "Consequence Assessment of Hydrological Communications Through Borehole Plugs," Contractor Report SAND 81-7164, Prepared for Sandia National Laboratories, Albuquerque, NM, November.

IRG, 1978, "Isolation of Radioactive Wastes in Geologic Repositories: Status of Scientific and Technical Knowledge," a working paper for the Interagency Review Group on Nuclear Waste Management, prepared by Subgroup for Alternative Technology Strategies.

Irish, E.R., 1980, "Safety Assessment for the Underground Disposal of Radioactive Wastes - The IAEA Programme," pp. 39-43, Radionuclide Release Scenarios for Geologic Repositories, Proceedings of the NEA Workshop, Paris, September 1980. Published by The OECD Nuclear Energy Agency, Paris, 1981.

Iwai, K., 1976, "Fundamental Studies on Fluid Flow Through a Single Fracture," Ph.D. Thesis, University of California, Berkeley, 208 pp.

Jacob, C.E. and S.W. Lohman, 1952, "Nonsteady flow to a Well of Constant Drawdown in an Extensive Aquifer," Transactions, American Geophysical Union, Vol. 33, No. 4, pp. 559-569.

Kalia, H.N., 1986, "ERG and GRG Review of the Draft of 'Preliminary Test Plan for In Situ Testing From an Exploratory Shaft in Salt - October 1983,'" BMI/ONWI-591, Technical Report, Office of Nuclear Waste Isolation, Battelle Memorial Institute, Columbus, Ohio, March.

Kantey, C.A. and A.B.A. Brink, 1962, "Laboratory Criteria for the Recognition of Expansive Soils," National Building Research Institute, South African Council for Scientific and Industrial Research, Bulletin No. 9.

Kassiff, G., M. Livneh, and G. Wiseman, 1969, Pavements on Expansive Clays, Jerusalem Academic Press, Jerusalem.

Keith, S.B., S.J. Reynolds, P.E. Damon, M. Shafiqullah, D.E. Livingston, and P.D. Pushkar, 1980, "Evidence for Multiple Intrusion and Deformation within the Santa Catalina-Rincon-Tortolita Crystalline Complex, Southeastern Arizona," Geological Society of America Memoir 153, Cordilleran Metamorphic Core Complexes, pp. 217-267.

Klingsberg, C. and J. Duguid, 1980, "Status of Technology for Isolating High-Level Radioactive Wastes in Geologic Repositories," DOE/TIC 11207 (Draft), U.S. Department of Energy, Office of Waste Isolation, Washington, DC, October.

Knutsson, S., 1977, Thermal Conductivity Tests on Buffer Material of Compacted Bentonite, KBS Teknisk Rapport 72, Karnbranslesakerhet, Stockholm.

Kocher, D.C., A.L. Sjoreen, and C.S. Bard, 1983, "Uncertainties in Geologic Disposal of High-level Wastes - Groundwater Transport of Radionuclides and Radiological Consequences," NUREG/CR-2506; ONRL-5838; 214 + xiv pp., prepared for the U.S. Nuclear Regulatory Commission by Oak Ridge National Laboratory, Oak Ridge, Tennessee, July.

Kruseman, G.P. and N.A. De Ridder, 1970, "Analysis and Evaluation of Pumping Test Data," Bulletin No. 11, International Institute for Land Reclamation and Improvement, Wageningen, The Netherlands.

Ladd, C.C. and Lambe, T.W., 1963, "The Strength of Undisturbed Clay Determined from Undrained Tests," Laboratory Shear Testing of Soils, ASTM Special Technical Publication No. 361, pp. 342-371. American Society for Testing and Materials, Philadelphia.

Lambe, T.W., 1951, Soil Testing for Engineers, John Wiley and Sons.

Lambe, T.W. and R.V. Whitman, 1979, Soil Mechanics, SI Version, John Wiley and Sons, Inc., New York, 553 pp.

Lin, W., 1977, "Compressible Fluid Flow Through Rocks of Variable Permeability," Lawrence Livermore Laboratory, Livermore, California, Report UCRL-52304, 1977

Liu, C. and J.B. Evett, 1981, Soils and Foundations, Prentice-Hall, Inc., New Jersey.

Lowe, J. and T.C. Johnson, 1960, "Use of Back Pressure to Increase Degrees of Saturation of Triaxial Test Specimens," Research Conference on Shear Strength of Cohesive Soils, Soil Mechanics and Foundations Division of American Society of Civil Engineers , pp. 819-836.

Malinowski, R., 1982, "Ancient Mortars and Concretes: Aspects of Their Durability," History of Technology, Seventh Annual Volume, A. Rupert Hall and Norman Smith, eds., Mansell Publishing Limited, London, 1982.

McHenry, J.R., "Theory and Application of Neutron Scattering in the Measurement of Soil Moisture," Soil Science, 95, 294-307, 1963.

Meyer, D. and J.J. Howard, eds., 1983, "Evaluation of Clays and Clay Minerals for Application to Repository Sealing," ONWI-486, prepared by D'Appolonia Consulting Engineers, Inc., and Material Research Laboratory, The Pennsylvania State University, for Office of Nuclear Waste Isolation, Battelle Memorial Institute, Columbus, Ohio.

Mindess, S. and J.F. Young, 1981, Concrete, Prentice Hall, Englewood Cliffs.

Mitchell, James K., 1976, Fundamentals of Soil Behavior, John Wiley and Sons, Inc., New York, 422 pp.

Moore, P.L., 1974, Drilling Practices Manual, The Petroleum Publishing Company, Tulsa, Oklahoma.

Moore, P.L., 1986, Drilling Practices Manual, Second Edition, PennWell Publishing Co., Tulsa, OK.

National Research Council, 1983, "A Study of the Isolation System for Geologic Disposal of Radioactive Wastes," Waste Isolation Systems Panel, Board on Radioactive Waste Management, Commission on Physical Sciences, Mathematics, and Resources, National Academy Press, Washington, DC.

National Research Council Commission on Natural Resources, 1979, "Geologic Criteria for Repositories for High-Level Radioactive Wastes," National Academy of Sciences, Washington, D.C.

Nelson, P. and W.E. Glenn, 1975, "Influence of Bound Water on the Neutron Log in Mineralized Igneous Rocks," Paper M, Transactions of the SPWLA Sixteenth Annual Logging Symposium, New Orleans, Louisiana, Society of Professional Well Log Analysts, Inc., Houston, Texas.

Nelson, P.B. Paulsson, R. Rachiele, L. Anderson, T. Schrauf, W. Hustrulid, O. Duran, and K.A. Magnusson, 1979, "Preliminary Report on Geophysical and Mechanical Borehole Measurements at Stripa," Technical Information Report No. 16, Swedish-American Cooperative Program on Radioactive Waste Storage, Lawrence Berkeley Laboratory, LBL-8280, 1979.

Neretnieks, I., 1979, "Transport Mechanism and Rates of Transport of Radionuclides in the Geosphere as Related to the Swedish KBS Concept," IAEA-SM-234/108, presented at OECD International Symposium, Helsinki.

Neuzil, C.E., C. Cooley, S.E. Silliman, J.D. Bredehoeft, and P.A. Hsieh, 1981, "A Transient Laboratory Method for Determining the Hydraulic Properties of 'Tight' Rocks - II. Applications," Internationl Journal of Rock Mechanics, Mineral Science and Geomechanical Abstracts, Vol. 18, pp. 253-258.

Neville, A.M., 1981, Properties of Concrete, Pitman Publishing, London.

Nuclear Regulatory Commission, 1982, "Disposal of High-Level Radioactive Wastes in Geologic Repositories: Technical Criteria," 10 CFR Part 60, Final Rule, U.S. Nuclear Regulatory Commission, Washington, D.C.

Oakes, D.T., 1960, "Solids Concentration Effects in Bentonite Drilling Fluids," Clays and Clay Minerals, Vol. 8, pp. 252-273.

OECD, 1980, Borehole and Shaft Plugging, Proceedings of the Workshop on, organized by the OECD Nuclear Energy Agency and the U.S. Department of Energy, Columbus, Ohio, Published by The OECD Nuclear Energy Agency, Paris.

OECD, 1984, Geological Disposal of Radioactive Waste, An overview of the current status of understanding and development. An Experts' Report sponsored by the Commission of the European Communities and The OECD Nuclear Energy Agency. Published by Organization for Economic Co-Operation and Development, Paris, February.

Papadopulos, S.S., J.D. Bredehoeft, and H.H. Cooper, Jr., 1973, "On the Analysis of 'Slug Test' Data," Water Resources Research, Vol. 9, no. 4, pp. 1087-1089.

Pedersen, A. and K.E. Lindstrom-Jensen, 1980, "Selection of Release Scenarios for a Danish Waste Repository in a Salt Dome, pp. 181-196, Radioactive Release Scenarios for Geologic Repositories, Proceedings of the NEA Workshop, Paris, September 1980. Published by The OECD Nuclear Energy Agency, Paris, 1981.

Popovics, S., 1979, Concrete Making Materials, Hemisphere Publishing, Washington, D.C..

Pusch, R., 1979, "Water Uptake and Swelling of Montmorillonite Clay Seams in Rock," pp. 273-8, Vol. 1, Proceedings, Fourth International Congress on Rock Mechanics, Montreux, Switzerland. Published by A.A. Balkema, Rotterdam.

Pusch, R., 1983, "Borehole Sealing for Underground Waste Storage," Journal of Geotechnical Engineering, Vol. 109, no. 1, pp. 113-119, ASCE, January.

Pusch, R. and A. Bergstrom, 1980, "Highly Compacted Bentonite for Borehole and Shaft Plugging," pp. 161-167, Proceedings, OECD/ONWI Workshop on Borehole and Shaft Plugging, Columbus, Ohio. Published by OECD, Paris.

Pusch, R. and T. Carlsson, 1985, "The Physical State of Pore Water of Na Smectite used as Barrier Component," Engineering Geology, Vol. 21, No. 3/4, pp. 257-265, June.

Pusch. R., T. Eriksen, and A. Jacobsson, 1982, "Ion/Water Migration Phenomena in Dense Bentonites," pp. 649-658, Scientific Basis for Nuclear Waste Management V, W. Lutze, editor, Proceedings of the Symposium, June 7-10, 1982, Berlin, Germany. Elsevier Science Publishing Co., Inc., New York.

Pusch, R., A. Jacobson, and A. Bergstrom, 1979, "Bentonite-Based Buffer Substances for Isolating Radioactive Waste Products at Great Depth in Rock, and Discussion," in Underground Disposal of Radioactive Wastes, Vol. I, Proceedings of a Symposium held at Otaniemi, Finland, July 2-6, published by the International Atomic Energy Agency, Vienna, Austria, 1980, pp. 487-502.

Rehrig, W.A. and S.J. Reynolds, 1980, "Geologic and Geochronologic Reconnaissance of a Northwest-Trending Zone of Metamorphic Core Complexes in Southern and Western Arizona," Geological Society of America Memoir 153, Cordilleran Metamorphic Core Complexes, pp. 131-157.

Roy, D.M., M.W. Grutzeck, P.H. Licastro, 1979, "Evaluation of Cement Borehole Plug Longevity," ONWI-30, Office of Nuclear Waste Isolation, Battelle Memorial Institute, Columbus, Ohio.

Sarkar, A.K., M.W. Barnes, and D.M. Roy, 1982, "Longevity of Borehole and Shaft Sealing Materials: Thermodynamic Properties of Cements and Related Phases Applied to Repository Sealing, ONWI-201, Office of Nuclear Waste Isolation, Battelle Memorial Institute, Columbus, Ohio.

Sawyer, W.D. and J.J.K. Daemen, 1987, "The Sealing Performance and Permeability of Bentonite Borehole Plugs," Topical Report to the U.S. Nuclear Regulatory Commission, Division of Health, Siting and Waste Management, for Contract NRC-04-78-271, by the Department of Mining and Geological Engineering, University of Arizona. (In preparation)

Seitz, R.R., B. Sager, and J.D. Davis, 1987, "Numerical Modeling of Radionuclide Transport Through Repository Seals," Waste Management '87, Tucson, Arizona, March 1-5, 1987.

Singh, S.K., 1982, "Chemical, Physical, and Engineering Characterization of Candidate Backfill Clays and Clay Admixtures for a Nuclear Waste Repository - Part I," in Scientific Basis for Nuclear Waste Management V, Materials Research Society Symposia Proceedings, Vol. 6, pp. 413-433.

Sitz, P. 1981, "Querschnittsabdichtungen untertaegiger Hohlraeume durch Daemme und Pfropfen" (Sealing the cross-section of underground excavations with dams or plugs), Freiberger Forschungshefte A643, 151 pp., VEB Deutscher Verlag fur Grundstoffindustrie, Leipzig.

Skibitzke, H.E., 1963, "Determination of the Coefficient of Transmissibility from Measurements of Residual Drawdown in a Bailed Well," pp. 293-298, Geological Survey Water-Supply Paper 1536-I, Methods of Determining Permeability, Transmissibility and Drawdown, R. Bentall, Compiler. U.S. Government Printing Office, Washington, D.C.

South, D.L. and J.J.K. Daemen, 1986, "Permeameter Studies of Water Flow Through Cement and Clay Borehole Seals in Granite, Basalt and Tuff," NUREG/CR-4748, Technical Report prepared for the U.S. Nuclear Regulatory Commission, Division of Engineering Safety, Office of Nuclear Regulatory Research, by the Department of Mining and Geological Engineering, University of Arizona, Tucson.

Stormont, J.C., 1984, "Plugging and Sealing Program for the Waste Isolation Pilot Plant," SAND 84-1057, Sandia National Laboratories, Albuquerque, New Mexico, November.

Taylor, D.W., 1948, Fundamentals of Soil Mechanics, John Wiley and Sons, New York.

Terzaghi, K., 1943, Theoretical Soil Mechanics, John Wiley and Sons, Inc., New York.

Tittman, J., 1956, "Radiation Logging," in Fundamentals of Logging, University of Kansas Petroleum Engineering Conference. pp. 115-136: Physical Principles; pp. 137-154: Applications.

Todd, D.K., 1980, Groundwater Hydrology, Second Edition, John Wiley and Sons, New York.

U.S. Department of Energy, 1979, "Management of Commercially Generated Radioactive Waste," DOE/EIS-0046-D, Vol. 1 of 2, Draft Environmental Impact Statement, Washington, DC, April.

U.S. Department of Energy, 1982, "NWTS Program Criteria for Mined Geologic Disposal of Nuclear Waste: Repository Performance and Development Criteria," DOE/NWTS-33(3), Office of NWTS Integration, Battelle Memorial Institute, Columbus, Ohio, July, Public Draft.

U.S. Department of Energy, 1983, "Summary of the Results of the Evaluation of the WIPP Site and Preliminary Design Validation Program," WIPP-DOE-161, Waste Isolation Pilot Plant, Albuquerque, New Mexico, March.

U.S. Environmental Protection Agency, 1986, "Environmental Standards and Federal Radiation Protection Guidance for Management and Disposal of Spent Nuclear Fuel, High-Level and Transuranic Radioactive Wastes," 40 CFR 191, Federal Register, Final Rule.

U.S. Nuclear Regulatory Commission, 1983, "Disposal of High-Level Radioactive Wastes in Geologic Repositories," Final Rule 10 CRF 60, Federal Register, Vol. 48, No. 120, June 30.

U.S. Nuclear Regulatory Commission, 1985, "Disposal of High-Level Radioactive Wastes in Geologic Repositories," Final Rule, Unsaturated Zone Amendment, Federal Register, Vol. 50, No. 140, pp. 29641-8, Monday, July 22.

Van Olphen, H., 1977, Clay and Colloid Chemistry, John Wiley and Sons, New York, 318 pp.

Westsik, J.H., Jr., L.A. Bray, F.N. Hodges, and E.J. Wheelwright, 1982, "Permeability, Swelling and Radionuclide Retardation Properties of Candidate Backfill Materials," Scientific Basis for Nuclear Waste Management, Materials Research Society Annual Meeting, November 1981, Boston, Mass., Symposia Proceedings, Vol. 6, S.V. Topp, editor, pp. 329-336. North-Holland, New York.

Whitherspoon, P.A., S.S.Y. Wang, K. Iwai, and J.E. Gale, 1980, "Validity of the Cubic Law for Fluid FLow in a Deformable Rock Fracture," Water Resources Research, Vol. 16, no. 6, December, pp. 1016-1024.

Wilson, S.D., 1970, "Suggested Method of Test for Moisture-Density Relations of Soils Using Harvard Compaction Apparatus," Special Procedures for Testing Soil and Rock for Engineering Purposes, 5th Ed., ASTM Special Technical Publication 479, pp. 101-103. American Society for Testing and Materials, Philadelphia, PA.

Winterkorn, H.F. and H.Y. Fang, 1975, "Soil Technology and Engineering Properties of Soils," Ch. 2, pp. 67-120 of Foundation Engineering Handbook, H.F. Winterkorn and H.Y. Fang, editors, Van Nostrand Reinhold Company, Inc., New York, NY, 751 pp.

Zeigler, T.W., 1976, "Determination of Rock Mass Permeability," Technical Report S-76-2, U.S. Army Engineer Waterways Experiment Station, Vicksburg, Mississippi.

Znidarcic, Dobroslav, 1982, "Laboratory Determination of Consolidation Properties of Cohesive Soil," Ph.D. Dissertation, University of Colorado, Boulder, 172 pp.

APPENDIX A

PRESSURE TRANSDUCER CALIBRATION CURVES

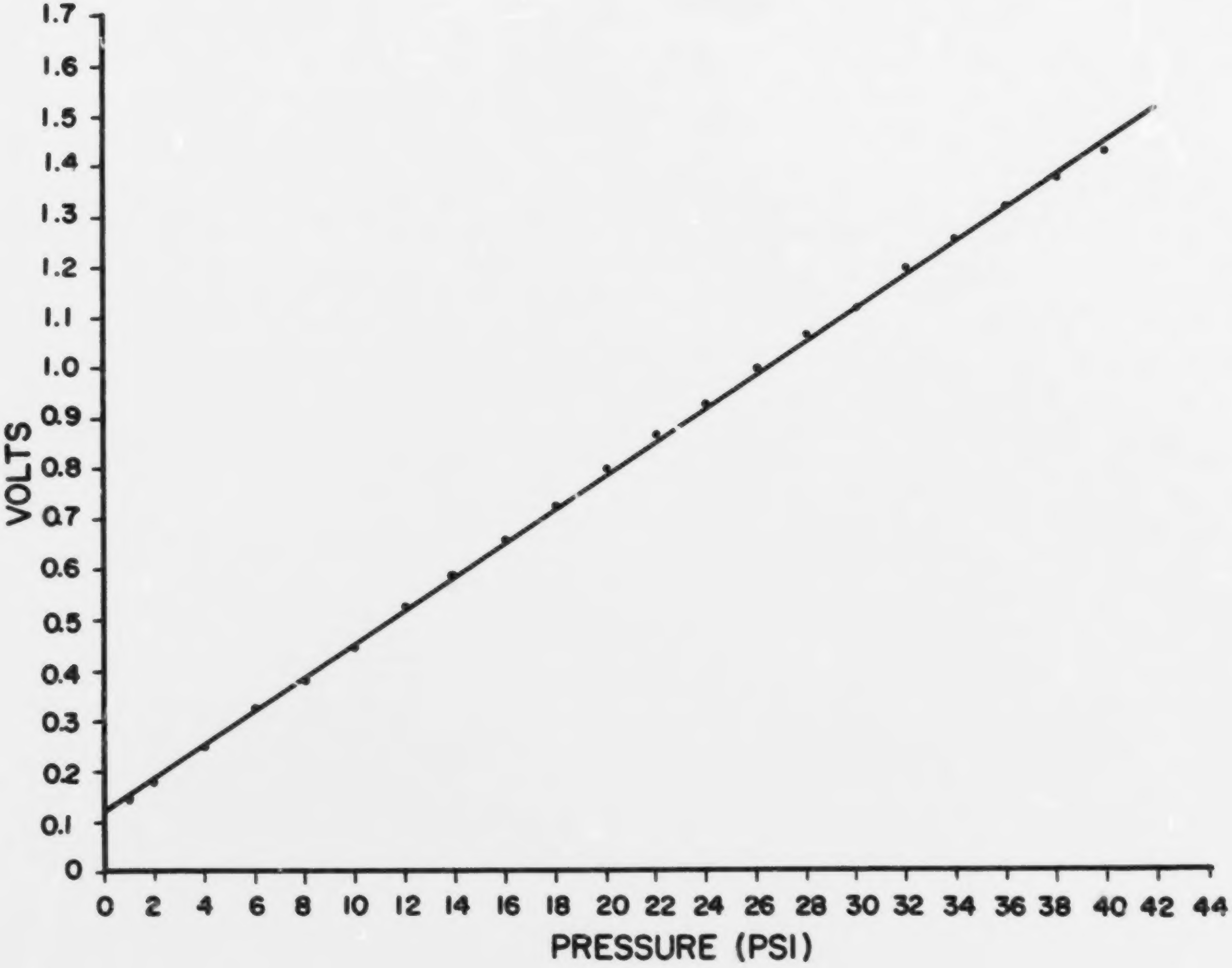

Figure A.1 Calibration curve for 345 kPa (50 psi) Dynisco pressure transducer.

BEST COPY AVAILABLE

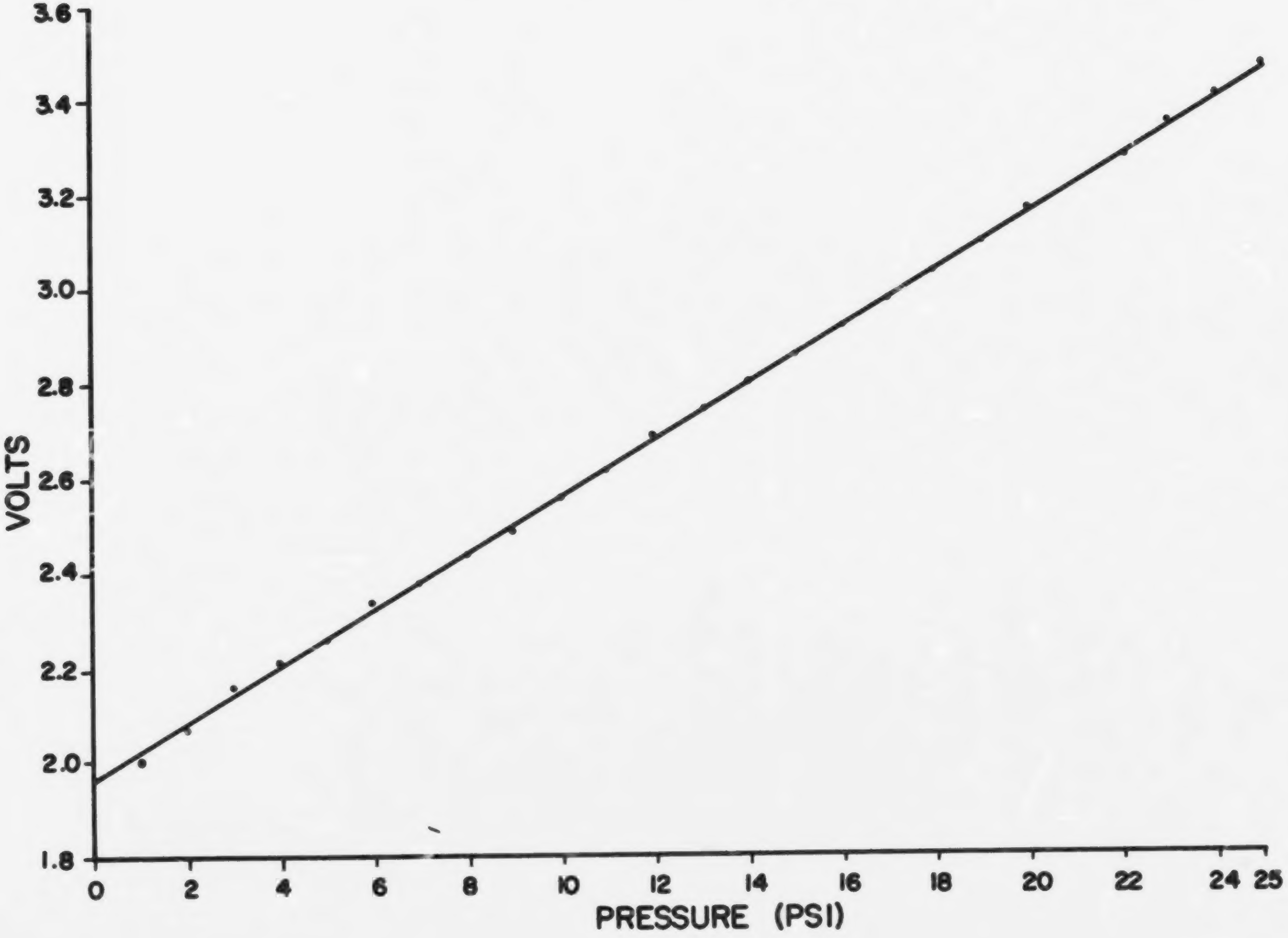

Figure A.2 Calibration curve for 172 kPa (25 psi) Dynisco pressure transducer.

APPENDIX B

TYPE CURVES FOR SLUG TEST ANALYSIS

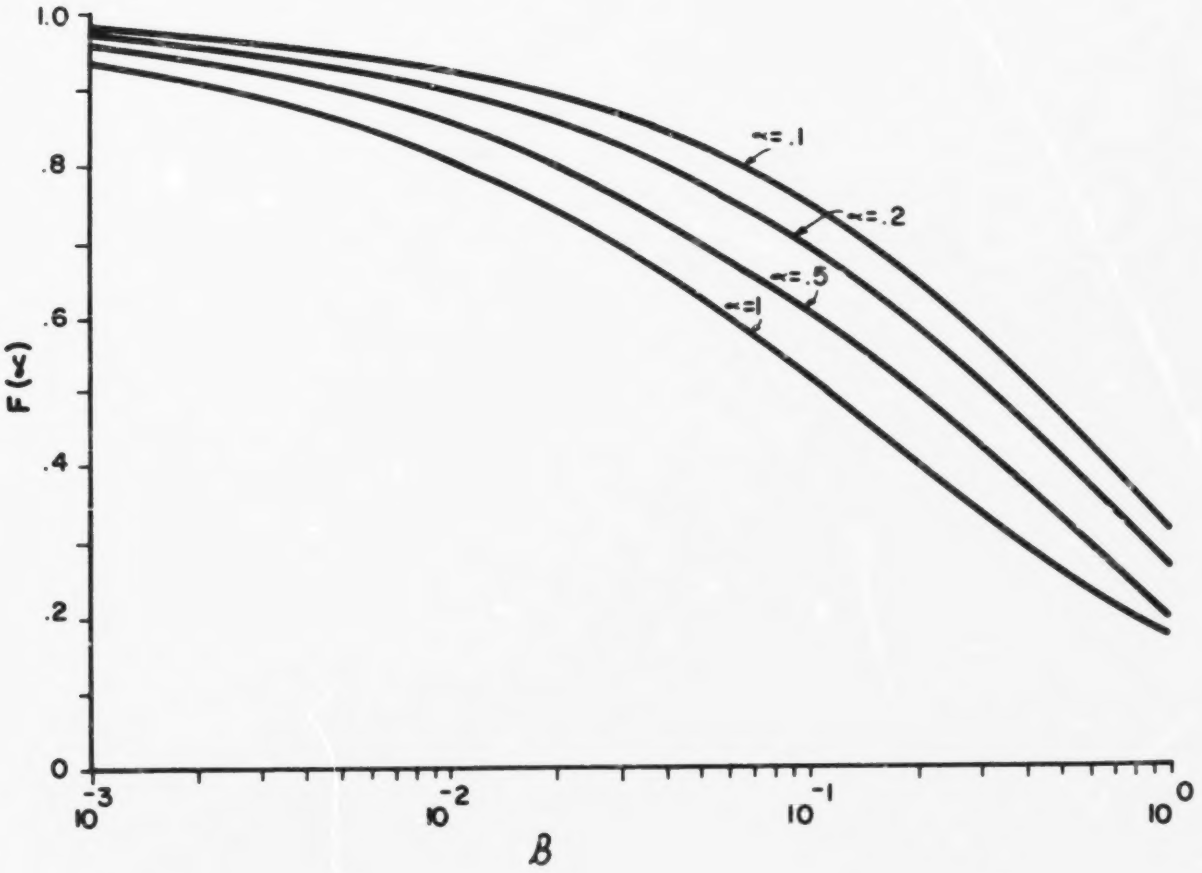

Figure B.1 Type curves for slug test analysis, i.e. head change as a function of time after a sudden pressure increase. [Section 3.4.1.6, equation (3.12); Section 3.5.2, equation (3.33)]

BEST COPY AVAILABLE

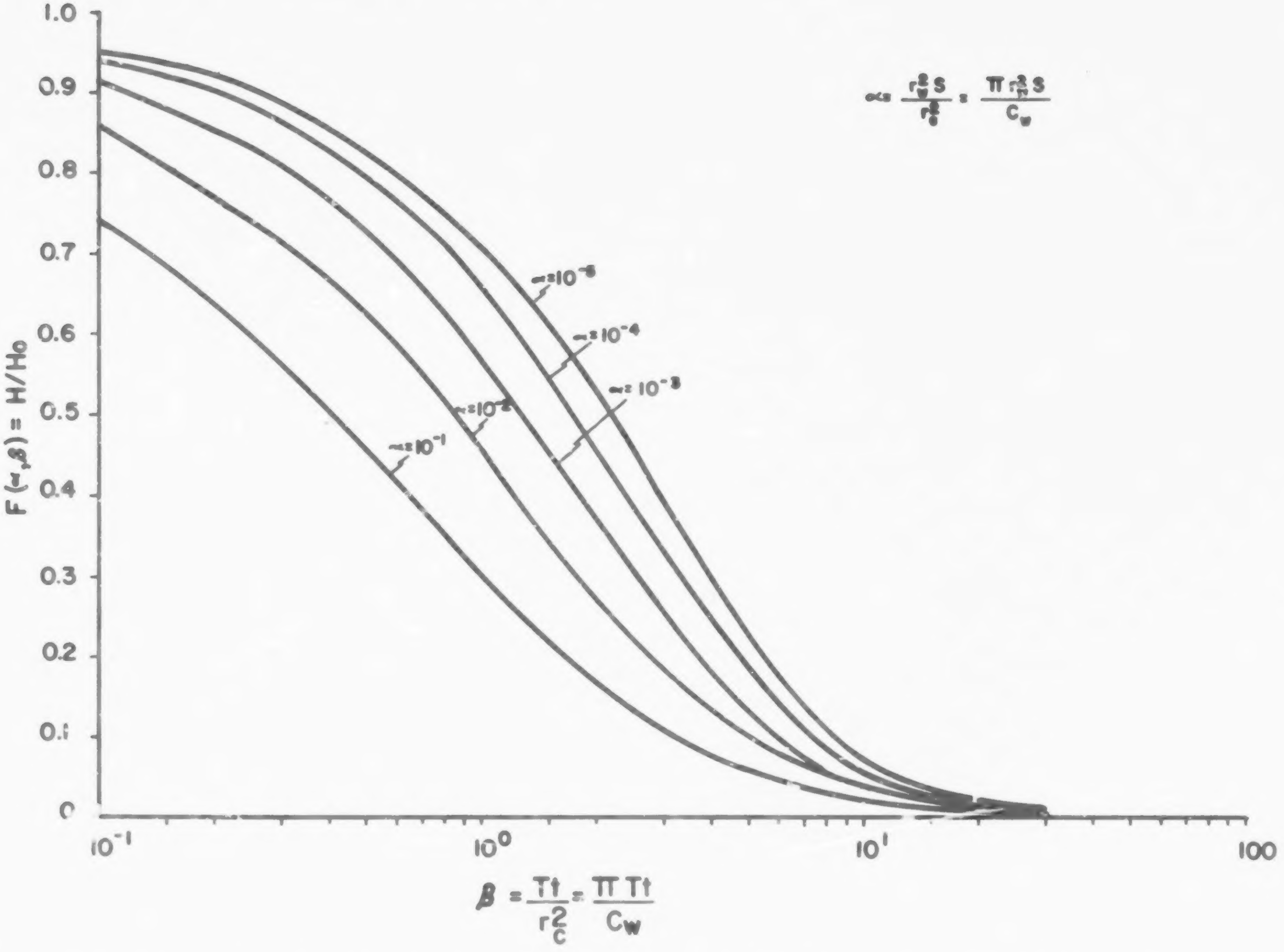

Figure B.2 Type curves for slug test analysis, i.e. head change as a function of time after a sudden pressure increase. [Section 3.4.1.6, equation (3.12); Section 3.5.2, equation (3.33)]

BEST COPY AVAILABLE

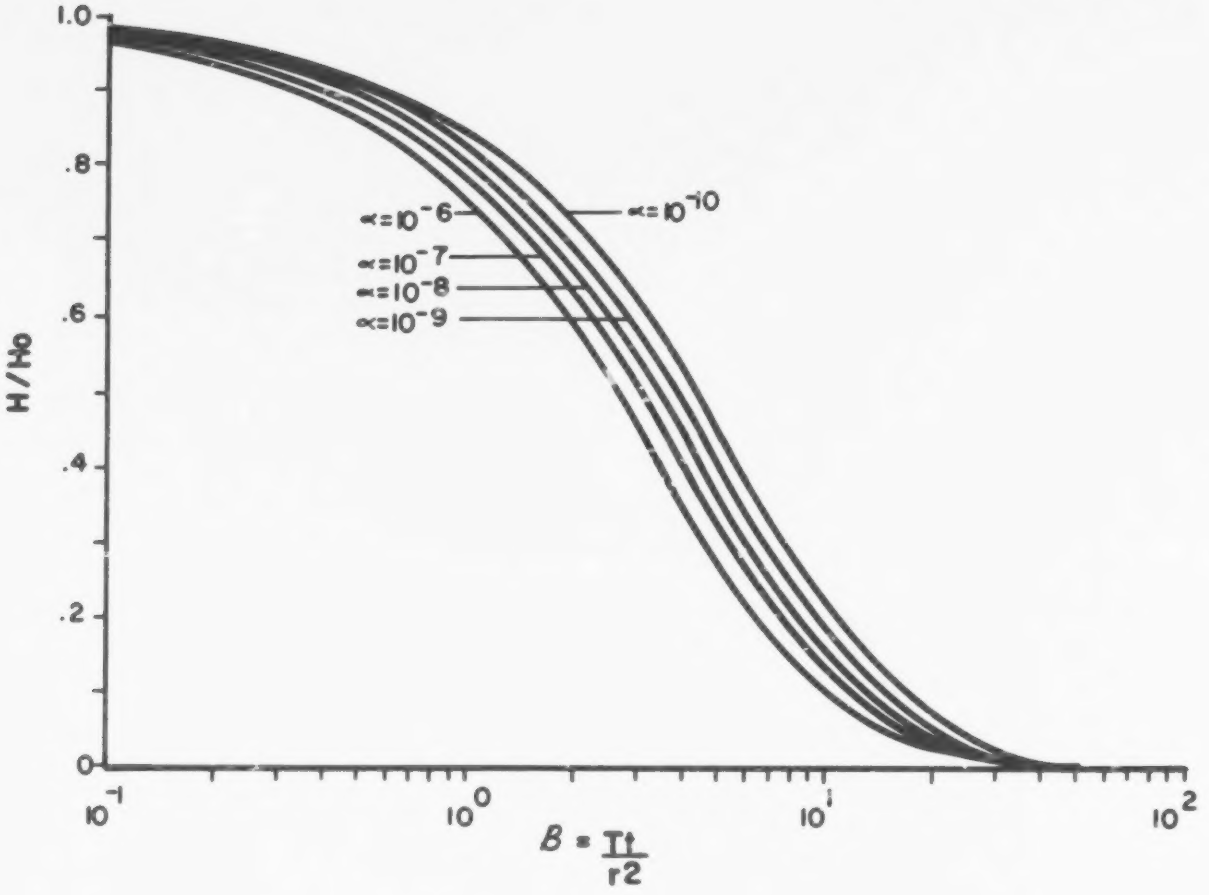

Figure B.3 Type curves for slug test analysis, i.e. head change as a function of time after a sudden pressure increase. [Section 3.4.1.6, equation (3.12); Section 3.5.2, equation (3.33)]

BEST COPY AVAILABLE

APPENDIX C

LABORATORY MEASUREMENTS OF BENTONITE PLUG HYDRAULIC CONDUCTIVITY AND DEGREE OF SATURATION

Table C.1 Hydraulic Conductivity (injection pressure = 34 kPa (5 psi))

Date of Reading	Time Between Reading (sec)	Total Volume In (cm^3)	Volume Out/Tube (cm^3)				Unadjusted Hydraulic Conductivity (x 10^{-8} cm/s)			
			1	2	3	4	1	2	3	4
May										
051915	12300	9.01	0.6	0.4	0.35	0.4	2.17	1.45	1.27	1.45
061150	59700	38.29	2.0	1.6	1.15	1.5	1.49	1.19	0.858	0.112
061440	10200	4.83	0.4	0.4	0.3	0.45	1.75	1.75	1.31	1.96
061535	3300	0.97	0.2	0.15	0.0	0.1	2.70	2.02	0.0	1.35
061540	300	–	–	–	–	–	–	–	–	–
061718	5880	3.22	0.3	0.26	0.25	0.36	2.27	1.97	1.89	2.73
062316	21480	11.58	0.7	0.4	0.45	0.54	1.45	0.831	0.933	1.12
071800	67440	20.59	2.65	2.05	1.3	1.9	1.75	1.35	0.858	1.26
071835	2100	–	–	–	–	–	–	–	–	–
072320	17100	3.86	0.85	0.45	0.45	0.6	2.22	1.17	1.17	1.56
090850	120600	–	-1.6	-1.25	-0.65	-0.3	0.0	0.0	0.0	0.0
091229	13140	1.29	-0.65	0.5	0.4	0.5	0.0	1.70	1.36	1.70
091426	7020	0.97	-0.1	0.2	0.23	0.3	0.0	1.27	1.46	1.91
091700	9240	1.61	-0.11	0.4	0.27	0.35	0.0	1.93	1.30	1.69
101730	88200	14.16	0.11	2.3	1.6	2.15	.056	1.16	8.07	1.09
140925	316500	–	–	–	–	–	–	–	–	–
141238	11580	5.79	0.9	1.1	1.1	0.95	3.46	4.23	4.23	3.66
141421	6180	2.57	0.3	0.4	0.4	0.35	2.16	2.89	2.89	2.52
151003	70920	–	–	–	–	–	–	–	–	–
151129	5160	0.64	0.15	0.3	0.2	0.25	1.30	2.59	1.73	2.16
151322	6780	1.93	0.25	0.3	0.35	0.35	1.64	1.97	2.30	2.30
151512	6600	1.29	0.23	0.3	0.3	0.3	1.55	2.02	2.02	2.02
151610	3480	0.64	0.08	0.2	0.15	0.2	1.06	2.56	2.31	2.56
160804	57240	14.16	0.72	1.8	1.7	1.5	.559	1.40	1.32	1.17
161000	6960	1.29	0.02	0.2	0.2	0.2	.128	1.28	1.28	1.28
161316	11760	1.93	0.3	0.5	0.45	0.5	1.14	1.89	1.70	1.89
161520	7440	1.29	0.2	0.3	0.3	0.3	1.20	1.80	1.80	1.80
171024	68640	–	–	–	–			–	–	–
171150	5160	1.29	0.3	0.35	0.35	0.4	2.59	3.02	3.02	3.45

Table C.1 Hydraulic Conductivity (injection pressure = 34 kPa (5 psi))--Continued

Date of Reading	Time Between Reading (sec)	Total Volume In (cm^3)	Volume Out/Tube (cm^3)				Unadjusted Hydraulic Conductivity ($\times 10^{-8}$ cm/s)			
			1	2	3	4	1	2	3	4
182011	116460	21.88	2.25	3.7	3.55	4.05	.862	1.42	1.36	1.55
201002	136260	23.81	2.1	4.35	3.45	3.85	.685	1.45	1.13	1.26
201005	180	-	-	-	-	-	-	-	-	-
211175	93120	-	-	-	-	-	-	-	-	-
211430	9180	1.29	0.35	0.4	0.4	0.4	1.70	1.94	1.94	1.94
211743	11580	1.93	0.3	0.5	0.4	0.5	1.15	1.93	1.54	1.93
211746	180	-	-	-	-	-	-	-	-	-
221310	69840	12.23	1.3	2.1	2.05	1.9	.831	1.34	1.31	1.21
230951	74460	12.23	1.33	2.25	2.05	2.0	.795	1.35	1.23	1.20
230952	60	-	-	-	-	-	-	-	-	-
231615	22980	3.22	1.0	1.1	0.9	1.1	1.94	2.13	1.74	2.13
240757	56520	9.65	0.9	1.6	1.5	1.4	.709	1.26	1.18	1.10
241830	37980	5.79	1.4	1.6	1.6	1.7	1.64	1.88	1.88	2.00
241835	300	-	-	-	-	-	-	-	-	-
251620	78300	13.51	1.85	2.6	2.55	2.2	1.05	1.52	1.45	1.25
280924	234240	-	-	-	-	-	-	-	-	-
290953	88140	12.87	1.8	3.0	2.7	2.6	.909	1.52	1.37	1.31
291223	9000	1.29	0.25	0.35	0.3	0.3	1.24	1.73	1.48	1.48
291227	240	-	-		-	-	-	-	-	-
291619	13920	10.94	0.6	0.7	0.7	0.7	1.92	2.24	2.24	2.24
300800	56460	9.33	0.7	1.45	1.3	1.25	.551	1.15	1.03	.988
301549	28140	2.90	0.85	1.0	1.0	1.05	1.35	1.58	1.58	1.66
310845	60960	-	-	-	-	-	-	-	-	-
311311	15960	1.93	0.7	0.75	0.75	0.75	1.95	2.09	2.09	2.09
June										
051549	-	-	-	-	-	-	-	-	-	-
060745	57360	11.58	0.6	1.0	1.05	0.85	.465	.776	.815	.661
061739	35640	1.93	1.3	1.35	1.35	1.30	1.63	1.69	1.69	1.63
071025	60360	8.37	0.5	1.05	1.10	1.05	3.69	.776	.811	.776

Table C.1 Hydraulic Conductivity (injection pressure = 34 kPa (5 psi))--Continued

Date of Reading	Time Between Reading (sec)	Total Volume In (cm^3)	Volume Out/Tube (cm^3) 1	2	3	4	Unadjusted Hydraulic Conductivity (x 10^{-8} cm/s) 1	2	3	4
071053	1680	–	–	–	–	–	–	–	–	–
071651	21480	7.08	1.4	1.5	1.55	1.35	2.91	3.11	3.22	2.80
081518	80820	17.37	2.45	2.65	1.6	2.50	1.35	1.46	.882	1.38
100822	147840	–	–	–	–	–	–	–	–	–
101640	29880	25.10	1.55	1.45	1.15	1.45	2.31	2.16	1.72	2.16
111645	86700	14.80	2.55	2.55	1.75	2.55	1.31	1.31	.898	1.31
111656	660	–	–	–	–	–	–	–	–	–
120809	54780	10.62	0.9	1.0	0.6	.95	.732	.815	.488	.772
121029	8400	0.32	0.2	0.2	0.15	.25	1.06	1.06	.795	1.33
121836	29220	1.29	1.1	1.05	0.7	0.9	1.68	1.60	1.07	1.68
130612	41760	5.47	0.3	0.55	1.25	0.65	.320	.587	1.33	.693
131816	43440	2.57	1.55	2.5	2.2	1.25	1.59	2.56	2.26	1.28
131820	240	–	–	–	–	–	–	–	–	–
141052	59520	7.72	0.9	.95	.85	.85	.673	.713	.638	.638
150730	74280	6.44	1.5	1.5	.75	1.45	.902	.902	.449	.870
151520	28200	2.57	.85	.85	.25	.80	1.34	1.34	.394	1.26
161700	84720	9.01	1.9	1.95	.35	1.9	1.00	1.03	.184	1.00
161705	300	–	–	–	–	–	–	–	–	–
171046	63660	6.44	1.1	1.1	.25	1.0	.772	.772	.175	.701
171730	24220	1.93	.95	.95	.65	1.05	1.75	1.75	1.20	1.93
171730	–	–	–	–	–	–	–	–	–	–
181615	89100	9.65	1.4	1.4	.90	1.4	.701	.701	.449	.701
191117	68520	6.44	1.0	1.1	0.4	1.0	.650	.717	.260	.650
191648	19860	1.29	1.2	1.15	0.8	1.1	2.69	2.58	1.80	2.47
191650	120	–	–	–	–	–	–	–	–	–
200852	57720	8.37	0.5	0.7	0.1	0.6	.386	.539	.077	.465
201617	26700	.32	1.2	1.1	0.8	1.1	2.00	1.83	1.33	1.83
210930	61980	13.19	.25	.35	0.05	.35	.180	.252	.036	.252
211525	21300	6.44	.85	1.45	.55	.85	1.78	1.67	1.15	1.78
211544	1140	18.66	.05	0	0.1	.05	1.95	0	3.63	1.95

Table C.1 Hydraulic Conductivity (injection pressure = 34 kPa (5 psi))--Continued

Date of Reading	Time Between Reading (sec)	Total Volume In (cm^3)	Volume Out/Tube (cm^3)				Unadjusted Hydraulic Conductivity (x 10^{-8} cm/s)			
			1	2	3	4	1	2	3	4
221551	86820	37.32	2.15	2.25	1.1	1.85	1.10	1.15	.563	.949
221601	600	–	–	–	–	–	–	–	–	–
231545	85440	15.44	2.7	2.7	2.0	2.5	1.41	1.41	1.04	1.30
240805	58800	11.58	1.45	1.5	.9	1.35	1.10	1.14	.681	1.02
240808	180	–	–	–	–					–
241603	28500	4.50	1.7	1.6	1.45	1.6	2.66	2.50	2.27	2.50
250825	58920	11.58	1.0	1.05	.75	.90	.756	.795	.567	.681
251512	24420	2.57	1.15	1.15	.85	1.15	2.10	2.10	1.55	2.10
251519	420	–	–	–	–	–	–	–	–	–
260809	60600	11.58	1.0	1.05	.85	.95	.736	.772	.626	.697
261452	24180	3.22	1.1	1.1	.90	1.05	2.03	2.03	1.66	1.94
261507	900	–	–	–	–	–	–	–	–	–
270807	61200	14.80	1.4	1.45	.80	1.25	1.02	1.06	.583	.909
280723	83760	13.51	1.1	.65	4.0	3.55	.587	.346	2.13	1.89
280726	180	–	–	–	–	–	–	–	–	–
281714	35280	4.50	1.9	1.8	1.35	1.75	2.40	2.27	1.70	2.21
291525	79860	–	–	–	–	–	–	–	–	–
July										
010524	136740	34.75	3.65	3.6	2.05	3.35	1.19	1.17	.669	1.09
011656	41520	5.47	1.7	1.7	1.0	1.7	1.82	1.82	1.07	1.82
020740	52980	9.97	1.1	1.2	.9	1.05	.925	1.01	.756	.882
021621	31260	3.22	1.65	1.55	1.25	1.55	2.35	2.21	1.78	2.21
030337	40560	6.11	.70	.75	.45	.7	.768	.823	.496	.768
030823	17460	3.22	.30	.35	.1	.3	.764	.894	.255	.764
030947	4740	.32	.25	.20	.15	.25	2.35	1.88	1.41	2.35
031329	13320	1.93	.7	.7	.45	.65	2.34	2.34	1.50	2.17
031333	240	–	–	–	–	–	–	–	–	–
031845	18720	1.61	.85	.80	.7	.8	2.02	1.91	1.67	1.91
041112	59220	11.91	.95	1.05	.75	.9	.717	.791	.563	.677

Table C.1 Hydraulic Conductivity (injection pressure = 34 kPa (5 psi))--Continued

Date of Reading	Time Between Reading (sec)	Total Volume In (cm^3)	Volume Out/Tube (cm^3) 1	2	3	4	Unadjusted Hydraulic Conductivity (x 10^{-8} cm/s) 1	2	3	4
041741	23340	2.57	1.2	1.15	.9	1.15	2.29	2.20	1.72	2.20
050413	37920	6.44	.55	.6	.25	.5	.646	.705	.294	.587
050416	180	–	–	–	–	–	–			
051520	39840	4.50	1.5	1.5	1.3	1.5	1.68	1.68	1.45	1.68
071940	188400	–	–	–	–	–	–		–	–
080745	43500	7.08	.9	.7	.6	.7	.921	.717	.614	.717
081630	31500	1.93	1.6	1.5	1.25	1.6	2.26	2.12	1.77	2.26
081632	120	–	–	–	–	–	–	–	–	–
090334	39720	7.08	0.45	0.5	0.5	0.4	.504	.559	.559	.449
091548	44040	5.79	1.9	1.85	1.65	1.8	1.92	1.87	1.67	1.82
100545	50220	7.40	0.25	0.35	0.4	0.3	.220	.311	.354	.268
101730	42300	4.18	1.75	1.65	1.4	1.6	1.84	1.74	1.48	1.69
101735	300	–	–	–	–	–	–			
111610	81300	10.30	2.45	2.45	2.5	2.35	1.34	1.34	1.37	1.29
111619	540	–	–	–						–
120916	61020	9.97	1.25	1.3	1.4	1.15	.913	.949	1.02	.839
121718	28920	2.25	1.45	1.4	1.35	1.45	2.24	2.16	2.08	2.24
131509	78660	12.23	1.4	1.45	1.45	1.3	2.01	2.09	2.09	1.87
131515	360	–	–	–	–	–	–			
141532	83820	12.23	2.15	2.2	2.2	2.05	1.14	1.17	1.17	1.09
150933	68460	8.69	1.15	1.2	1.3	1.1	.748	.780	.846	.717
151549	22560	1.61	1.6	1.5	1.4	1.4	3.16	2.96	2.76	2.76
151758	7740	–	–	–	–	–	–	–	–	–
160821	51780	7.72	0.7	0.8	0.9	0.65	.602	.689	.776	.559
161647	30360	–	–			–	–	–		–
170817	55800	-3.54	-0.05	0.1	0.2	0	0	.079	.161	0
171703	31560	10.94	1.25	1.15	1.1	1.15	1.76	1.62	1.56	1.62
171706	180	–	–	–	–	–	–	–	–	–
180818	54720	7.08	0.95	1.05	1.15	0.9	.776	.854	.937	.732
181508	24600	3.22	0.9	0.85	0.85	0.9	1.63	1.54	1.54	1.63

Table C.1 Hydraulic Conductivity (injection pressure = 34 kPa (5 psi))--Continued

Date of Reading	Time Between Reading (sec)	Total Volume In (cm^3)	Volume Out/Tube (cm^3)				Unadjusted Hydraulic Conductivity ($\times 10^{-8}$ cm/s)			
			1	2	3	4	1	2	3	4
190812	61440	9.65	0.85	0.9	1.05	0.75	.618	.654	.760	.543
191736	33840	2.90	1.2	1.25	1.15	1.2	1.58	1.65	1.52	1.58
191740	240	–	–	–	–	–	–	–	–	–
201930	93000	11.91	2.0	2.0	2.2	1.9	.957	.957	1.06	.909
211314	63480	8.37	1.35	0.4	1.45	1.3	.941	.976	1.01	.906
211322	480	–	–			–	–			–
220741	65940	8.37	1.5	1.45	1.6	1.4	1.01	.980	1.08	.945
221709	34080	2.57	1.3	1.3	1.3	1.3	1.70	1.70	1.70	1.70
230801	53520	7.72	0.6	0.65	0.8	0.55	.500	.539	.665	.457
231000	7140	–	–							
231832	30720	3.22	1.4	1.4	1.4	1.4	2.03	2.03	2.03	2.03
231834	120	–	–	–	–	–	–			
240757	48180	7.72	0.8	0.9	1.1	0.75	.740	.831	1.02	.693
241655	32280	2.57	1.5	1.4	1.4	1.45	2.07	1.93	1.93	2.00
250806	54660	10.30	0.45	0.6	0.7	0.4	.366	.488	.567	.327
251815	36540	3.86	1.4	1.35	1.4	1.4	1.71	1.65	1.71	1.71
251818	180	–	–				–	–		
260819	50460	7.72	0.75	0.8	1.05	0.75	.661	.705	.929	.661
261615	28560	3.22	1.3	1.25	1.3	1.25	2.03	1.95	2.03	1.95
270809	57240	6.76	0.95	0.95	1.05	0.85	.740	.740	.819	.661
270816	420	–	–							–
290817	172860	23.17	4.0	4.2	4.6	3.95	1.03	1.08	1.19	1.02
290838	1260	–	–	–	–	–	–			
291713	30900	1.93	1.95	1.2	2.0	1.3	2.81	1.73	1.70	1.87
300711	50280	14.48	.6	.7	.85	.55	.531	.622	.752	.488
300720	540	--	–			–	–			
301653	34380	6.44	1.45	1.4	1.45	1.45	1.88	1.54	1.88	1.88
310746	53580	4.50	0.55	0.4	0.8	0.5	.457	.500	.665	.417
310800	840	–	–	–						
311720	33600	2.90	1.55	1.5	1.6	1.55	2.06	1.99	2.12	2.06

Table C.1 Hydraulic Conductivity (injection pressure = 34 kPa (5 psi))--Continued

Date of Reading	Time Between Reading (sec)	Total Volume In (cm^3)	Volume Out/Tube (cm^3)				Unadjusted Hydraulic Conductivity ($\times 10^{-8}$ cm/s)			
			1	2	3	4	1	2	3	4
August										
010755	52500	8.69	0.35	0.45	0.65	0.3	.295	.382	.551	.256
011659	32640	2.25	1.25	1.2	1.25	1.2	1.70	1.64	1.70	1.64
011717	1080	-	-			-	-	-	-	-
020814	53820	8.04	0.75	0.8	1.0	0.7	.622	.661	.827	.579

Table C.2 Loss of Saturation (injection pressure = 34 kPa (5 psi))

Date of Reading	Time Between Reading (sec)	Total Volume In (cm^3)	Volume Out/Tube (cm^3) 1	2	3	4	Loss to Saturation/Tube (cm^3) 1	2	3	4
May										
051915	12300	9.01	0.6	0.4	0.35	0.4	1.65	1.85	1.90	1.85
061150	59700	38.29	2.0	1.6	1.15	1.5	7.57	7.97	8.42	8.07
061440	10200	4.83	0.4	0.4	6.3	0.45	0.81	0.81	0.91	0.76
061535	3300	0.97	0.2	0.15	0.0	0.1	0.04	0.09	0.24	0.14
061540	300	–	–	–	–	–	–	–		
061718	5580	3.22	0.3	0.26	0.25	0.36	0.50	0.54	0.55	0.44
062316	21480	11.58	0.7	0.4	0.45	0.54	2.20	2.50	2.45	2.36
071800	67440	20.59	2.65	2.05	1.3	1.9	2.50	3.10	3.85	3.25
071835	2100	–	–			–	–	–		–
072320	17100	3.86	0.85	0.45	0.45	0.6	-0.05	0.35	0.35	0.20
090850	120600	–	-1.6	-1.25	-0.65	-0.3	4.84	6.19	5.79	6.14
091229	13140	1.29	-0.65	0.5	0.4	0.5	-0.33	-0.18	-0.08	-0.18
091426	7020	0.97	-0.1	0.2	0.23	0.3	0.14	0.04	0.01	-0.06
091700	9420	1.61	-0.11	0.4	0.27	0.35	0.29	0.002	0.13	0.05
101730	88220	14.16	0.11	2.3	1.6	2.15	3.43	1.24	1.94	1.39
140925	316500	–	–	–	–	–				
141238	11580	5.79	0.9	1.1	1.1	0.95	0.55	0.35	0.35	0.50
141421	6180	2.57	0.3	0.4	0.4	0.35	0.34	0.24	0.24	0.29
151003	70920	–	–	–	–	–				
151129	5160	0.64	0.15	0.3	0.2	0.25	0.01	-0.14	-0.04	-0.09
151322	6780	1.93	0.25	0.3	0.35	0.35	0.23	0.18	0.13	0.13
151512	6600	1.29	0.23	0.3	0.3	0.3	0.09	0.02	0.02	0.02
151610	3480	0.64	0.08	0.2	0.15	0.2	0.08	-0.04	0.01	-0.04
160804	57240	14.16	0.72	1.8	1.7	1.5	2.82	1.74	1.84	2.04
161000	6960	1.29	0.02	0.2	0.2	0.2	0.30	0.12	0.12	0.12
161316	11760	1.93	0.3	0.5	0.45	0.5	0.18	-0.02	0.03	-0.02
161520	7446	1.29	0.2	0.3	0.3	0.3	0.12	0.02	0.02	0.02
171024	68640	–	–							–
171150	5160	1.29	0.3	0.35	0.35	0.4	0.02	-0.03	-0.03	-0.08

Table C.2 Loss of Saturation (injection pressure = 34 kPa (5 psi))--Continued

Date of Reading	Time Between Reading (sec)	Total Volume In (cm^3)	Volume Out/Tube (cm^3)				Loss to Saturation/Tube (cm^3)			
			1	2	3	4	1	2	3	4
182011	116460	21.88	1.25	3.7	3.55	4.05	3.22	1.77	1.92	1.42
201002	136260	23.81	2.1	4.35	3.45	3.85	3.85	1.60	2.50	2.10
201005	180	-	-	-	-	-	-			
211157	93120	-	-	-		-	-	-	-	-
211430	9180	1.29	0.35	0.4	0.4	0.4	-0.03	-0.08	-0.08	-0.08
211743	11580	1.93	0.3	0.5	0.4	0.5	0.18	-0.02	0.08	-0.02
211746	180	-	-	-	-	-	-	-	-	
221310	69840	12.23	1.3	2.1	2.05	1.9	1.76	0.96	1.01	1.16
230951	74460	12.23	1.33	2.25	2.05	2.0	1.73	0.81	1.01	1.06
230952	60	-	-	-	-	-	-	-		
231615	22980	3.22	1.0	1.1	0.9	1.1	-0.20	-0.30	-0.10	-0.30
240757	56520	9.65	0.9	1.6	1.5	1.4	1.51	0.81	0.91	1.01
241830	37980	5.79	1.4	1.6	1.6	1.7	0.05	-0.15	-0.15	-0.25
241835	300	-	-	-	-	-				
251620	78300	13.51	1.85	2.6	2.55	2.2	1.53	0.78	0.83	1.18
280924	234240	-	-	-	-	-	-			
290953	88140	12.87	1.8	3.0	2.7	2.6	1.42	0.22	0.52	0.62
291223	9000	1.29	0.25	0.35	0.3	0.3	0.07	-0.03	0.02	0.02
291227	240	-	-		-	-	-	-	-	-
291619	13920	10.94	0.6	0.7	0.7	0.7	-0.12	-0.22	-0.22	-0.22
300800	56460	9.33	0.7	1.45	1.3	1.25	1.63	0.88	1.03	1.08
301549	28140	2.90	0.85	1.0	1.0	1.05	-0.13	-0.28	-0.28	-0.33
310845	60960	-	-	-	-			-	-	-
311311	15960	1.93	0.7	0.75	0.75	0.75	-0.22	-0.27	-0.27	-0.27
June										
051549	-	-	-	-	-	-	-	-	-	-
060745	57360	11.58	0.6	1.0	1.05	0.85	2.30	1.90	1.85	2.05
061739	35640	1.93	1.3	1.35	1.35	1.30	-0.82	-0.87	-0.87	-0.82
071025	60360	8.37	0.5	1.05	1.10	1.05	1.59	1.04	0.99	1.04

Table C.2 Loss of Saturation (injection pressure = 34 kPa (5 psi))--Continued

Date of Reading	Time Between Reading (sec)	Total Volume In (cm^3)	Volume Out/Tube (cm^3) 1	2	3	4	Loss to Saturation/Tube (cm^3) 1	2	3	4
071053	1680	-	-	-						
071651	21480	7.08	1.4	1.5	1.55	1.35	0.37	0.27	0.22	0.42
081518	80820	17.37	2.45	2.65	1.6	2.5	1.89	1.69	2.74	1.84
100822	147840	-	-	-	-	-	-	-	-	-
101640	29880	25.10	1.55	1.45	1.15	1.45	-0.50	-0.40	-0.10	-0.40
111645	86700	14.80	2.55	2.55	1.75	2.55	1.15	1.15		
111656	660	-	-	-			-	-	-	-
120809	54780	10.62	0.9	1.0	0.6	0.95	1.95	1.65	2.05	1.70
121029	8400	0.32	0.2	0.2	0.15	0.25	-0.72	-0.12	-0.07	-0.17
121836	29220	1.29	1.1	1.05	0.7	0.9	-0.78	-0.73	-0.38	-0.78
130612	41760	5.47	0.3	0.55	1.25	0.65	1.07	0.82	0.12	0.72
131816	43440	2.57	1.55	2.5	2.2	1.25	-0.91	-1.86	-1.56	-0.61
131820	240	-	-	-	-	-	-	-	-	-
141052	59520	7.72	0.9	0.95	0.85	0.85	1.03	0.98	1.08	-13.07
150730	74280	6.44	1.5	1.5	0.75	1.45	0.11	0.11	0.86	0.16
151520	28200	2.57	0.85	0.85	0.25	0.80	-0.21	-0.21	0.39	-0.16
161500	84720	9.01	1.9	1.95	0.35	1.9	0.35	0.30	1.9	0.35
161705	7500	-	-	-	-	-	-	-	-	-
17104	63660	6.44	1.1	1.1	0.25	1.0	0.51	0.51	1.36	0.61
171730	24240	1.93	0.95	0.95	0.65	1.05	-0.47	-0.47	-0.17	-0.57
171730	-	-	-	-	-	-	-	-	-	-
181615	89100	9.65	1.4	1.4	0.90	1.4	1.01	1.01	1.51	1.01
191117	68520	6.44	1.0	1.1	0.4	1.0	0.61	0.51	1.21	0.61
191648	19860	1.29	1.2	1.15	0.8	1.1	-0.88	-0.83	-0.48	-0.78
191650	120	-	-	-	-	-	-	-	-	-
200852	57720	8.37	0.5	0.7	0.1	0.6	1.59	1.39	1.99	1.49
201617	26700	0.32	1.2	1.1	0.8	1.1	-1.12	-1.02	-0.72	-1.02
210930	61980	13.19	0.25	0.35	0.05	0.35	3.05	2.95	3.25	2.95
211525	21300	6.44	0.85	1.45	0.55	0.85	0.76	0.81	1.06	0.76
211544	1140	18.66	0.05	0	0.1	0.05	4.62	4.67	4.57	4.62

Table C.2 Loss of Saturation (injection pressure = 34 kPa (5 psi))--Continued

Date of Reading	Time Between Reading (sec)	Total Volume In (cm^3)	Volume Out/Tube (cm^3)				Loss to Saturation/Tube (cm^3)			
			1	2	3	4	1	2	3	4
221551	86820	37.32	2.15	2.25	1.1	1.85	7.18	7.08	8.23	7.48
221601	600	–	–	–	–	–	–	–	–	–
231545	85440	15.44	2.7	2.7	2.0	2.5	1.16	1.16	1.86	1.36
240805	58800	11.58	1.45	1.5	0.9	1.35	1.45	1.40	2.00	1.55
240808	180	–	–	–	–	–	–	–	–	–
241603	28500	4.50	1.7	1.6	1.45	1.6	–0.57	–0.47	–0.32	–0.47
250825	58920	11.58	1.0	1.05	0.75	0.90	1.9	1.85	2.15	2.00
251512	24420	2.57	1.15	1.15	0.85	1.15	–0.51	–0.51	–0.21	–0.51
251519	420	–	–	–	–	–	–	–	–	–
260809	60600	11.58	1.0	1.05	0.85	0.95	1.90	1.85	2.05	1.95
261452	24180	3.22	1.1	1.1	0.90	1.05	–0.3	–0.3	–0.1	–0.25
261507	900	–	–	–	–	–	–	–	–	–
270807	61200	14.80	1.4	1.45	0.80	1.25	2.30	2.25	2.90	2.45
280723	83760	13.51	1.1	0.65	4.00	3.55	2.28	2.73	–0.62	–0.17
280726	180	–	–	–	–	–	–	–	–	–
281714	35280	4.50	1.9	1.8	1.35	1.75	–0.77	–0.67	–0.22	–0.62
291525	79860	–	–	–	–	–	–	–	–	–
July										
010524	136740	34.75	3.65	3.6	2.05	3.35	5.04	5.09	6.64	5.34
011656	41520	5.47	1.7	1.7	1.0	1.7	–0.33	–0.33	0.37	–0.33
020740	52980	9.97	1.1	1.2	.9	1.05	1.39	1.29	1.59	1.44
021621	31260	3.22	1.65	1.55	1.25	1.55	–0.85	–0.75	–0.45	–0.75
030337	40560	6.11	.70	.75	.45	.7	0.83	0.78	1.08	0.83
030828	17460	3.22	.30	.35	.1	.3	0.50	0.45	0.70	0.50
030947	4740	.32	.25	.20	.15	.25	–0.17	–0.12	–0.07	–0.17
031329	13320	1.93	.7	.70	.45	.65	–0.22	–0.22	0.03	–0.17
031333	240	–	–	–	–	–	–	–	–	–
031845	18720	1.61	.85	.80	.7	.8	–0.45	–0.4	–0.3	–0.4
041112	59220	11.91	.95	1.05	.75	.9	2.03	1.93	2.23	2.08

Table C.2 Loss of Saturation (injection pressure = 34 kPa (5 psi))--Continued

Date of Reading	Time Between Reading (sec)	Total Volume In (cm^3)	Volume Out/Tube (cm^3)				Loss to Saturation/Tube (cm^3)			
			1	2	3	4	1	2	3	4
041741	23340	2.57	1.2	1.15	.9	1.15	-0.56	-0.51	-0.26	-0.51
050413	37920	6.44	.55	.6	.25	.5	1.06	1.01	1.36	1.11
050416	180	-	-	-	-	-	-	-	-	-
051520	39840	4.50	1.5	1.5	1.3	1.5	-0.37	-0.37	-0.17	-0.37
071940	188400	-	-	-	-	-	-	-	-	-
080745	43500	7.08	.9	.7	.6	.7	0.87	1.07	1.17	1.07
081630	31500	1.93	1.6	1.5	1.25	1.6	-1.12	-1.02	-0.77	-1.12
081632	120	-	-	-	-	-	-	-	-	-
090334	39720	7.08	.45	.5	.5	.4	1.32	1.27	1.27	1.37
091548	44040	5.79	1.9	1.85	1.65	1.8	-0.45	-0.40	-0.20	-0.35
100545	50220	7.40	.25	.35	.4	.3	1.60	1.50	1.45	1.55
101730	42300	4.18	1.75	1.65	1.4	1.6	-0.70	-0.60	-0.35	-0.55
101735	300	-	-	-	-	-	-	-	-	-
111610	81300	10.30	2.45	2.45	2.5	.35	0.12	0.12	0.07	0.22
111619	540	-	-	-	-	-	-	-	-	-
120916	61020	9.97	1.25	1.3	1.4	1.15	1.24	1.19	1.09	1.34
121718	28920	2.25	1.45	1.4	1.35	1.45	-0.89	-0.84	-0.79	-0.89
131509	78660	12.23	1.4	1.45	1.45	1.3	-	-	-	-
131515	360	-	-	-	-	-	-	-	-	-
141432	83820	12.23	2.15	2.2	2.2	2.05	0.91	0.86	0.86	1.01
150933	68460	8.69	1.15	1.2	1.3	1.1	1.02	0.97	0.87	1.07
151549	22560	1.61	1.6	1.5	1.4	1.4	-1.20	-1.10	-1.00	-1.00
151758	7740	-	-	-	-	-	-	-	-	-
160821	51780	7.72	.7	.8	.9	.65	1.23	1.13	1.03	1.28
161647	30360	-	-	-	-	-	-	-	-	-
170817	55800	-3.54	-0.05	.1	.2	0	0.83	0.78	0.68	0.88
171703	31560	10.94	1.25	1.15	1.1	1.15	1.48	1.58	1.63	1.58
171706	180	-	-	-	-	-	-	-	-	-
180818	54720	7.08	.95	1.05	1.15	.9	0.82	0.72	0.62	0.87
181508	24600	3.22	.9	.85	.85	.9	-0.10	-0.05	-0.05	-0.10

Table C.2 Loss of Saturation (injection pressure = 34 kPa (5 psi))--Continued

Date of Reading	Time Between Reading (sec)	Total Volume In (cm^3)	Volume Out/Tube (cm^3)				Loss to Saturation/Tube (cm^3)			
			1	2	3	4	1	2	3	4
190812	61440	9.65	.85	.9	1.05	.75	1.56	1.51	1.36	1.66
191736	33840	2.90	1.2	1.25	1.15	1.2	−0.48	−0.53	−0.43	−0.48
191740	240	–	–	–	–	–	–	–	–	–
201930	93000	11.91	2.0	2.0	2.2	1.9	0.98	0.98	0.78	1.08
211314	63840	8.37	1.35	.4	1.45	1.3	0.74	0.69	0.64	0.79
211322	480	–	–	–	–	–	–	–	–	–
220741	65940	8.37	1.5	1.45	1.6	1.4	0.59	0.64	0.49	0.69
221709	34080	2.57	1.3	1.3	1.3	1.3	−0.66	−0.66	−0.66	−0.66
230801	53520	7.72	.6	.65	.8	.55	1.33	1.28	1.13	1.38
231000	7140	–	–	–	–	–	–	–	–	–
231832	30720	3.22	1.4	1.4	1.4	1.4	−0.6	−0.6	−0.6	−0.6
231834	120	–	–	–	–	–	–	–	–	–
240757	48180	7.72	.8	.9	1.1	.75	1.13	1.03	0.83	1.18
241655	32280	2.57	1.5	1.4	1.4	1.45	−0.86	−0.76	−0.76	−0.81
250806	54660	10.30	.45	.6	.7	.4	2.12	1.97	1.87	2.17
251815	36540	3.86	1.4	1.35	1.4	1.4	−0.43	−0.38	−0.43	−0.43
251818	180	–	–	–	–	–	–	–	–	–
260819	50460	7.72	.75	.8	1.05	.75	1.18	1.13	0.88	1.18
261615	28560	3.22	1.3	1.25	1.3	1.25	−0.5	−0.45	−0.5	−0.45
270809	57240	6.76	.95	.95	1.05	.85	0.74	0.74	0.64	0.84
270816	420	–	–	–	–	–	–	–	–	–
290817	172860	23.17	4.0	4.2	4.6	3.95	1.79	1.59	1.19	1.84
290838	1260	–	–	–	–	–	–	–	–	–
291713	30900	1.93	1.95	1.2	2.0	1.3	−1.47	−0.72	−1.52	−0.82
300711	50280	14.48	.6	0.7	.85	.55	3.02	2.92	2.77	3.07
300720	540	–	–	–	–	–	–	–	–	–
301653	34380	6.44	1.45	1.4	1.45	1.45	0.16	0.21	0.16	0.16
310746	53580	4.50	.55	.4	.8	.5	0.58	0.53	0.33	0.63
310800	840	–	–	–	–	–	–	–	–	–
311720	33600	2.90	1.55	1.5	1.6	1.55	−0.83	−0.78	−0.88	−0.83

Table C.2 Loss of Saturation (injection pressure = 34 kPa (5 psi))--Continued

Date of Reading	Time Between Reading (sec)	Total Volume In (cm^3)	Volume Out/Tube (cm^3) 1	2	3	4	Loss to Saturation/Tube (cm^3) 1	2	3	4
August										
010755	52500	8.69	.35	.45	.65	.3	1.82	1.72	1.52	1.87
011659	32640	2.25	1.25	1.2	1.25	1.2	-0.69	-0.64	-0.69	-0.64
011717	1080	-	-	-	-	-	-	-	-	-
020814	53820	8.04	.75	.8	1.0	.7	1.26	1.21	1.01	1.31

APPENDIX D

BENTONITE PLUG CONSOLIDATION TEST DATA

Table D.1 Consolidation Outflow from Bentonite Plug in Tube 5 at 69 kPa (10 psi)

Time (min)	Outflow (cc)
0	0
5	2.6
30	4.4
55	6.0
170	7.8
370	11.3
970	16.3
1454	19.8
1753	21.1
2151	22.5
2813	25.3
2863	25.8
3868	38.3
5108	41.45
7125	46.4
8598	49.7
9683	51.1
11107	56.8
12843	61.6
15711	66.2
17959	77.5
20366	82.0
23193	87.4
25122	92.2
28114	98.8
30192	103.1
32926	108.9
35285	117.2
37327	120.4
39605	124.7
41992	136.6
42472	138.4
43808	143.1
44886	144.3
45394	146.1
46703	148.05

Table D.2 Consolidation Outflow from Bentonite Plug in Tube 6 at 69 kPa (10 psi)

Time (min)	Outflow (cc)
0	0
5	2.2
30	4.0
55	5.0
170	7.1
370	10.5
970	25.8
1454	29.1
1753	30.4
2151	31.8
2813	34.6
2863	35.0
3868	47.5
5108	50.15
7125	54.2
8598	57.3
9683	58.5
11107	67.8
12843	69.2
15711	74.7
17959	84.4
20366	87.9
23193	92.6
25122	97.9
28114	103.8
30192	107.6
32926	112.6
35285	123.5
37327	125.4
39605	129.4
41992	143.1
42472	144.7
43808	148.2
44886	149.4
45394	151.0
46703	162.7

Table D.3 Consolidation Outflow from Bentonite Plug in Tube 7 at 69 kPa (10 psi)

Time (min)	Outflow (cc)
0	0
5	2.6
30	4.6
55	5.9
170	8.3
370	12.0
970	30.3
1454	33.8
1753	35.2
2151	36.6
2813	39.5
2863	40.8
3868	61.5
5108	65.2
7125	70.2
8598	73.7
9683	75.0
11107	79.9
12843	83.3
15711	90.0
17959	97.4
20366	101.7
23193	107.5
25122	112.3
28114	118.5
30192	123.1
32926	129.8
35285	137.9
37327	141.1
39605	145.1
41992	157.6
42472	159.4
43808	163.8
44886	165.2
45394	166.2
46703	168.85

Table D.4 Consolidation Outflow from Bentonite Plug in Tube 8 at 69 kPa (10 psi)

Time (min)	Outflow (cc)
0	0
10	0.1
830	0.1
1300	0.1
2847	1.7
3900	1.3
5235	1.8
5665	1.9
6829	1.8
8120	1.8
9595	1.9
11433	1.8
12855	1.9
13208	1.8
15080	1.9
16493	1.8
17526	1.8
18915	1.8
20358	1.9
23139	1.8
25239	1.8
26821	1.8
27687	4.1
28077	6.3
28648	8.2
29317	11.3
31007	33.1
31863	36.2
33049	41.0
34623	50.1
36688	69.5
38194	67.8
39530	71.4
41116	71.4
41977	97.9

Table D.5 Consolidation Outflow from Bentonite Plug in Tube 5 at 138 kPa (20 psi)

Time (min)	Outflow (cc)
0	0
0.5	2.45
1	3.25
2	3.85
4	4.35
8	5.45
16	5.85
32	7.85
72	9.55
342	14.05
907	20.15
1430	23.25
2262	32.75
4054	38.15
5154	42.95
5719	46.05
6724	49.85
7246	51.95
8048	54.75
8584	57.85
9499	60.65
10107	63.75
10952	66.45
11428	69.15
12382	72.25
15271	83.85
15806	86.05
16642	87.65
17227	89.45
18117	90.35
18122	90.75

Table D.6 Consolidation Outflow from Bentonite Plug in Tube 6 at 138 kPa (20 psi)

Time (min)	Outflow (cc)
0	0
0.5	1.8
1	2.4
2	3.0
4	3.4
8	4.4
16	5.7
32	6.8
72	7.8
342	12.1
907	17.9
1430	20.8
2262	32.9
4054	37.3
5154	41.7
5719	44.6
6724	48.1
7246	51.9
8048	54.5
8584	57.2
9499	59.8
10107	63.2
10952	65.2
11428	67.6
12382	70.6
15271	82.9
15806	85.3
16642	86.35
17227	87.8
18117	88.7
18122	89.0

Table D.7 Consolidation Outflow from Bentonite Plug in Tube 7 at 138 kPa (20 psi)

Time (min)	Outflow (cc)
0	0
0.5	3.5
1	3.3
2	4.1
4	4.6
8	5.8
16	6.6
32	8.5
72	9.7
342	14.2
907	20.2
1430	23.4
2262	32.7
4054	38.3
5154	43.3
5719	46.6
6724	51.2
7246	52.3
8048	55.3
8584	58.5
9499	61.4
10107	64.6
10952	67.5
11428	70.1
12382	73.6
15271	83.4
15806	87.2
16642	88.5
17227	90.1
18117	91.2
18122	91.6

Table D.8 Consolidation Outflow from Bentonite Plug in Tube 5 at 207 kPa (30 psi)

Time (min)	Outflow (cc)
0	0
.5	1.7
1	2.7
2	3.6
4	4.0
8	4.6
16	5.3
360	9.5
496	12.1
1336	18.95
1832	22.9
2736	27.1
3349	30.9
4328	34.0
4821	36.8
4951	37.7
5886	41.7
6374	45.5
7331	48.4
8017	43.0
9156	57.3
10565	63.0
11521	67.2
12036	70.1
12967	73.2
13596	76.3
14396	78.6

Table D.9 Consolidation Outflow from Bentonite Plug in Tube 6 at 207 kPa (30 psi)

Time (min)	Outflow (cc)
0	0
.5	2.1
1	2.3
2	2.9
4	3.4
8	3.9
16	4.8
360	8.4
496	10.9
1336	17.5
1832	21.2
2736	25.3
3349	29.0
4328	32.0
4821	34.6
4951	35.3
5886	38.6
6374	42.2
7331	44.9
8017	48.3
9156	52.4
10565	57.9
11521	61.9
12036	64.6
12967	67.6
13596	70.5
14396	72.7

Table D.10 Consolidation Outflow from Bentonite Plug in Tube 7 at 207 kPa (30 psi)

Time (min)	Outflow (cc)
0	0
.5	2.7
1	3.0
2	3.5
4	3.9
8	4.5
16	5.4
360	9.4
496	12.1
1336	19.1
1832	23.0
2736	27.4
3349	31.4
4328	34.6
4821	37.5
4951	38.2
5886	40.8
6374	44.6
7331	47.6
8017	52.2
9156	56.7
10565	62.7
11521	67.1
12036	69.9
12967	73.2
13596	76.5
14396	78.7

APPENDIX E

LATE TIME SOLUTIONS FOR TRANSIENT TEST LABORATORY PLUG HYDRAULIC CONDUCTIVITY TESTING

(Section 5.7.2)

Upstream reservoir head (pressure) H_u decays
as a fraction of applied pulse H

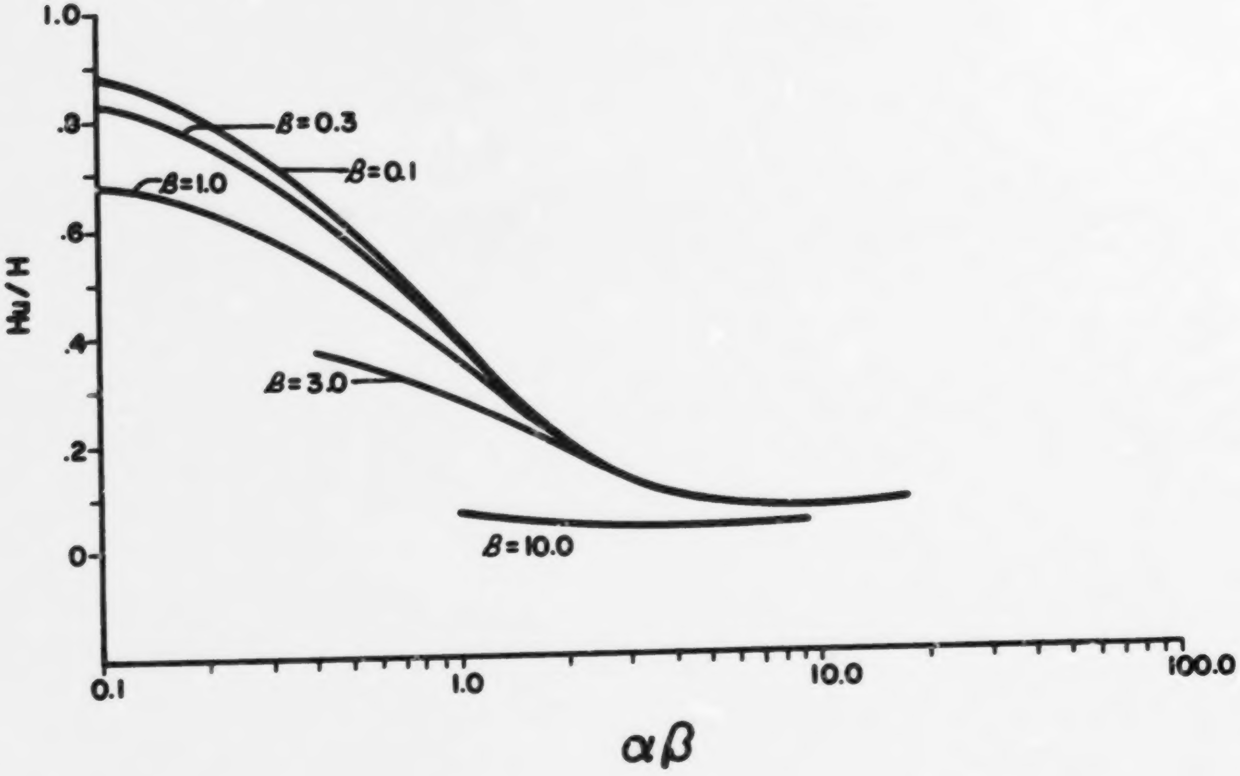
1.0
.8
.6
.4
.2
0
Hu/H
β=0.3
β=0.1
β=1.0
β=3.0
β=10.0
0.1
1.0
10.0
100.0
αβ

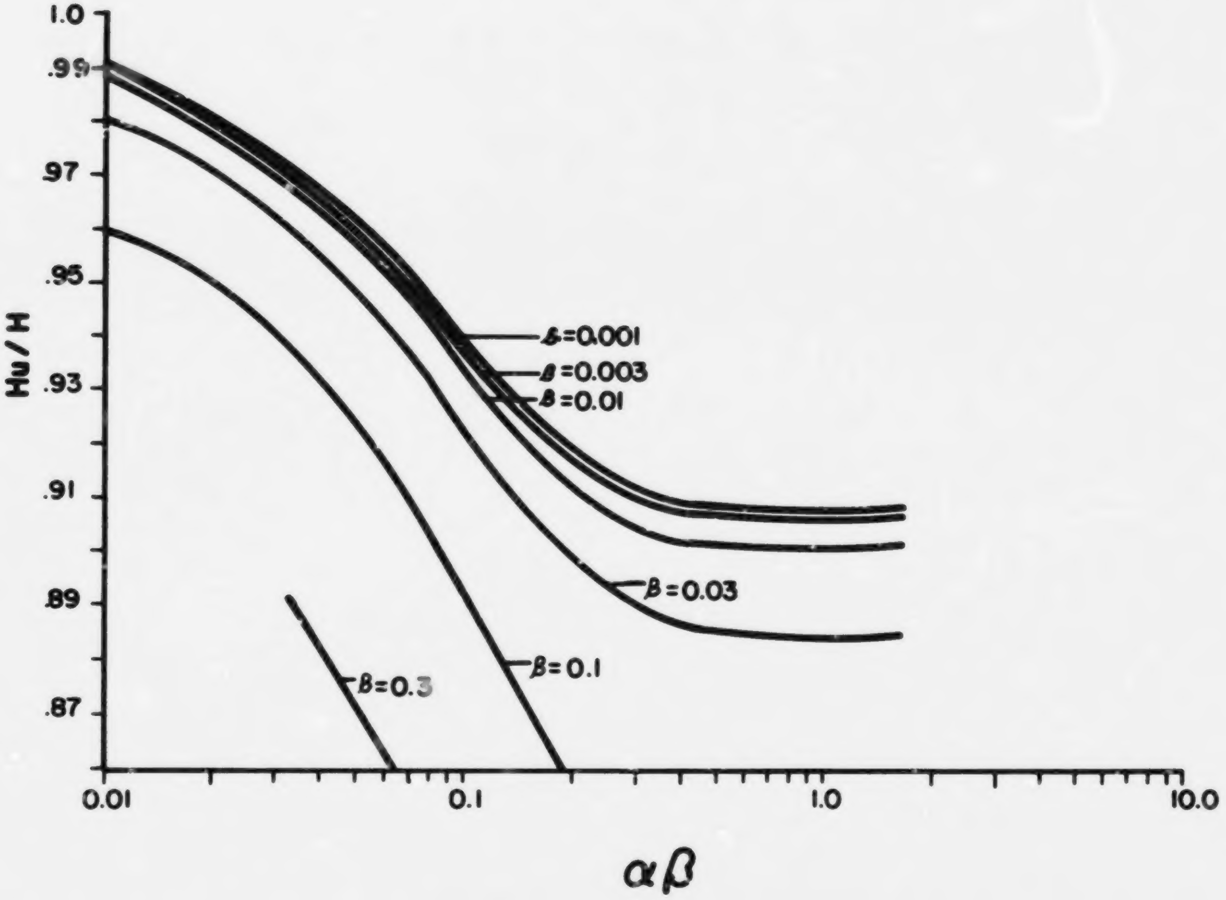
Hu / H
1.0
.99
.97
.95
.93
.91
.89
.87
0.01
0.1
1.0
10.0
$\alpha\beta$
β=0.001
β=0.003
β=0.01
β=0.03
β=0.1
β=0.3

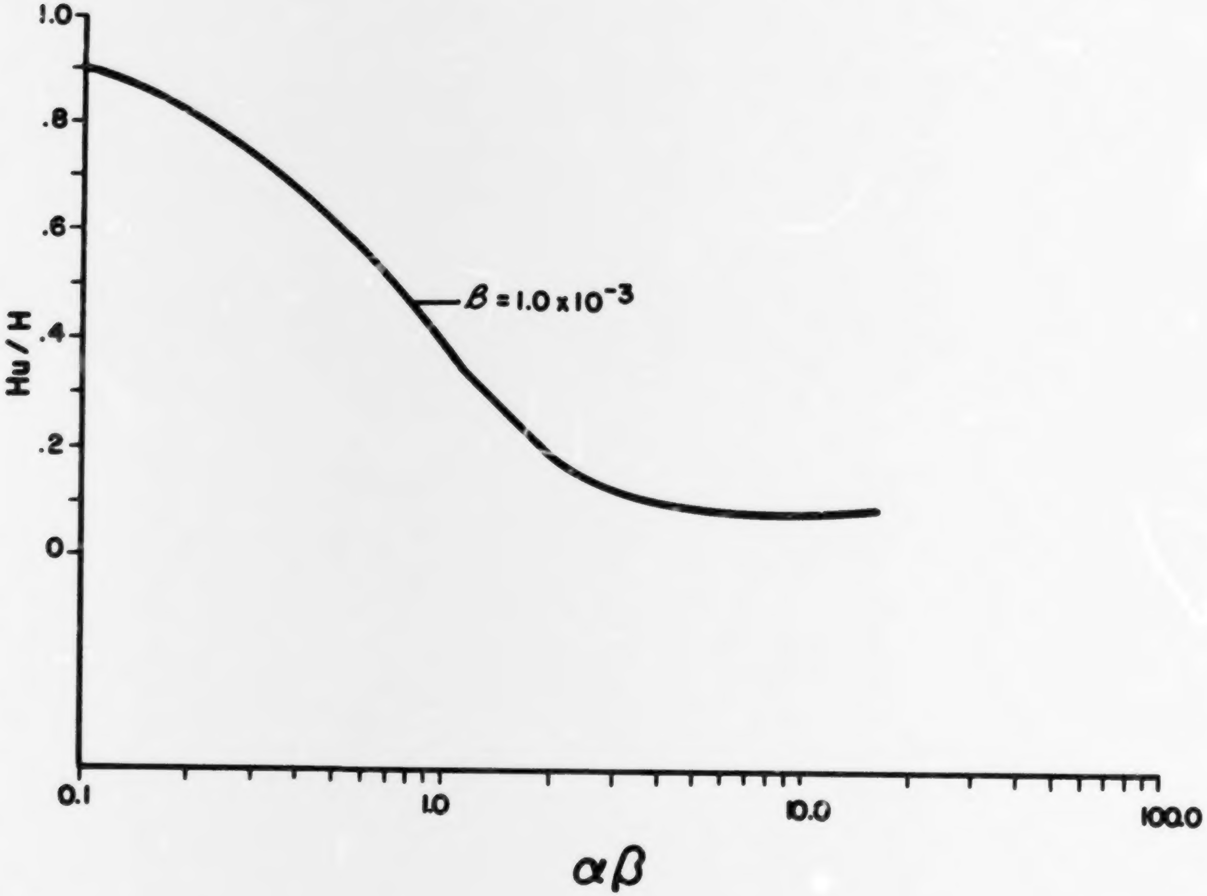
1.0
.8
.6
.4
.2
0
Hu / H
$\beta = 1.0 \times 10^{-3}$
0.1
1.0
10.0
100.0
$\alpha\beta$

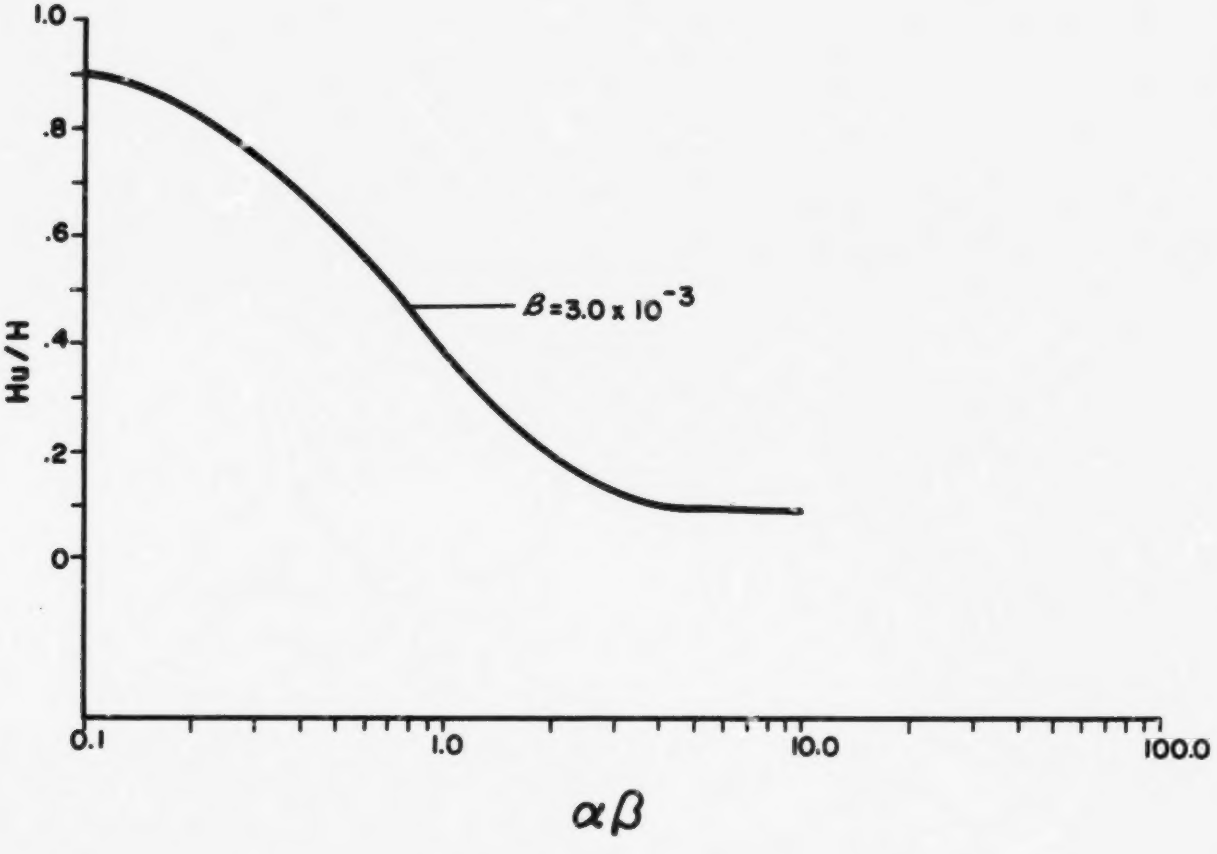
1.0
.8
.6
.4
.2
0
Hu/H
$\beta = 3.0 \times 10^{-3}$
0.1
1.0
10.0
100.0
$\alpha\beta$

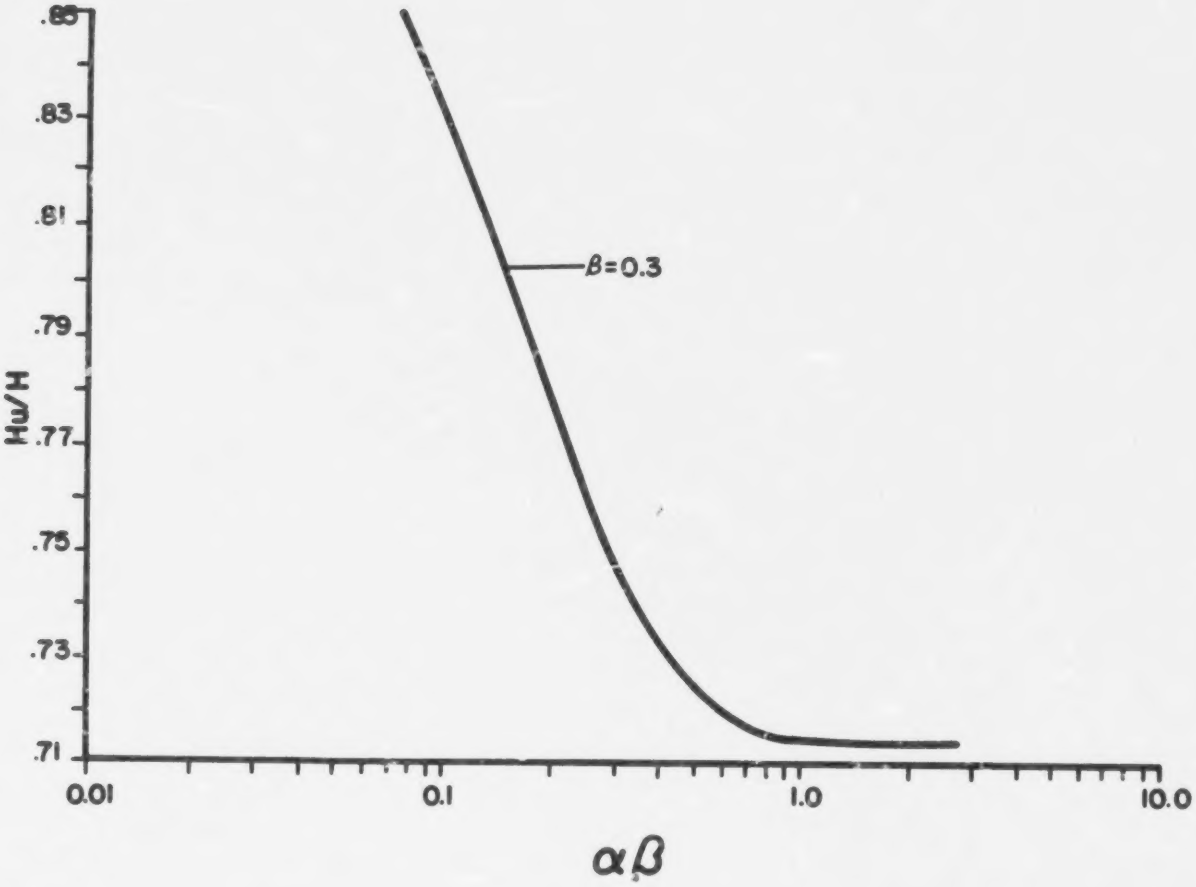
.85
.83
.81
.79
.77
.75
.73
.71
Hw/H
β=0.3
0.01
0.1
1.0
10.0
αβ

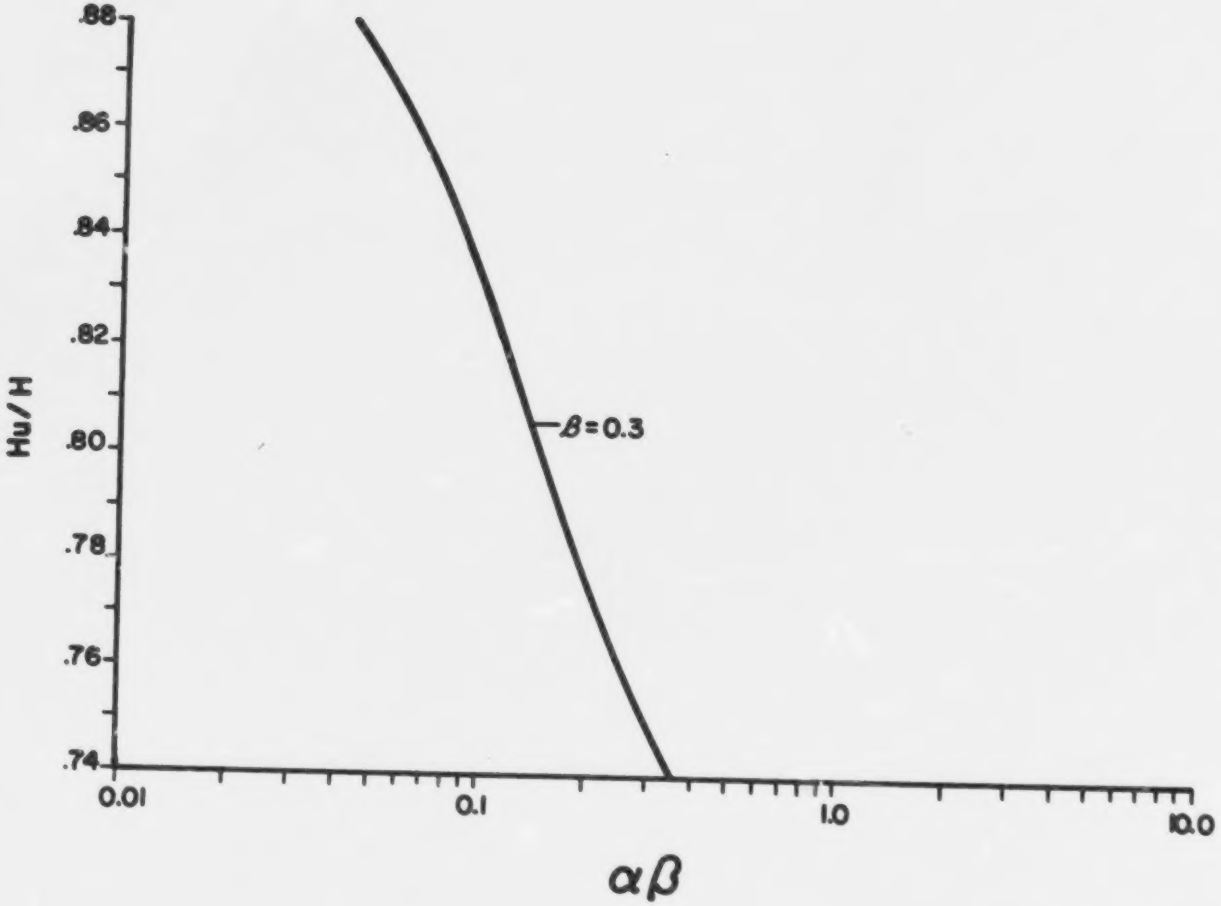
.88
.86
.84
.82
.80
.78
.76
.74
Hu/H
β=0.3
0.01
0.1
1.0
10.0
αβ

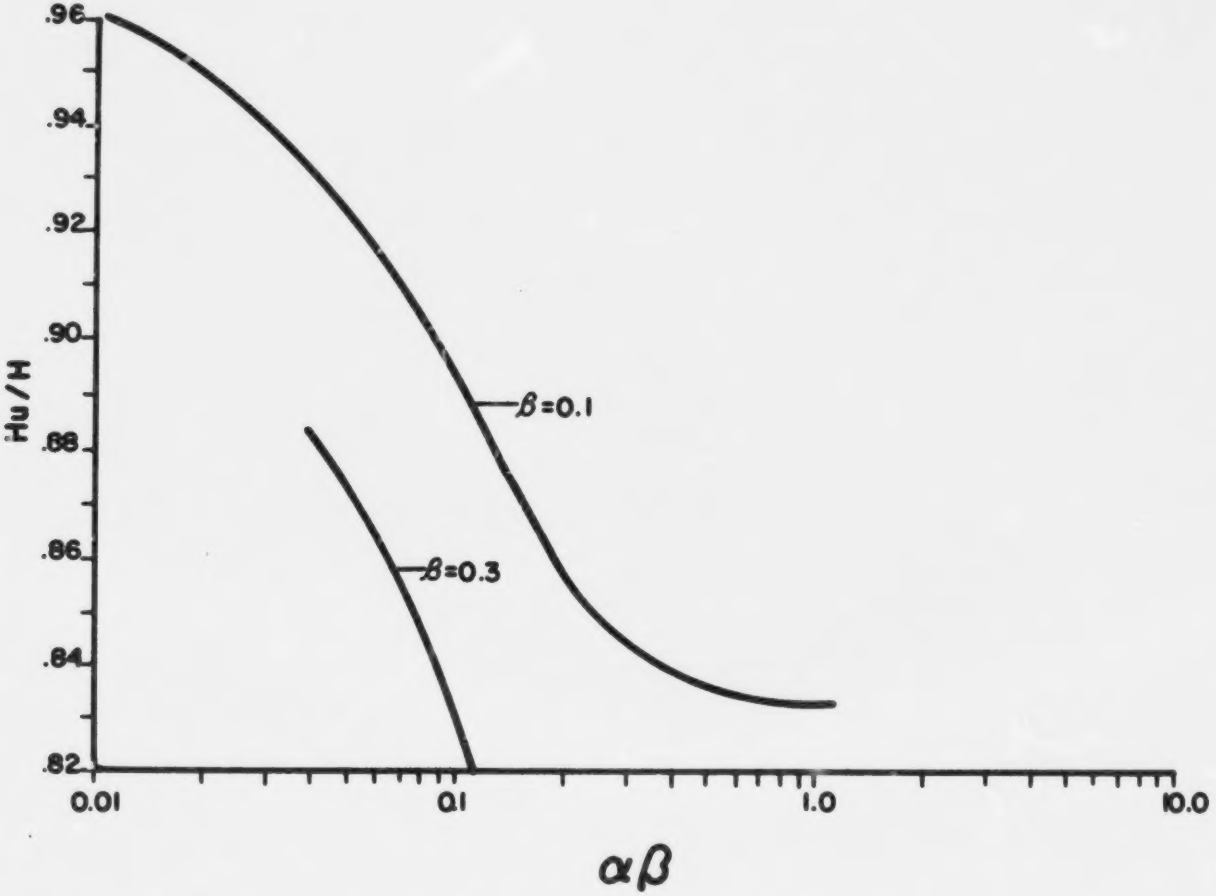
.96
.94
.92
.90
.88
.86
.84
.82
Hu/H
β=0.1
β=0.3
0.01
0.1
1.0
10.0
αβ

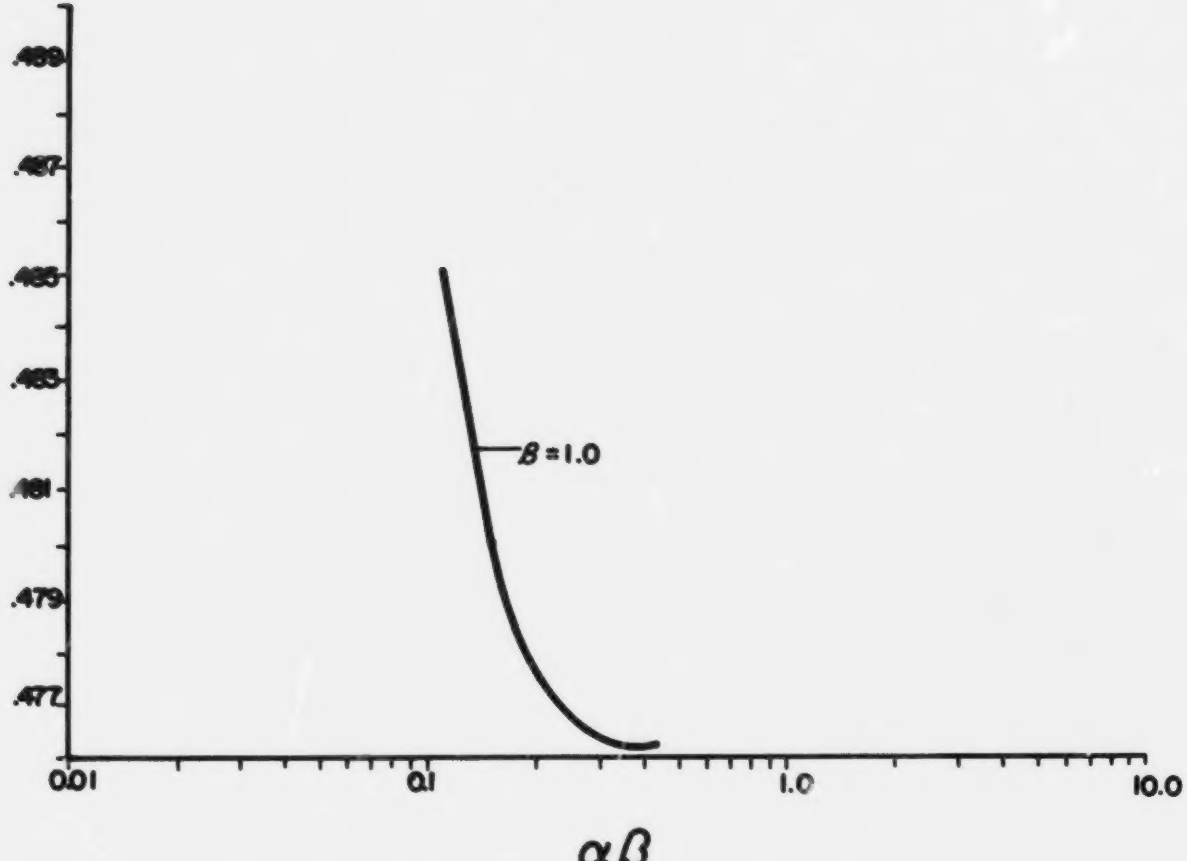
Hu/H
.489
.487
.485
.483
.481
.479
.477
β = 1.0
0.01
0.1
1.0
10.0
αβ

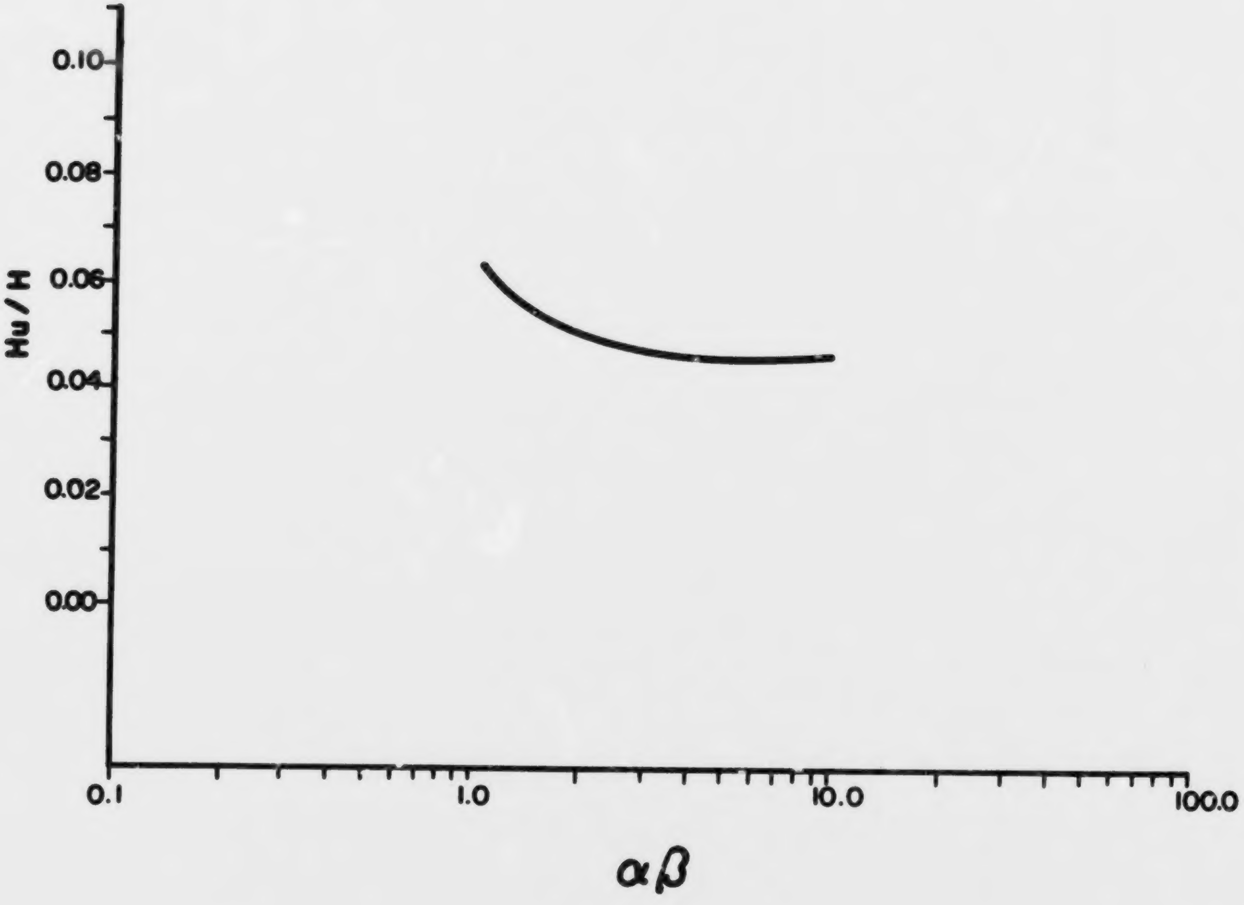
Hu / H
0.10
0.08
0.06
0.04
0.02
0.00
0.1
1.0
10.0
100.0
αβ

APPENDIX F

TYPE CURVES FOR LABORATORY PLUG TRANSIENT HYDRAULIC CONDUCTIVITY TESTING

H_u: upstream reservoir head (pressure) decay as a fraction of applied pulse H

H_d: downstream reservoir head (pressure) build-up as a fraction of applied pulse H

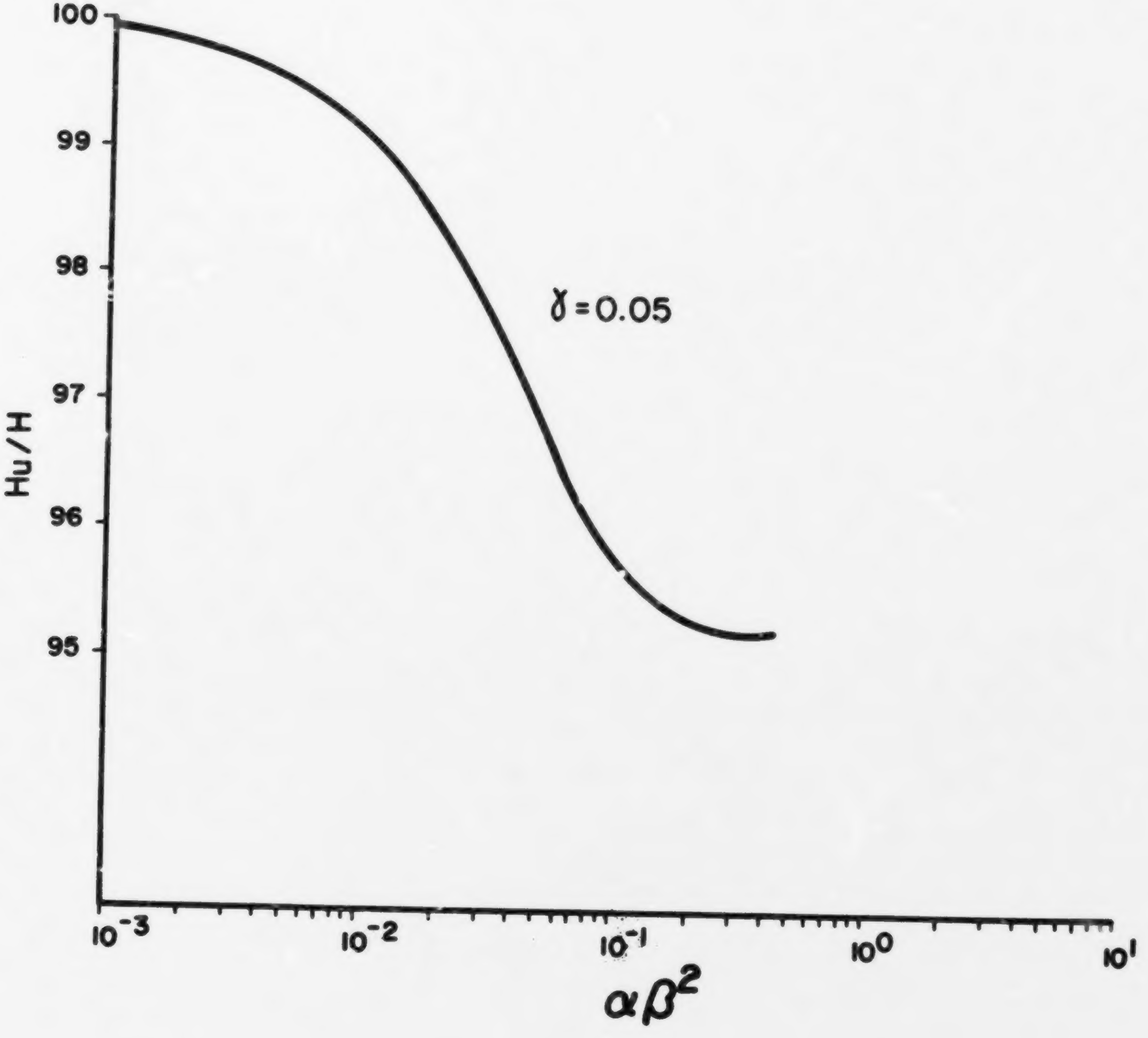
100
99
98
97
96
95
Hu/H
$\gamma = 0.05$
10^{-3}
10^{-2}
10^{-1}
10^{0}
10^{1}
$\alpha\beta^2$

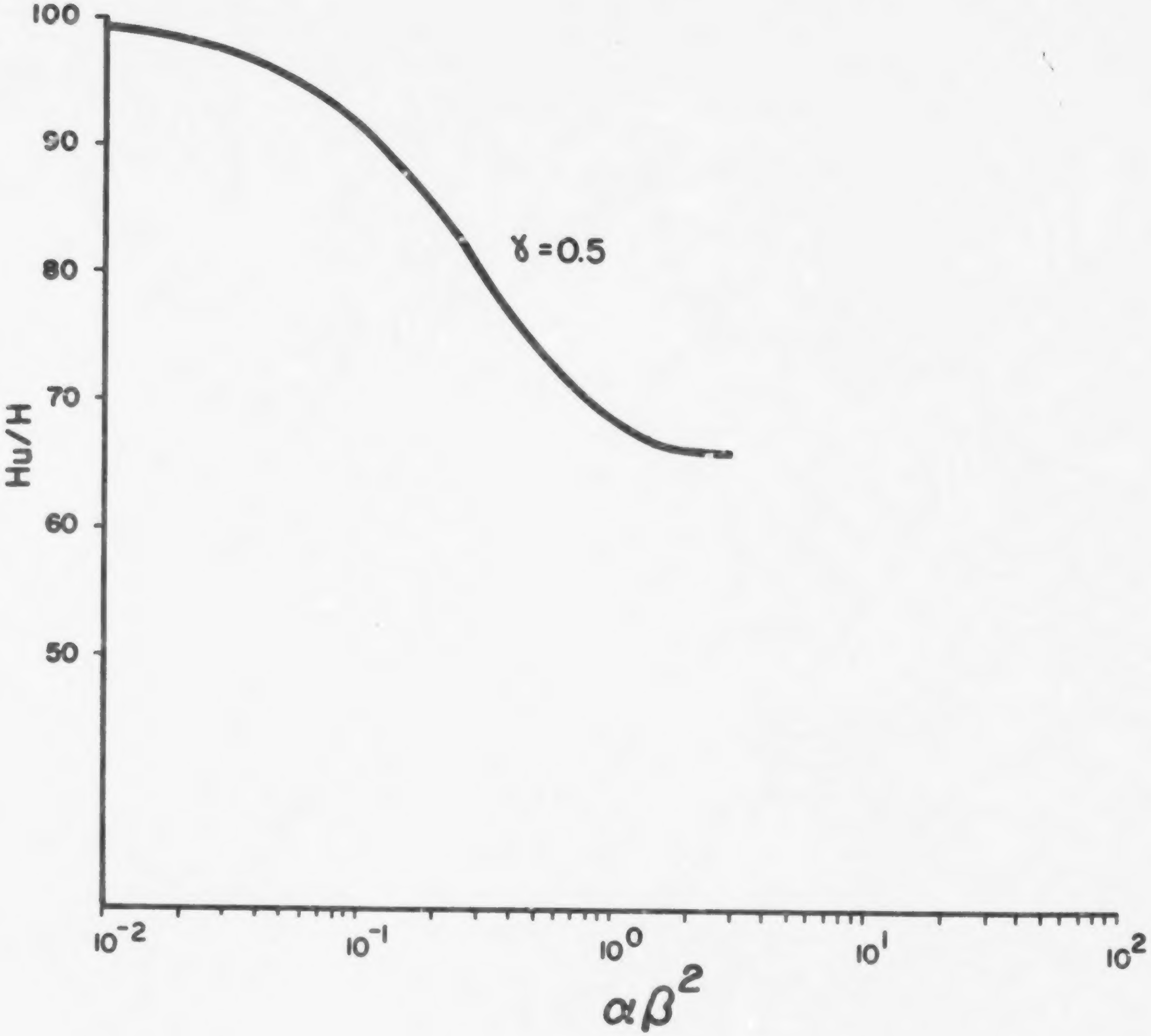
100
90
80
70
60
50
Hu/H
γ = 0.5
10^{-2}
10^{-1}
10^{0}
10^{1}
10^{2}
$\alpha\beta^2$

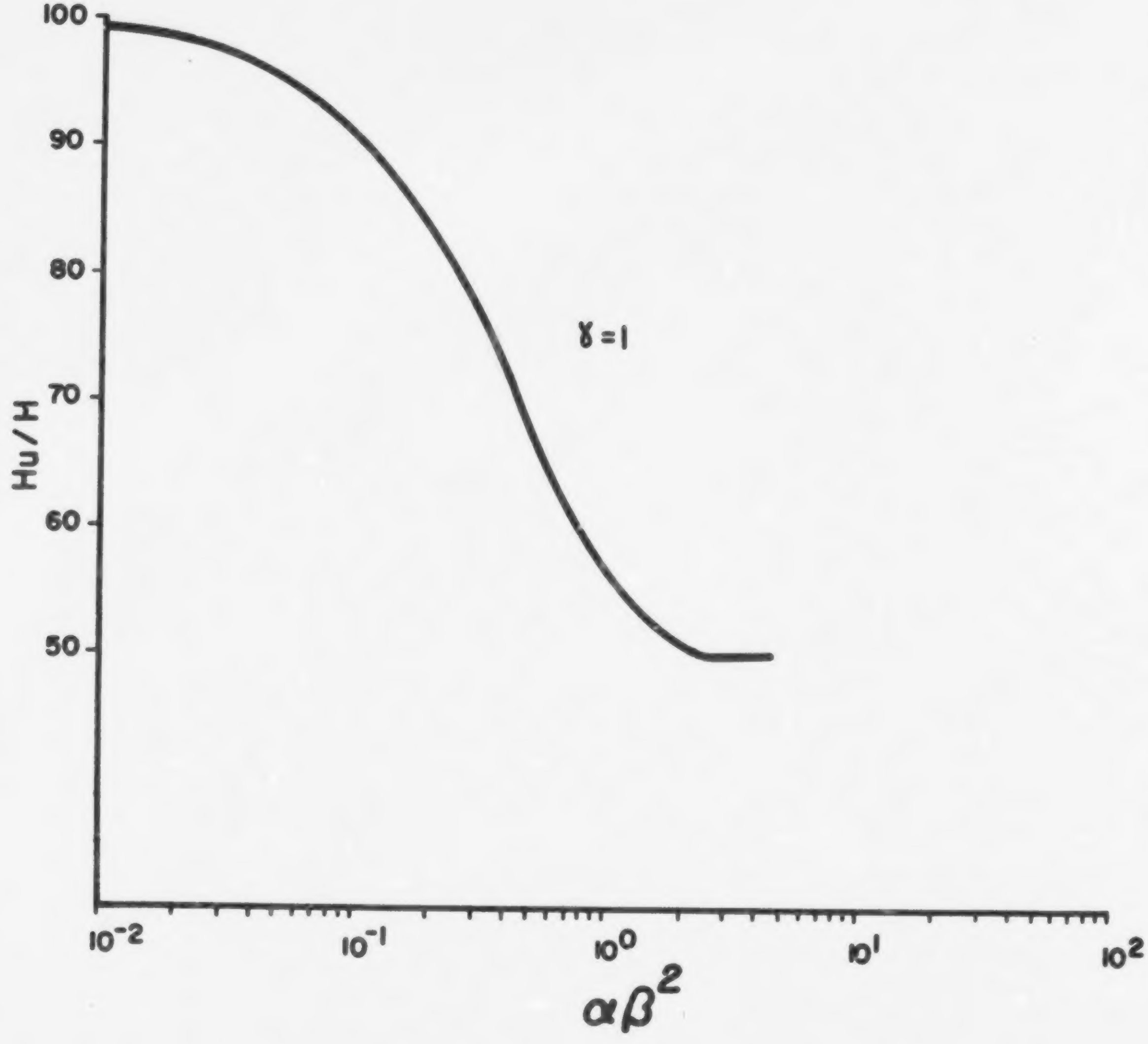
100
90
80
70
60
50
Hu/H
γ = 1
10⁻²
10⁻¹
10⁰
10¹
10²
αβ²

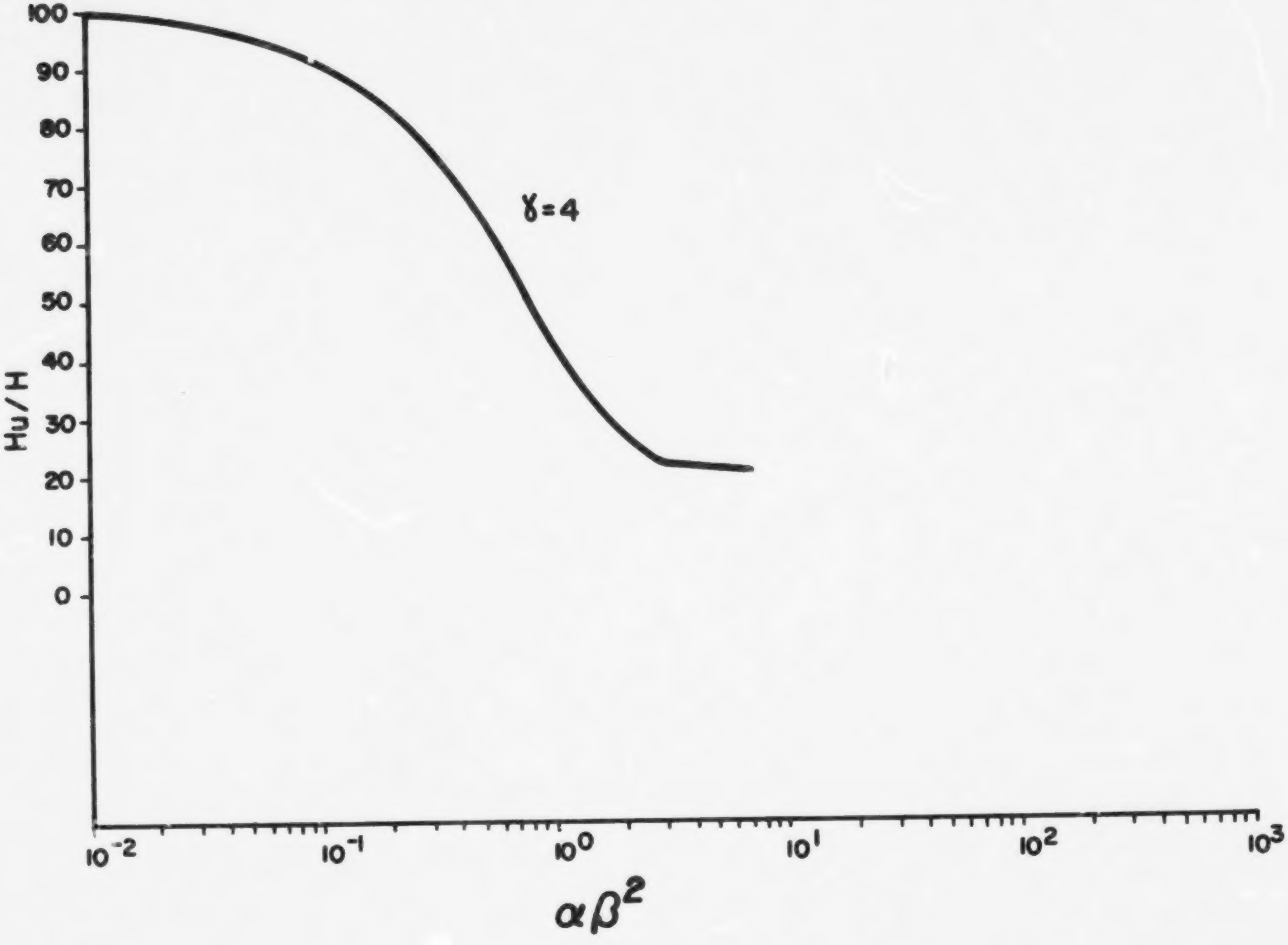
100
90
80
70
60
50
40
30
20
10
0
Hu/H
γ=4
10^{-2}
10^{-1}
10^{0}
10^{1}
10^{2}
10^{3}
$\alpha\beta^2$

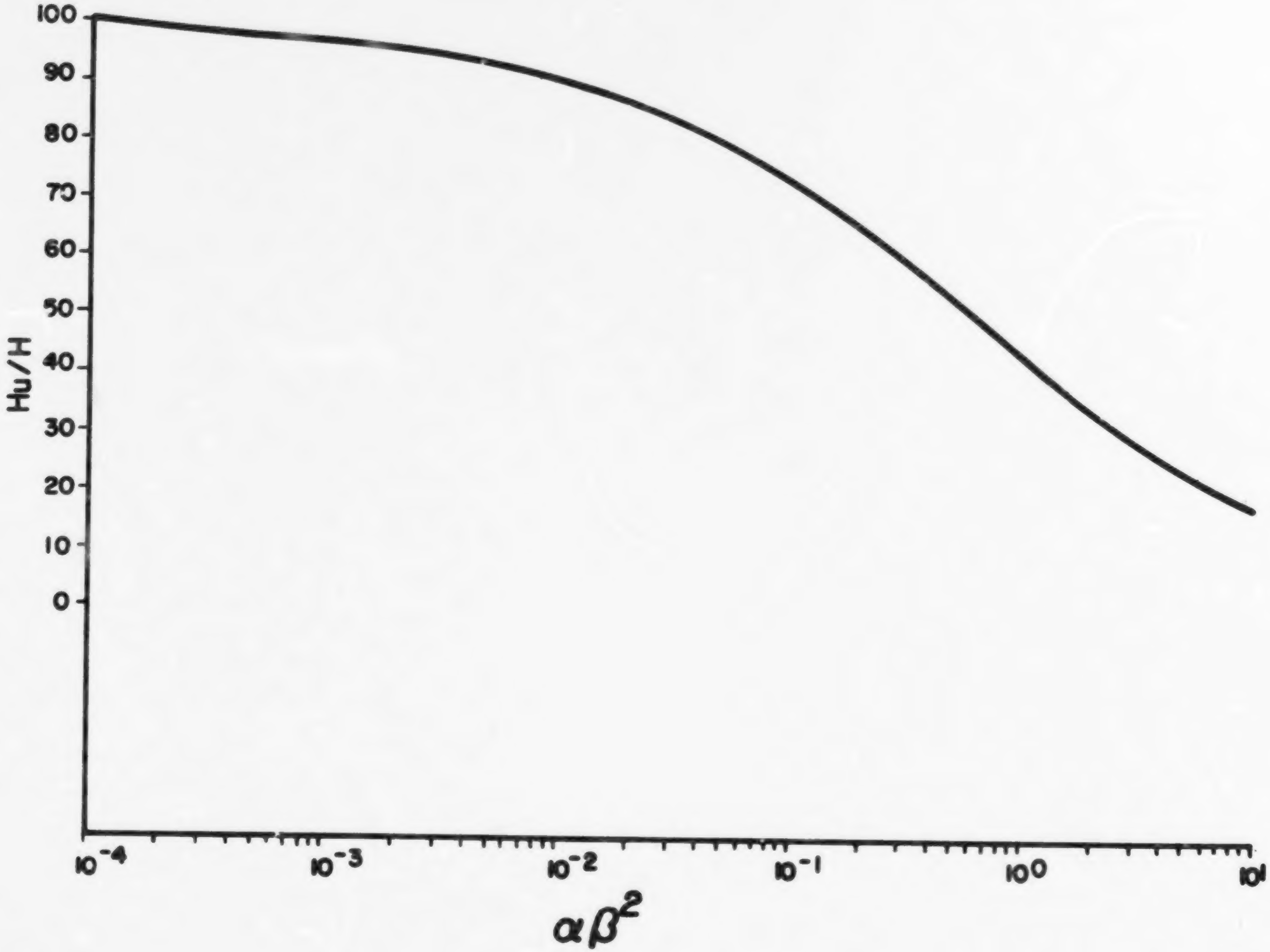
100
90
80
70
60
50
40
30
20
10
0
Hu/H
10^{-4}
10^{-3}
10^{-2}
10^{-1}
10^{0}
10^{1}
$\alpha\beta^2$

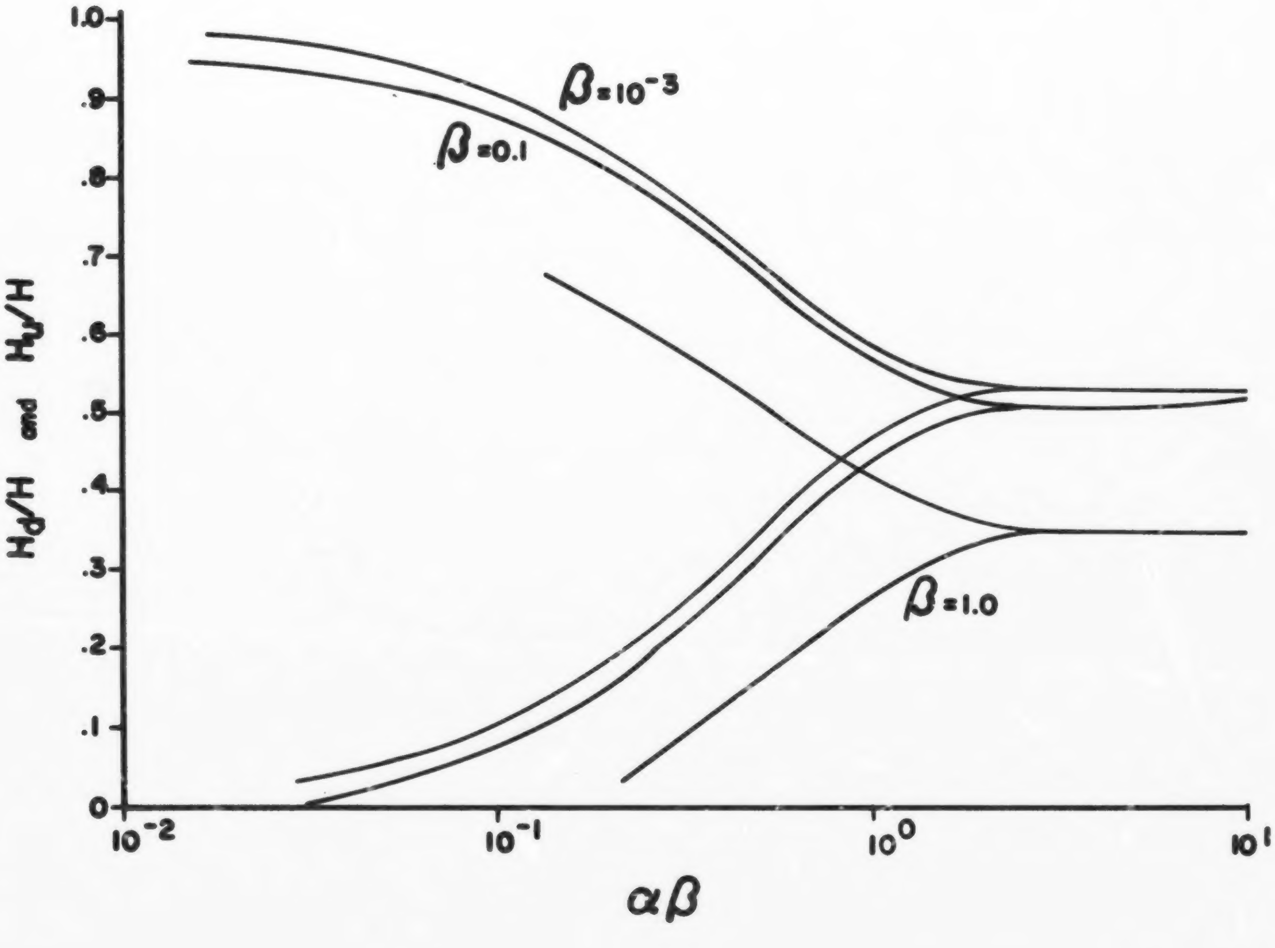
1.0
.9
.8
.7
.6
.5
.4
.3
.2
.1
0
H_d/H and H_u/H
10^{-2}
10^{-1}
10^{0}
10^{1}
$\alpha\beta$
$\beta = 10^{-3}$
$\beta = 0.1$
$\beta = 1.0$

NRC FORM 335
(6 83)

U.S. NUCLEAR REGULATORY COMMISSION

BIBLIOGRAPHIC DATA SHEET

1 REPORT NUMBER (Assigned by TIDC, add Vol. No., if any)
NUREG/CR-4919

2 Leave blank

3 TITLE AND SUBTITLE
Field Testing of Bentonite and Cement Borehole Plugs
in Granite

4 RECIPIENT'S ACCESSION NUMBER

5 DATE REPORT COMPLETED

MONTH	YEAR
March	1987

6 AUTHOR(S)
A.F. Kimbrell, T.S. Avery, and J.J.K. Daemen

7 DATE REPORT ISSUED

MONTH	YEAR
July	1987

8 PERFORMING ORGANIZATION NAME AND MAILING ADDRESS (Include Zip Code)

Department of Mining and Geological Engineering
University of Arizona
Tucson, AZ 85721

9 PROJECT/TASK/WORK UNIT NUMBER

10 FIN NUMBER
FIN B6627
NRC-04-78-271

11 SPONSORING ORGANIZATION NAME AND MAILING ADDRESS (Include Zip Code)

Division of Engineering
Office of Nuclear Regulatory Research
U.S. Nuclear Regulatory Commission
Washington, DC 20555

12a TYPE OF REPORT
Technical Report

12b PERIOD COVERED (Inclusive dates)

13 SUPPLEMENTARY NOTES

14 ABSTRACT (200 words or less)

This technical report describes in-situ flow tests on bentonite and cement borehole plugs installed in granite, and laboratory back-up experiments on similar plugs. Prior to sealing, the hydraulic conductivity of the boreholes is tested. These measurements, together with core and borehole videologs, permit the selection of seal test intervals. Commercial expansive cement and standard waterwell sealing bentonite products and emplacement procedures are used. Transient (short-term) and steady-state (long-term) tests determine the sealing performance of the plugs under various stress conditions.

Laboratory and field experiments confirm the difficulty of obtaining even moderately accurate performance values for bentonite plugs as installed here, due to the simultaneous saturation, swelling, and consolidation. Nevertheless, conventional installation of readily available seals can provide adequate borehole seals (i.e., seals with a hydraulic conductivity of about the same magnitude as that of intact granite). Bentonite plugs of this type are heterogeneous and weak. Improved testing procedures and analyses are needed if actual conductivity values are to be obtained in a reasonable testing time (e.g., months). Laboratory investigations on failure mechanisms in cementitious and bentonitic plugs, not covered in this research study, are needed to identify and prevent plug failure.

15a KEY WORDS AND DOCUMENT ANALYSIS
Permeability testing
Borehole plugging
Borehole sealing
Rock Mass sealing
Bentonite borehole plugs
Cement borehole plugs
Borehole plug testing

15b DESCRIPTORS
Granite hydraulic conductivity
Cement hydraulic conductivity
Bentonite hydraulic conductivity
Seal testing
Bentonite consolidation
Transient pulse testing

16 AVAILABILITY STATEMENT
Unlimited

17 SECURITY CLASSIFICATION
(This report)
Unclassified

18 NUMBER OF PAGES

19 SECURITY CLASSIFICATION
(This page)
Unclassified

20 PRICE
$

*U.S. GOVERNMENT PRINTING OFFICE:1987-181-682:60175

321

UNITED STATES
NUCLEAR REGULATORY COMMISSION
WASHINGTON, D.C. 20555

OFFICIAL BUSINESS
PENALTY FOR PRIVATE USE, $300

SPECIAL FOURTH-CLASS RATE
POSTAGE & FEES PAID
USNRC
WASH. D.C.
PERMIT No. G-67

BEST COPY AVAILABLE

329